THE AMERICAN JOURNAL OF PATHOLOGY

VOLUME XXXIII JULY–AUGUST, 1957 NUMBER 4

HISTOLOGIC AND PHYSIOLOGIC CHARACTERISTICS OF HORMONE-SECRETING TRANSPLANTABLE ADRENAL TUMORS IN MICE AND RATS*

ARTHUR I. COHEN, Ph.D.; JACOB FURTH, M.D., and RITA F. BUFFETT, Ph.D.

From the Children's Cancer Research Foundation, Children's Medical Center; the Department of Pathology, Harvard Medical School; and the Cancer Research Institute of the New England Deaconess Hospital, Boston, Mass.

Adrenocortical tumors which occur spontaneously are infrequent in mice and rats.[1-7] They have been induced in several strains of mice by castration shortly after birth[8-11] and in the rat by implantation of estrone pellets[12] or by inclusion of the carcinogenic agent "butter yellow" in the diet.[13] Histologic studies of tissues of hosts bearing tumor transplants indicated the production of estrogenic or androgenic hormones, or both, by some experimental tumors. To our knowledge, adrenocortical tumors which secrete corticoids have not been observed in mice or rats. However, transplants of an adrenocortical carcinoma in the Osborne-Mendel strain of rats induced atrophy of the adrenal glands of the hosts, indicating inhibition of ACTH by adrenocorticoid secretions.[13]

The present investigation concerns two adrenocortical tumors, one occurring in the LAF_1 strain of mice and the other in the WR strain of rats. Neither of these tumors gives evidence of secretion of gonadal hormone of either type, feminizing or masculinizing, and both are characterized by the presence of excessive adrenocorticoid secretion.

MATERIALS AND METHODS

Origin of the Adrenal Tumor of Mouse. During April, 1951, a group of LAF_1 mice was exposed to the irradiation of a test atomic bomb explosion (Operation Greenhouse). Adrenal tumors were observed in less than 1 per cent, and it is questionable whether these were induced by the irradiation or arose spontaneously. One male mouse that re-

* These investigations have been supported by Grant C-2259 of the National Institutes of Health.

Received for publication, July 23, 1956.

ceived 318 rep and was sacrificed in October, 1953, had a tumor in the right adrenal cortex measuring 12 by 20 mm.; the left adrenal gland was atrophic. The tumor was excised and finely minced in a small amount of isotonic saline solution and implanted intramuscularly in the thigh of male and female LAF_1 mice.

Origin of the Adrenal Tumor of Rat. A group of young WR male rats was radiothyroidectomized with I^{131} (400 μc. injected subcutaneously) for the purpose of inducing pituitary tumors. Two of the animals were sacrificed 1½ years later, when a tumor measuring 8 by 10 mm. was found in the right adrenal cortex of one rat, and in the other a tumor with an average diameter of 6 mm. was found in the left adrenal cortex. It is uncertain whether radiothyroidectomy caused these tumors. The two tumors were combined, finely minced with a small amount of isotonic saline solution, and implanted in the thigh muscles of WR rats.

Animals. The WR rats were bred in our laboratory; the LAF_1 mice were obtained from the Jackson Memorial Laboratory, Bar Harbor, Maine. The animals were fed a standard diet of Purina Chow pellets. Rats that were to be radiothyroidectomized were given a low iodine diet* and distilled drinking water for several weeks before administration of the I^{131} (120 μc. subcutaneously). Following adrenalectomy, the mice were given a single intramuscular injection of 1 mg. of desoxycorticosterone trimethylacetate.†

All animals into which the tumors were implanted were subsequently necropsied. Tissues were fixed in Zenker's solution and stained with hematoxylin and eosin.

Electrolyte Studies. Blood was obtained by cardiac puncture of etherized animals. Twenty-four hour samples of urine were collected from animals placed in metabolism cages. The electrolyte analyses were made with a flame photometer.

Eosinophil Counts. The technique of Speirs[14] was followed.

Results

Adrenal Tumor of Mouse, Strain 2

Original Tumor. At necropsy, the mouse bearing the original tumor displayed the following changes: emaciation with no edema, atrophy of lymph nodes and thymus, atrophy of testes and seminal vesicles, and slight enlargement of the thyroid gland. The tumor cells were fairly uniform in size and shape; the cytoplasm was scanty and ill-defined. There were few mitotic figures. Metastases in the lungs were numerous.

* Obtained from Nutritional Biochemicals Corp., Cleveland, Ohio.
† Percorten, Ciba, generously supplied by Dr. Robert Gaunt.

Transplantations. The tumor transplants took well in mice of the host strain in all passages: in males nearly 100 per cent and in females, 92 per cent (Table I). The average latent periods of the original passage in males and females were 106 and 133 days, respectively. After several passages, the average latencies decreased to 23 days in females in the seventh passage and to 16 days in males in the ninth passage.

TABLE I

Growth of Transplants of an Adrenal Tumor of a Mouse, Strain 2, in Isologous Strain

Treatment of hosts	Recipients	
	Male	Female
None	201/202*	77/84*
Adrenalectomy	13/14	4/4
Gonadectomy	11/11	8/9
Hypophysectomy		4/4

* Number of takes over number grafted.

The tumor took in eight of nine female gonadectomized recipients, but in these the average latency was about 35 per cent longer than in untreated controls. No change in the latency was observed in gonadectomized males. Adrenalectomy did not affect the latency in males but increased it slightly in females. Hypophysectomy, performed only in females, doubled the latent period.

Necropsy Findings. At necropsy, the transplanted tumors weighed 5 to 10 gm. each, were brown, soft, well vascularized, and sometimes spotted with opaque areas of necrosis. Microscopic examination of the tumor showed solid sheaths of polygonal epithelial cells of uniform size with scanty cytoplasm, spherical nuclei, and a few mitotic figures (Fig. 1). Most tumor cells resembled those of the adrenal cortex; rarely, they were elongated or sarcoma-like. Connective tissue septa separated groups of cells into nodules. The absence of distinct anaplasia was significant in the almost invariable presence of pulmonary metastases. Some tumor cells possessed a certain degree of polarity, being lined up on a basement membrane with nuclei located close to the membrane. Calcification and ossification were noted in a few tumors. The tumor cells contained little fat and the impression was gained that it was more abundant in the degenerating parts of the tumor.

Minute metastatic tumor nodules were disseminated throughout all lobes of the lungs (Fig. 2). In several cases these were not seen on gross examination, but were present in all sections taken. Most metastases were intravascular "tumor emboli." Where tumor cells had gained entry into alveoli and bronchi, they appeared to have grown there uninhibited. Edema and cavernous dilatation of pulmonary capillaries frequently accompanied the pulmonary metastases.

The most characteristic change associated with this transplanted tumor was a very marked atrophy of all three layers of the adrenal

cortex (Fig. 3). The adrenal medulla appeared unchanged in all tumor-bearing hosts. Some adrenal glands were enlarged, but this was due to congestion of adrenal sinusoids and not to hyperplasia of the cortex (Fig. 4). Similar cavernous dilatation of vessels was noted in the liver, ovaries, lungs, and in a few other organs, suggesting that the tumor growth was sometimes associated with a marked hypervolemia.[15]

A marked thymic atrophy was evident in all tumor-bearing animals. It was present even in animals bearing only small tumors and was interpreted as due to secretion of corticoids by the tumor. Animals bearing tumors other than those secreting ACTH or steroid hormones did not cause thymic atrophy until the tumors were large, while involution of the thymus occurred soon in all mice bearing this adrenal tumor.

TABLE II

Polyuria and Polydipsia in Mice Bearing Transplants of an Adrenal Tumor, Strain 2

Mouse	Days of observation	Water consumed, mean (range)	Urine excreted, mean (range)
		ml./mouse/day	*ml./mouse/day*
Control*	38	6.5 (5.8–7.0)	1.2 (1.0–2.2)
Tumor-bearing	10	37 (29–43)	23 (18–27)
Tumor-bearing	10	23 (17–26)	13 (10–18)
Tumor-bearing	10	57 (53–67)	36 (30–44)
Tumor-bearing	10	61 (53–69)	34 (27–41)
Tumor-bearing	10	29 (27–34)	18 (15–22)
Tumor-bearing	5	31 (28–33)	16 (12–20)
Tumor-bearing†	5	50 (47–55)	28 (20–38)
Tumor-bearing‡	8	33 (29–35)	13 (9–19)
Tumor-bearing‡	6	24 (20–34)	16 (10–23)

* Five animals were used to secure the control values. Other values are for individual mice.

† Gonadectomized mouse.

‡ Adrenalectomized and gonadectomized mouse.

Thymic involution is, in our experience, the most sensitive indicator of hyperstimulation by adrenocorticoids.

The testes and ovaries appeared normal or atrophic. Leydig cells were fewer than normal. The latter observation suggested some secretion of androgenic steroids by the tumor, but this supposition was not supported by the finding that in castrated tumor-bearing animals the seminal vesicles remained atrophic.

In the ovaries, lutein bodies were conspicuously absent and luteinization of the stroma was deficient. The uterine horns were slightly elongated and dilated or thickened. The mammary glands were usually normal except for marked ductal hyperplasia in a few animals, a change

not uncommon in old female mice. In ovariectomized hosts, the uterine horns were sometimes dilated and elongated, and sometimes thin and atrophic. These changes suggested the possibility of some secretion of estrogens. The ovaries of female adrenalectomized hosts were atrophic; their uteri were slightly dilated and elongated.

The pituitary and thyroid glands of tumor-bearing mice appeared normal. The liver showed no conspicuous change other than that of an occasional slight congestion of the hypervolemic type and/or a leukemoid reaction. Hemopoiesis was evident in the spleen, but such changes are common in animals bearing diverse tumors of large size. The kidneys showed no noteworthy change. There was no indication of a masculinizing effect in female mice.

Water Balance and Electrolytes. When the adrenal tumor in the mouse grew to 2 or 3 cm. in diameter, a profound polyuria and polydipsia, with no edema, were observed in the hosts (Table II). The

TABLE III

Serum Electrolyte Values of Mice Bearing an Adrenal Tumor, Strain 2

Serum electrolyte	Control mice*	Tumor-bearing mice*
Na, meq./l.	166.7 ± 12.7†	189.1 ± 7.9†
K, meq./l.	5.6 ± 0.7	4.9 ± 0.5
Cl, meq./l.	115.2 ± 10.1	121.7 ± 10.6
Na/K ratio	30.3 ± 5.4	38.8 ± 4.4

* Five mice in each group.
† Standard deviation of the mean.

presence of these changes in adrenalectomized and gonadectomized mice indicated that they were caused by secretions of the tumor.

A study of the serum electrolyte changes was made in mice with grafted adrenal tumors of later passages when hormonal secretions appeared to have diminished (Table III). The serum sodium levels were elevated and the potassium levels were slightly depressed. Polyuria and polydipsia were not so prominent in these mice as noted earlier. Increased sodium retention and polyuria pointed to an increased secretion of aldosterone or of another mineralocorticoid by the tumor. It is noteworthy that adrenalectomized mice bearing the tumor could be maintained on tap water.

Eosinophils. The eosinophil counts of the blood in adrenal tumor-bearing mice (strain 2) dropped to very low levels soon after the grafted tumor became palpable (Table IV). This occurred also in adrenalectomized, adreno-gonadectomized, and hypophysectomized tumor-bearing hosts (Table IV).

The change in levels of eosinophilic leukocytes was followed in 12 mice. A representative example is shown in Table V. The tumor was not yet palpable at 26 days, when the level of eosinophils was 378 per cmm. and the leukocyte count was 25,800. As the tumor grew, both eosinophil and total leukocyte counts dropped progressively to 19 per cmm. and 9,800, respectively. Bilateral adrenalectomy was performed 57 days after the graft. In normal animals, adrenalectomy is followed promptly by regeneration of the thymus and recovery from eosinopenia. In these animals, the eosinopenia persisted, the progressive drop in the levels of leukocytes and eosinophils was not arrested (terminal counts 1,600 and 3 per cmm., respectively), while the animals gained weight and the tumors continued to grow (Table V). Additional gonadectomy had no effect on the levels of eosinophils.

Eosinopenia was consistent in all adrenal tumor-bearing mice, but leukopenia was variable and usually slight. There was, however, a marked lymphopenia which occurred late in the presence of large tumors. In tumor-bearing mice, adrenalectomy was not followed by regeneration of the thymus. These data indicate that adrenal tumors of strain 2 secrete glucocorticoids.

TABLE IV

Eosinophil Levels of the Blood in Mice Bearing Adrenal Tumors, Strain 2*

Tumor size†	Normal			Adrenalectomized			Adreno-gonadectomized			Hypophysectomized		
	No. of counts	Mean	(Range)	No. of counts	Mean	(Range)	No. of counts	Mean	(Range)	No. of counts	Mean	(Range)
+	14	33	(0–150)	1	9					1	16	
+ to ++	8	6	(0–19)	5	9	(3–25)	2	25	(12–37)	2	6	(3–9)
++ to +++	3	6	(3–12)	5	7	(3–12)	1	12				
+++ to ++++	3	22	(9–48)	3	8	(3–12)						
Controls	55	409	(75–1373)	37	178	(22–318)	5	259	(97–612)	8	573	(250–967)

* Eosinophil counts per cmm. Blood obtained from tails at 8:00 a.m.

† Each plus sign indicates an approximate average diameter of 1 cm.

Adrenal Tumor of Mouse, Strain 3

Another adrenal tumor occurring also in an irradiated mouse was studied earlier in four passages. This tumor grew very rapidly, causing death with large tumors in about 1 month. It caused only slight involution of the thymus; the gonads and adrenal glands of the hosts appeared normal or were only slightly altered. Transplantation of this malignant non-secreting or low-secreting adrenocortical tumor was discontinued.

TABLE V

Sequence of Changes in a Mouse Bearing an Adrenal Tumor, Strain 2

Days after graft	Body weight	Tumor size*	Eosinophils	White blood cells	Lymphocytes	
					%	Total
	gm.		cmm.	cmm.		cmm.
26	26.3	o	378	25,800	91	23,478
33	27.2	?	150	26,750	82	21,935
41	28.6	±	41	20,100	87	17,487
47	28.0	± to +	12	8,600	83	7,138
54	30.2	+ to + ±	19	9,800	70	6,860
57†						
63	33.0	++	25	12,500	48	6,000
70	34.9	++±	12	8,300	37	3,071
77	36.0	++±	3	1,600		

* Each + indicates an average of 1 cm.
† Bilateral adrenalectomy.

Adrenal Tumor of Rat, Strain 1

Original Tumor. The two rats bearing the original adrenal tumors were emaciated and anemic. Malnutrition could be attributed to overgrown incisor teeth. There was advanced atrophy of the thymus and lymph nodes. The testes were small, with degenerative changes in spermatogenic tubules and reduction in number of Leydig cells. Small remnants of the thyroid gland were present; other changes at thyroid sites were those of "radiothyroidectomy." There were distinct "thyroidectomy cells" in the pituitary body[16] with decrease in the number of acidophils. The adrenal tumors appeared to be typical cortical adenomas with no evidence of malignancy. The adrenal glands of the opposite side also contained minute tumor nodules and the cortical layers were thin. No metastases were observed.

Transplantation. The original passage was made by grafting the pooled tumors on radiothyroidectomized and gonadectomized rats of the strain of origin. In untreated rats there were no tumor takes even

after 615 days. The thyroidectomized animals, on the other hand, developed tumors with an average latency of 221 days; and gonadectomized rats, of 485 days.

Table VI summarizes the results of transplantations in animals variously treated. The tumors grew best in hosts made deficient of thyroid hormone either by radiothyroidectomy or low iodine diet. They took well in gonadectomized males and females, but in the latter after a much longer latent period. These periods were longer in gonadectomized than in radiothyroidectomized animals, and longer in the females than in males. The tumors grew well in animals that were both adrenalectomized and gonadectomized, but the average latent period was still about twice that of the radiothyroidectomized rats.

TABLE VI

Transplantation of Adrenal Tumor of Rat, Strain 1

Treatment of hosts	Recipients	
	Males	Females
None	6/28*	0/8*
Gonadectomy	11/13	4/4
Adrenalectomy and gonadectomy	4/4	
Radiothyroidectomy	10/10	9/9
Low iodine diet	5/5	

* Number of takes over number of grafts.

In the course of successive transfers, there was a decrease in the latent periods, but the relative differences in latency in animals which were variously treated persisted. These data indicate that growth of this adrenal tumor is greatly influenced by some hormonal imbalance in the hosts. Growth promotion by adrenalectomy can be adequately explained by increase of ACTH, but that by thyroidectomy is puzzling.

Necropsy Findings. At death, the grafted tumors were approximately 4 cm. in average diameter and weighed 10 to 15 gm. They had a characteristic, yellow-brown hue and were spotted with hemorrhagic and necrotic areas. Rarely, disseminated areas of calcification, and sometimes of ossification, were noted. The adrenal tumor cells of the rat (Fig. 6) were similar to those of the mouse: polygonal, closely packed, often forming palisades. Mitotic figures were numerous, but anaplasia was scant. Pulmonary metastases were noted in a few animals (Fig. 7).

There was atrophy of all layers of the adrenal cortex of tumor-bearing hosts; the medulla appeared unchanged (Fig. 8). The thymus was atrophic. These observations indicate that the tumor secreted corticoids. The thyroid gland appeared normal in the gonadectomized and untreated hosts. There was marked atrophy of the testes and seminal vesicles (Fig. 10) of the non-operated animals. Leydig cells were few or absent and spermatogenesis was depressed. In the gonad-

ectomized males, there was advanced atrophy of the seminal vesicles. The testes and seminal vesicles of radiothyroidectomized hosts were atrophic. These findings indicate lack of secretion of androgens. The ovaries and uteri of female radiothyroidectomized hosts were of normal size or atrophic; in no case was there evidence of gonadal stimulation.

The pituitary bodies of the gonadectomized and thyroidectomized animals possessed large numbers of hypertrophied cells with hyalinization and vacuolization of the cytoplasm.[16] These changes were similar to Crooke's hyalinization of pituitary basophils, which is considered to be pathognomonic of Cushing's disease. They were absent in untreated rats bearing the adrenal tumor.

Obesity, a characteristic change in mice bearing grafted adrenotropic tumors,[23] was present in most rats, but absent in most mice with grafted adrenal tumors.

Preliminary studies have shown the tumor-bearing rats to be slightly polyuric, with about two or three times the daily urine output of controls. The serum sodium and potassium values appeared unchanged in the few tumor-bearing rats examined. However, adrenalectomized hosts survived well on tap water once the tumor started to grow.

Discussion

The physiologic effects of functional adrenocortical tumors in man and animals vary with the type of hormones secreted. In general, four types of hormonal effects have been noted: those influencing carbohydrate or electrolyte metabolism and male or female sexuality. The clinical picture most frequently observed suggests the simultaneous overproduction of a mixture of several hormones in various proportions, sometimes of only two types and rarely of only one type.[17] Table VII surveys functional adrenal tumors in several animal species. In earlier reports of others, only gonadal effects (masculinizing, feminizing, or both) were recorded, while our adrenal tumor strains in both mice and rats exhibited glucocorticoid and mineralocorticoid but no gonadal activities. Studies are now being made on the rates and types of corticoids secreted by the tumor slices *in vitro*[21] and on urinary steroidal products of the hosts.[22] The results of the former[21] indicate secretion of corticoids and responsiveness of the tumor cells to ACTH. The results of the latter[22] indicate a large increase in urinary 17-ketosteroids, particularly the 11-oxygenated 17-ketosteroids.

It is noteworthy that all three layers of the adrenal cortex of tumor-bearing hosts were inhibited. Atrophy of the zona glomerulosa and polyuria indicate secretion of mineralocorticoids. Confirmatory evi-

TABLE VII

Physiologic Effects of Functional Adrenocortical Tumors and Transplants in Several Animal Species

Host	Strain and sex	Induction procedure	Presumed secretion			
			Andro-genic	Estro-genic	Gluco-corticoid	Mineralo-corticoid
Mouse	NH ♂ and ♀,[8,11] DBA ♀ [18]	Castration	−	+	−	−
Mouse	A ♀ [11]	Castration	+	−	−	−
Mouse	CE ♂ and ♀,[9,10] C_3H ♀, CBA ♀, Bagg albino ♂ and ♀ [11]	Castration	+	+	−	−
Mouse	LAF_1 ♂ (Cohen *et al.*, 1957)	Irradiation(?)	−	−	+	+
Mouse	NH x A ♂ [8]	Irradiation(?)	−	?	−	−
Mouse	Old NH ♀ [8]	Spontaneous	−	+	−	−
Mouse	C ♀ [2]	Spontaneous	−	−	−	−
Rat	WR ♂ (Cohen *et al.*, 1957)	Radiothyroidectomy(?)	−	−	+	+
Rat	Osborne-Mendel ♀ [13]	Carcinogenic diet	−	−	?	−
Guinea pig	♂ [19]	Castration	+	−	−	−
Rabbit	♂ [20]	Spontaneous	−	−	−	−

dence for this is the hypernatremia co-existing with polyuria. The hypoplasia of the zona glomerulosa is probably caused by a process analogous to its inhibition by administration of salt. The early severe depression of eosinophil counts is indicative of excessive secretion of glucocorticoids and, correspondingly, the marked atrophy of the zona fasciculata and zona reticularis indicates inhibition of ACTH discharge.

In parallel studies the levels of eosinophils of mice bearing transplanted tumors of diverse types have been investigated. A marked and early drop in levels of eosinophils occurred in mice with grafted adrenal or adrenotropic pituitary tumors. Following this drop, adrenalectomy caused a rise in levels of eosinophils in mice bearing adrenotropic pituitary tumors, while in animals with adrenal tumors the drop continued until almost all eosinophils disappeared from the circulation.

It is most desirable to identify the corticoids secreted by such tumors. While it is possible that they merely represent a spectrum of the usual adrenocorticoids, it is also conceivable that some of them have little or no hormonal activity, yet exert a specific pituitary inhibition. Such compounds may characterize the neoplastic cell and be of therapeutic value in inhibiting secretion by adrenotropes.

Routine morphologic examinations disclosed no significant change in the mouse or rat pituitary bodies of the tumor-bearing hosts. Theoretically, one would expect atrophy or hypoplasia of the adrenotropic cells. The morphologic characteristics of adrenotropic cells are unknown. They are believed to be variants of basophils, but none of our three transplantable adrenotropic tumors is composed of distinctly basophilic cells.[23] All are chromophobic or amphophilic even though they are highly secretory. The absence of Crooke's change in the pituitary bodies of untreated mice and rats bearing adrenal tumor grafts is noteworthy. Crooke's change has been reproduced in man by administration of cortisone or hydrocortisone.[24] The literature on Crooke's change in rodents given ACTH or cortisone is contradictory. Our findings with adrenotropic pituitary tumors[23] and with adrenal tumors here described agree with those of Halmi and Barker,[25] who failed to find any changes in the pituitary bodies of rats and mice given corticoids or ACTH; we fail to explain the contradictory findings of Golden and Bondy.[26] A sharp differentiation of the changes in the pituitary gland caused by gonadectomy, thyroidectomy, and lack or excess of corticoids remains to be worked out.

Prolonged cortisone treatment in mice usually causes a fatal infection with a diphtheroid organism (*Corynebacterium pseudotuberculosis murium kutscheri*), with pleurisy and pericarditis and tumor-like

granulomas in the lung, kidneys, and liver.[27] Mice bearing transplantable ACTH-secreting tumors almost invariably die of a fatal infection by this microorganism[23] when the tumor measures barely more than a few millimeters. Absence of such changes in mice bearing the transplantable adrenal tumors can be taken as biologic evidence indicating that these tumors do not secrete cortisone, hydrocortisone, or a related steroid which depresses body resistance. Clarification of these problems awaits identification of the steroids secreted by these tumors and determination of the range of changes caused in the animal body by each of these.

Summary

Adrenocortical tumors originating in mice and rats were transplanted in series in the strain of origin.

In mice, the transplanted tumor of strain 2 grew in normal, gonadectomized, adrenalectomized, and hypophysectomized hosts. It caused marked atrophy of all layers of the adrenal cortex (but not the medulla), hypernatremia with profound polyuria, thymic involution, and marked depression of the levels of eosinophils. Grafted adrenotropic pituitary tumors also caused a marked and early drop in levels of eosinophils and involution of the thymus; however, while with adrenotropic tumors adrenalectomy is followed by regeneration of the thymus and a rise in levels of eosinophils, in adrenal tumor-bearing animals the eosinopenia and thymic involution persisted. These effects indicate that this adrenal tumor secretes glucocorticoids and mineralocorticoids. In preliminary experiments, the tumor responded to ACTH *in vitro*.

In spite of retention of secretory abilities and lack of anaplasia, this tumor is highly malignant, as indicated by extensive pulmonary metastases, a behavior rarely exhibited by common tumors of mice.

The transplants of the adrenal tumors in the rat grew best in adrenalectomized and in radiothyroidectomized, less well on gonadectomized, and least in untreated hosts. Males were much more susceptible than females.

Secondary changes produced by the adrenal tumors in the rat were similar to those of the tumors in the mouse and indicated secretion of glucocorticoids. Polyuria, however, was less extensive in the rat, and levels of serum electrolytes were normal. Obesity was common in the rat, but not in the mouse.

Evidence for secretion of feminizing or masculinizing gonadal hormones by adrenal tumors of either the mouse or rat was lacking.

The courtesy of Dr. Alexander Hollaender in releasing the tumor strains isolated at the Oak Ridge National Laboratory is gratefully acknowledged.

REFERENCES

1. Slye, M.; Holmes, H. F., and Wells, H. G. Primary spontaneous tumors in the kidney and adrenal of mice. Studies on the incidence and inheritability of spontaneous tumors in mice. *J. Cancer Research,* 1921, **6**, 305–336.
2. Dalton, A. J.; Edwards, J. E.; Andervont, H. B., and Briggs, V. C. A spontaneous, transplantable, adrenal cortical tumor arising in a strain C mouse. *J. Nat. Cancer Inst.,* 1943–44, **4**, 329–338.
3. Kirschbaum, A.; Frantz, M., and Williams, W. L. Neoplasms of the adrenal cortex in noncastrate mice. *Cancer Research,* 1946, **6**, 707–711.
4. McCoy, G. W. A preliminary report on tumors found in wild rats. *J. M. Research,* 1909, **21**, 285–296.
5. Woolley, P. G., and Wherry, W. B. Notes on twenty-two spontaneous tumors in wild rats (*M. norvegicus*). *J. M. Research,* 1911–12, **25**, 205–215.
6. Bullock, F. D., and Curtis, M. R. Spontaneous tumors of the rat. *J. Cancer Research,* 1930, **14**, 1–115.
7. Ratcliffe, H. L. Spontaneous tumors in two colonies of rats of the Wistar Institute of Anatomy and Biology. *Am. J. Path.,* 1940, **16**, 237–254.
8. Gardner, W. U. Estrogenic effects of adrenal tumors of ovariectomized mice. *Cancer Research,* 1941, **1**, 632–637.
9. Woolley, G. W., and Little, C. C. The incidence of adrenal cortical carcinoma in gonadectomized female mice of the extreme dilution strain. II. Observations on the accessory sex organs. *Cancer Research,* 1945, **5**, 203–210.
10. Woolley, G. W., and Little, C. C. The incidence of adrenal cortical carcinoma in gonadectomized male mice of the extreme dilution strain. *Cancer Research,* 1945, **5**, 211–219.
11. Frantz, M. J., and Kirschbaum, A. Sex hormone secretion by tumors of the adrenal cortex of mice. *Cancer Research,* 1949, **9**, 257–266.
12. Dunning, W. F.; Curtis, M. R., and Segaloff, A. Strain differences in response to estrone and the induction of mammary gland, adrenal, and bladder cancer in rats. *Cancer Research,* 1953, **13**, 147–152.
13. Mulay, A. S., and Eyestone, W. H. Transplantable adrenocortical adenocarcinomas in Osborne-Mendel rats fed a carcinogenic diet. *J. Nat. Cancer Inst.,* 1955, **16**, 723–729.
14. Speirs, R. S. Assay of ACTH activity based on the eosinopenic response in normal and hypophysectomized mice. *Endocrinology,* 1953, **52**, 300–310.
15. Furth, J., and Sobel, H. Hypervolemia secondary to grafted granulosa-cell tumor. *J. Nat. Cancer Inst.,* 1946–47, **7**, 103–113.
16. Halmi, N. S. Two types of basophils in the anterior pituitary of the rat and their respective cytophysiological significance. *Endocrinology,* 1950, **47**, 289–299.
17. Harrison, J. H., and Desautels, R. E. The Adrenal Glands. In: Christopher's Textbook of Surgery, Davis, L. (ed.). W. B. Saunders Co., Philadelphia, 1956, ed. 6, pp. 775–797.
18. Woolley, G.; Fekete, E., and Little, C. C. Mammary tumor development in mice ovariectomized at birth. *Proc. Nat. Acad. Sc.,* 1939, **25**, 277–279.
19. Spiegel, A. Über das Auftreten von Geschwülsten der Nebennierenrinde mit vermännlichender Wirkung bei frühkastrierten Meerschweinchenmännchen. *Virchows Arch. f. path. Anat.,* 1939–40, **305**, 367–393.

20. Hueper, W. C., and Ichniowski, C. T. Carcinoma of the adrenal cortex in a rabbit. *Cancer Research,* 1944, 4, 176–178.

21. Cohen, A. I.; Bloch, E., and Celozzi, E. *In vitro* response of functional experimental adrenal tumors to corticotropin (ACTH). *Proc. Soc. Exper. Biol. & Med.* (In press.)

22. Bloch, E. Urinary steroids in adrenal tumor-bearing mice. In preparation.

23. Furth, J. Experimental Pituitary Tumors. In: Recent Progress in Hormone Research, Pincus, G. (ed.). Academic Press, Inc., New York, 1955, 11, 221–255.

24. Laqueur, G. L. The human hypophysis in diseases of the adrenal cortex. *Stanford M. Bull.,* 1951, 9, 75–87.

25. Halmi, N. S., and Barker, S. B. Histo-physiological effects of cortisone on rat pituitary and thyroid. *Endocrinology,* 1952, 51, 127–134.

26. Golden, A., and Bondy, P. K. Cytologic changes in rat adenohypophysis following administration of adrenocorticotrophin or cortisone. *Proc. Soc. Exper. Biol. & Med.,* 1952, 79, 252–255.

27. Antopol, W.; Glaubach, S., and Quittner, H. Experimental observations with massive doses of cortisone. *Rheumatism,* 1951, 7, 187–196.

LEGENDS FOR FIGURES

FIG. 1. Grafted adrenal tumor of a mouse, strain 2. × 400.

FIG. 2. Extensive pulmonary metastases of grafted adrenal tumor of a mouse, strain 2. × 150.

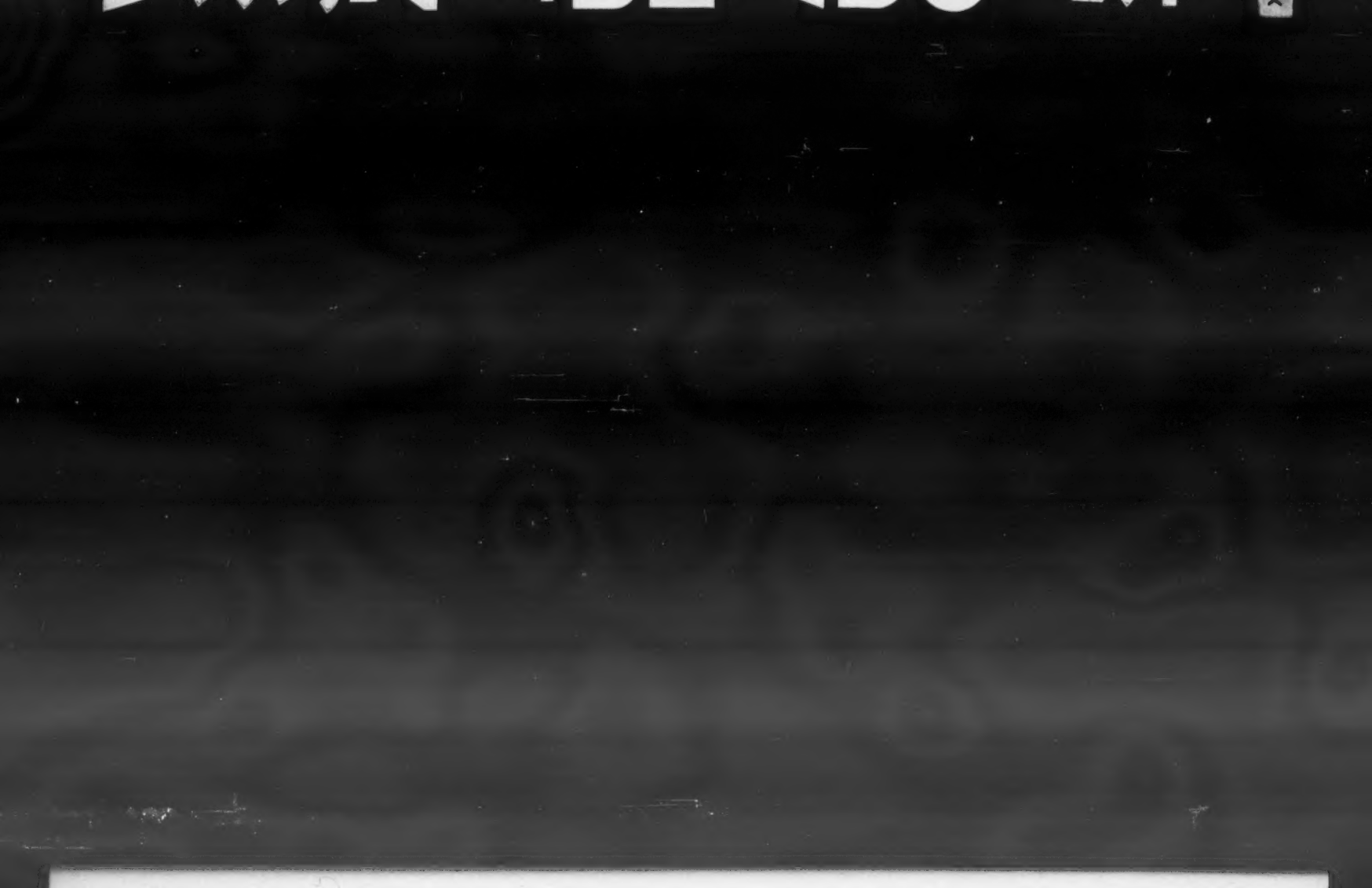

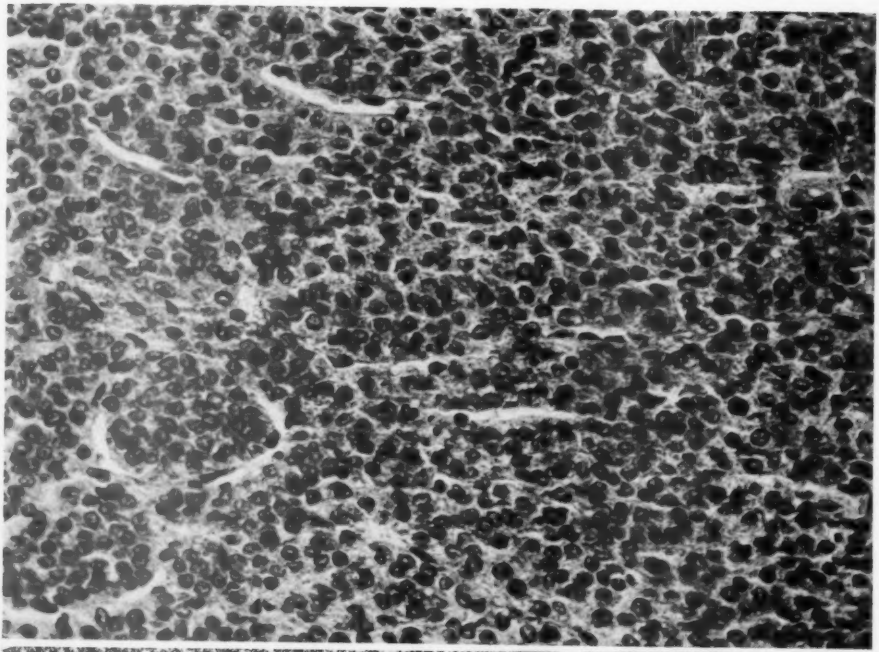

1

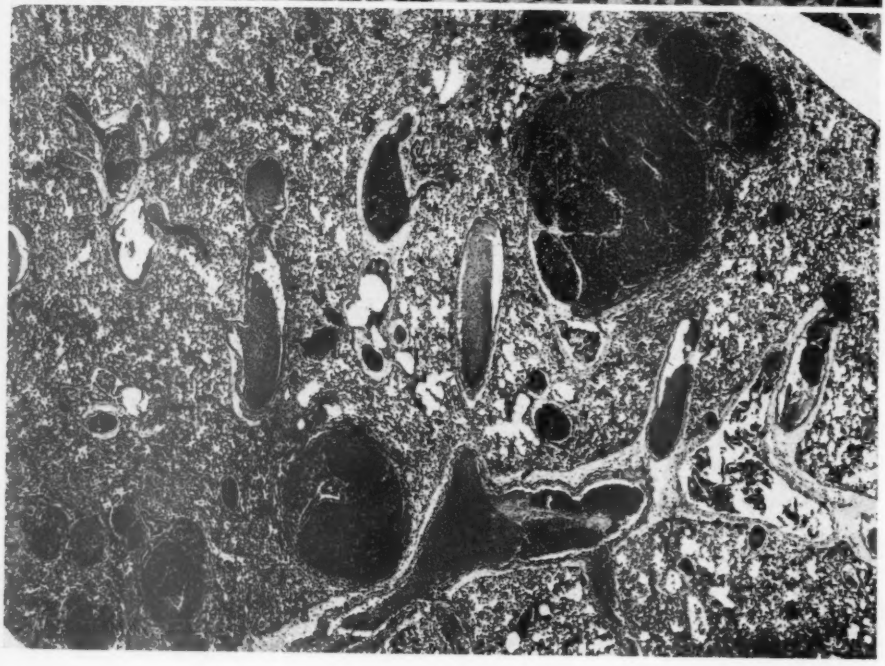

2

FIG. 3. Advanced atrophy of the adrenal cortex of a male mouse bearing transplanted adrenal tumor, strain 2. × 200.

FIG. 4. Advanced atrophy of the adrenal cortex with moderate congestion in a male mouse bearing a grafted adrenal tumor, strain 2. × 200.

FIG. 5. Adrenal cortex of a normal adult male mouse. × 200.

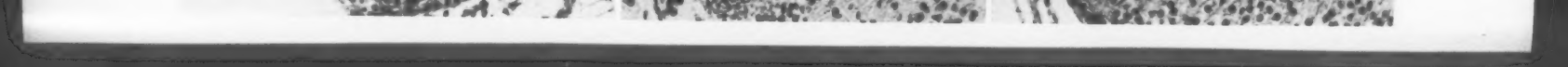

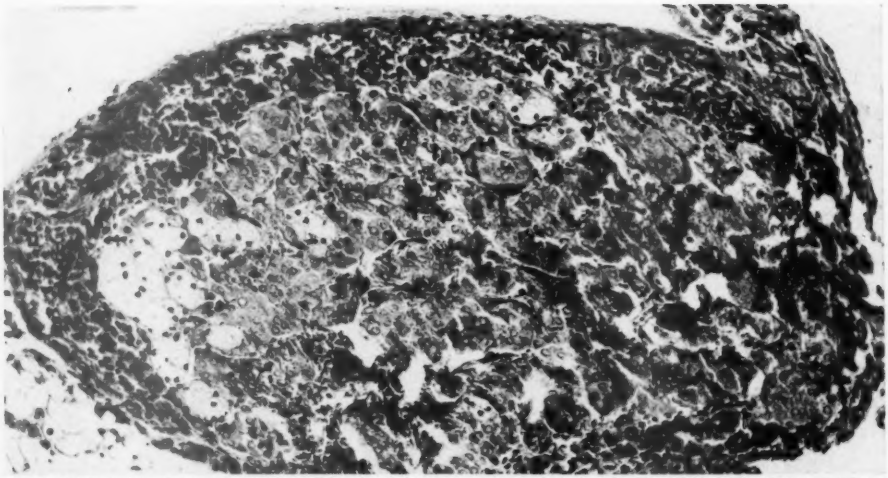

3

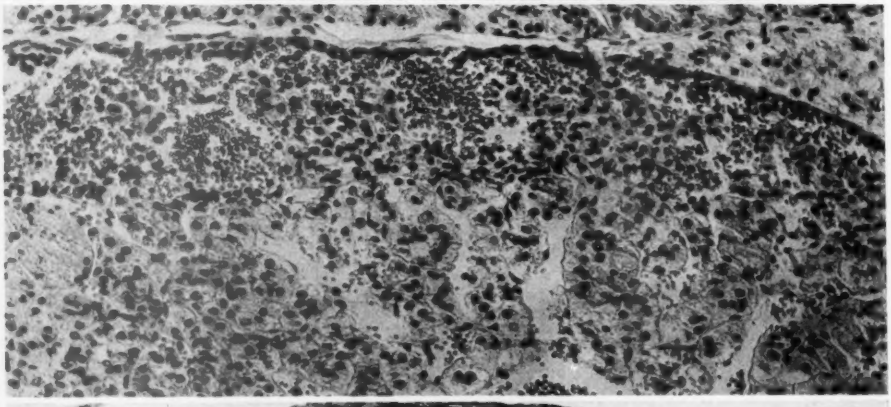

4

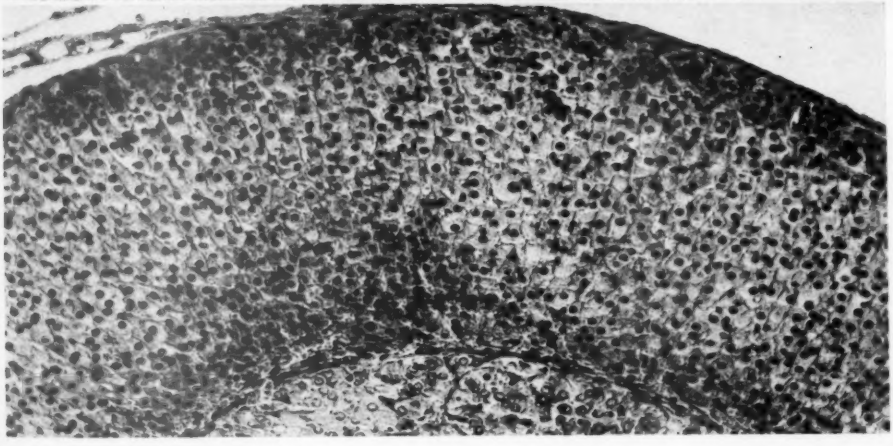

5

FIG. 6. Grafted adrenal tumor of rat, strain 1. × 400.

FIG. 7. Pulmonary metastases from grafts of adrenal tumor of rat, strain 1. × 100.

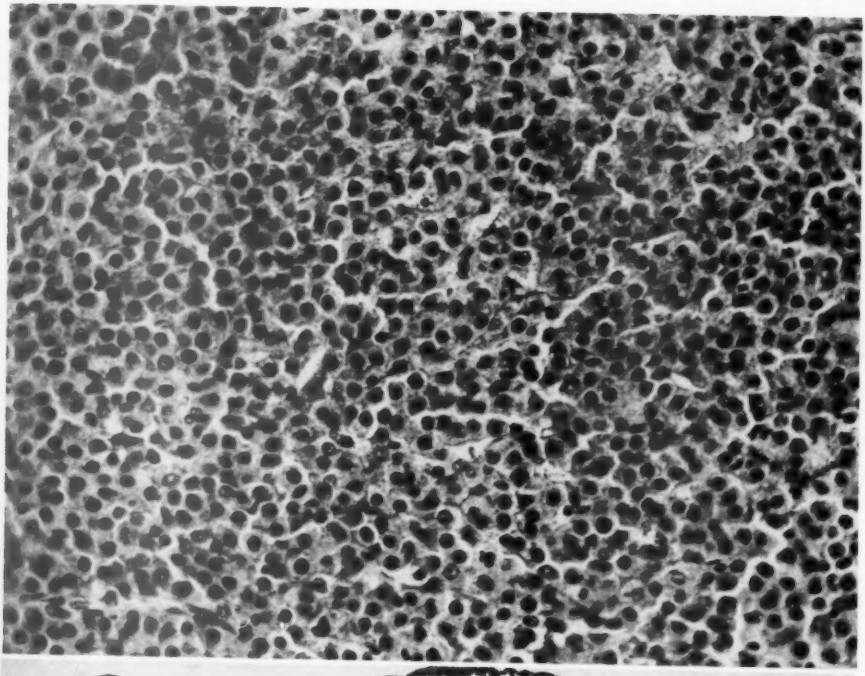

6

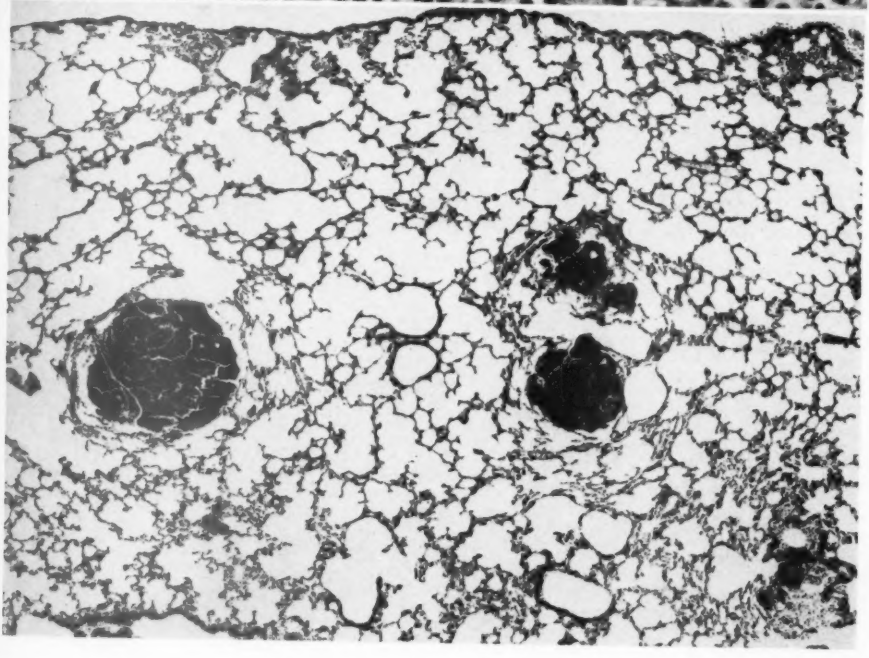

7

FIG. 8. Advanced atrophy of the adrenal cortex of a male rat bearing a grafted adrenal tumor, strain 1. × 150.

FIG. 9. Adrenal cortex of a normal male rat. × 150.

FIG. 10. Advanced atrophy of spermatogenic tubules with an area of calcification in a rat bearing a grafted adrenal tumor, strain 1. × 100.

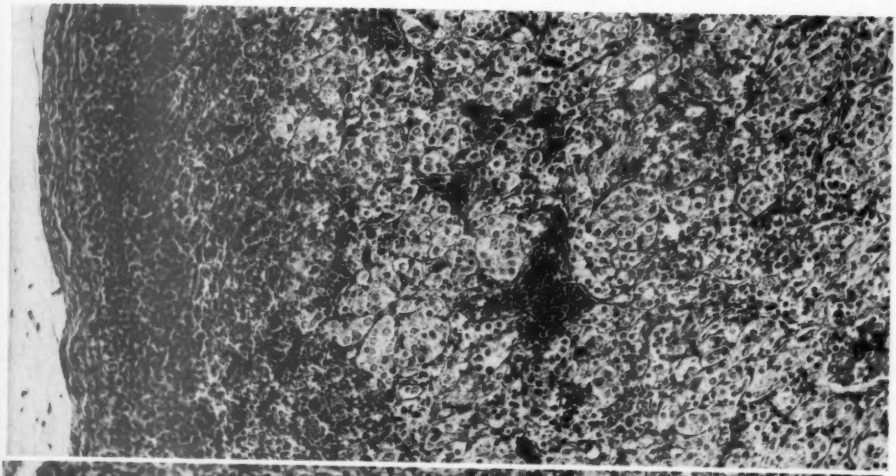

8

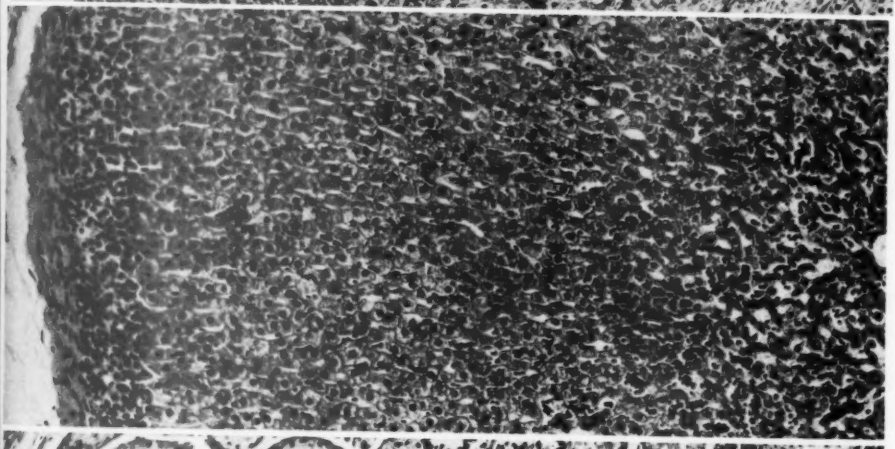

9

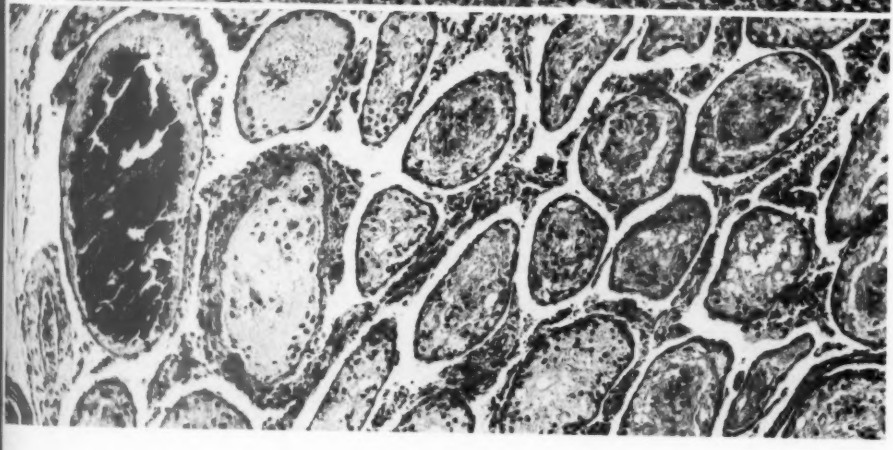

10

GENESIS OF TERATOMAS OF THE TESTIS

A Study of Normal and Zinc-injected Testes of Roosters*

Albert G. Smith, M.D., and Leon Powell, M.D.
From the Department of Pathology, Duke University School of Medicine, and Veterans Administration Hospital, Durham, N.C.

It has been postulated that teratomas of man and of the experimental rooster arise from within seminiferous tubules, probably from germ cells.[1,2] Before this theory of origin can be accepted, it is necessary to evaluate critically the possible origin of teratomas from groups of embryonal cells or "rests." The following study was initiated to determine whether there are cell rests which give rise to teratomas in the testes of roosters. We have examined histologically whole testes of many roosters by serial and skipped serial sections for cells which could be interpreted as embryonal rests. Since teratomas can be produced in 5 to 13 per cent of testes of roosters injected with zinc,[3] cell rests must be present in at least 5 per cent of the testes if they are the nidus from which teratomas develop. It is also necessary to show that cell masses which may be rests, if present, actually are associated with the development of teratomas. To show this relation, we injected zinc into testes of roosters and subsequently examined them.

Materials and Methods

The testes of 103 roosters were examined histologically. Roosters were from 8 weeks to 18 months of age and were New Hampshire reds except for a few white leghorns. Twenty-four roosters were injected intratesticularly with zinc. Seventy-nine were normal untreated roosters. The testes of 55 of the 79 were sectioned serially, and those of the remaining roosters were examined by skipped serial sections or multiple blocks. Since teratomas are produced ordinarily only when injections of zinc are performed in the first 3 months of the year, gonads from the untreated roosters were obtained at different times of the year. The testes were removed, weighed, fixed in Helly's fluid, dehydrated, embedded in paraffin, sectioned, and stained with hematoxylin and eosin. Weights varied from 0.1 to 25 gm. Most of the testes examined were the smaller gonads from the younger roosters.

In early March, the right testes of seven 10-week-old roosters were injected with 0.3 cc. of 10 per cent zinc sulfate, and the right testes of

* Supported in part by grants C-1636 and C-2499 from the National Institutes of Health, U.S. Public Health Service.
Received for publication, September 19, 1956.

nine roosters with 0.3 cc. of 5 per cent zinc chloride; two roosters remained as controls. All of the roosters died or were sacrificed at periods varying from 4 days to 6 months following injection. In a second series, initiated in February, both testes of eight 18-month-old New Hampshire red roosters were injected with 0.3 cc. of 5 per cent zinc chloride. Of these, two died 2 months after injection and were necropsied; the remainder were killed 6 months following injection.

Results and Observations

Histologic Appearance of Uninjected Testes

The histologic features of testes of roosters seldom have been described in the literature,[4] but they are very similar to those of man. The tubules contain germ cells, Sertoli cells, and, in the very young rooster, undifferentiated cells. In the actively proliferating testis of the mature rooster, the cells within the tubules are mostly germ cells with few Sertoli cells. Immediately underlying the basement membrane of the tubules is a flat layer of fibrocytes. The tubules so pack the testes that frequently the basement layer of one tubule is adjacent to the basement layer of another, leaving no interstitial tissue. In other areas, Leydig cells with clear, sometimes light pink cytoplasm and with Sudan-positive material are seen. Blood vessels, tubuli recti, epididymis, and a fibrous capsule are present as they are in man.

In serial or skipped serial sections, groups of cells of three basic types were found: large eosinophilic granulated cell, lymphocytic cell, and reticulum-like cell.

Groups of eosinophilic granulated cells were found in 15 of the 206 testes examined, an incidence of 7.3 per cent. They were not found in the testes of any rooster over 14 weeks of age. The cells were large, round, or elongated and they frequently formed small glands (Figs. 8 and 10). Eosinophilic granules were prominent within the cytoplasm. The nuclei were round or oval and generally had prominent nucleoli and chromatin networks, but there were some pyknotic forms. The cytoplasm, slightly red in the periodic acid-Schiff stain, had positive black granules in the Sudan black stains, and brilliant fuchsinophilic granules in Masson's trichrome stain. These cells were located in the interstitial areas, in the central portion of the testicular substance, around blood vessels, and beneath the capsule. Wherever a great mass of these large granulated cells occurred, marginal cells threaded out into surrounding interstitial areas and were associated with groups of lymphoid and reticulum-like cells. When these cells occurred in small numbers, it sometimes was quite difficult to distinguish them from juvenile eosinophils.

Accumulations of cells of the lymphocytic type occurred in every testis examined—206 in all. These accumulations occurred in every part of the testis: between the tubules, beneath the capsule, in the capsule, around ruptured or open testicular tubules (Fig. 2), around blood vessels, and subendothelially in blood vessels. Some reticulum or endothelial cells and young lymphocytes were seen, but most of the cells were small and round with large, round, dark nuclei and scanty cytoplasm (Fig. 1). Degenerated cells with particulate globules of chromatin for nuclei were present also.

Accumulations of the reticulum-like cell, which were similar to lymphoid germinal follicles, occurred in about two thirds of the testes. It sometimes was difficult to distinguish between groups of these cells and those of the lymphocytic type, since one group graded into the other. Groups of reticulum-like cells usually were quite circumscribed and were found at any site where cell groups of the lymphocytic type were present. Some of the most peculiar cell groups were subendothelial and perivascular. The predominant cell in the groups was the large reticulum-like cell with rounded or irregular cytoplasmic borders, prominent round or slightly oval nuclei, dense chromatinic network, and prominent nucleoli (Fig. 16). These reticulum-like cells, together with small cells, degenerated cells, and eosinophils, sometimes formed a mass encircled by fibroblasts (Figs. 3 to 7). It was thought originally that these cells might be rests of germ cells because of the large vesicular nuclei and prominent, clumped chromatin. However, examination of other lymphoid tissue of the rooster revealed lymphoid germinal follicles without a surrounding zone of small lymphocytes and with a fibrous capsule similar to some of the reticulum-like cell masses found in the testis. Of 103 roosters examined, only one with generalized lymphomatosis was encountered.

The presence and character of the three types of cell groups did not vary in relation to the season in which the testes were removed. However, the age of the rooster did have some relation to their presence or absence. None of the three types was found in a study of random sections of testes from 14 to 21 day embryos. The granulated cell groups appeared only in roosters 8 to 14 weeks old. The lymphoid and reticulum-like cell groups occurred in roosters from 8 weeks to 2 years of age.

Histologic Appearance of Zinc-Injected Testes

No teratomas were produced in the 16 roosters, 10 weeks of age, which were injected in March, an indication of the need for adult roosters for this experiment. A small teratoma of one testis was discovered 6 months following injection in one of the 8 roosters, 18

months of age, which were injected in February. This teratoma arose in a fibrous scar produced by zinc and was a rounded mass surrounded by a fibrous capsule (Fig. 15). Its central core consisted of fatty tissue, possible ectodermal cells with basophilic cytoplasmic inclusions (Fig. 15), and large glands lined by mucus-secreting columnar epithelium of intestinal type (Fig. 14). The mucin was Schiff and mucicarmine positive. In addition to the teratoma, we found histologic changes in the injected testes of roosters as previously described by Carleton, Friedman, and Bomze.[3] These changes were initial coagulation necrosis of the tubules with subsequent macrophagic reaction and fibrosis, and hematomas with giant cell reaction. In the fibrous areas, there were masses of cells similar to the reticulum-like cells found in uninjected testes and reminiscent of embryonal anlage (Figs. 11, 12, and 13). Numerous small and altered germinal tubules, some cords of germinal epithelium, and a few germinal cells also were isolated in the fibrous tissue (Fig. 9). Many of the injected testes were atrophic, weighing considerably less than the opposite uninjected testis. In some instances, the injected testis was not demonstrable 6 months after injection. It is interesting that in two instances of advanced atrophy, there was aspermatogenesis and marked proliferation of the interstitial cells. However, interstitial cell tumors have not been induced in roosters as they have been in other species.[5,6]

Discussion

Theories of Teratogenesis

To understand which cells possibly may give rise to teratomas, we must consider classical theories of teratogenesis. These theories include the fertilization of polar bodies (Marchand,[7] Ribbert[8]); splitting off and totipotent development of blastomeres (Bonnet[9]); cell rest theory (Cohnheim,[10] Meyer[11]); parthenogenesis (Waldeyer,[12] Langhans[13]); and an organizer theory (Spemann,[14] Krafka[15]). Cohnheim called these cell groups "embryonale anlage," not "rests," and stated that "the new-born infant brings with it into the world, not the tumour, but merely the superabundant cell material and from the latter, if circumstances be favorable, a tumour may grow later on." Cohnheim did not localize the precise stage at which these superabundant cells appear other than that they may appear at "an early stage of embryonic development." It is obvious that such embryonal anlagen must originate very early in the development of the embryo if all germ layers are to be represented in a teratoma, and that chorionic elements and fetal membranes should not be present unless the "superabundant cell ma-

terial" be germ cells of the embryo or blastomere cells. Willis[16] mentioned the possibility of organizers and displaced blastomeres contributing to the development of teratomas. According to Krafka, deranged organizers induce embryonic axes other than the prime axis in the embryonic plate, such extra axes becoming enveloped in branchial cleft, gonadal or other regions, as body growth progresses.

An alternate to the theory of origin of teratomas from unusual embryonal cell groups is that they arise from tubular germ cells. Michalowsky,[17–19] Falin,[20,21] Champy and Lavedan,[22,23] and Carleton, Friedman, and Bomze[3] agreed that the neoplastic process which initiates development of teratomas in the zinc-injected testes of the rooster begins in the tubules. Friedman[24] stated that in human testicular tumors the germ cells give rise to germinomas (seminomas), which in turn give rise to "embryonal" or primitive cell carcinoma of biphasic potency. The embryonal carcinoma then may be the site for teratogenesis or trophogenesis (chorio-epithelioma). Dixon and Moore[2] explained teratogenesis on a similar basis, except that seminomas "although of germinal origin, . . . are not intimately related to other types of germinal tumors." The finding of early intratubular epithelial proliferations in the zinc-injected testes of the rooster, followed by extratubular proliferations resembling human embryonal carcinoma, and finally by teratogenesis,[3] support this germ cell theory of origin of teratomas. The concept of development of teratomas from germ cells is related to the old idea of parthenogenesis, requiring for teratomas produced in roosters by zinc or copper an initiating stimulus (artificial parthenogenesis) similar to the mechanical pricking of the ovum that induces parthenogenesis in the frog.[25,26] Seminomas have been produced in birds simply by regeneration following partial amputation[22,23] or transplantation.[27]

Interpretation of Our Findings

When adapted to the problem of experimental teratogenesis in roosters, it is obvious that all of the above theories except the one of parthenogenesis require some cells to be present in the testes other than strict anatomical components. These extra cells would, therefore, be displaced polar bodies, blastomeres, cell rests, or cells that result from displaced organizers acting upon embryonic cells. Our studies were aimed at the discovery of such groups. Since these cell groups must be present from embryonal life, testes of young roosters not subjected to zinc or any other injections or trauma were examined. In our studies, we found granulated, lymphoid, and reticulum-like cell groups.

The identity of the large eosinophilic granulated cells is not certain. Such cells are probably the "pancreatic acini" which were "so regularly intermingled with testicular tubules that the possibility of a 'rest' could not be eliminated," described by Carleton, Friedman, and Bomze[3] in a zinc-injected testis of a rooster. These cells probably are not germ cells because their granules indicate much greater differentiation. They occurred in 7.5 per cent of the testes of 103 roosters, and since teratomas can be produced by zinc injection in 5 per cent[17] to 13 per cent[3] of testes, the percentage occurrence of these masses is within the range of percentage occurrence of teratomas. Despite this correlation, it is difficult for us to believe that these cells form a nidus which is affected by zinc to produce teratomas. We think the most likely explanation is that they are Leydig cells or Leydig cell precursors or derivatives. Both these cells and Leydig cells may have fuchsinophilic granules, both contain formalin-fixed lipid as demonstrated by the Sudan black stain, both may be eosinophilic, and both occur in the interstitial areas; but the usual interstitial cells of the testes of embryos as well as of adult roosters are light pink or colorless, have few prominent granules, and have more fat than the more eosinophilic cells. Why these granulated cells should appear in the 8-week-old rooster is unknown, but they may be a developmental stage in the life of Leydig cells. Some of the granulated cell groups interdigitated with disrupted seminiferous tubules and germ cells in such fashion as to raise the question of their relation to germ cells (Fig. 10). Since the granulated cell groups and the two other cell types discussed below may occur in juxtaposition to one another, we wonder if all three groups may have a common origin. At any rate, it would seem that cells so differentiated as to have striking fuchsinophilic granules probably do not possess totipotential powers.

The cell groups of lymphocytic type which were found in the testes may be, in many instances, inflammatory lymphocytic infiltrates, since they occur around ruptured tubules and are mixed with eosinophils and degenerating white blood cells. Spermatic nucleoproteins are said to induce a granulomatous and lymphocytic response; therefore, this lymphoid reaction near ruptured tubules is not surprising.[28] However, most of the accumulations occurred in areas where there were no ruptured tubules, and particularly near blood vessels.

The reticulum-like cell groups are not characteristic of mammalian testes, nor are they found in the testes of chicken embryos. Indentation of the lumen of blood vessels by subendothelial reticulum-like cells suggests that such cells may arise from the endothelium, or, that they are related to germ cells that travel by blood vessels[29] or omphalo-

mesenteric mesenchyme[30] from the yolk sac to the urogenital ridge. Since primitive germ cells do not have certain cytologically characteristic features of more mature germ cells, it is difficult to identify them and to demonstrate their relation to reticulum-like cells. The latter are found in the scars of the testes of roosters produced by zinc, and their appearance resembles embryonal anlage. These masses of cells in the zinc-produced scars may be proliferations of germ cells in segments of tubules enmeshed in the fibrous tissue, but which can no longer be recognized as tubules. The similarity of these cell masses in zinc scars to reticulum-like cell groups in the uninjected testes of the young rooster is striking, and it is possible that both represent groups of multipotent cells or "rests" (Figs. 5, 12, and 13). If these "rests" developed from superabundant cell proliferation within the gonad late in the development of the embryo, it is possible that they may represent germ cell proliferations of unusual form occurring in embryonal life. If this were the case, it would still be a correct generalization to say that the teratomas develop from germ cells. Thus, the reticulum-like cells may represent the embryonal anlage or overabundant cell masses described by Cohnheim,[10] which may in particular originate from embryonal germ cells. On the other hand, the number of peculiar cell groups in the zinc scars is greater than in equal areas of uninjected testes, indicating that the cell groups may arise from cell proliferations of injured tubules. Thus, some observations support the theory that zinc-induced teratomas originate from proliferating tubular germ cells which have been altered by zinc and entrapped in scar tissue, and others indicate that there are cell rests in uninjected testes of roosters which could be affected by zinc, giving rise to teratomas. Some of the reticulum-like cells clearly resemble lymphoid tissue found in other organs of the rooster, and they almost surely are not always inflammatory reactions. They may be simply lymphoid tissue, but still they may be capable of germinating teratomas in response to some stimuli. Reticulum-like cells in the uninjected testes, in zinc scars, and in lymphoid tissue may have certain histologic resemblances and may be identical cells possessing different powers of growth in different environments. On the other hand, this histologic resemblance may obscure true differences in metabolism, function, and growth. Thus, cells which appear to be lymphoid cells may be germ cells with growth potential, and only additional basic knowledge of minute functions of cells will enable us to determine their true nature.

In the teratomas which we produced, there were no adjacent glandular or sheet proliferations of cells resembling human embryonal carci-

noma. This fact would lead us to believe that testicular teratomas may arise in some instances without the associated epithelial proliferation of embryonal carcinoma. Perhaps the stage of embryonal carcinoma that precedes the development of teratomas as postulated by Friedman *et al.*[1,3,31] should not be regarded as true carcinoma, but as masses of embryonic cells developing from stimulated germ cells. The embryonic cell masses may be represented by the reticulum-like cell groups in zinc scars (Fig. 12), and may become the mature tissue elements of the teratoma. In contrast to metastasizing embryonal carcinoma, the pre-teratoma anlage stage (reticulum-like cell groups) should be regarded as a local non-metastasizing phenomenon under the influence of organizers. Little or no embryonal carcinoma remains around the developed teratomas after 4 or more months following injection, and neither the embryonal carcinoma-like tissue nor the teratomas in roosters metastasize. If it is theorized that these pre-teratoma cell masses are embryonal carcinoma, it must follow that the masses of cells representing embryonal carcinoma completely and relatively simultaneously reach a stage where teratomatous differentiation takes place—a rather peculiar behavior for carcinoma. No fetal membranes were seen in the teratomas we produced, nor were they found in the 11 tumors produced by Carleton, Friedman, and Bomze.[3] This may be due to difficulties in recognizing simple membranes, since the chick does not form a placenta or chorionic villi. If the teratoma arose from embryonal anlage as described by Cohnheim,[10] membranes would not be expected as the original cells are embryonal and capable only of genesis of portions of embryos.

Conclusions gained from the study of gonadal tumors of man or rooster are not entirely applicable to each other because of the peculiarity in roosters of induction of teratomas by zinc, and the failure of these teratomas or associated proliferating tissue to metastasize. Nevertheless, we must consider teratomas in mammals in order to gain a greater knowledge of the over-all problem of teratogenesis. "Rests" have not been observed in the human testis. The theory of origin of testicular teratomas from intratubular germ cells would explain the genesis of human testicular and ovarian teratomas, but does not explain extragenital teratomas.[32,33] The comparison of the histology of pinealomas, thymomas, pineal and thymic teratomas to gonadal tumors prompted Friedman[24] to point out their similarities and therefore the possible germ cell origin of all of these tumors. If germ cells reach the testes by migration from the yolk sac, it is not too difficult to imagine

that this migration might be misdirected, lodging cells at other sites, which later become teratomas or the tumors that resemble gonadal tumors, although Krafka[15] did not think this likely. It would probably be impossible to prove that such is the case, since single germ cells resemble other cells in some stages of their development, and it would be nearly impossible to distinguish such variants of germ cells from cells of the thymus, pineal, or other extragenital organs. In extragenital teratomas arising in a metastasis of embryonal carcinoma of the human testis, the teratoma probably arises from embryonal carcinoma cells, derivatives of germ cells. This supports the theory of origin of human embryonal carcinoma and teratomas of the testes from intratubular germ cells, but it should again be emphasized that these conclusions do not necessarily apply to avian tumors. The similarity of tumors of lymphoid organs to gonadal tumors, and the finding of teratomas in lymphoid organs call to mind other relations of gonadal tumors to the lymphoid system, as the lymphocytosis in seminomas, lymphoid tumors in young males,[34] and the lymphoid cells of reticulum cell groups that we found in the testes of roosters. Is this relation a purely inflammatory or chance relation, or are cells that we recognize as lymphoid or reticulum-like sometimes members of a motley group, histologically similar, but biochemically and in growth potential, very different?

Summary

A histologic survey was made of 206 testes of roosters by serial and skipped serial sections in a search for cell groups that might be multipotential cells or the abnormal embryonal anlagen described by Cohnheim.[10] Unusual cell groups were seen in the interstitial area of normal testes and these were labeled reticulum-like cell, eosinophilic granulated cell, and lymphocytic cell groups.

The groups of reticulum-like cells occurred in the uninjected testes and may be rests of germ cell origin, arising by abnormal proliferations before or shortly after hatching. These groups also occurred in scars produced by zinc in testes, where they may have been present before injection or may have been new intratubular proliferations of germ cells. In zinc scars, they are the probable antecedents of teratomas, and they probably develop into teratomas by organized processes rather than carcinomatous transformation. However, we cannot completely exclude the possibility that the reticulum-like cell groups are lymphoid tissue.

The groups of large eosinophilic granulated cells are possibly related to Leydig cells.

The groups of lymphocytic cells may be inflammatory, may represent normal lymphoid tissue in the testes, or may be related to the reticulum-like cell groups or teratomas.

REFERENCES

1. Friedman, N. B., and Moore, R. A. Tumors of the testis. A report on 922 cases. *Mil. Surgeon*, 1946, **99**, 573–593.
2. Dixon, F. J., and Moore, R. A. Tumors of the Male Sex Organs. Atlas of Tumor Pathology, Section VIII, Fascicles 31B and 32, p. 50, Subcommittee on Oncology of the Committee on Pathology of the National Research Council, Armed Forces Institute of Pathology, Washington, D.C., 1952.
3. Carleton, R. L.; Friedman, N. B., and Bomze, E. J. Experimental teratomas of the testis. *Cancer*, 1953, **6**, 464–473.
4. Kumaran, J. D. S., and Turner, C. W. The normal development of the testes in the White Plymouth Rock. *Poultry Sc.*, 1949, **28**, 511–520.
5. Peyron, A., and Samsonoff, N. Sur la production expérimentale des tumeurs de la glande interstitielle du testicule chez le rat. *Compt. rend. Soc. de biol.*, 1941, **135**, 922–925.
6. Hooker, C. W.; Gardner, W. U., and Pfeiffer, C. A. Testicular tumors in mice receiving estrogens. *J. A. M. A.*, 1940, **115**, 443–445.
7. Marchand, F. Zur Kenntniss der Embolie und Thrombose der Gehirnarterien, zugleich ein Beitrag zur Casuistik der primären Herztumoren und der gekreuzten Emboli. *Berl. klin. Wchnschr.*, 1894, 31, 36–38. (Cited by Krafka.[15])
8. Ribbert, H. Beiträge zur Kenntniss der Rhabdomyome. *Virchows Arch. f. path. Anat.*, 1892, **130**, 249–278. (Cited by Krafka.[15])
9. Bonnet, R. Giebt es bei Wirbeltieren Parthenogenesis? *Ergebn. d. Anat. u. Entwcklngsgesch.*, 1899, **9**, 820–870. (Cited by Krafka.[15])
10. Cohnheim, J. Lectures on General Pathology. A Handbook for Practitioners and Students. (Translated from the second German edition by Alexander B. McKee.) The New Sydenham Society, London, 1889, 821 pp.
11. Meyer, R. Über embryonale Gewebseinschlüsse in den weiblichen Genitalien und ihre Bedeutung für die Pathologie diesen Organe. *Ergebn. d. allg. Path. u. path. Anat.*, 1905, **9**, 685.
12. Waldeyer, W. Die Entwickelung der Carcinome. *Virchows Arch. f. path. Anat.*, 1872, **55**, 67–158. (Cited by Krafka.[15])
13. Langhans, T. Kystoma et Adenoma testis. *Deutsche Chir.* (Abt. B), 1887, **50**, 414. (Cited by Krafka.[15])
14. Spemann, H. Ueber die Determination der ersten Organanlagen des Amphibienembryo. *Arch. f. Entwcklngsmechn. d. Organ.*, 1918, **43**, 448–555. (Cited by Krafka.[15])
15. Krafka, J., Jr. Teratoma, an explanation of its cause based on the organizer theory of embryology. *Arch. Path.*, 1936, **21**, 756–764.
16. Willis, R. A. Teratomas. Atlas of Tumor Pathology, Section III, Fascicle 9, Subcommittee on Oncology of the Committee on Pathology of the National Research Council, Armed Forces Institute of Pathology, Washington, D.C., 1951, pp. 12–13.

17. Michalowsky, I. Die experimentelle Erzeugung einer teratoiden Neubildung der Hoden beim Hahn. Vorläufige Mitteilung. *Centralbl. f. allg. Path. u. path. Anat.*, 1926, **38**, 585–587.

18. Michalowsky, I. Eine experimentelle Erzeugung teratoider Geschwülste der Hoden beim Hahn. *Virchows Arch. f. path. Anat.*, 1928, **267**, 27–62.

19. Michalowsky, I. Das 10. experimentelle Zink-Teratom. *Virchows Arch. f. path. Anat.*, 1929–30, **274**, 319–325.

20. Falin, L. I. Experimental teratoma testis in the fowl. *Am. J. Cancer*, 1940, **38**, 199–211.

21. Falin, L. I., and Anissimowa, W. W. Zur Pathogenese der experimentellen teratoiden Geschwülste der Geschlechtsdrüsen. Teratoide Hodengeschwulst beim Hahn, erzeugt durch Einführung von $CuSo_4$-Lösung. *Ztschr. f. Krebsforsch.*, 1940, **50**, 339–351.

22. Champy, C., and Lavedan, J. P. Seminomes par régénérations testiculaires chez les oiseaux. *Bull. Assoc. franç. p. l'etude du cancer*, 1939, **28**, 503–526.

23. Champy, C., and Lavedan, J. Séminomes par régéneration chez les oiseaux. *Compt. rend. Soc. de biol.*, 1938, **127**, 1197–1199.

24. Friedman, N. B. The comparative morphogenesis of extragenital and gonadal teratoid tumors. *Cancer*, 1951, **4**, 265–276.

25. Arey, L. B. Developmental Anatomy. A Textbook and Laboratory Manual of Embryology. W. B. Saunders Co., Philadelphia, 1946, ed. 5, 616 pp.

26. Pincus, G. Comparative behavior of mammalian eggs in vivo and in vitro; development of fertilized and artificially activated rabbit eggs. *J. Exper. Zool.*, 1939, **82**, 85–129.

27. Biskind, M. S., and Biskind, G. R. Tumor of rat testis produced by heterotransplantation of infantile testis to spleen of adult castrate. *Proc. Soc. Exper. Biol. & Med.*, 1945, **59**, 4–8.

28. Russell, M., and Friedman, N. B. Studies in general biology of sperm: experimental production of spermatic granuloma. *J. Urol.*, 1951, **65**, 650–654.

29. Patten, B. M. The Early Embryology of the Chick. P. Blakiston's Son & Co., Philadelphia, 1929, ed. 3, 228 pp.

30. Witschi, E. Migration of the germ cells of human embryos from the yolk sac to the primitive gonadal folds. *Contrib. Embryol.*, 1948, **32**, 67–80.

31. Friedman, N. B. Germinoma of the pineal; its identity with germinoma ("seminoma") of the testis. *Cancer Research*, 1947, **7**, 363–368.

32. Schlumberger, H. G. Teratoma of the anterior mediastinum in the group of military age; a study of sixteen cases, and a review of theories of genesis. *Arch. Path.*, 1946, **41**, 398–444.

33. Laipply, T. C. Cysts and cystic tumors of the mediastinum. *Arch. Path.*, 1945, **39**, 153–161.

34. Kretschmer, H. L. Embryoma of the testicle in a five-year-old child. *Am. J. Surg.*, 1948, **76**, 99–101.

[*Illustrations follow*]

LEGENDS FOR FIGURES

FIG. 1. Uninjected testis of a 2½-month-old rooster. A cell group of lymphocytic type with small lymphocytes and some larger mononuclear cells in the interstitial area. × 236.

FIG. 2. Uninjected testis. A cell group of lymphocytic type around and in a ruptured tubule. × 630.

FIG. 3. Uninjected testis of an 18-month-old rooster. Three cell groups of reticulum-like type are present in the adventitia of the epididymis at upper left; a seminiferous tubule is just visible at lower right. × 113.

FIG. 4. Uninjected testis of a 2½-month-old rooster. High-power view of Figure 5, showing mixture of large reticulum-like cells and smaller round cells. × 630.

FIG. 5. Cell groups of reticulum-like type are present just beneath the capsule with a cell group of diffuse lymphocyte type on the left. × 214.

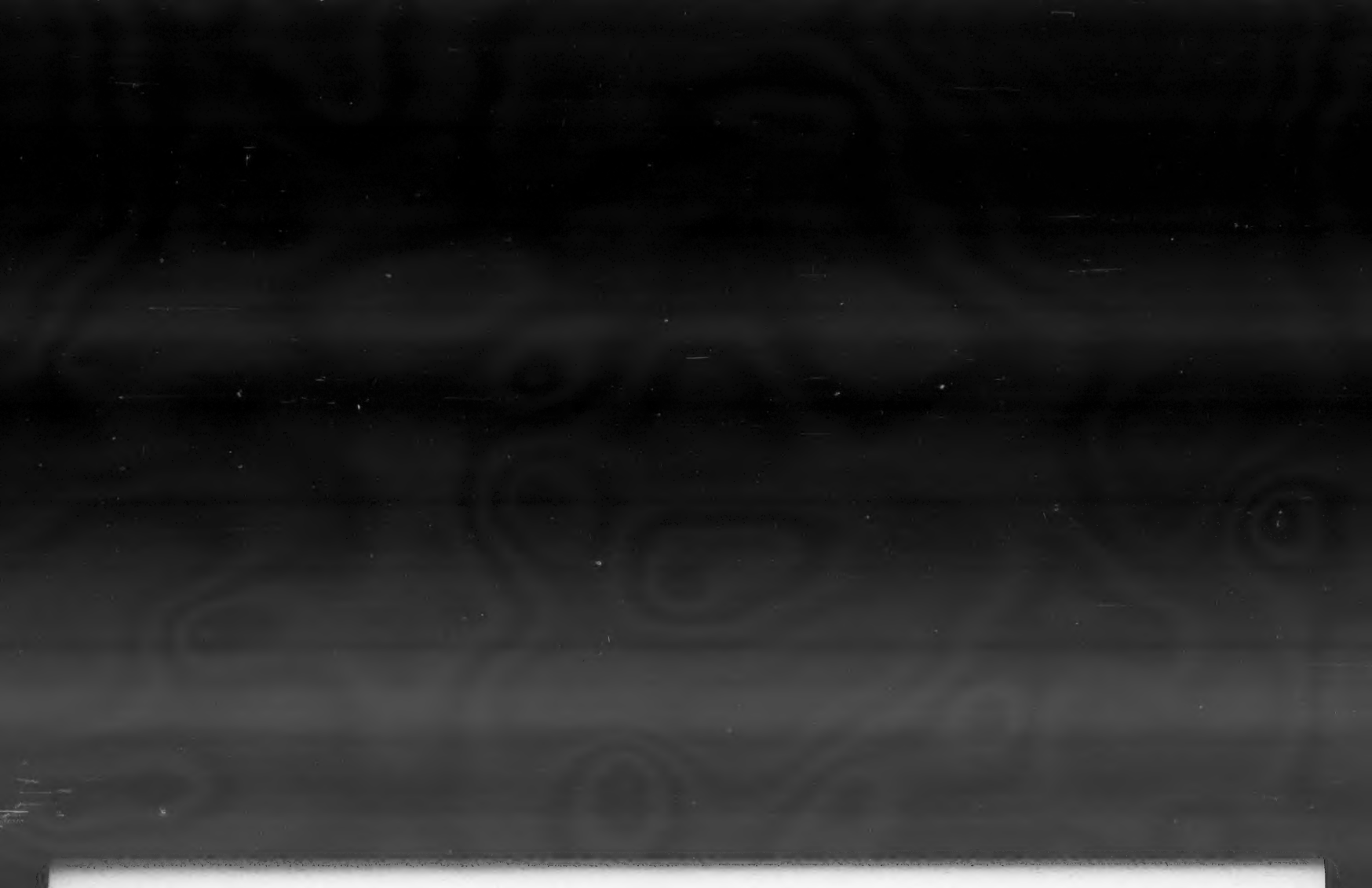

1

3

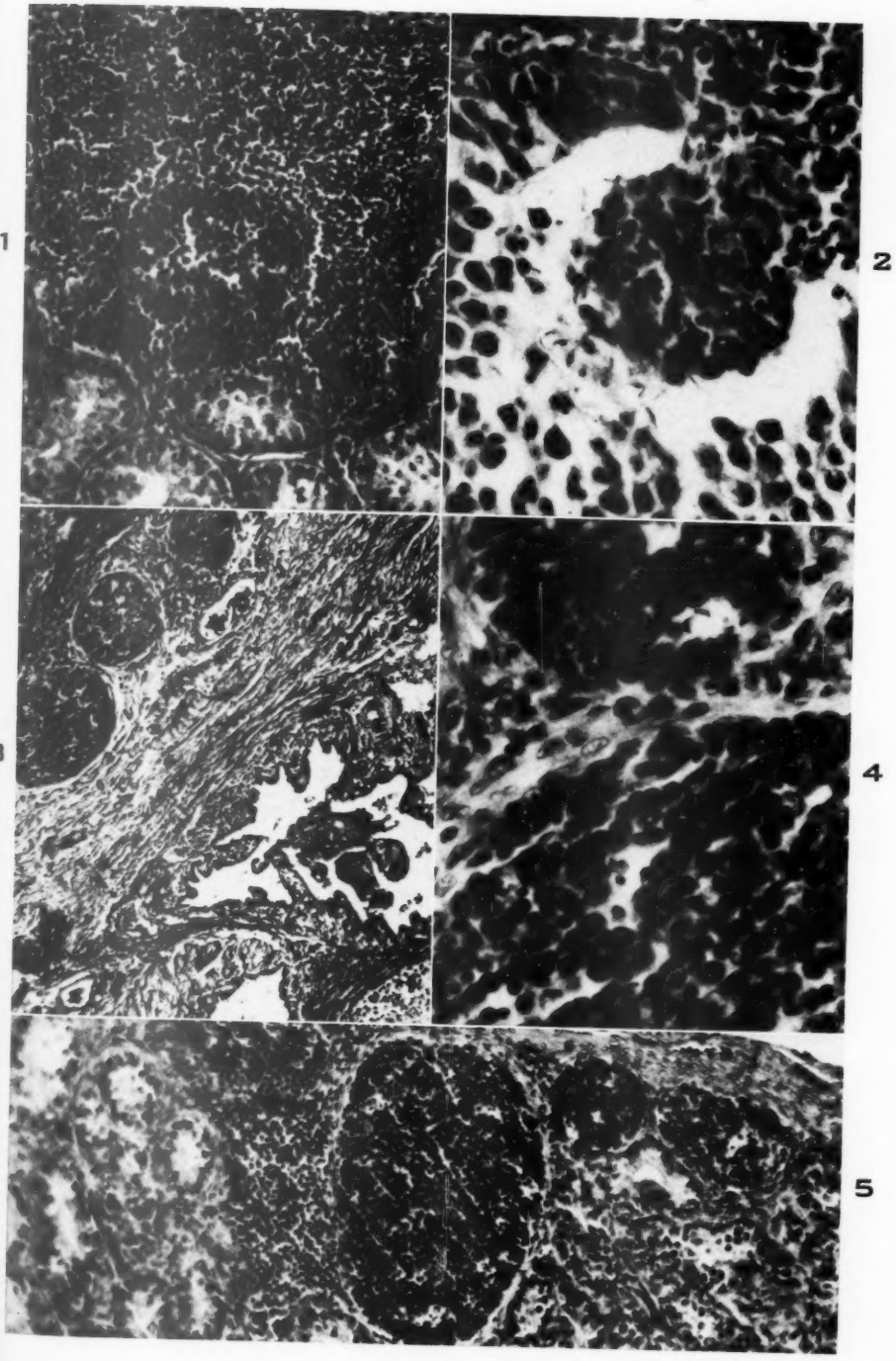
1
2
3
4
5

FIG. 6. Uninjected testis. Section of blood vessel with lumen on right and blood cells at upper right. A large subendothelial mass of reticulum-like cells may be noted on the left. × 630.

FIG. 7. Uninjected testis. Another mass of large mononuclear reticulum-like cells around a blood vessel in the capsule at top. A portion of a seminiferous tubule is at the bottom. × 630.

FIG. 8. Uninjected testis. Cell groups of eosinophilic granulated type are represented by the large dark cells in gland-like groups and single cells at lower left and lower right. Seminiferous tubules are present in the upper and central portions of the field, and some are markedly distorted. × 200.

FIG. 9. Zinc-injected testis. Portions of seminiferous tubules are at lower and upper left, and a tubule which is probably distorted is present in the scar at low center. Other cells with large prominent nuclei are scattered through the scar in the right, central, and left portions of the field. × 200.

FIG. 10. High-power view of Figure 8. Of note are the acinus of granulated cells at lower left and single cords of cells to the right of the acinus. Single large granulated cells interdigitate with germ cells in the disrupted seminiferous tubules, two large granulated cells being noted particularly at the very center of the field. × 630.

6

8

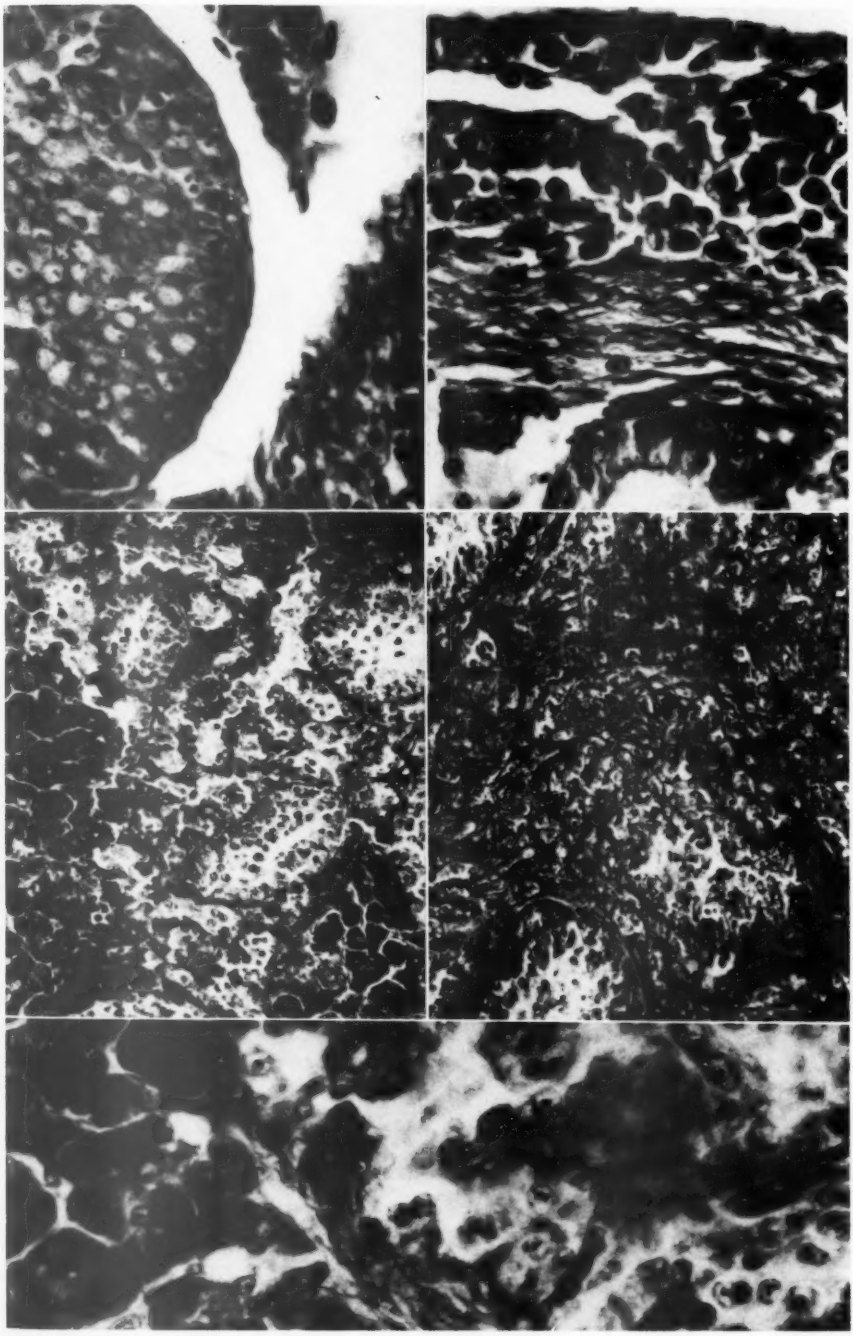
6
7
8
9
10

FIG. 11. Zinc-injected testis. A zinc produced scar is on the left. Partially atrophied seminiferous tubules may be noted on the right with loose scattering of intratubular germ cells. On the margin of the larger tubules at upper right is a small, greatly altered, dark tubule with a dense collection of intratubular cells. × 236.

FIG. 12. Zinc-injected testis. A zinc produced scar occupies almost the entire field except for portions of tubules at upper right and lower left. Anlage-like masses of cells are present in the scar at lower central left, central right, and lower right. × 200.

FIG. 13. Zinc-injected testis. A small portion of a hematoma is seen at upper left, and a segment of a seminiferous tubule at lower left. The remainder of the field is a zinc produced scar with a heavy infiltrate of lymphocytes and a cell group of reticulum-like type seen in lower center. Similarity may be noted to groups in Figures 5 and 12. × 250.

FIG. 14. Zinc-injected testis. A view of the teratoma produced with epithelium of intestinal type lining large cysts. × 80.

FIG. 15. Zinc-injected testis. Another section of the teratoma showing how it arises in the zinc produced scar at the center. Fatty tissue and probable ectodermal elements are present. × 33.

FIG. 16. Uninjected testis. High-power view of a reticulum-like cell group as seen in Figure 5, to show nuclear and cytologic detail of the large reticulum-like cells. × 1,300.

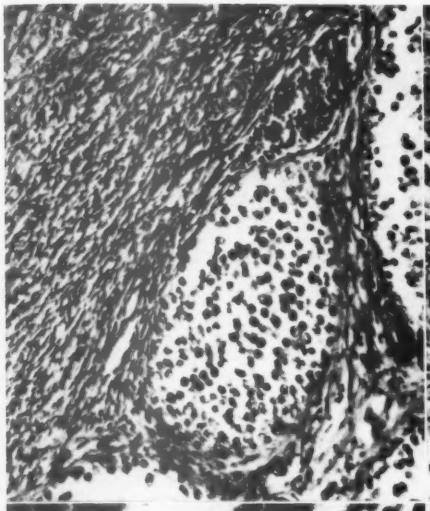

11

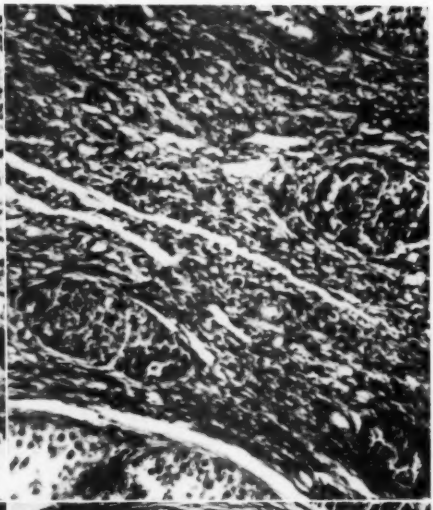

12

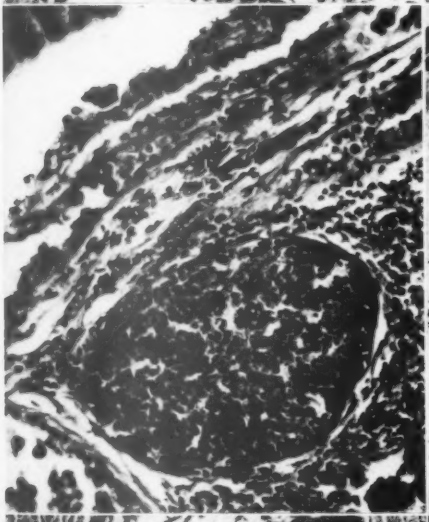

13

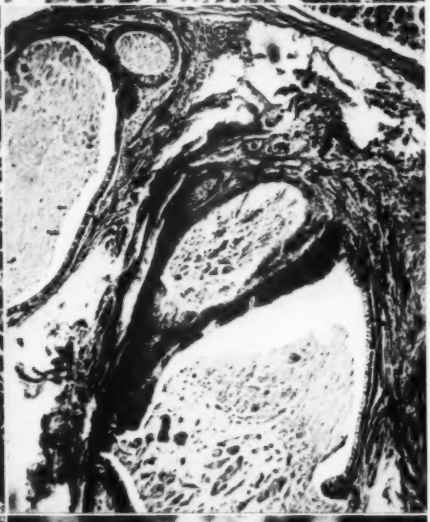

14

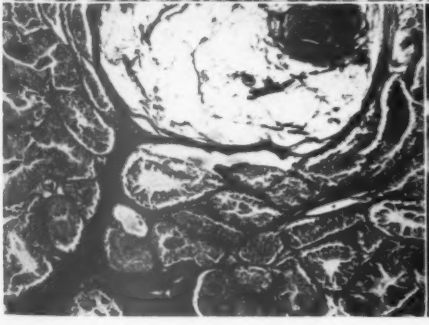

15

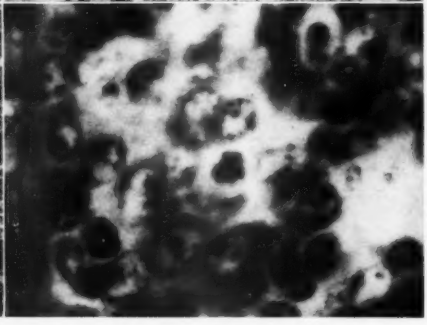

16

EARLY HISTOLOGIC CHANGES IN INDUCED TUMORS OF THE SUBMAXILLARY SALIVARY GLANDS OF THE RAT*

SAMUEL M. STANDISH, D.D.S.
From the Department of Oral Pathology, Indiana University School of Dentistry, Indianapolis, Ind.

Sporadic attempts to induce tumors of salivary glands in animals have been made since 1910 when Löwenstein[1] produced epithelial proliferation of the parotid ducts of rabbits by injecting scharlach R. Subsequent investigators prior to 1939 utilized such agents as tar, scharlach R, arsenicals, and balsam of Peru with indifferent success. Macchiarulo and Büngeler,[2] in 1929, reported squamous epithelial cysts arising from the ductal epithelium of the parotid glands of rats following the repeated injection of tar. Tadaki,[3] in 1932, induced adenocarcinomas of ductal origin in the submaxillary glands of rabbits by injecting tar. Berberich,[4] also in 1932, presumably induced malignant parotid tumors in experimental animals, although details of the study were not given. Abb,[5] in 1932, employed several different agents to produce cysts with squamous metaplasia of the ductal epithelium in the parotid glands of rabbits and rats.

Investigators[6-11] subsequent to 1932 utilized refined aromatic hydrocarbons to induce malignant tumors consistently, principally epidermoid carcinomas and fibrosarcomas, in the salivary glands. However, with few exceptions, little attention was given to the study of the histogenesis of these tumors. Steiner,[10] in 1942, used methylcholanthrene, 1,2,5,6-dibenzanthracene, and 3,4-benzpyrene in mice, rats, guinea pigs, and rabbits in an attempt to produce tumors of the submaxillary gland. All of the animals except rabbits responded with tumor induction, usually squamous cell carcinoma. In an incidental study using 21 mice sacrificed at weekly intervals from 1 to 13 weeks, Steiner stated that the epithelial metaplasia originated from both acinar and ductal epithelium.

Bauer and Byrne,[11] in 1950, conducted experiments similar to those of Steiner[10] and were able to induce papillary cystadenomas, papillary cystadenocarcinomas, and undifferentiated carcinomas of myo-epithelial origin. Like Steiner, they failed to produce tumors in the salivary gland of the rabbit. These workers used 1,2,5,6-dibenzanthracene, methylcholanthrene, 1,2-benzanthracene, and 9,10-dimethyl-1,2,-ben-

* This study was supported by research grant C-2622 from the National Cancer Institute of the National Institutes of Health, U.S. Public Health Service. Preliminary investigations were supported by funds from the Indiana Cancer Society.

Presented, in part, at the Thirty-fourth General Meeting of the International Association for Dental Research, St. Louis, March 22, 1956.

Received for publication, September 21, 1956.

zanthracene in the parotid glands of rabbits, mice, and rats. They concluded that the pluripotential epithelial cells which line the intercalated ducts[12] undergo the initial metaplasia in tumor formation and that the acinar cells apparently do not participate in the process.

Gross,[13] in 1953, reported carcinoma of the salivary gland in mice given leukemic extracts. Details of the histopathology of these tumors were not given other than that they appeared to arise in the parotid glands and were probably of myo-epithelial origin.

Stewart,[14] in 1955, produced adrenal tumors and "multinodular pleomorphic tumors of the parotid gland" in mice inoculated with cell-free extracts of filtrates of leukemic mouse tissues. Gross[15] and Law, Dunn, and Boyle[16] pursued this line of investigation also and discussed the parotid tumors induced.

Critical analysis of the existing literature concerning experimental induction of tumors in the salivary glands indicates that the various investigators, for the most part, have been concerned primarily with tumor production, per se. While there are notable exceptions, earlier experiments were based largely upon an evolvement of histogenesis from a study of the fully developed induced tumor. It was believed that this problem might better be resolved by investigation of parenchymal changes that occur during carcinogenesis, not after it has already occurred.

Marked histologic differences exist between the submaxillary salivary glands of weanling and adult rats. That this factor (namely, the absence of the so-called granular ducts in the weanling) might influence the mechanism of carcinogenesis in some manner has to be considered.

Therefore, in the present study, tumor production was not a primary objective; rather, by sacrifice of animals at certain stated time intervals an attempt was made to map the parenchymal cell and other tissue changes through the early phases of experimental carcinogenesis, utilizing two different hydrocarbons having comparatively long and short latent periods. In addition, comparative studies were carried out to determine possible differences in the character of the response in weanling and adult animals.

Materials and Methods

On the basis of past experience in this laboratory,[17] it was suggested that 3-methylcholanthrene* and 7,12-dimethylbenz(α)anthracene*

* Obtained from Distillation Products, Division of Eastman Kodak Company, Rochester, N.Y.

might fulfil, respectively, the requirement of carcinogens with comparatively long and short latent periods.

Accordingly, these agents were prepared, using Carbowax* (15 per cent Carbowax 1500, 85 per cent Carbowax 4000) as a carrier, to make a 20 per cent mixture by weight. The Carbowax and carcinogenic mixture was placed in an oven at 59° C. until the Carbowax melted. The mixture was stirred until it appeared homogeneous and was then drawn up into warm, glycerine-lubricated glass tubules with an inside diameter of 3 mm. and cooled. The tubes were stored in a refrigerated desiccator.

A total of 188 weanling and 206 adult male albino rats (Sprague-Dawley strain) was used throughout this study.[18] The weanling animals were from 27 to 30 days of age and averaged 80 gm. in weight. The adult animals were from 90 to 100 days of age and averaged 190 gm. in weight. Under Nembutal Sodium† anesthesia, the ventral neck hair was clipped, a midline incision was made, and the left salivary glands were dissected free from the overlying fascia. A pellet of the carcinogen approximately 1 mm. long was expelled from the glass tube by forcing it out with a swab stick from the opposite end. By a stab wound, a pocket was produced in the lower pole of the left submaxillary salivary gland, the pellet inserted, and the skin incision closed with silk sutures. The animals were placed two in a cage and fed a commercial laboratory stock diet.

Both weanling and adult animals implanted with methylcholanthrene (MCA) were sacrificed at 1, 2, 4, 8, 12, 16, 20, and 24 weeks after operation. Since the response to the implantation of dimethylbenzanthracene (DMBA) pellets appeared significantly more violent both grossly and microscopically, animals of this group were sacrificed at 4 days and 1, 2, 4, 8, and 12 weeks after operation. The intervals of sacrifice of 16, 20, and 24 weeks were not carried out in this group as it was quickly established that tumors could be induced with this agent at earlier periods.

The salivary glands were removed en masse and fixed in Zenker-formol (Helley's) solution. The tissues were processed in the routine manner and tissue sections prepared at 6 μ. Harris' hematoxylin and eosin stains were used in every instance and special stains were used as indicated.

Controls consisted of six sham-operated animals sacrificed at 1, 2, 4, and 20 weeks to determine the possible effect of incision and repair

* Obtained from Carbide and Carbon Chemicals Company, New York, N.Y.
† Obtained from Pentobarbital Sodium, Abbott Laboratories, North Chicago, Ill.

upon the parenchymal cells. Also, 11 animals implanted with pure Carbowax were sacrificed at 4 days and 1, 2, 4, and 20 weeks to determine the effect of the carrier upon the salivary glands.

Results

Multinucleated Giant Cell Response

The initial response to the implantation of carcinogen-Carbowax pellets was characterized by a marked multinucleated giant cell reaction (Figs. 1 and 2). While it usually was possible to observe the presence of the pellet in the paraffin block, the finding of multinucleated giant cells with rhombic spaces in the tissue section was considered a priori evidence that the carcinogen was properly placed within or in apposition to the submaxillary gland and was, therefore, potentially capable of exerting a carcinogenic effect.

Connective Tissue Response

Considerable early repair with connective tissue proliferation was elicited in all instances. It is of particular significance that many animals with properly implanted pellets showed little or no parenchymal reaction to the carcinogen and demonstrated a well organized connective tissue barrier between the implant and the surrounding parenchyma.

It was noted that DMBA provoked a violent reparative response in almost every instance. This connective tissue hyperplasia appeared to replace the surrounding glandular tissue and seemed to be further provoked by a comparatively high incidence of abscesses at the early intervals of sacrifice. Except in those animals showing frank production of sarcomas, the histologic features of the connective tissue were similar in all groups. Four animals of the group that received MCA developed malignant connective tissue tumors which were diagnosed as fibrosarcomas (Fig. 3). These tumors occurred at 20 weeks (two weanlings) and 24 weeks (two adults). While one is impressed by the fibroblastic activity in the DMBA-implant animals, production of sarcoma was not observed in this group. However, since this group was not carried past the sacrifice intervals of 12 weeks, this is probably not significant.

Inflammatory Reaction

Inflammatory cell infiltration, while present, was not remarkable in either carcinogen-implant group and appeared unrelated to the degree of parenchymal change.

Sham-Operated and Carbowax Control Animals

Except for a mild inflammatory cell infiltration at the interval of 1 week, it was impossible to determine where the original incision had been in the sham-operated controls. Semiserial sections failed to reveal any alteration of the normal glandular architecture in the animals of this group.

The Carbowax control animals likewise failed to demonstrate parenchymal changes. In no instance could the Carbowax pellet be observed grossly at sacrifice or in the paraffin block. However, in two animals sacrificed after 4 days and 14 days, an empty space surrounded by well organized connective tissue was noted in the tissue sections and this was presumed to be the retained Carbowax pellet (Fig. 4). Cleft-like spaces with giant cells were not found in any of the controls.

Parenchymal Reaction

The essential response of the parenchyma of the submaxillary gland to carcinogen-Carbowax implants usually was manifest as a transition of normal ductal epithelium to a stratified squamous type. These changes were graded according to degree of metaplasia into five categories for purposes of scoring and analysis, only. Incipient metaplasia was identified as a disorganization of ductal cells with a reduction in stainability of nuclear chromatin (Fig. 5). With time, these columnar or cuboidal cells became flattened, with squamous layering of progressively increasing thickness (Figs. 6, 7, and 8). Eventual malignant transformation compatible at least with carcinoma-*in-situ* through epidermoid carcinoma presented the characteristic features of loss of orderly maturation and polarity, numerous typical and atypical mitotic figures, and variation in size and staining of cells (Figs. 9 to 13).

Since the metaplastic epithelium appeared to be derived exclusively from the striated ductal epithelium in both groups, no differences could be established in the histogenesis of induced tumors in weanling and adult rats. The metaplastic process was initiated in the striated ductal epithelium with a flattening of the cuboidal cells and a squamous layering to produce a well differentiated stratified squamous epithelium. These structures tended to retain the lumen which almost invariably became at least partially occluded with various structures, principally desquamated epithelial cells, inflammatory cells, and secretion granules. In many sections epithelial pearls were noted early in the metaplastic process, often by the time the ductal wall had reached the stage of being three cells thick (Fig. 7). This metaplastic epithe-

lium resembled striated ductal epithelium in staining qualities although the striations characteristic of these ducts obviously disappeared with the development of squamous features. In adult animals the granular tubules were conspicuously absent from that portion of the gland immediately adjacent to the site of implantation.

The fate of the acinar epithelium in the metaplastic process was noticeably inconsistent and indefinite. The acini seemed to disappear in the face of the connective tissue activity associated with the implant whereas the ductal epithelium tended to persist in these regions. The acini occasionally were noted to be disorganized, with plumping and paling of the nuclei. Metaplastic activity of acinar epithelium could not be established.

In the MCA-implant group, the incidence of metaplasia was remarkably consistent in both weanlings and adults provided that the pellet was retained well within the submaxillary gland. Metaplasia was demonstrated in 88 per cent of the weanling and 80 per cent of the adult animals in which the pellet was optimally located whereas only 51 per cent of all animals implanted that survived until sacrifice showed metaplasia. Thus, while metaplasia is much more likely to occur with the MCA-implant ideally placed deep within the submaxillary gland, metaplasia can occur if the pellet is located adjacent to the gland. On the other hand, the fact that the pellet may be located in the substance of the submaxillary gland does not assure metaplasia.

In the DMBA group, metaplasia of ductal epithelium was noted from the sacrifice interval of 4 days. The incidence of metaplasia in those animals showing evidence of the DMBA implant in or adjacent to the submaxillary gland was markedly higher than in the MCA animals. Metaplasia was demonstrated in 98 per cent of the weanling animals and 94 per cent of the adult animals with optimally implanted DMBA pellets. Metaplasia was noted in 77 per cent of all animals of this group implanted regardless of the location of the implant. Thus, the reactivity of the submaxillary gland was greater in the DMBA group both as to incidence and degree of metaplasia noted at each sacrifice interval. Malignant features were noted first at markedly earlier sacrifice intervals (8 weeks) for the DMBA implant group than for the MCA implant group (16 weeks).

Formation of Epidermoid Cysts

Formation of epidermoid cysts was noted from the 2 week interval in the MCA group and from the 1 week interval in the DMBA group. In every case, the epidermoid cysts appeared to arise from the striated ductal epithelium and presented squamous epithelium from 4 to 10

cell layers thick. These cysts varied as to their contents, relation to the implant, and the activity of the lining cells. One cyst was located within the implant and contained, within its lumen, crystals with multinucleated giant cells (Fig. 6). The other epidermoid cysts were located peripheral to the implant but within areas of connective tissue replacement of gland tissue. Certain of the cysts discovered at the later intervals of sacrifice contained large masses of keratin (Fig. 12).

The incidence of epidermoid cysts appeared to bear a relationship to the parenchymal reactivity and specifically to the degree of squamous metaplasia. This finding is further augmented by the observation that all animals, save one, that demonstrated grade 4 metaplasia (carcinoma-*in-situ* or epidermoid carcinoma) manifested this alteration in a cyst wall. The exception showed a focus of malignant cells in the vicinity of an epidermoid cyst and this probably represented tortuous, infiltrating fingers of cells originating from the cyst, although subsequent sectioning could not substantiate this.

Reaction to Blockage(?) of Ducts

Histologic features resembling those seen in duct-ligated salivary glands were observed in both groups of rats that received carcinogens. These appeared in focal areas made up entirely of duct-like structures and essentially devoid of recognizable acini (Fig. 14). Attempts to demonstrate hyperplasia of the ductal system or the transition of acini to these duct-like structures failed. It did appear that the acini disappeared or at least underwent atrophy with a concomitant relative increase in the number of ducts in a given field. This response was particularly evident in those animals showing marked connective tissue replacement of glandular tissue or in glands with occluded and/or metaplastic ducts. It was considered significant that 78 per cent of all MCA-treated animals demonstrating any degree of metaplasia also exhibited some metaplastic ducts filled with varying amounts of desquamated epithelial cells, cellular débris, histiocytes, inflammatory cells, and/or rarely a granular secretion similar to the granules found in the granular tubules. DMBA-implanted animals exhibited similar findings and, again, the possible relationship to this phenomenon suggested itself.

Epidermoid Carcinoma

The histologic features compatible with a diagnosis of epidermoid carcinoma (or carcinoma-*in-situ*) were found in seven weanling and two adult animals of the MCA-implanted group. Three weanlings and one adult developed carcinoma at 16 weeks and the remainder of the carcinomas were discovered at 20 and 24 weeks. In each case epider-

moid carcinoma developed in relation to an epidermoid cyst, although occasional apparently independent foci of neoplastic cells could be found.

The DMBA-implanted group exhibited nine instances of epidermoid carcinoma at a markedly earlier interval of sacrifice. Two weanling and two adult animals demonstrated malignant transformation at the 8 week interval. At the 12 week interval, two weanling and three adult animals showed malignant change. No apparent histologic difference could be noted in either implant group showing these changes.

Discussion

While 3-methylcholanthrene and 7,12-dimethylbenz(α)anthracene produced a variety of tissue responses, certain behavior patterns seem to have been established.

Parenchymal Reaction

Steiner[10] reported that the acinar cells, as well as the ductal epithelium, participated in the neoplastic process initiated in the submaxillary glands. Bauer and Byrne,[11] on the other hand, produced a variety of parotid tumors which they considered had origin in intercalated ducts and myo-epithelial cells. However, in this present study, cellular activity initiated with carcinogen-Carbowax implants in the submaxillary glands appeared to involve only the cells of the striated ducts. It is to be noted that the granular tubules located in the immediate vicinity of the implant lost their distinctive cytologic features and could not be distinguished from the striated ducts. Thus, while the fate of these granular tubules following their morphologic reversion cannot be accurately determined, it can be theorized that they adopt the characteristics of cells of the striated ducts and undergo metaplasia and eventual malignant transformation. In no instance could proliferative activity of acinar epithelium be observed. Rather, the acini were remarkable in that they promptly disappeared from the region of the implant, whereas the ductal epithelium tended to persist, oftentimes within the mass of the carcinogenic crystals proper.

Age of Animal

Berenblum,[19] in an extensive summary of the literature, stated: "Age, sex, pregnancy, castration, and other forms of hormonal influence, play an insignificant role in determining the response to carcinogenic action." This present study likewise failed to establish clearly any remarkable

difference in the incidence of tumors in weanling and adult rats, although the weanling MCA-implanted animals demonstrated a slight tendency toward earlier malignant transformation than the adult MCA-implanted animals. If only those MCA-treated animals that demonstrated the presence of the implant within the glandular parenchyma are considered, this tendency of weanling animals to have earlier and a greater percentage of epidermoid carcinoma (or carcinoma-*in-situ*) is only weakly supported by a slightly higher incidence of metaplasia in the younger animals. This finding is even less apparent in the DMBA-treated animals (short-acting carcinogen), as might be expected. Further, the relatively consistent parallelism of incidence of epidermoid cyst in both age groups appears to bear a direct relationship to the incidence and degree of metaplasia and therefore to tumor production inasmuch as most of the epidermoid carcinomas induced were associated with epidermoid cysts. No differences in the degree of malignancy could be observed either cytologically or histologically in the two carcinogen-treated or age groups.

Reaction to Blockage(?) of Ducts

The histologic features of a relative increase in the number of ducts with atrophy of the acini were noted almost invariably in connection with actively metaplastic ducts with occluded lumina. This response was considered to be a reaction to the blockage of ducts. These changes resemble, to a remarkable degree, those reported by Junqueira,[20] Rabinovitch,[21] Fernandes and Junqueira,[22] Junqueira and Rabinovitch,[23] and Valeri[24] following ligation of the submaxillary ducts. Clark,[25] in an unreported investigation, presented histologic sections of duct-ligated submaxillary glands that could not be differentiated from these areas.

These foci obviously were located proximally to the carcinogen-implant and therefore unaffected by the carcinogenic stimulus. The effect of carcinogenic agents implanted directly into these altered areas should be investigated.

While no conclusions can be drawn from these observations, it is proposed that herein lies the possible mechanism for the production of some of the various neoplasms encountered in the salivary glands. Obviously, blockage of ducts alone is not capable of initiating the growth of tumors but, coupled with certain unknown factors, it presents interesting possibilities.

Summary

The effects of implantation in the submaxillary salivary gland of a slow-acting carcinogen (3-methylcholanthrene) and a fast-acting carcinogen (7,12-dimethylbenz(α)anthracene) in a Carbowax carrier have been studied.

A variety of cellular and tissue responses were noted. These included a multinucleated giant cell reaction to the carcinogenic crystals, connective tissue hyperplasia, central abscess formation, metaplasia of glandular epithelium, formation of epidermoid and keratin cysts, carcinoma-*in-situ*, and production of epidermoid carcinoma and fibrosarcoma. Connective tissue hyperplasia and central abscess formation, while more intense in the 7,12-dimethylbenz(α)anthracene group, appeared to have little effect upon the incidence of metaplasia and tumor production in either group. Inflammatory cell infiltration could be correlated only with central abscess formation or surface ulceration and did not in any way affect the metaplastic process.

The incidence of formation of epidermoid cysts had a direct relationship to the potency of the carcinogen, the incidence and degree of metaplasia, and to tumor production inasmuch as the malignant transformation occurred in the wall of epidermoid cysts in nearly every instance.

Parenchymal metaplasia originated in the cells of striated ducts in all cases and was noted from the first interval of sacrifice in both groups (3-methylcholanthrene, 1 week; 7,12-dimethylbenz(α)anthracene, 4 days). The acinar epithelium did not appear to participate in the metaplastic process in this study and instead tended to disappear promptly from the implantation site.

The fate of cells of the granular tubules was not readily apparent. However, these cells appeared to lose their characteristic staining properties and to undergo morphologic reversion to cells indistinguishable from the cells of striated ducts.

With 3-methylcholanthrene, seven weanling animals and two adult animals demonstrated carcinoma-*in-situ* or epidermoid carcinoma, three tumors occurring at the 16 week interval in the weanling group and one tumor noted at 16 weeks in the adult group. With 7,12-dimethylbenz(α)anthracene, four weanling and five adult animals demonstrated malignant change, with the earliest tumors (two tumors occurring in each group) appearing at the sacrifice interval of 8 weeks. Production of fibrosarcoma occurred only with the slow-acting carcinogen, two being noted in the adult group at 20 weeks and two in the weanling group at 24 weeks.

REFERENCES

1. Löwenstein, C. Über atypische Epithelwucherungen und Tumoren der Speicheldrüsen, besonders der Parotis. *Frankfurt. Ztschr. f. Path.*, 1910, **4**, 187–202.
2. Macchiarulo, O., and Büngeler, W. Durch Teer erzeugte eigenartige Veränderungen der Parotisdrüse. *Frankfurt. Ztschr. f. Path.*, 1929, **37**, 211–221.
3. Tadaki, Y. Experimentelle Studien über die Entstehung des Teercarcinoms an Gl. submaxillaris bei Kaninchen. *Mitt. a. d. med. Akad. zu Kioto*, 1932, **6**, 377–378.
4. Berberich, J. Experimentelle Erzeugung von Tumoren am Ohr, an der Nase, den Nebenhöhlen und der Parotis. *Ztschr. f. Hals-, Nasen- u. Ohrenh.*, 1932, **31**, 343–345. (Abstract in: *Am. J. Cancer*, 1933, **18**, 628.)
5. Abb, M. Zur experimentellen Erzeugung von Parotistumoren. *Arch. f. Ohren-, Nasen- u. Kehlkopfh.*, 1932, **133**, 117–130. (Abstract in: *Am. J. Cancer*, 1933, **18**, 627–628.)
6. Steiner, P. E. Induced Tumors of the Salivary Glands. Program of the Third International Cancer Congress, Atlantic City, N.J., 1939, p. 138.
7. Benecke, E., and Schröder, J. Über experimentelle Geschwulsterzeugung in Speicheldrüsen. *Ztschr. f. Krebforsch.*, 1939–40, **49**, 505–514. (Abstract in: *Am. J. Cancer*, 1940, **39**, 255.)
8. Rusch, H. P.; Baumann, C. A., and Maison, G. L. Production of internal tumors with chemical carcinogens. *Arch. Path.*, 1940, **29**, 8–19.
9. Franseen, C. C.; Aub, J. C., and Simpson, C. L. Experimental tumors in lymph nodes and in endocrine and salivary glands. *Cancer Research*, 1941, **1**, 489–493.
10. Steiner, P. E. Comparative pathology of induced tumors of the salivary glands. *Arch. Path.*, 1942, **34**, 613–624.
11. Bauer, W. H., and Byrne, J. J. Induced tumors of the parotid gland. *Cancer Research*, 1950, **10**, 755–761.
12. Schaper, A., and Cohen, C. Beiträge zur Analyse des thierischen Wachstums. II. Teil. Ueber zellproliferatorische Wachstumszentren und deren Beziehungen zur Regeneration und Geschwulstbildung. *Arch. f. Entwcklngsmechn. d. Organ.*, 1905, **19**, 348–445.
13. Gross, L. A filterable agent, recovered from Ak leukemic extracts, causing salivary gland carcinomas in C3H mice. *Proc. Soc. Exper. Biol. & Med.*, 1953, **83**, 414–421.
14. Stewart, S. E. Neoplasms in mice inoculated with cell-free extracts or filtrates of leukemic mouse tissues. I. Neoplasms of the parotid and adrenal glands. *J. Nat. Cancer Inst.*, 1954–55, **15**, 1391–1415.
15. Gross, L. Induction of parotid carcinomas and/or subcutaneous sarcomas in C3H mice with normal C3H organ extracts. *Proc. Soc. Exper. Biol. & Med.*, 1955, **88**, 362–368.
16. Law, L. W.; Dunn, T. B., and Boyle, P. J. Neoplasms in the C3H strain and in F_1 hybrid mice of two crosses following introduction of extracts and filtrates of leukemic tissues. *J. Nat. Cancer Inst.*, 1955, **16**, 495–539.
17. Shafer, W. G. Personal communication, 1954.
18. Standish, S. M. Early Cytologic and Histologic Changes in Experimentally Induced Tumors in the Submaxillary Glands of Weanling and Adult Albino Rats. Master of Science thesis, Indiana University, 1956.

19. Berenblum, I. Carcinogenesis and Tumor Pathogenesis. In: Advances in Cancer Research, Greenstein, J. P., and Haddow, D. (eds.). Academic Press, Inc., New York, 1954, **2**, 142.

20. Junqueira, L. C. U. Cytological, cytochemical and biochemical observations on secreting and resting salivary glands. *Exper. Cell Research*, 1951, **2**, 327–338.

21. Rabinovitch, M. Doctoral thesis, Universidade de Sao Paulo, 1951.

22. Fernandes, J. F., and Junqueira, L. C. U. Respiration, glycolysis and energy rich phosphorus compounds in secreting and non-secreting rat submaxillary glands. *Exper. Cell Research*, 1953, **5**, 329–334.

23. Junqueira, L. C., and Rabinovitch, M. Reversibility of the phenomena induced by excretory duct ligature in the rat submaxillary gland. *Texas Rep. Biol. & Med.*, 1954, **12**, 94–97.

24. Valeri, V. Nuclear volume and testosterone-induced changes in secretory activity in the submaxillary gland of mice. *Science*, 1954, **120**, 984–986.

25. Clark, P. G. Personal communication, 1955.

LEGENDS FOR FIGURES

FIG. 1. Methylcholanthrene-implant in a weanling rat, 1 week old. Implant localized within submaxillary parenchyma. Hematoxylin and eosin stain. × 120.

FIG. 2. Methylcholanthrene-implant in a weanling rat, 8 weeks old. Carcinogenic crystal spaces within multinucleated giant cells. The metaplastic focus of cells is cut tangentially in this section. Hematoxylin and eosin stain. × 260.

FIG. 3. Methylcholanthrene-implant in a weanling rat, 24 weeks of age. Fibrosarcoma. Hematoxylin and eosin stain. × 160.

FIG. 4. Carbowax control in an adult rat, 2 weeks old. The large, empty space represents the retained Carbowax which dissolved in preparation of the specimen. The encapsulated Carbowax rapidly disappeared from the implant site in all other Carbowax controls. Hematoxylin and eosin stain. × 190.

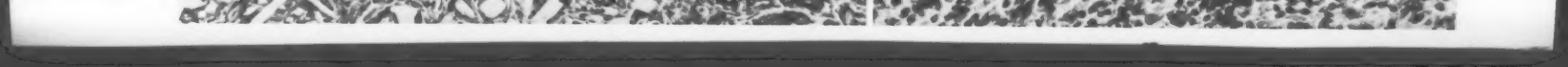

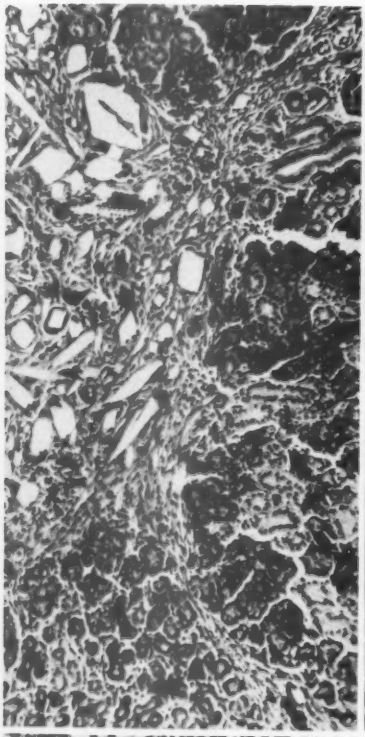

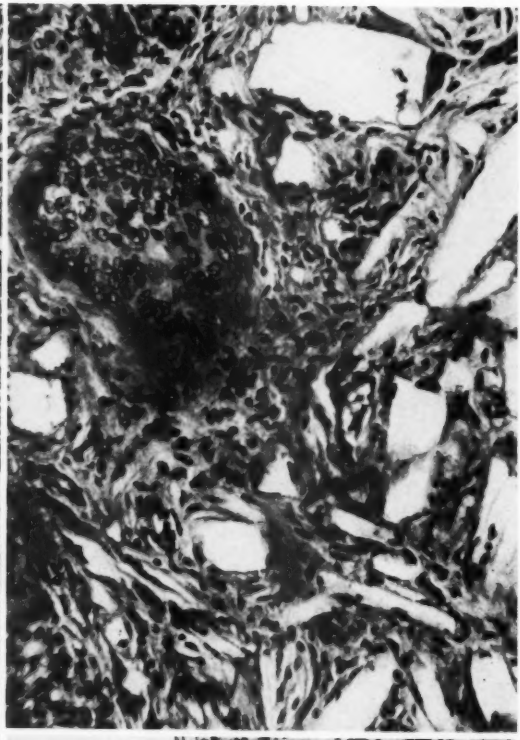

2

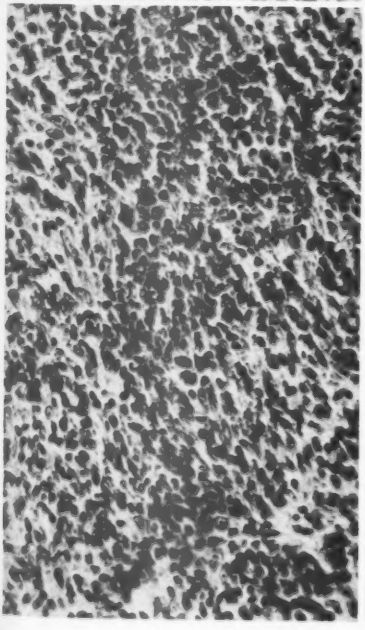

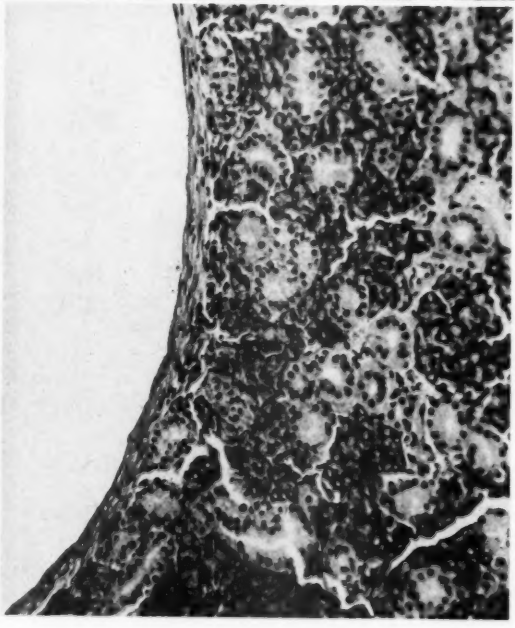

4

FIG. 5. Methylcholanthrene-implant in an adult rat, 2 weeks of age. Early alteration of striated ducts suggestive of incipient metaplasia. Hematoxylin and eosin stain. × 350.

FIG. 6. Methylcholanthrene-implant in a weanling rat, 2 weeks old. This specimen demonstrates early formation of epidermoid cysts. In this case the ductal epithelium persisted within the implant itself. Hematoxylin and eosin stain. × 200.

FIG. 7. Methylcholanthrene-implant in an adult rat, 1 week old. Squamous layering of ducts with a tendency to form keratin pearls. Hematoxylin and eosin stain. × 290.

FIG. 8. Methylcholanthrene-implant in a weanling rat, 16 weeks of age. Advanced squamous metaplasia in a portion of the wall of a cyst. Hematoxylin and eosin stain. × 290.

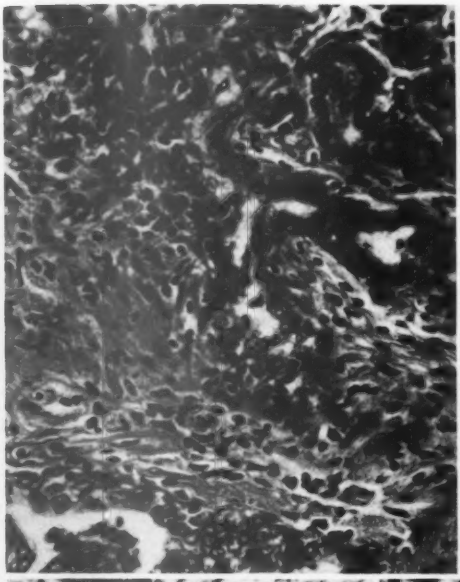

5

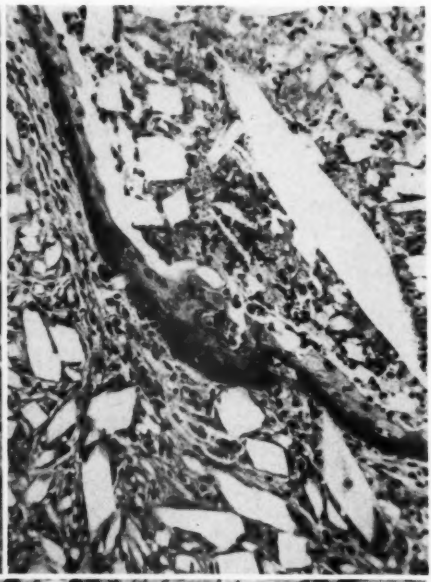

6

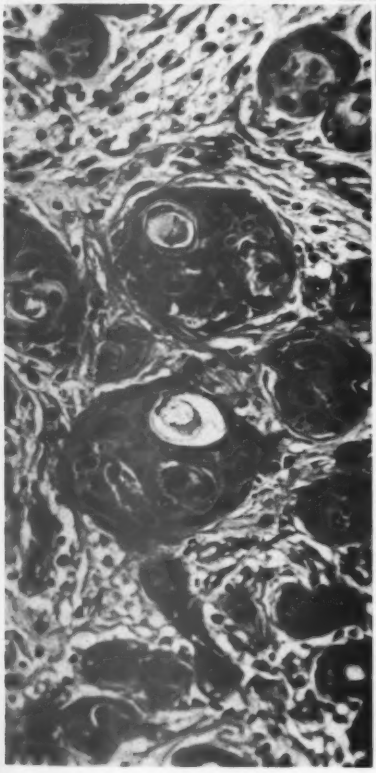

7

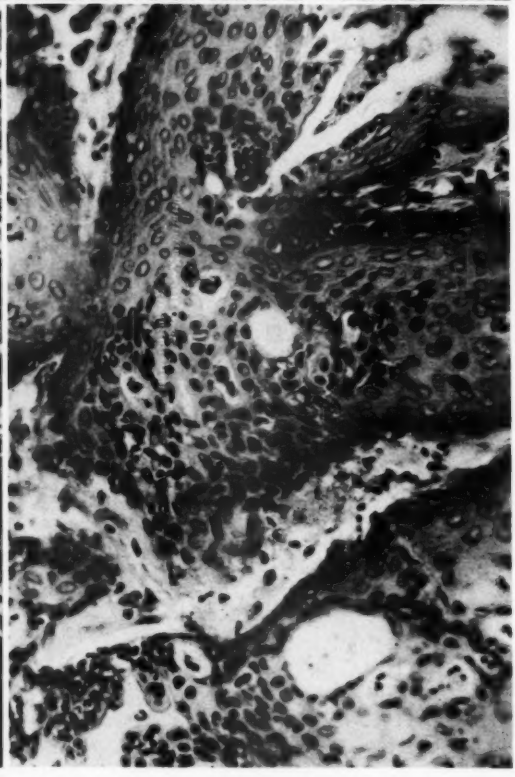

8

FIG. 9. Methylcholanthrene-implant in a weanling rat, 16 weeks of age. This photomicrograph demonstrates focal areas of dyskeratosis in a portion of the wall of an epidermoid cyst. Carcinoma-*in-situ*. Hematoxylin and eosin stain. × 280.

FIG. 10. Methylcholanthrene-implant in a weanling rat, 20 weeks of age. Epidermoid carcinoma. Cystic degeneration is occurring in the wall of an epidermoid cyst. Hematoxylin and eosin stain. × 200.

FIG. 11. Dimethylbenzanthracene-implant in an adult rat, 12 weeks old. Epidermoid carcinoma. Elsewhere in this specimen an epidermoid cyst was found but its relation to this neoplastic focus could not be established. Hematoxylin and eosin stain. × 250.

FIG. 12. Dimethylbenzanthracene-implant in an adult rat, 12 weeks old. Epidermoid carcinoma. The lumina of the metaplastic ducts tend to persist even through the advanced stages of metaplasia. Cellular inclusions and débris may be noted in the section. Hematoxylin and eosin stain. × 200.

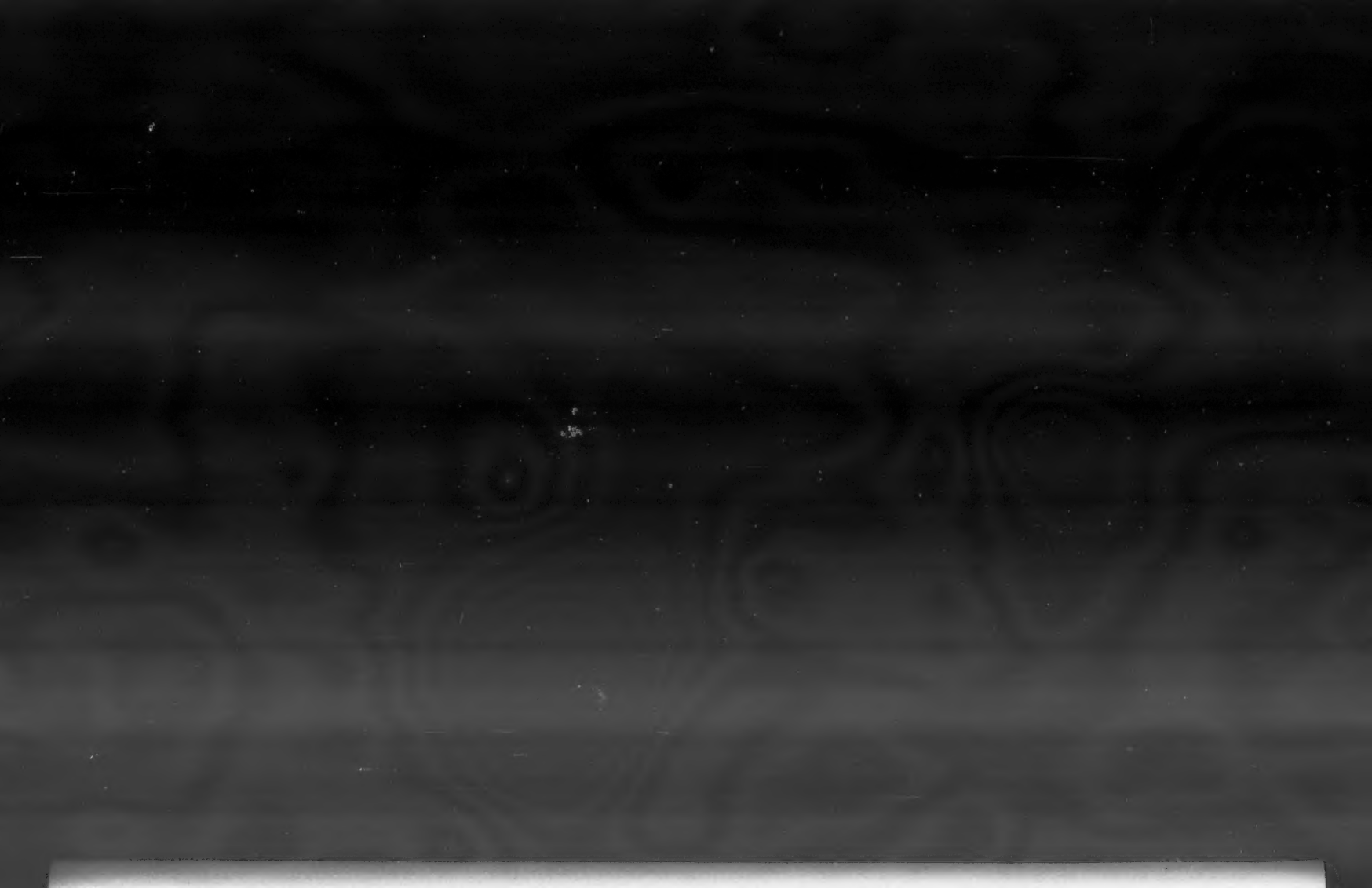

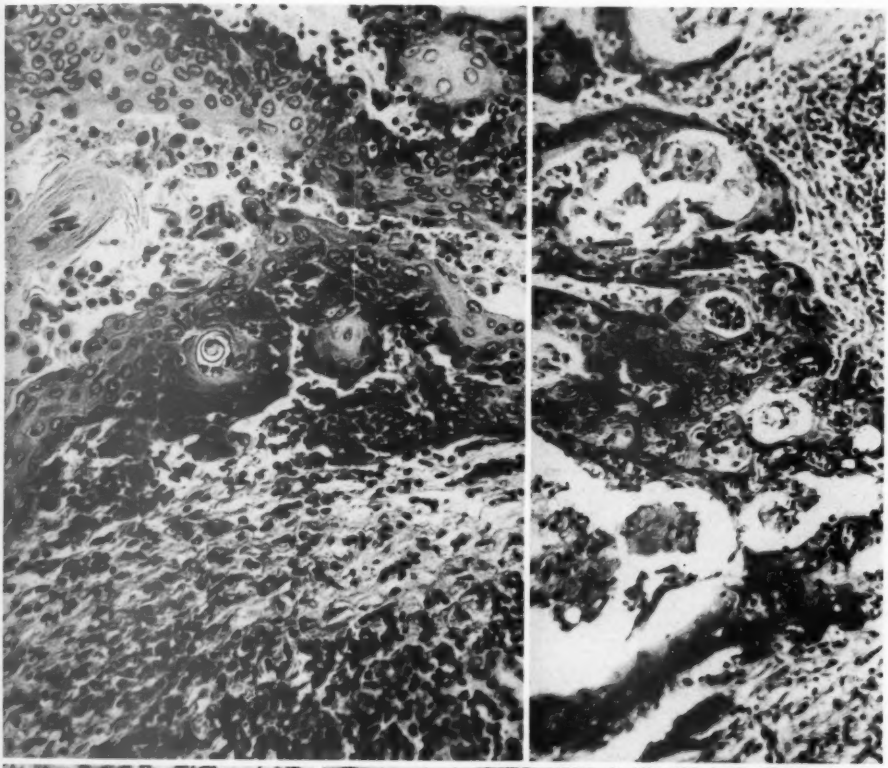

10

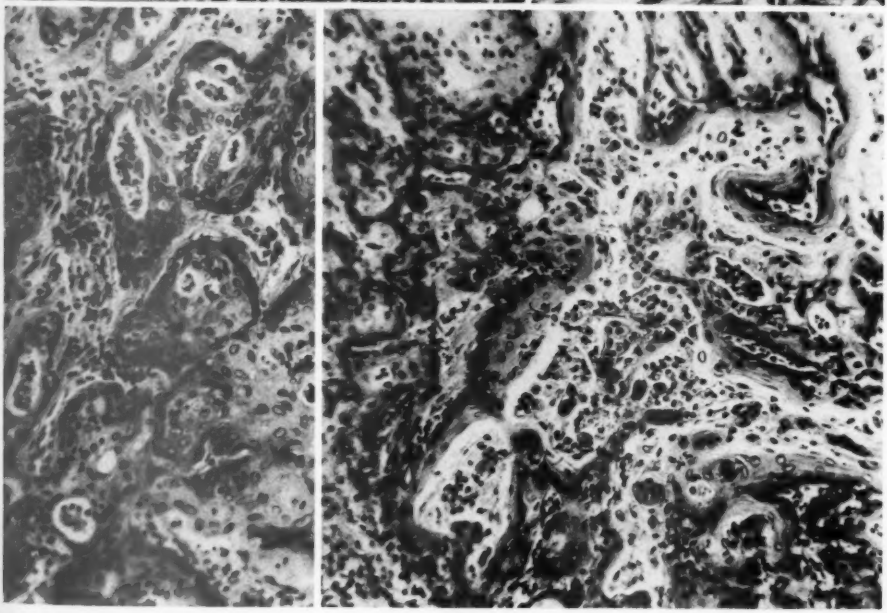

12

FIG. 13. Methylcholanthrene-implant in a weanling rat, 16 weeks old. Epidermoid carcinoma. Of note is the low-grade cellular activity in the wall of a keratin cyst. Hematoxylin and eosin stain. × 350.

FIG. 14. Methylcholanthrene-implant in an adult rat, 16 weeks of age. Blockage of ducts. Duct-like structures predominate. This phenomena resembles those changes observed following the ligation of ducts. Hematoxylin and eosin stain. × 300.

13

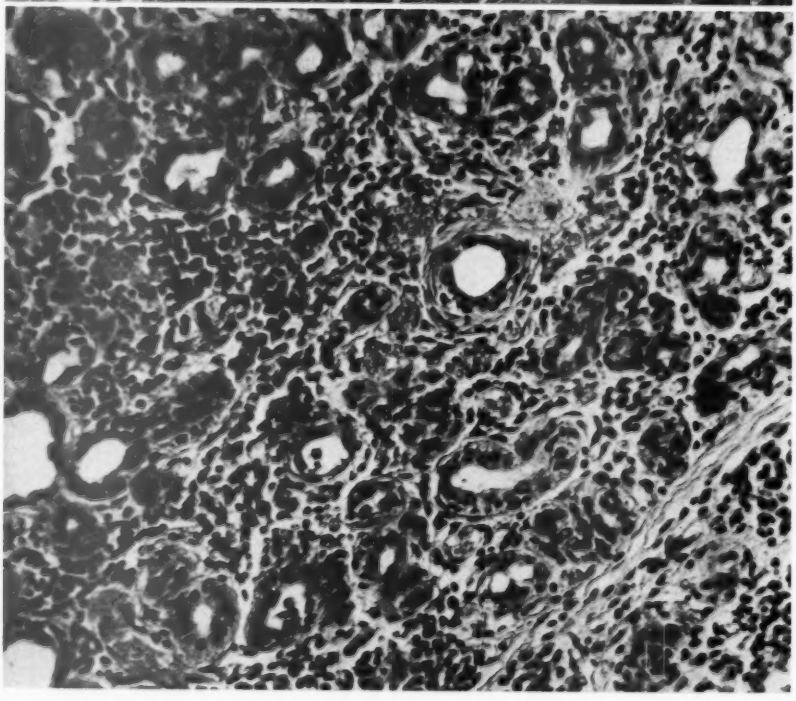

14

CYTOPATHOLOGY OF POLIOMYELITIS VIRUS IN TISSUE CULTURE

Fluorescent Antibody and Tinctorial Studies*

Sonja M. Buckley, M.D.

From the Division of Laboratories and Research, New York State Department of Health, Albany 1, N.Y.

Since the introduction of the technique of tissue culture for the propagation of poliomyelitis virus by Robbins, Enders, and Weller,[1] many investigators have studied the changes induced by infection of cells with these agents.[2-11] Feulgen-positive,[2] basophilic[4] granules occurring in the cytoplasm of cells of human origin infected with strains of type I and type III poliomyelitis virus have been reported. Antigen-containing cytoplasmic granules have been demonstrated by Coons's method[12] in kidney cells of the monkey inoculated with the Mahoney strain.[11]

In the present study, the development of cellular injury, particularly the presence or absence of cytoplasmic granules, was studied in kidney cells of the monkey and in cells of human origin inoculated with the Mahoney, MEF1, and Leon strains of poliomyelitis virus. The fluorescent antibody technique and tinctorial methods were employed.

Materials and Methods

Tissue Culture

Monkey Kidney. Trypsinized kidney cells were cultured as described previously.[11]

Cells of Human Origin. Conditions under which various lines of human cells are maintained in this laboratory are summarized in Table I. Cells were grown in tubes for 4 to 7 days. The sheets of cells were then retrypsinized and transferred to coverglasses placed in the flat bottom of Leighton tubes.† The composition of the respective growth of media is described in Table I. Explants of human origin were washed once with Syverton's maintenance solution before inoculation with virus. For experiments, the medium consisted of beef amniotic fluid[13] (85 per cent), inactivated horse serum (10 per cent), beef-embryo extract (5 per cent), penicillin (100 units per ml.), and dihydrostreptomycin (100 μg. per ml.).

Virus. Poliomyelitis virus type I (Mahoney strain), type II (MEF1 strain), and type III (Leon strain) were used. The titers of fluids from infective tissue cultures of kidneys of monkey were $10^{-5.5}$ for type I, $10^{-5.75}$ for type II, and $10^{-5.85}$ for type III.

* Received for publication, August 21, 1956.

† Obtained from Microbiological Associates, Bethesda, Md.

Fluorescent Antibody Technique. The indirect method[14] as applied in this laboratory[11,15] was used. The specificity of the immunocytochemical method has been discussed previously.[11] The same sample of human gamma globulin was employed as source of antibodies throughout the study. The log of the 50 per cent end-point dilution of the

TABLE I
Human Cell Lines

Cell line no.	Strain	Source	Date received	Growth fluid*				Transfer intervals	No. of cells per tube
				H	HAS	BEE	MS		
				%	%	%	%	(*days*)	
2	HeLa	Tuskegee Institute	7/8/54	60	40			10–14	40,000
7	Conjunctiva	Dr. R. S. Chang† via Sterling Winthrop Research Institute	3/3/55	55	40	5		7–10	30,000
8	Kidney	Dr. R. S. Chang† via Sterling Winthrop Research Institute	3/3/55	55	40	5		7–10	50,000
9	Liver	Dr. J. E. Smadel, Army Medical Service Graduate School	4/28/55	65	30	5		7–10	25,000
10	Embryonic intestine	Dr. G. Henle, Children's Hospital of Philadelphia	5/20/55		40	4	56	7–10	94,000

* Containing 50 units of penicillin and 50 μg. of streptomycin per ml.
H = Hanks's balanced salt solution adjusted to pH 7.4 to 7.6.
HAS = Human adult serum.
BEE = Beef embryo extract.
MS = Syverton's maintenance solution.
† Department of Microbiology, Harvard School of Public Health.

sample of gamma globulin[16] was 2.75 for type I, 2.85 for type II, and 2.40 for type III. For fluorescent antibody tests, the human gamma globulin was diluted 1:10 with buffered saline solution (sodium chloride solution, phosphate buffered to pH 7.0), whereas the fluorescein-labeled pseudoglobulin of the anti-human gamma globulin horse serum was diluted 1:20.

Tinctorial Methods

Giemsa's Method. Cultures were fixed in Bouin's fluid for 5 minutes and were allowed to stand overnight in 70 per cent ethyl alcohol; then they were washed, stained in an inverted position in dilute Giemsa's stain* (1 ml. of stock solution to 39 ml. of Sôrensen's phosphate buffer,

* Obtained from Merck & Co., Darmstadt, Germany.

pH 7.2) for 2½ hours, differentiated and dehydrated in acetone, acetone-xylene (1:1), and xylene.

Gram's Method. Cultures were air-dried (1 hour at 37° C.) and treated with acetone for 10 minutes. They were then stained by Gram's method. Preparations of renal cells of monkey were decolorized with 95 per cent ethyl alcohol, whereas cells of human origin were decolorized with a mixture of 95 per cent ethyl alcohol and acetone (1:1).

Experimental Findings

Monkey Kidney

Comparison of the Evolution of the Cytologic Lesions. In four experiments, the appearance of specific fluorescence after large doses of all three types of virus was analyzed at different intervals. Results were correlated with the development of cytopathogenic effects observed on unstained cultures or on preparations stained by tinctorial methods. The procedure described previously[11] was followed closely in this investigation. Table II shows the results obtained in a typical

Table II

Specific Fluorescence of Kidney Tissue of the Monkey*

Time	Poliomyelitis virus types			Uninoculated control
	I	II	III	
hrs.				
0	±	±	±	±
3	+	±	±	±
5	2+	1+	2+	−
10	3+	1+	2+	±
15	3+	3+	3+	±
20	4+	3+	2+†	−
25	2+†	3+	2+†	±

* Grading of results explained in text.

† Beginning of destruction in groups inoculated with types I and III.

experiment by the immunocytochemical method. The findings were graded according to the number of cells exhibiting specific fluorescence as well as by the degree of intensity of fluorescence: minus sign indicates absence of specific fluorescence; plus-minus, dull green coloring of cells; 1 plus to 3 plus, the presence of specific, brilliant yellow-green intracellular fluorescence in few to many cells; 4 plus, intense fluorescence in many cells. Uninoculated control preparations showed either gray-blue autofluorescence or a dull green coloring of cells. The appearance of specific fluorescence preceded the beginning of the cytopatho-

genic effect by a few hours. There was little difference among the three types in this qualitative study. Type I stained somewhat brighter than types II and III, and type II was slower in the evolution of changes. Within 5 hours, the cytoplasm of some scattered cells was stained diffusely. No antigen was localized within the nucleus at that time. In the 10-hour groups, the picture was more varied. The distribution of fluorescence was either diffuse and granular, or, occasionally, brilliant fluorescent granules were present. Fifteen hours after inoculation, peripheral fluorescent zones corresponding to hyaline zones[8] were observed. Other cells exhibited distinct fluorescent granules[11] (Figs. 1, 2, and 3). Cellular projections, some of which showed stippling, beading, or bulbous enlargements,[6,11] fluoresced. The bubbling phenomenon of Barski *et al.*[5] was present. Some of the cells were shrunken, rounded, and characterized by diffuse, brilliant fluorescence. A similar pleomorphism was present in preparations stained by Giemsa's method. Uninoculated kidney cells of the monkey have been discussed.[11] In inoculated tissue explants, there appeared to be a parallelism between the distribution of basophilic and fluorescent material: diffuse fluorescence was conformable to increased diffuse basophilia; peripheral fluorescent zones to basophilic ectoplasmic layers; and fluorescent granules to basophilic granules (Figs. 7, 8, and 9). Such forms varied in size and shape, were confined either to the ectoplasmic layer of the cell[2] or were distributed diffusely throughout the cytoplasm with intranuclear localization or overlay the nucleus. They were sometimes surrounded by a clear halo. At times, they were placed within a bulbous enlargement[11] or were clearly extracellular (Fig. 9). The cytoplasm of cells containing basophilic granules stained either deep blue or purple or had lost its affinity for basophilic dyes (Fig. 8). In such cells, chromatolysis was common (Fig. 7). In size, shape, and distribution, the granules corresponded to the antigen-containing fluorescent granules. In cells showing a peripheral basophilic zone, the remaining central portion often appeared as a granular, strongly eosinophilic mass.[2,9,10]

Cytoplasmic granules, when stained by Gram's method, were either Gram-negative or Gram-labile (Figs. 13, 14, and 15). The smaller size of the granules is explained by the different mode of fixation.

Cells of Human Origin

In ten experiments, five lines of human cells were tested for distribution of specific fluorescence 15 hours after inoculation of large doses of all three types of virus. Tissue cultures were harvested and processed

according to procedures described previously.[11] Table III summarizes the results. The same grading system was applied as for the tissue cultures of monkey kidney. The changes observed in cells of human origin were quite similar to those reported for the monkey kidney. There were no apparent basic tissue or type differences, except that

TABLE III

Specific Fluorescence of Cells of Human Origin (Time of Harvest: 15 Hours after Inoculation)*

Experiment no.	Cell line	Poliomyelitis virus types			Uninoculated control
		I	II	III	
VI	Hela	3+	2+	2+	±
XIV	Conjunctiva	3+	2+	2+	±
IXc	Kidney	3+	3+	3+	±
XV	Liver	4+	2+	2+	±
IVc	Intestine	3+	1+	2+	± to +

* Grading of results explained in text.

explants inoculated with type I virus occasionally stained brighter. Preparations of human liver inoculated with all three types will illustrate the changes observed in cells of human origin. The specific fluorescence was either diffuse or granular, whereby the size of granules varied extensively (Figs. 4, 5, and 6). Fluorescent material often was localized in the peripheral ectoplasmic layer (Fig. 6). Fluorescent cellular processes, some of them stippled (Fig. 4) or occasionally exhibiting beading or bulbous enlargements, were demonstrated. In Giemsa-stained preparations, uninoculated human hepatic cells showed a considerable difference in size and shape, some of the cells being five times as large as others. Binucleated or giant cells were present. A few "bubbling" cells, as well as some pyknotic, basophilic staining cells, were observed. The finely granular cytoplasm stained blue with a slight purple tinge. Occasionally, cytoplasmic vacuoles were noted, some of which were filled with an eosinophilic mass. A few cells contained basophilic cytoplasmic granules. The nuclei, round, oval, or lobulated, stained homogeneously blue and contained one to five deeply basophilic nucleoli which were round, oval, or bizarre in shape. Inoculated preparations exhibited many cells with purple cytoplasm containing deeply basophilic granules, irregular in size and shape (Figs. 10, 11, and 12), or generalized basophilia, or cells characterized by strongly basophilic ectoplasmic layers. In such cells, the central cytoplasmic portion frequently stained eosinophilic.

In infected preparations stained by Gram's method, cytoplasmic

granules were Gram-negative or Gram-labile (Figs. 16, 17, and 18).

As described for kidney cells of the monkey, there was a striking multiplicity of morphologic changes. Again the distribution of the fluorescent antigen-containing material appeared to parallel the distribution of the basophilic material.

Hematoxylin and eosin stains were inadequate in our experience for demonstrating the changes brought out so well by Giemsa's method.

Discussion

The immunocytochemical method demonstrated the antigen of each of the three types of poliomyelitis virus to be localized in the kidney cells of the monkey 5 hours after massive inoculation. The results correlate well with the findings obtained in studies on virus release by other investigators.[4,8,10] In early stages, focally distributed cells showed diffuse specific fluorescence in the cytoplasm, but not in the nucleus. The cytoplasm has been considered as the site of the primary action of poliomyelitis virus.[2,11,17-20] Five hours following inoculation, no alteration in structure was detectable, with the possible exception of a slight increase in the volume of cells. This has been mentioned also by Klöne[7] who reasoned that such an increase in volume might not be measurable, since measurements usually are made in two dimensions, neglecting the third. By 6 hours, there was a direct correlation between the cytopathogenic effect and the presence of antigen in the cells. Especially at the 15-hour period and thereafter, a multiplicity of morphologic changes[2-11] was apparent in fluorescent antibody studies and in preparations examined by tinctorial methods in the host cells of monkey or man. Diffuse or granular specific fluorescence or fluorescence localized in the peripheral cytoplasm of infected cells was a feature. In later stages, many cells also showed intranuclear antigen.[21]

In Giemsa-stained preparations, increased basophilia, or basophilic cytoplasmic granules, or peripheral basophilic zones were present regularly following inoculation of the host cells with all three types of virus. Similar phenomena have been described by Barski *et al.*[2] and Ackermann and associates.[4] Deeply blue pyknotic cells or less shrunken, purple cells with or without basophilic granules were indicative of infection. Quite frequently, normally configurated cells contained basophilic granules which often were surrounded by a halo. Sometimes also they were located within the nucleus or overlay the nucleus. In such cells, the protoplasm stained pale blue or not at all; the nucleoli often were very faintly stained; and there was general chromatolysis.

This indicates that both pyknosis as well as lysis of cells can occur as a sequence of infection. Barski *et al.* have described as an early lesion the appearance of a cytoplasmic, eosinophilic mass preceding a definite increase in basophilia both of nucleus and of the remainder of cytoplasm. It also has been reported that this granular, eosinophilic mass is characterized by low, brownian movement, whereas the peripheral, basophilic staining cytoplasm shows active brownian movement.[10] Other investigators have emphasized the formation of an ectoplasmic layer[7] or hyaline zone[8] beautifully illustrated by Harding *et al.*[10] in their Plate II. This peripheral cytoplasm apparently underwent profound changes during the release of virus.[8] In our studies, similar ectoplasmic layers surrounding an eosinophilic cytoplasmic mass showed an affinity for basophilic dyes and contained antigen as shown by Coons's method (Fig. 6). The cytoplasmic acidophilic mass might very well be of passive nature and of secondary importance. Generally, the distribution of basophilic material correlated with the distribution of fluorescent material.

Basophilic granules, when stained by Gram's method, were Gram-negative or Gram-labile. The conventional hematoxylin and eosin stain was inadequate in our experience.

The most striking feature was the multiplicity of changes as illustrated by both the immunocytochemical and Giesma methods. Bulbous enlargements within processes or beaded processes were perhaps more frequently observed in kidney tissue of the monkey than in human cells, but the difference was not striking. Such forms, as well as "bubbling" cells and peculiar projections, might be transitory stages during the release of virus from an infected cell.

On a purely qualitative basis, there was no type difference nor was there any basic difference in the reaction of the many cell systems in their response to virus infection.[22] The multiplicity of changes in the later infectious stages has been stressed. One wonders whether this multiplicity indicates the existence of a life cycle. Bedson and Bland[23] appear to have first considered the possibility that viruses other than those of psittacosis pass through a developmental cycle. Basophilic or fluorescent granules might then be part of that cycle. In view of the specificity of the immunocytochemical method, this possibility must be considered.

Preliminary *in vitro* studies on several ECHO viruses, as well as on Coxsackie virus, type B, indicate a similarity in histopathology for enteric viruses.

SUMMARY

The antigens of poliomyelitis types I, II, and III were identified in the cytoplasm and in the nucleus of kidney cells of the monkey, and in cells of human origin, by means of the fluorescent antibody technique. More antigen appeared to be formed in the cytoplasm than in the nucleus.

On a qualitative basis, there was no type difference, nor was there any basic difference in the reaction of the many cell systems in their response to virus infection.

The multiplicity of changes as seen by fluorescent antibody technique, as well as by tinctorial methods, suggests the possibility of a sequential life cycle of poliomyelitis virus.

REFERENCES

1. Robbins, F. C.; Enders, J. F., and Weller, T. H. Cytopathogenic effect of poliomyelitis viruses *in vitro* on human embryonic tissues. *Proc. Soc. Exper. Biol. & Med.*, 1950, **75**, 370–374.
2. Barski, G.; Endo, M., and Monaci, V. Étude préliminaire des lésions cellulaires de la poliomyélite en culture *in vitro* sur une souche de fibroblastes humains. *Ann. Inst. Pasteur*, 1953, **85**, 264–268.
3. Stoler, M., and Gey, M. K. Destruction of a human fibrosarcoma strain (A.Fi.) in tissue cultures following the growth of poliomyelitis viruses. *Bull. Johns Hopkins Hosp.*, 1953, **92**, 385–393.
4. Ackermann, W. W.; Rabson, A., and Kurtz, H. Growth characteristics of poliomyelitis virus in HeLa cell cultures: lack of parallelism in cellular injury and virus increase. *J. Exper. Med.*, 1954, **100**, 437–450.
5. Barski, G.; Robineaux, R., and Endo, M. Phase contrast cinematography of cellular lesion produced by poliomyelitis virus *in vitro*. *Proc. Soc. Exper. Biol. & Med.*, 1955, **88**, 57–59.
6. Hogue, M. J.; McAllister, R.; Greene, A. E., and Coriell, L. L. The effect of poliomyelitis virus on human brain cells in tissue culture. *J. Exper. Med.*, 1955, **102**, 29–36.
7. Klöne, W. Untersuchungen zur Cytopathogenität des Poliomyelitisvirus (Typ Leon). *Arch. f. Virusforsch.*, 1954, **6**, 36–44.
8. Lwoff, A.; Dulbecco, R.; Vogt, M., and Lwoff, M. Kinetics of the release of poliomyelitis virus from single cells. *Virology*, 1955, **1**, 128–139.
9. Beale, A. J.; Stevens, P. F.; Davis, N.; Stackiw, W., and Rhodes, A. J. The development of inclusions in tissue cultures of monkey kidney epithelial cells infected with poliomyelitis virus. *Canad. J. Microbiol.*, 1956, **2**, 298–303.
10. Harding, C. V.; Harding, D.; McLimans, W. F., and Rake, G. Cytological changes accompanying the growth of poliomyelitis virus in cells of human origin (strain HeLa). *Virology*, 1956, **2**, 109–125.
11. Buckley, S. M. Visualization of poliomyelitis virus by fluorescent antibody. *Arch. f. Virusforsch.*, 1955, **6**, 388–400.

12. Coons, A. H., and Kaplan, M. H. Localization of antigen in tissue cells. II. Improvements in a method for the detection of antigen by means of fluorescent antibody. *J. Exper. Med.*, 1950, **91**, 1–13.

13. Enders, J. F. Bovine amniotic fluid as tissue culture medium in cultivation of poliomyelitis and other viruses. *Proc. Soc. Exper. Biol. & Med.*, 1953, **82**, 100–105.

14. Weller, T. H., and Coons, A. H. Fluorescent antibody studies with agents of varicella and herpes zoster propagated *in vitro*. *Proc. Soc. Exper. Biol. & Med.*, 1954, **86**, 789–794.

15. Buckley, S. M.; Whitney, E., and Rapp, F. Identification by fluorescent antibody of developmental forms of psittacosis virus in tissue culture. *Proc. Soc. Exper. Biol. & Med.*, 1955, **90**, 226–230.

16. Opton, E. M.; Nagaki, D., and Melnick, J. L. Poliomyelitis antibodies in human gamma globulin. *J. Immunol.*, 1955, **75**, 178–185.

17. Meloni, G. A., and Molina, A. M. La localizzazione intracellulare del virus poliomielitico nei vari stadi della malattia sperimentale. *Igiene mod.*, 1954, **47**, 816–826. (Abstracted in *Bull. Hyg.*, 1955, **30**, 1031.)

18. Bodian, D. Poliomyelitic changes in multinucleated neurons, with special reference to the site of action of virus in the cell. *Bull. Johns Hopkins Hosp.*, 1945, **77**, 49–59.

19. Schwerdt, C. E., and Pardee, A. B. The intracellular distribution of Lansing poliomyelitis virus in the central nervous system of infected cotton rats. *J. Exper. Med.*, 1952, **96**, 121–136.

20. Kaplan, A. S., and Melnick, J. L. The intracellular localization of poliomyelitis virus. *J. Exper. Med.*, 1953, **97**, 91–116.

21. Ruska, H.; Stuart, D. C., Jr., and Winsser, J. Electron microscopic visualization of intranuclear virus-like bodies in epithelial cells infected with poliomyelitis virus. *Arch. f. Virusforsch.*, 1955, **6**, 379–387.

22. Dunnebacke, T. H. Correlation of the stage of cytopathic change with the release of poliomyelitis virus. *Virology*, 1956, **2**, 399–410.

23. Bedson, S. P., and Bland, J. O. W. A morphological study of psittacosis virus, with the description of a developmental cycle. *Brit. J. Exper. Path.*, 1932, **13**, 461–466.

[*Illustrations follow*]

LEGENDS FOR FIGURES

Figs. 1 to 6. All preparations were harvested 15 hours after inoculation and stained by the fluorescent antibody technique. The bright white areas represent the specific yellow-green fluorescence indicative of the presence of poliomyelitis antigen. × 400.

FIG. 1. Kidney tissue of the monkey inoculated with the Mahoney strain. Diffuse or granular fluorescence or presence of individual fluorescent granules.

FIG. 2. Kidney tissue of the monkey inoculated with the MEF1 strain. Large cell shows granular distribution of specific fluorescence within the cytoplasm. Nucleus contains less antigen.

FIG. 3. Kidney tissue of the monkey inoculated with the Leon strain. Fluorescent granules are located within the cytoplasm and in the cellular process in the left upper corner.

FIG. 4. Human liver cells inoculated with the Mahoney strain. Diffuse or granular distribution of specific fluorescence and fluorescent granules of different size and shape within the cellular processes.

FIG. 5. Human liver cells inoculated with the MEF1 strain. Cell in the center contains large fluorescent bodies located in the peripheral zone.

FIG. 6. Human liver cells inoculated with the Leon strain. Fluorescent material most concentrated in the peripheral cytoplasmic layer and in the cellular process.

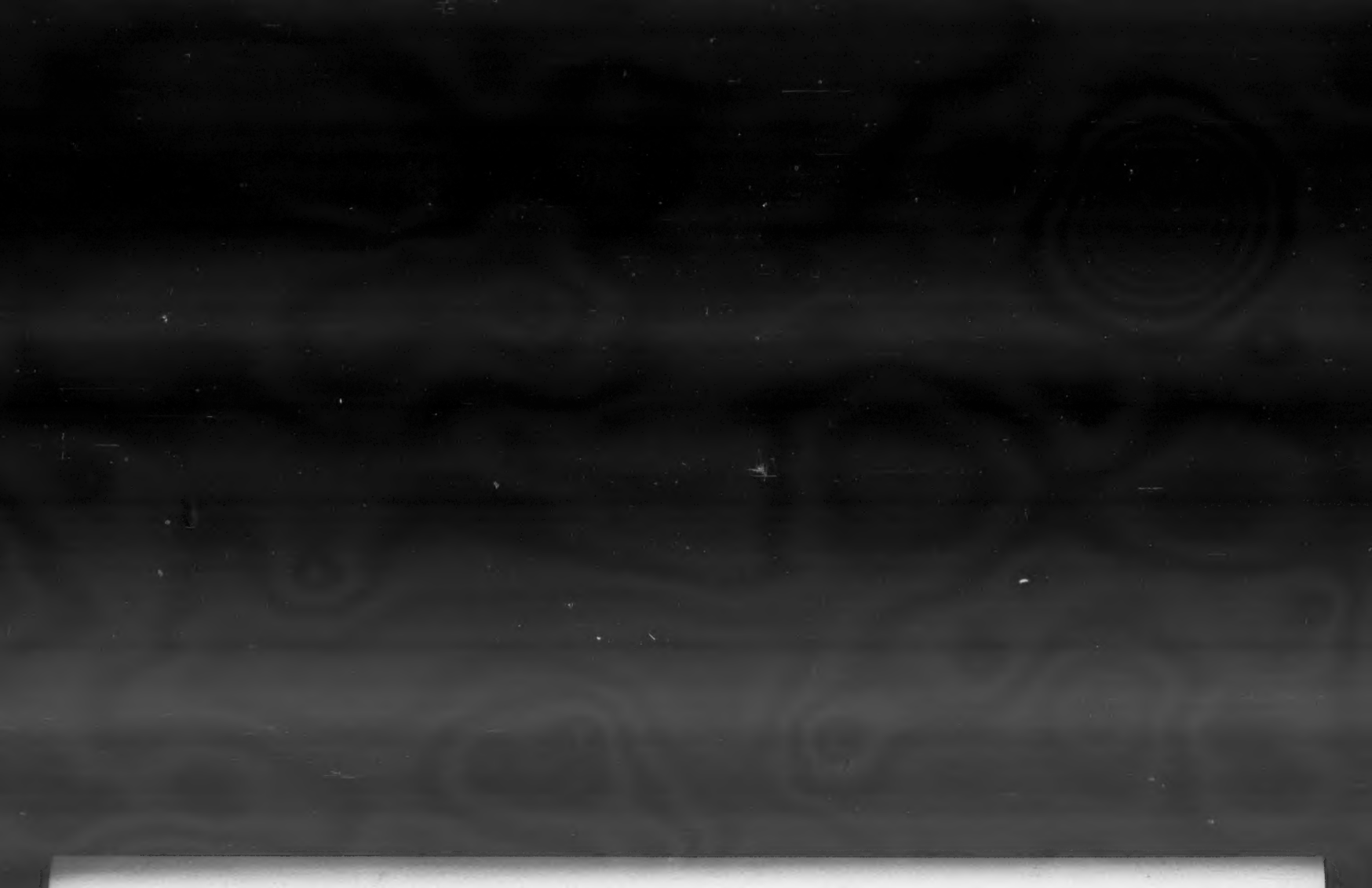

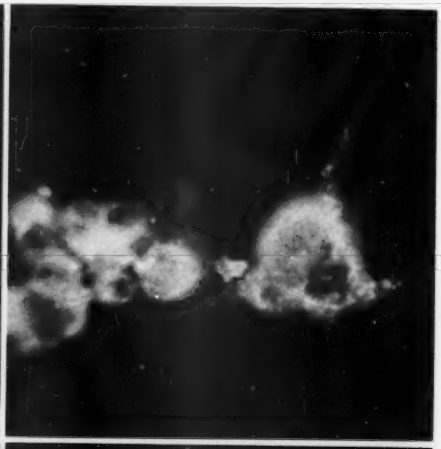

4

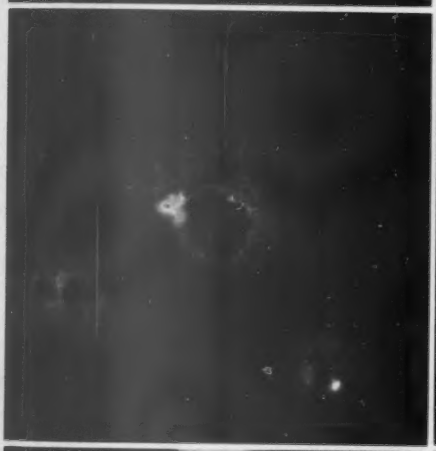

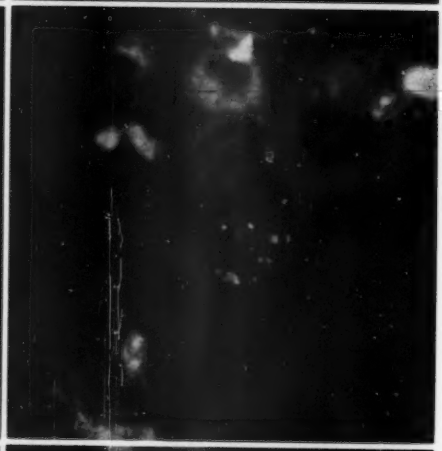

5

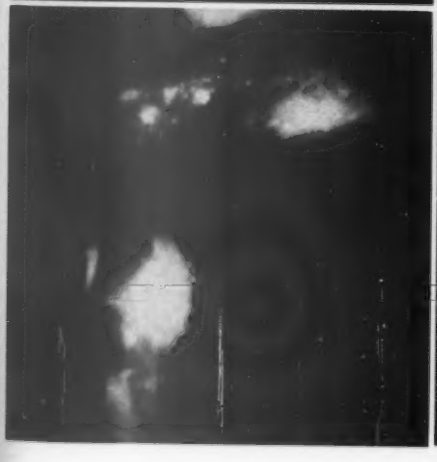

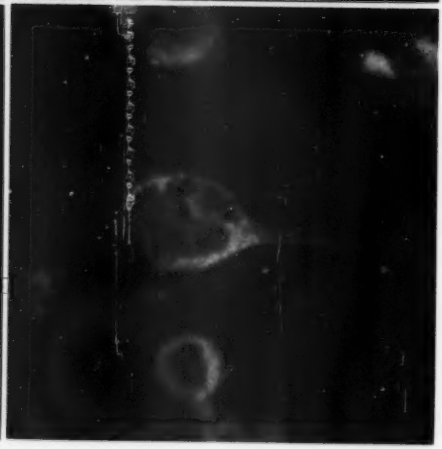

6

Figs. 7 to 9. All preparations harvested 15 hours after inoculation and stained by Giemsa's method. × 800.

FIG. 7. Kidney tissue of the monkey inoculated with the Mahoney strain. Basophilic granules varying greatly in size and shape are localized mostly in the periphery of the cytoplasm.

FIG. 8. Kidney tissue of the monkey inoculated with the MEF1 strain. Two cells characterized by pale-staining cytoplasm contain numerous basophilic granules, many of which appear to be surrounded by a clear halo.

FIG. 9. Kidney tissue of the monkey inoculated with the Leon strain. Extracellularly located basophilic granules.

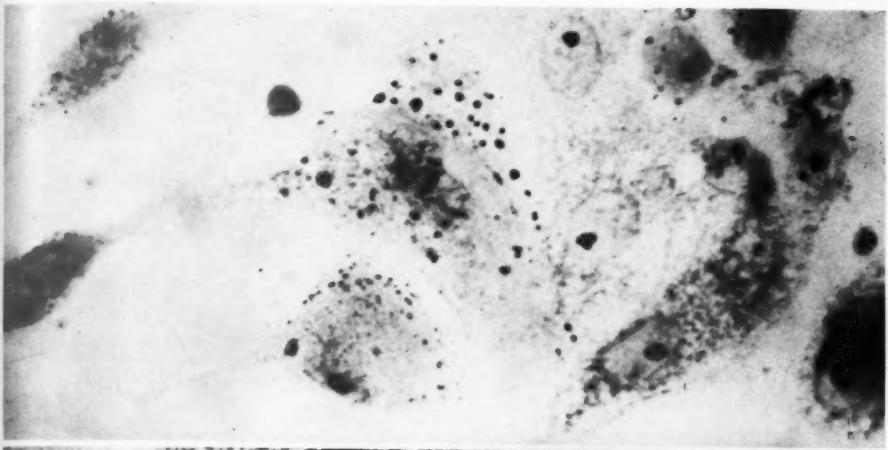

7

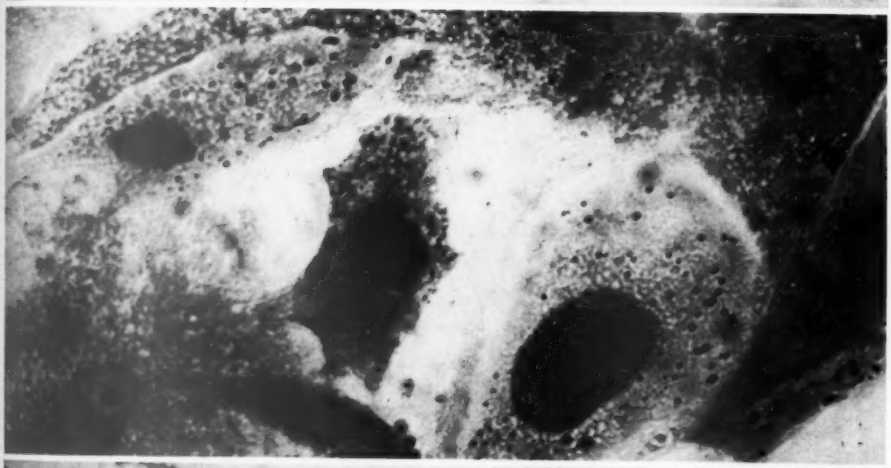

8

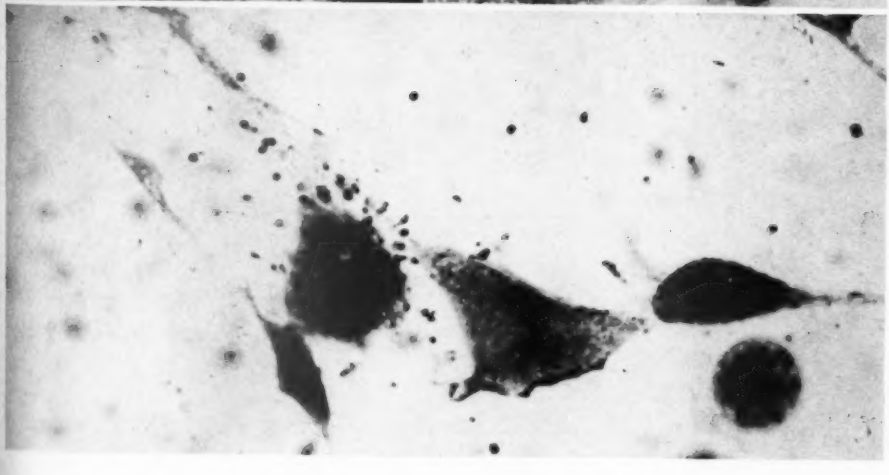

9

Figs. 10 to 12. All preparations harvested 15 hours after inoculation and stained by Giemsa's method. × 800.

FIG. 10. Human liver cells inoculated with the Mahoney strain. Pleomorphic basophilic granules located mostly in the ectoplasmic layer and in the cellular process.

FIG. 11. Human liver cells inoculated with the MEF1 strain. Large basophilic bodies corresponding in size and localization to fluorescent granules, Figure 5.

FIG. 12. Human liver cells inoculated with the Leon strain. Basophilic granules located mostly in the ectoplasmic layer of the cytoplasm.

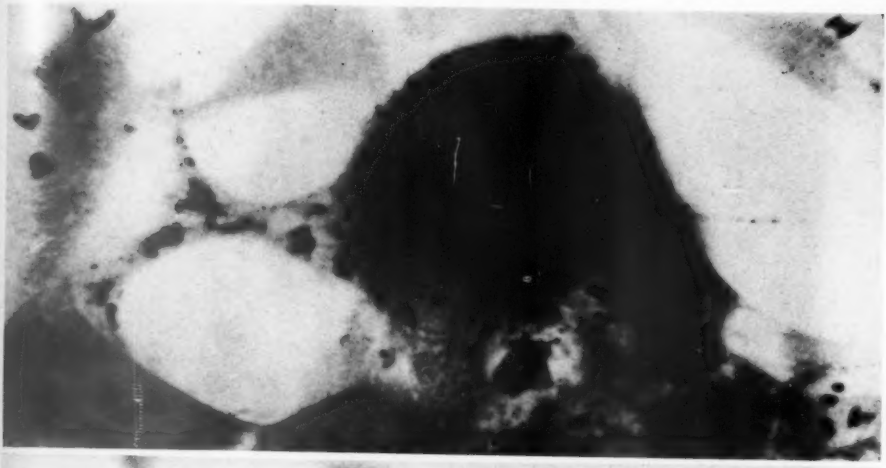

10

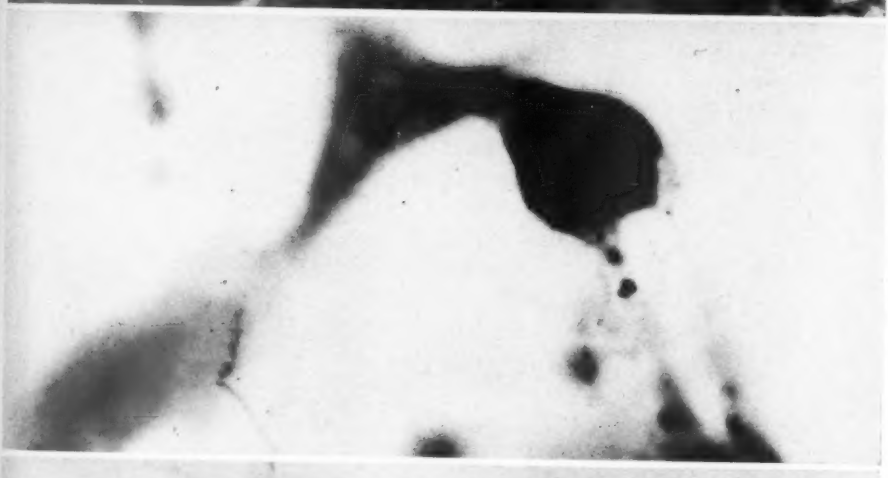

11

12

Figs. 13 to 18. All preparations harvested 15 hours after inoculation and stained by Gram's method. × 800.

FIG. 13. Kidney tissue of the monkey inoculated with the Mahoney strain. Gram-negative granules located in the periphery of cells.

FIG. 14. Kidney tissue of the monkey inoculated with the MEF1 strain. Gram-negative granules located throughout the cytoplasm.

FIG. 15. Kidney tissue of the monkey inoculated with the Leon strain. Gram-negative granules located throughout the cytoplasm.

FIG. 16. Human liver cells inoculated with the Mahoney strain. Gram-negative granules localized throughout the cytoplasm.

FIG. 17. Human liver cells inoculated with the MEF1 strain. Large Gram-negative granules located mostly in the periphery of the cytoplasm.

FIG. 18. Human liver cells inoculated with the Leon strain. Fine Gram-negative granules distributed throughout the cytoplasm.

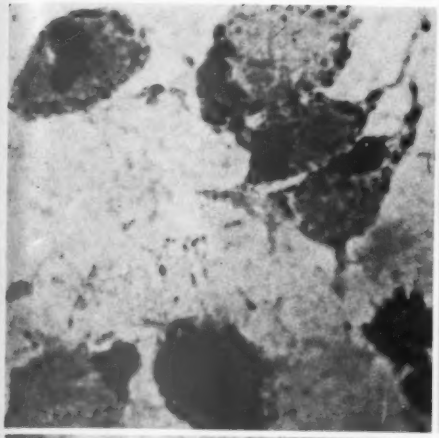

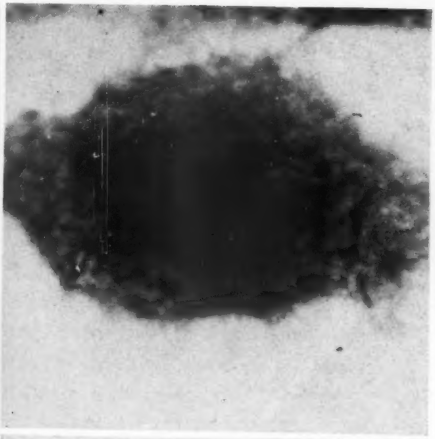

16

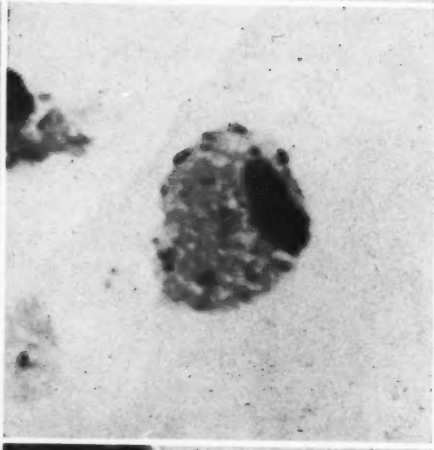

17

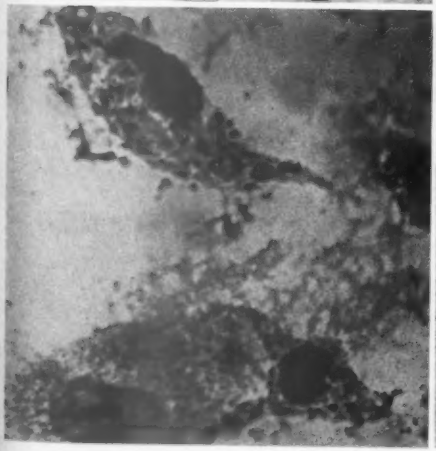

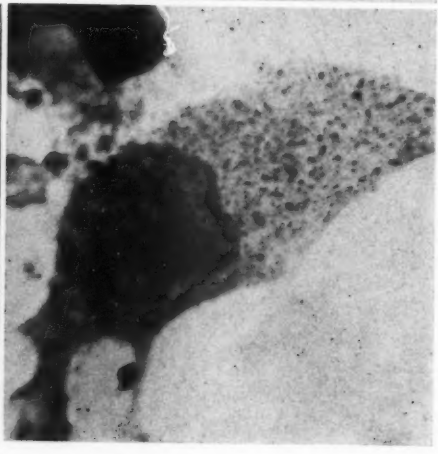

18

STUDIES ON HEPATITIS IN HAMSTERS INFECTED WITH EQUINE ABORTION VIRUS

I. Sequential Development of Inclusions and the Growth Cycle*

Charles C. Randall, M.D., and E. C. Bracken, Ph.D.
From the Department of Microbiology, Vanderbilt University School of Medicine, Nashville, Tenn.

The nature of the intranuclear inclusion body of virus-infected cells has long been a subject of investigation, most extensively with virus of herpes simplex. Goodpasture[1] apparently was the first investigator to trace the development of the intranuclear inclusion. He noted that early changes often consisted of several irregular eosinophilic particles which seemed to coalesce to form one structure and tended to increase in size and eventually to fill the nuclear space. Scott and his coworkers[2-5] have made a thorough sequential study of infection by the virus of herpes simplex and have correlated morphologic nuclear changes with the growth cycle. In one stage the inclusion completely fills the nucleus and is referred to as "full" or "complete," in comparison to classical inclusions designated as "shrunken." In contrast, the oft mentioned "classical type A" eosinophilic inclusion with halo and marginated chromatin was described by Cowdry[6] without reference to the possibility of progressive morphologic changes. Attention is invited to the apt remarks of Scott *et al.*[7] relative to the fallacy of making a narrow definition of the morphology and staining properties of the inclusions of herpes simplex.

It is important to study in some detail another virus infection in which intranuclear inclusions are demonstrated. Anderson and Goodpasture[8] presented histologic evidence of infection of Syrian hamsters by equine abortion virus. Later, Doll and coworkers[9,10] succeeded in adapting various strains to this host. Tissue culture methods have shown that a variety of animal tissues are susceptible to infection.[11] The hepatitis produced in hamsters is striking and uniform, regularly culminating in death in 18 to 24 hours. Classical intranuclear inclusions are present in the great majority of parenchymal cells.

It is the purpose of this study to relate the sequential morphologic

* Aided, in part, by a grant from the Grayson Foundation.
Reported, in part, at the Annual Meeting of the Federation of American Societies for Experimental Biology, Atlantic City, 1956.
Received for publication, September 17, 1956.

changes of a virus-infected cell with certain physical and chemical changes in isolated nuclei. Toward this end morphologic studies and the growth curve will be presented in this paper and in a second, the results of cell fractionation studies.

Materials and Methods

Virus. The Kentucky A strain of equine abortion virus adapted to the hamsters by Doll *et al.*[9] was used in this study, which was initiated with 80th passage hamster liver. Subsequent passages were made at intervals of 1 to 4 weeks. Infected frozen livers were stored at −45° to −50° C. prior to grinding before use.

Inoculation of Animals. Syrian hamsters, 18 to 21 days old and weighing 20 to 30 gm., were used within 24 hours after arrival in the laboratory. Each animal was inoculated intraperitoneally with 1.0 ml. of a 1:5 dilution of freshly ground liver containing approximately 5×10^8 LD_{50} per gm. Controls received a comparable inoculum of normal hamster liver. Following inoculation of five to ten animals, each was sacrificed, with controls, under ether at intervals of 3, 6, 9, 12, and 15 hours. The few remaining infected animals died between 18 and 24 hours and were harvested fresh. The livers taken at those intervals were sampled for sequential histologic hematoxylin and eosin and histochemical (Feulgen) studies, and the bulk was pooled and stored at −45° to −50° C. for cell fractionation procedures to be described in a succeeding issue of this journal.

Histologic and Histochemical Methods. Representative pieces of liver were fixed in neutral 10 per cent formalin and separately in a mixture of 95 per cent Zenker's fluid and 5 per cent glacial acetic acid. Tissues embedded in paraffin were cut at 6 μ and stained with hematoxylin and eosin and by the Feulgen nucleal reaction. Schiff's reagent was prepared according to de Tomasi[12] and the Feulgen reaction was performed by the modified method of Feulgen and Rossenbeck as presented by Pearse.[13] Control sections, both infected and normal, were treated with cold Schiff's reagent without prior hydrolysis to eliminate false positive reactions.

Titration of Virus. In order to determine the amount of virus in the blood and liver, a sufficient number of 3-week-old hamsters were inoculated as previously described (passage 123). Five animals for each interval of time were etherized, the pleural cavity opened, and the heart and great vessels excised, followed by removal of the liver. Small representative pieces of liver were fixed in formalin and stained with

hematoxylin and eosin as a check on the sequential development of inclusions as described above. Homologous material was pooled and stored at −45° to −50° C. until ready for titration. The LD_{50} values were determined by the classical method of Reed and Muench.[14]

Experimental Results

The Sequential Development of Nuclear Changes. Livers of animals from the 110th, 118th, and 124th passages were harvested at intervals of 3, 6, 9, 12, 15, and 18 to 24 hours following inoculation. All tissues were fixed in formalin and Zenker's solutions except for the last passage which was fixed only in formalin.

Hematoxylin and Eosin Sections

Normal Tissue. The microscopic structure of the fixed and stained nucleus of the animal cell is well known and does not merit more than passing comment. The nucleoli were spheroid with a dense, dark-staining, sometimes irregular, thin peripheral ring. The eosinophilic interior of the nucleolus was homogeneous and lighter staining. The chromatin filaments showed some variation and the karyosomes sometimes were quite prominent. Figure 1 demonstrates the architecture of an uninfected cell.

Three Hours after Inoculation. The majority of cells 3 hours after inoculation could not be distinguished from those of the control sections; however, in scattered cells the architecture appeared altered (Figs. 2 and 3). The chromatinic filaments appeared distorted, assuming bizarre configurations, or were sometimes fragmented. In an occasional cell the nuclear margin appeared irregularly thickened. In a few of the altered nuclei, small, irregular, single to multiple, very pale eosinophilic masses were recognized. This precipitable substance was interpreted as being the first evidence of "inclusion material."

Six Hours. At 6 hours the first evidence of hepatitis was noted, with focal areas of necrosis and usually light infiltration by neutrophils and mononuclear cells. The nuclear changes were now more accentuated, with many cells showing disarrangement of the chromatin including margination around the periphery of the nucleus. Inclusion material was more abundant, occurring at single or multiple, light to medium pink-staining areas (Fig. 4), simulating type A inclusions in some cells (Fig. 5). The nucleoli showed some distortion and were unrecognizable in some infected cells.

Nine Hours. The great majority of cells appeared involved 9 hours after inoculation (Figs. 6 and 7). Scattered nuclei showed changes

described at 3 and 6 hours. The majority of nuclei showed what were interpreted as more advanced changes. The outstanding picture concerned inclusions which were larger and optically denser than those seen at 6 hours, in many instances filling the cell and are illustrated in a Feulgen preparation. Scattered inclusions with clear halos ranged from eosinophilic to basophilic, whereas those filling the cells were usually basophilic. In practically all of the cells with "full" inclusions, as well as in many of the others in which the changes were interpreted as being less advanced, the internal nuclear structure was not evident; where the nucleolus was recognized it was often distorted. The irregular thickening of the nuclear periphery by chromatin, was, in general, more pronounced. Both the nucleolus and nucleus have been shown by others to increase in size during virus infection and data concerning this will be presented under a separate heading.

Twelve and 15 Hours. At 12 and 15 hours practically every parenchymal cell showed evidence of infection (Figs. 8, 9, and 10). The great majority of inclusions filled the cell; other forms were relatively infrequent. It was impossible to differentiate the 12 and 15 hour sections, and sometimes differences from the 9 hour period were often equivocal, depending on the field examined. The hepatitis, irrespective of the sections, was variable and focal and usually sparse without noticeable sequential differences. The areas of necrosis were usually lightly infiltrated by neutrophils.

Eighteen to 24 Hours. In the terminal stage of 18 to 24 hours, the livers were harvested as the animals became moribund. The livers from these animals were pooled and, since there is considerable variation in time, the sections were not strictly comparable. The irregular margination was now most pronounced and in some cells suggested a chain of beads (Fig. 11). The nuclei showed somewhat more variation. The majority contained full inclusions, many of which were adherent along a portion of the periphery and others were retracted and more or less resembled the classical type A variety. The inclusions showed some variation in staining. Those that filled the cell were usually, but not invariably, basophilic, while the shrunken inclusions tended to be more eosinophilic, sometimes resembling, except for their larger mass and deeper intensity of staining, the form seen at 6 hours.

It is now appropriate to emphasize that the changes described from 9 to 24 hours pertain to the study of large numbers of cells for any given time period and are more or less generalizations. There was some variation between different pieces of tissue and within one piece of tissue. Each period represented multiple pieces from at least five animals. It is necessary to point out that any given microscopic field may

be entirely composed of full inclusions, another may show an admixture, while quite rarely the classical inclusion may predominate. Casual and limited inspection could easily lead to an erroneous interpretation.

The type of fixative did not seem to make any appreciable difference in the microscopic appearance. It is plausible that fixation results in shrinkage of the inclusion. Cowdry[6] stated that the morphologic character and arrangement of inclusions is not much modified by fixatives, although some, such as Zenker's fluid, produce additional coagulation of the nucleoplasm. Reissig and Melnick[15] have shown that following fixation of tissues infected with herpes B virus in Zenker's fluid and immersion in 80 per cent alcohol for 24 hours, the nuclear substance underwent a slight retraction and appeared as inclusion bodies. The studies of Goodpasture,[1] Scott *et al.*,[2,4] and Dawson,[16] all employing

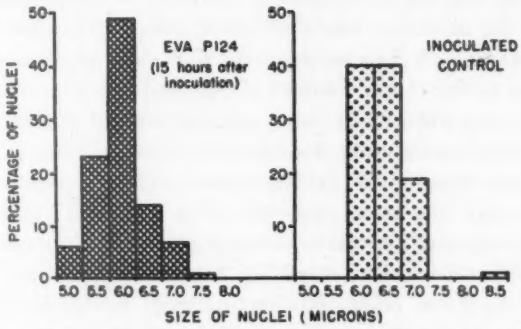

Text-figure 1. Comparison of the size of infected and control nuclei. P 124 represents the number of passages in hamsters.

Zenker's fixative, showed development of full inclusions. It appears that the effect of fixation on inclusions is unsettled and should be investigated further.

Measurement of Nuclei and Nucleoli. Several investigators have noted an increase in size of nuclei[1,16] and nucleoli[2,15] in other virus infections characterized by intranuclear inclusions. In the present study there seemed to be some variation in the size of nuclei which contained inclusions, according to the usual method of inspection with the light microscope. It seemed worth-while to make more objective measurements employing an accurately calibrated ocular micrometer. Comparisons were made of nuclei from infected and control groups 15 hours after inoculation. One hundred inclusion-bearing nuclei and control nuclei selected at random were compared at a magnification of 1,455 (oil). Examination of Text-figure 1 indicates that the two groups show distinct differences, with more than one fourth of the nuclei from the infected animals falling in the size-groups 5.0 and 5.5 μ. In contrast,

none of the cells of the control animal was in this range and nearly all were between 6.0 and 7.0 μ. The difference is obvious (probability $<< 0.001$). No attempt was made to fit normal distribution curves to the data obtained.

For the purpose of studying nucleoli, comparable 6 and 9 hour sections were used. This was necessary since after the latter period the majority of nucleoli are no longer evident. Several hundred nucleoli at each interval were examined without any trend being established. They were difficult to measure since they were very irregular.

Feulgen Nucleal Reaction

Control Sections. Uninfected nuclei (Fig. 12) stained by the Feulgen reaction contained chromatinic threads and karyosomes which stained with varying degrees of intensity. The thin, sometimes irregular periphery of the nucleolus was Feulgen-positive. This finding has been noted by others.[17,18] The background of nuclear sap was colorless to very faintly positive. The method of fixation was not a critical factor although tissues fixed in Zenker's solution seemed slightly more pale than those fixed in formalin, and for this reason all photographs are of formalin-fixed tissue. All Feulgen reactions were performed at the same time with the same reagents under identical conditions. The Feulgen nucleal reaction was arbitrarily graded pale, medium, or dark, or markedly positive, thus avoiding a rather ambiguous attempt at describing shades of color. Nuclear material is classically stained a brilliant purple color.[19]

Infected Sections. Many of the morphologic changes were similar to those seen in the sections stained with hematoxylin and eosin, allowing for differences in color. The description, therefore, will be abbreviated. At 3 hours the precipitable material, as observed in the hematoxylin and eosin preparation, was not evident with the Feulgen reaction. At 6 hours scattered nuclei contained pale to moderately staining inclusion material, which very rarely filled the nucleus (Figs. 13 and 14). The inclusions were generally not so distinct as in comparable hematoxylin and eosin sections. At 9 hours the inclusions (Fig. 15) presented some variation. The scattered type A inclusions were either pale, medium staining or rarely strongly positive. The more numerous full inclusions showed irregular and haphazard variation from pale to strongly positive, the latter being more numerous, without relation to a particular field. At 12 and 15 hours (Figs. 16, 17, and 18) the over-all reaction was more uniform and possibly more intense. The majority of inclusions were full and markedly positive, although a few were relatively

pale. Others of the classical variety presented considerable variation in staining from pale to dark. In general, it often was difficult, if not impossible, to distinguish the 12 to 15 hour preparations from those obtained at 9 hours. At 18 through 24 hours there was a tendency to greater variation in the intensity of staining of the inclusions. Shrunken inclusions were generally more pale, whereas the full variety maintained more intensity of color, though some were pale to almost colorless.

It should be re-emphasized that the changes from 9 to 24 hours are often indistinguishable and that the descriptions are at best broad generalizations, subject to the usual interpretations of a morphologic study.

Titration of Virus. Frozen liver and blood from passage 123 and blood from passage 134, obtained from animals sacrificed at previously stated intervals, were ground and diluted with physiologic saline solution. Four animals were used for each dilution. No deaths were recorded after 5 days. The data are summarized in Table I. It should

TABLE I

Comparison of Virus Content of Liver and Whole Blood

Time	Blood		Liver
	P 124	P 135	P 124
1 hour	4.0	Not done	Not done
3 hours	3.5	5.2	3.7
6 hours	Not done	4.5	5.3
9 hours	5.0	6.0	6.8
12 hours	5.7	7.0	8.0
15 hours	Not done	7.0	8.0

The results of hamster titrations are expressed as the negative log of the LD_{50}. P represents the passage number.

be kept in mind that the passages listed really represent material from the previous passage and the results indicate the virus content of that material. The figures given for the liver titration were quite representative of three different passages and are in agreement with those of Doll.[20] In Text-figure 2 a portion of the data is presented for emphasis and a representative liver titration is compared with whole blood. The amount of virus in the blood of P 123 as determined in P 124 is not indicated as several points are missing and graphing the data would give a false impression. In the one instance in which blood was titrated at 1 hour after intraperitoneal inoculation, the LD_{50} was surprisingly high and indicates quite rapid absorption. Probably the LD_{50} after 6

hours, in any case, represents a mixture of old absorbed and freshly replicated virus. It can be seen that viremia was present throughout the periods studied. It is interesting to note that at 6 hours the titer of the blood fell while that of the liver rose from 3 to 6 hours. After 6

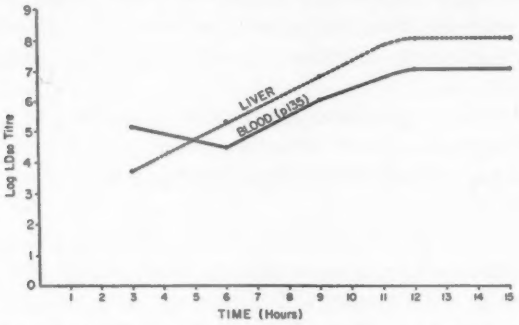

Text-figure 2. Graphic representation of the virus content of liver and whole blood. Data derived from Table I.

hours the titer of the blood and liver increased uniformly in almost parallel manner, the LD_{50} reaching a maximum and levelling off at 12 hours. This is in agreement with Doll,[20] whose data showed no significant change from 12 to 24 hours.

Sections from the donor animals (P 123 and P 134) obtained at the intervals previously noted were stained with hematoxylin and eosin and revealed the same sequential changes as previously noted under Experimental Results.

Discussion

The sequential development of inclusions of equine abortion virus is consistent in some degree with the findings of other workers.[1,15] Practically the same sequence of development was noted by Scott *et al.*[4] with the virus of herpes simplex in tissue culture, which contrasts with the development of the same virus in the chorioallantoic membrane.[2] In this latter study,[2] the earliest inclusion to appear (10 to 16 hours after inoculation) completely filled the nucleus of the infected cell; later, shrunken inclusions were evident.

In the present study a definite relationship was found to exist between the morphologic changes in the nucleus and the appearance of progeny virus both in the liver and in the blood of infected animals. Inclusion material was first noted at 3 hours and definite inclusions were observed at 6 hours following inoculation. This coincides with the rise in titer of hepatic virus from 3 to 6 hours. In contrast, the titer in the blood fell from 3 to 6 hours, but regrettably this latter datum is the

result of only one titration. If infectious virus had been replicated between 3 and 6 hours and not yet released, the mechanical rupture of the cells by freezing and grinding would account for the rise in titer.

If one accepts as a fact that the increase in virus in the liver from 3 to 6 hours indicates viral replication, then this phenomenon took place in cells in which the nuclei contained inclusions which were relatively small and poorly organized. Thereafter, inclusion material rapidly increased in amount, usually filling the cell from 9 to 12 hours. This coincided with the maximum titer of virus in blood and liver. Subsequently, there was little change in the growth curve or in the appearance of inclusions. It is possible that the Feulgen-positive inclusion would have become negative if the animals had survived longer. Crouse *et al.*[2] observed that in the chick chorioallantoic membrane infected with the virus of herpes simplex the inclusions were strongly Feulgen-positive at 24 hours and negative inclusions did not appear until 30 hours after inoculation.

The question arises as to the composition of the inclusion. According to the generally accepted interpretation of the Feulgen reaction,[20] the inclusion should contain desoxyribose nucleic acid (DNA). The possibility obtains that much of the DNA is somehow redistributed throughout the inclusion.

Admittedly, there is no evidence as far as this virus infection is concerned of the relationship of the intranuclear inclusion to the infectious units or to the site of replication. Electron microscopy with other virus infections does not elucidate this point as intranuclear inclusions apparently have not been visualized by this method of study.[15,21,22]* These excellent studies of thin sections of infected cells revealing the distribution of elementary bodies as yet do not define the relationship, if any, to the intranuclear inclusion. It is apparent from the present study that, even if production of infectious virus is related in some way to the intranuclear inclusion, release of virus does not significantly alter the appearance of the inclusion after 12 hours and the nucleus continues to be filled with Feulgen-positive material. It may be questioned that this indicates that release and production of virus material is in balance. In this connection experiences with another virus are worth summarizing. Feulgen-positive inclusions of herpes simplex become negative with time.[2,4,23] These late inclusions contain no nucleoprotein

* Since this article was submitted for publication, a significant paper by Bloch, Morgan, Godman, Howe, and Rose has appeared in the *J. Biophys. & Biochem. Cytol.*, 1957, 3, 1–8. These investigators have demonstrated by electron microscopy that in HeLa cells infected with adenovirus, the nucleus contains crystalline aggregates which are composed of virus particles. These crystals are Feulgen positive.

and therefore presumably no virus.[5] Depending on the stage of infection, there is apparently an association of the virus with the nucleus as determined by cell fractionation methods and subsequent disruption with M NaCl.[5] In late stages of infection there is no demonstrable virus associated with the nucleus.[5,24,25] It has been stated that the inclusions are not the virus of herpes.[24] The opposite view is taken by others who present evidence that the herpetic inclusion represents a virus colony inside a cellular matrix.[23]

Finally, it does not seem clear from the existing evidence that cytochemical changes in the intranuclear inclusion necessarily indicate liberation of virus or that particles of virus can be assumed to contain DNA or that viral inclusions represent virus colonies. It is plausible to consider the inclusion at least in part as a product of altered cellular metabolism, perhaps irrespective of the site of replication of the virus.

Certain chemical changes induced by viral infection will be presented in a second paper of this series.

Summary

A sequential study is reported of the morphologic changes occurring in hepatic parenchymal cells of the hamster following infection with equine abortion virus. At 3 hours the nuclei show disarrangement of the chromatinic network and small accumulations of inclusion material appear. With the development of the infection, there is progressive accumulation of Feulgen-positive material, filling the majority of nuclei in 9 to 12 hours. Subsequently, there is little change in the morphologic detail.

The virus content of blood and liver reaches a maximum from 9 to 12 hours, concomitant with the development of nuclear changes.

REFERENCES

1. Goodpasture, E. W. Intranuclear inclusions in experimental herpetic lesions of rabbits. *Am. J. Path.*, 1925, 1, 1–10.
2. Crouse, H. V.; Coriell, L. L.; Blank, H., and Scott, T. F. M. Cytochemical studies on the intranuclear inclusion of herpes simplex. *J. Immunol.*, 1950, 65, 119–128.
3. Scott, T. F. M.; Coriell, L. L.; Blank, H., and Gray, A. The growth curve of the virus of herpes simplex on the chorioallantoic membrane of the embryonated hen's egg. *J. Immunol.*, 1953, 71, 134–144.
4. Scott, T. F. M.; Burgoon, C. F.; Coriell, L. L., and Blank, H. The growth curve of the virus of herpes simplex in rabbit corneal cells grown in tissue culture with parallel observations on the development of the intranuclear inclusion body. *J. Immunol.*, 1953, 71, 385–396.
5. Gray, A., and Scott, T. F. M. Some observations on the intracellular localization of the virus of herpes simplex in the chick embryo liver. *J. Exper. Med.*, 1954, 100, 473–484.

6. Cowdry, E. V. The problem of intranuclear inclusions in virus diseases. *Arch. Path.*, 1934, **18**, 527–542.
7. Scott, T. F. M.; Blank, H.; Coriell, L. L., and Crouse, H. Pathology and Pathogenesis of the Cutaneous Lesions of Variola, Vaccinia, Herpes Simplex, Herpes Zoster, and Varicella. In: The Pathogenesis and Pathology of Viral Diseases, Kidd, J. G. (ed.). Columbia University Press, New York, 1950, pp. 74–98.
8. Anderson, K., and Goodpasture, E. W. Infection of newborn Syrian hamsters with the virus of mare abortion (Dimock and Edwards). *Am. J. Path.*, 1942, **18**, 555–561.
9. Doll, E. R.; Richards, M. G., and Wallace, M. E. Adaptation of the equine abortion virus to suckling Syrian hamsters. *Cornell Vet.*, 1953, **43**, 551–558.
10. Doll, E. R.; Bryans, J. T.; McCollum, W. H., and Crowe, E. W. Propagation of equine abortion virus in Syrian hamsters. *Cornell Vet.*, 1956, **46**, 68–82.
11. Randall, C. C. Propagation of equine abortion virus in tissues of other animals. *Federation Proc.*, 1954, **13**, 441.
12. de Tomasi, J. A. Improving the technic of the Feulgen stain. *Stain Technol.*, 1936, **11**, 137–144.
13. Pearse, A. G. E. Histochemistry: Theoretical and Applied. Little, Brown & Co., Boston, 1953, pp. 425–426.
14. Reed, L. J., and Muench, H. A simple method of estimating fifty per cent endpoints. *Am. J. Hyg.*, 1938, **27**, 493–497.
15. Reissig, M., and Melnick, J. L. The cellular changes produced in tissue cultures by herpes B virus correlated with the concurrent multiplication of the virus. *J. Exper. Med.*, 1955, **101**, 341–352.
16. Dawson, J. R., Jr. Herpetic infection of the chorio-allantoic membrane of the chick embryo. *Am. J. Path.*, 1933, **9**, 1–6.
17. Vincent, W. S. Structure and chemistry of nucleoli. *Internat. Rev. Cytol.*, 1955, **4**, 269–298.
18. Davidson, J. N., and Waymouth, C. Unpublished results, 1946. (Cited by Davidson, J. N. The distribution of nucleic acids in tissues. Symposia of the Society for Experimental Biology, 1947, no. 1, 77–85.)
19. Davidson, J. N. The Biochemistry of the Nucleic Acids, Methuen's Monographs, John Wiley & Sons, Inc., New York, 1953, ed. 2, p. 66.
20. Doll, E. R. Personal communication.
21. Morgan, C.; Ellison, S. A.; Rose, H. M., and Moore, D. H. Structure and development of viruses as observed in the electron microscope. I. Herpes simplex virus. *J. Exper. Med.*, 1954, **100**, 195–202.
22. Bang, F. B. Cellular changes in the chick chorio-allantoic membrane infected with herpes simplex and vaccinia. A study with thin sections for the electron microscope. *Bull. Johns Hopkins Hosp.*, 1950, **87**, 511–547.
23. Wolman, M., and Behar, A. Cytochemical evidence for the nature of herpes simplex inclusion bodies. *J. Infect. Dis.*, 1952, **91**, 63–68.
24. Francis, T., Jr., and Kurtz, H. B. The relation of herpes virus to the cell nucleus. *Yale J. Biol. & Med.*, 1949–50, **22**, 579–587.
25. Ackermann, W. W., and Kurtz, H. B. The relation of herpes virus to host cell mitochondria. *J. Exper. Med.*, 1952, **96**, 151–157.

[*Illustrations follow*]

LEGENDS FOR FIGURES

All preparations were fixed in formalin and stained with hematoxylin and eosin (Figs. 1 to 11) or by the method of Feulgen (Figs. 12 to 18). Certain representative features are marked with arrows.

FIG. 1. Uninfected control liver. One nucleolus is in relatively sharp focus with dark staining periphery. Oil immersion. × 1,134.

FIG. 2. Three hours after inoculation. The chromatin is conspicuously arranged in a figure which divides the nucleus into compartments in which there are ill-defined, pale-staining areas. The periphery of the nucleus is irregularly thickened. Oil immersion. × 1,134.

FIG. 3. Same preparation as that from which Figure 2 was taken. In various nuclei the chromatin is either finely or coarsely divided and may be interspersed with pale-staining, presumably inclusion material. Oil immersion. × 1,134.

FIG. 4. Six hours following inoculation. In addition to the changes seen at 3 hours (unmarked), it may be noted that in the nuclei marked by arrows the inclusion material is more conspicuous, stains more densely, and is less dispersed. Oil immersion. × 1,134.

FIG. 5. Same preparation as that from which Figure 4 was taken. A so-called typical inclusion is seen in the center of the field. × 598.

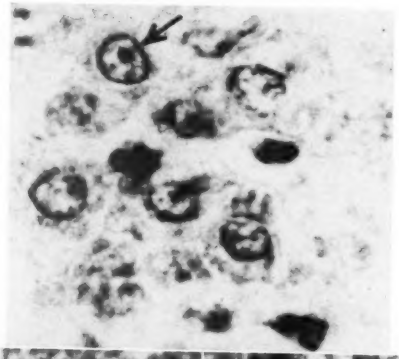

1

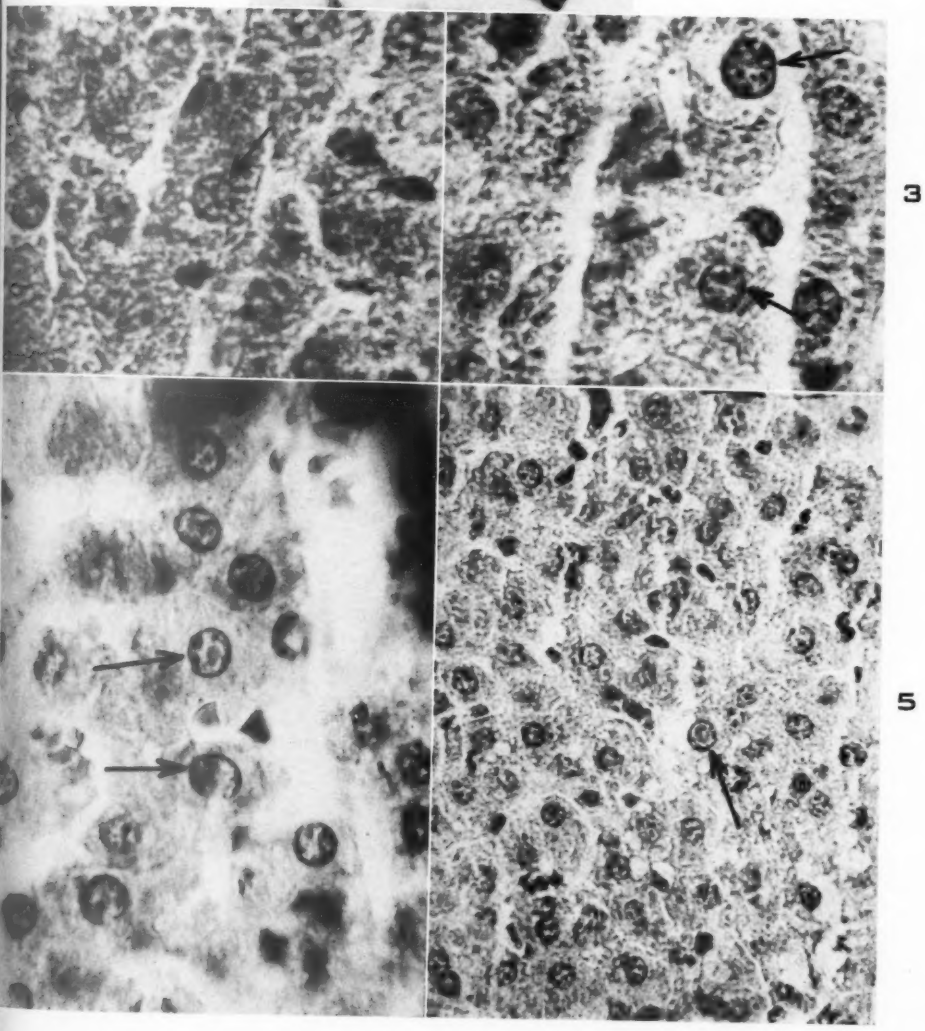

3

5

FIGS. 6 and 7. Nine hours after inoculation. Every cell shows some change with great variation in the appearance of infected cells, varying from changes seen at 3 hours to those in which the nucleus is filled with inclusion material (denoted by arrow). Margination of chromatin is conspicuous. Oil immersion. × 1,134. The more typical reaction seen at 9 hours is illustrated in a Feulgen preparation (Fig. 15).

FIG. 8. Twelve hours after inoculation. Most of the nuclei are filled with inclusion material. Oil immersion. × 1,134.

FIG. 9. Fifteen hours after inoculation. All nuclei contain full inclusions. Oil immersion. × 1,134.

FIG. 10. Same preparation as that from which Figure 9 was taken. A different field shows an unusual variety of inclusions for this period. Oil immersion. × 1,134.

FIG. 11. Twenty-four hours after inoculation. Irregular margination of chromatin around the periphery of the nucleus is conspicuous. Pink-staining inclusion material is interspersed between the beads of chromatin and on two sides is attached to an apparently shrunken inclusion. Oil immersion. × 1,455.

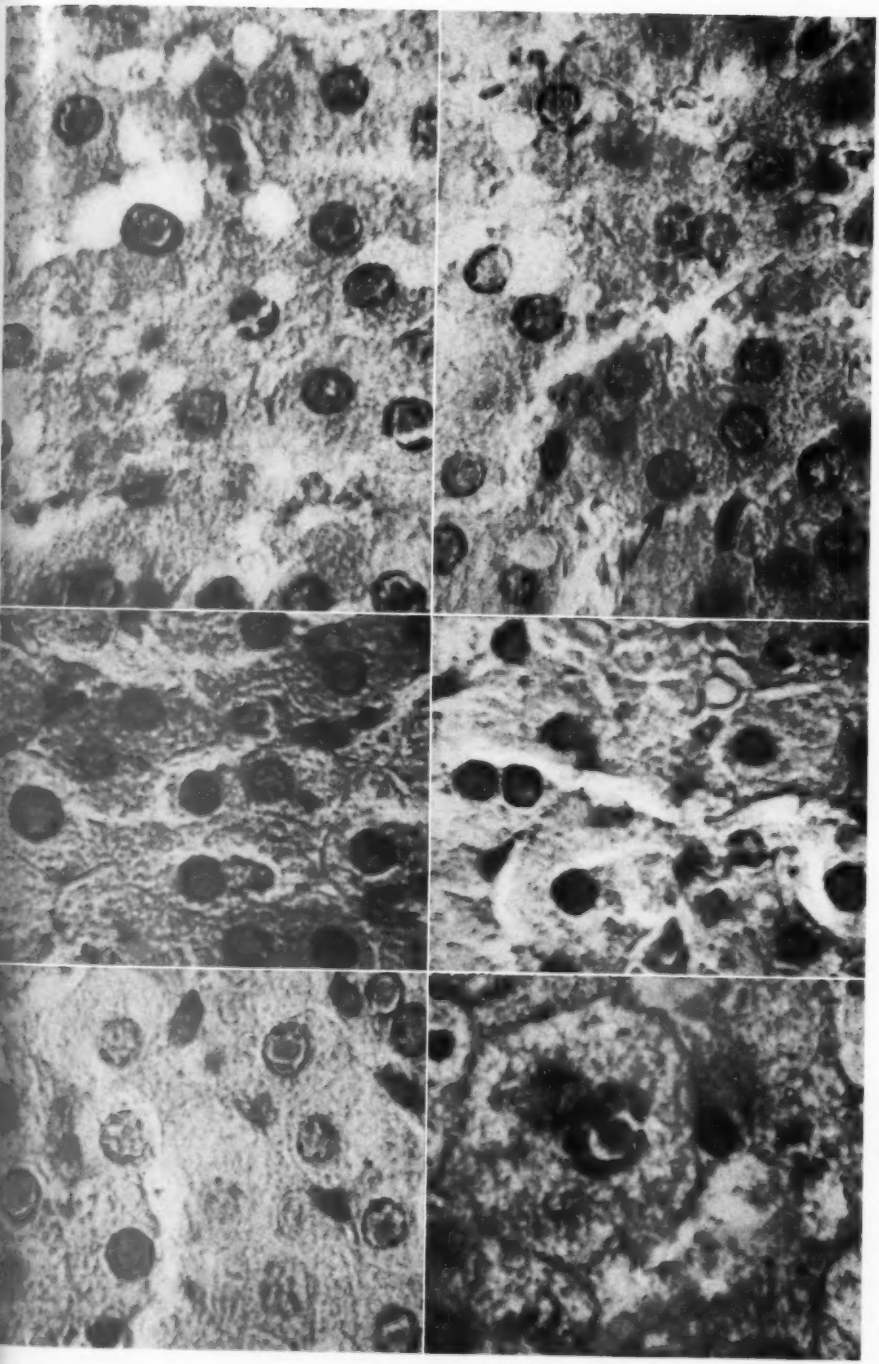

7

9

11

FIG. 12. Uninfected control liver. One nucleolus is in sharp focus. The Feulgen-positive nucleoli-associated material is irregularly distributed around the periphery. Oil immersion. × 1,134.

FIG. 13. Six hours after inoculation. Some of the nuclei show accumulation of inclusion material mingled with chromatin. In a large nucleus the changes are in sharp focus and margination of chromatin is conspicuous. Oil immersion. × 1,134.

FIG. 14. Same preparation as that from which Figure 13 was taken. The nucleus in the extreme upper left contains an example of an "incomplete" inclusion. The arrow indicates a moderate staining, rare (for this period) full inclusion, partially retracted along a portion of the circumference. Oil immersion. × 1,134.

FIG. 15. Nine hours after inoculation. The majority of nuclei are filled with inclusion material. There are scattered pale to dark staining inclusions which do not fill the nucleus. × 598.

FIG. 16. Fifteen hours after inoculation. A number of markedly positive inclusions completely filling the nucleus are sharply in focus. Oil immersion. × 1,134.

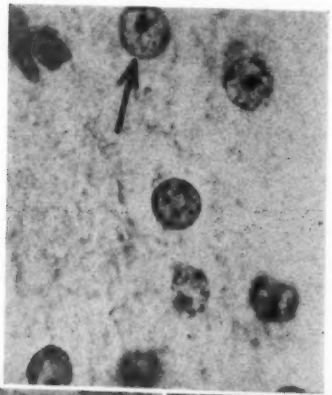

12

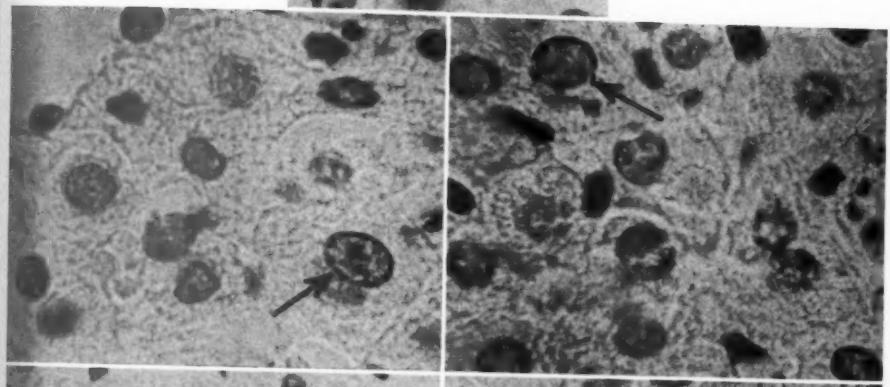

14

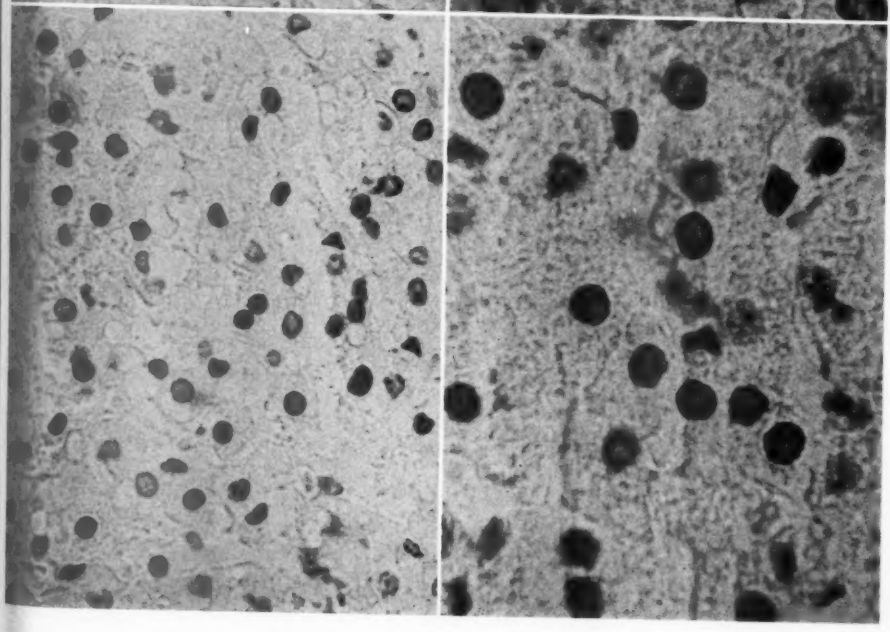

16

FIG. 17. Same preparation as that from which Figure 16 was taken. Most of the nuclei are filled with Feulgen-positive material. The arrows indicate the classical variety which are also strongly positive. Oil immersion. × 1,134.

FIG. 18. Same preparation as that from which Figure 16 was taken. The arrows point out pale-staining inclusions, which are relatively infrequent.

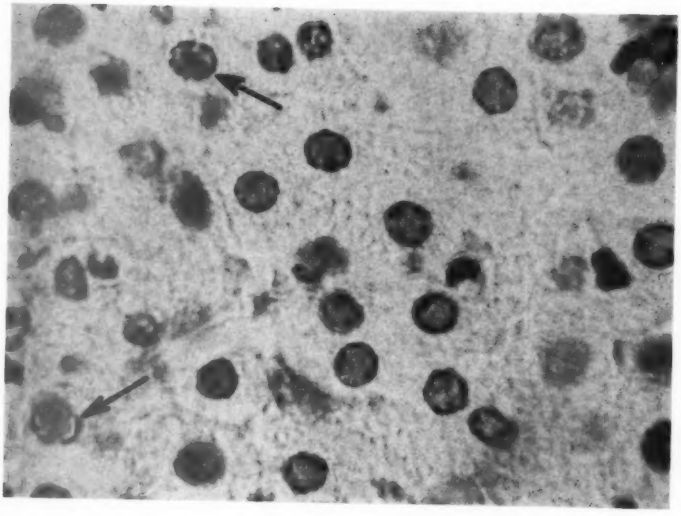

17

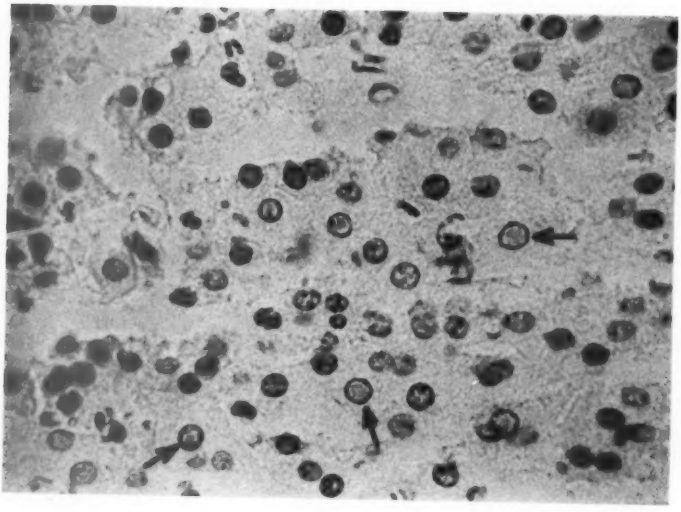

18

HISTOPATHOLOGY OF SWIMMERS' ITCH

II. Some Observations on the Pulmonary Lesions in the Unsensitized Mouse*

Peter J. Batten, Jr., M.D.

From the Departments of Pathology, St. Vincent's Hospital, Portland, Ore., and University of Michigan Medical School, Ann Arbor, Mich.

Since Cort[1] (1928) first demonstrated that various species of schistosome cercariae were the causative agents of swimmers' itch, Macfarlane[2] and Olivier[3] have shown that the dermatitis produced by these parasites is a sensitization phenomenon. Kagan and Meranze[4] and Batten[5] further demonstrated that only those cercariae which became immobilized within the epidermis of the host were capable of eliciting this papular response. They also were able to trace the fate of the cercariae that penetrated into the dermis and subcutaneous tissues; and it was found that in these locations the cercariae did not produce a dermatitis.

In 1941, Penner,[6] working with monkeys exposed to *Schistosomatium douthitti,* first demonstrated that schistosome cercariae were able to migrate to the lungs of abnormal hosts. Olivier,[7-9] in a series of papers (1949, 1952, and 1953), and Olivier and Weinstein[10] found pulmonary hemorrhages in laboratory animals which had been exposed to the cercariae of schistosomes of birds and muskrats. Kagan[11] also reported evidence of hemorrhage and damage in the lungs of monkeys exposed to cercariae of *S. douthitti.*

The pulmonary lesions in man which are caused by the migration of larvae of the three species of schistosomes of humans, *Schistosoma mansoni, Schistosoma japonicum,* and *Schistosoma haematobium,* consist of petechial hemorrhages and focal areas of leukocytic infiltration. The pulmonary lesions produced by the cercariae of these three schistosomes in laboratory animals have been described also. However, the microscopic pulmonary lesions produced by schistosome cercariae in laboratory animals have not been described.

The present paper describes the pulmonary lesions in the unsensitized white mouse after exposure to two species of schistosomes: *S. douthitti,* which reaches maturity in the mouse, and *Gigantobilharzia huronensis,* a parasite of birds. It was believed that this study would afford a comparison of the defense mechanisms against cercariae in the normal and abnormal hosts.

* Supported, in part, by a grant from the University of Michigan Medical School.
Received for publication, October 18, 1956.

Materials and Methods

White mice were exposed to the cercariae of *S. douthitti* and *G. huronensis*. A description of the collection and maintenance of infected snails, and of the exposure of the mice to the cercariae has been reported in a previous paper.[5] At necropsy, the lungs were examined in the fresh condition, and were then preserved in formalin. Portions of the lungs were prepared for microscopic examination by standard techniques.

Results

Pulmonary Lesions Produced by S. douthitti

The gross findings in the present investigation agree with, and confirm, those described by Olivier for *S. douthitti*[8] and for the three bird schistosomes, *Trichobilharzia ocellata, Trichobilharzia colae,* and *Trichobilharzia physellae*.[9] Hemorrhages were noted in the lungs of mice 20 hours after exposure, although more hemorrhage was found between the second and sixth days. At first the lesions were bright red, had distinct margins, and were of petechial size. They became progressively darker, the margins became less discrete, and the areas of hemorrhage became confluent, even to the extent of involving an entire lobe or lung. Colorless nodules, as described by Olivier, were observed infrequently between the fifth and twelfth days following exposure.

The first microscopic evidence of cercarial invasion of the lungs was noted 30 minutes after exposure, consisting of several focal areas of congestion of the interalveolar capillaries. A few alveoli contained erythrocytes but, as in the other lesions, there was little if any infiltration of leukocytes into the alveoli. The capillaries became progressively more congested, with a maximal degree of congestion being reached 4 days following exposure, and then a slow return to normal size. The alveolar hemorrhage increased and reached maximal intensity during the third to fifth days, when the greatest number of cercariae was observed. Tissue histiocytes containing hemosiderin were noted in the areas of hemorrhage 4 hours following exposure and persisted as long as 3 weeks after exposure. Many of the bronchioles were filled with blood during the second to the tenth days.

Sections of lung from one mouse exposed 2½ days previously showed a moderate perivascular and peribronchiolar infiltration with neutrophils; inasmuch as this inflammatory change was observed in a single animal, it was considered that the finding was probably unrelated to the cercarial infection.

All cercariae seen in the sections of lung were believed to have been

alive at the time of necropsy, as they stained well. Cercariae were observed in the alveoli and in the capillaries. No cellular reaction to the parasites was seen, in contrast to the response in the skin.[5]

Beginning on the tenth or twelfth day and continuing throughout the third week there was a diffuse subacute interstitial pneumonitis.

Pulmonary Lesions Produced by G. huronensis

The pulmonary lesions in mice exposed to *G. huronensis* were similar to those found following infection with *S. douthitti.* In only one experimental animal (exposed 2 days before), however, was evidence of gross hemorrhage seen. This consisted of a small bright red petechial hemorrhage with discrete margins. Evidence of interalveolar capillary congestion, and alveolar and bronchiolar hemorrhage was first noted 2 hours after exposure. Tissue histiocytes containing hemosiderin were observed 10 hours after exposure. No cercariae were observed in any of the sections of lungs, nor was there any evidence of cellular infiltration. Several animals showed focal areas of interstitial pneumonitis 10 days to 3 weeks after exposure.

The paucity of pulmonary changes in animals exposed to *G. huronensis* is attributed to the fact that large numbers of cercariae were previously noted[5] to have been destroyed in the dermis and subcutaneous tissues. That the pulmonary damage was caused by the cercariae is indicated by the similarity of these lesions to those produced by *S. douthitti.*

Discussion

Abundant information is available in the literature indicating that the larvae of schistosomes produce hemorrhages in the lungs of the definitive human and other animal hosts during migration. Olivier,[9] in his description of the migration of avian schistosomes in laboratory animals, summarized the criteria necessary for the establishment of the relationship between the pulmonary damage and the cercariae.

The gross pathologic findings of the present investigation agree with those detailed by Olivier.[8] The microscopic changes agree with those described by Faust and Meleney[12] in mice and rabbits exposed to cercariae of *S. japonicum.* With one exception, reports in the literature indicate that there is no cellular reaction to the larvae in the lungs. Olivier,[9] in a legend on a photomicrograph (Plate II, Fig. 4), noted that a cellular reaction surrounded a worm in the lung of a hamster exposed 4 days before necropsy. In the text, however, he stated: "Sectioned nodules from a hamster lung contained schistosomes which

were either moribund or dead." It can be inferred that the cellular response noted in this instance was the reaction to a dead worm.

The cercariae of *S. douthitti* and *G. huronensis* may become immobilized and destroyed within the epidermis, dermis, and subcutaneous tissues of mice, the host response consisting of edema and a cellular exudate.[5] It is apparent from the present investigation, however, that the cercariae are able also to migrate through the lungs without producing an inflammatory reaction. The capillary congestion, hemorrhage, hemosiderin-laden histiocytes, and interstitial pneumonitis are all believed to be due to the migration of the worms from the capillaries through the pulmonary tissue. These findings, as well as the complete absence of dead worms in the sections of lungs, indicate that cercariae which have passed the skin barrier are able to migrate through the lungs without eliciting an inflammatory reaction.

Summary

The gross and microscopic changes in the lungs of mice exposed to cercariae of *Schistosomatium douthitti* and *Gigantobilharzia huronensis* are very similar. There was congestion of the interalveolar capillaries, as well as alveolar and bronchiolar hemorrhage. Tissue histiocytes containing hemosiderin were a prominent feature in those areas where extensive hemorrhage occurred. Many cercariae were observed in the alveoli and in the capillaries, but there was no demonstrable cellular reaction to these parasites. There were no dead cercariae observed in the lungs. There was a diffuse interstitial pneumonitis present during the second and third weeks following exposure.

REFERENCES

1. Cort, W. W. Schistosome dermatitis in the United States (Michigan). *J. A. M. A.*, 1928, **90**, 1027–1029.
2. Macfarlane, W. V. Schistosome dermatitis in New Zealand. Part II. Pathology and immunology of cercarial lesions. *Am. J. Hyg.*, 1949, **50**, 152–167.
3. Olivier, L. J. Schistosome dermatitis, a sensitization phenomenon. *Am. J. Hyg.*, 1949, **49**, 290–302.
4. Kagan, I. G., and Meranze, D. R. The histopathology of immune and normal mouse skin exposed to cercariae of *Schistosomatium douthitti* (Trematoda: Schistosomatidae). *J. Infect. Dis.*, 1955, **97**, 187–193.
5. Batten, P. J., Jr. The histopathology of swimmers' itch. I. The skin lesions of *Schistosomatium douthitti* and *Gigantobilharzia huronensis* in the unsensitized mouse. *Am. J. Path.*, 1956, **32**, 363–377.
6. Penner, L. R. The possibilities of systemic infection with dermatitis-producing schistosomes. *Science*, 1941, **93**, 327–328.

7. Olivier, L. J. The fate of dermatitis-producing schistosome cercariae in laboratory animals. (Abstract.) *J. Parasitol.*, 1949, **35**, Suppl., 30–31.

8. Olivier, L. J. A comparison of infections in mice with three species of schistosomes, *Schistosoma mansoni, Schistosoma japonicum* and *Schistosomatium douthitti*. *Am. J. Hyg.*, 1952, **55**, 22–35.

9. Olivier, L. J. Observations on the migration of avian schistosomes in mammals previously unexposed to cercariae. *J. Parasitol.*, 1953, **39**, 237–246.

10. Olivier, L. J., and Weinstein, P. P. Experimental schistosome dermatitis in rabbits. *J. Parasitol.*, 1953, **39**, 280–291.

11. Kagan, I. G. Experimental infections of Rhesus monkeys with *Schistosomatium douthitti* (Cort, 1914). *J. Infect. Dis.*, 1953, **93**, 200–206.

12. Faust, E. C., and Meleney, H. E. Studies on *Schistosomiasis japonica*. *Am. J. Hyg.*, Monographic Series no. 3, 1924, 339 pp.

[*Illustrations follow*]

LEGENDS FOR FIGURES

The photomicrographs were taken from sections of lungs of mice which had been exposed to cercariae of *Schistosomatium douthitti*. These sections were fixed in formalin and stained with hematoxylin and eosin. × 530.

FIG. 1. Living cercaria in alveolus of lung (3 days after exposure). No evidence of host reaction.

FIG. 2. Living cercaria in arteriole of lung (3 days after exposure). No evidence of host reaction.

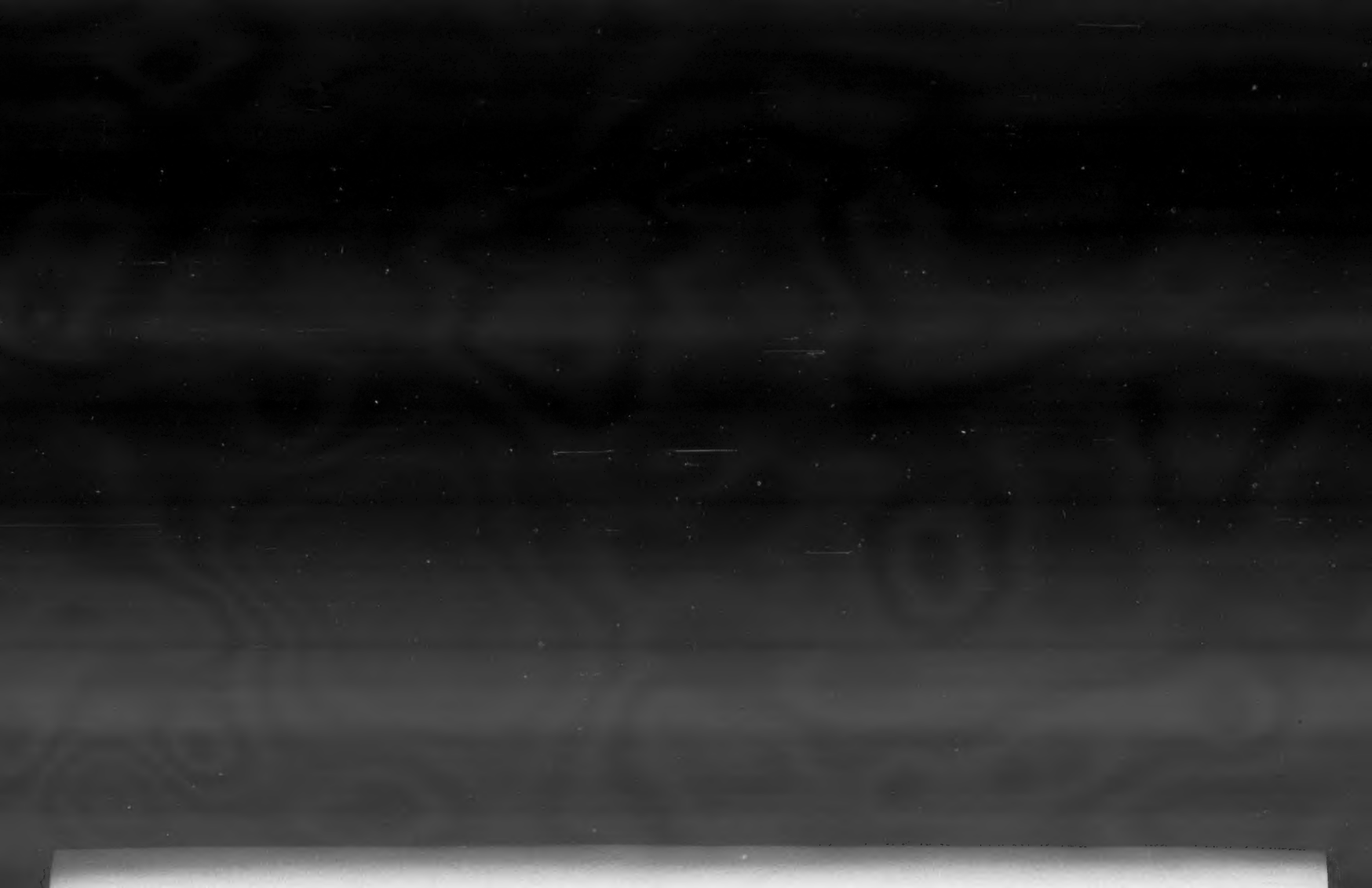

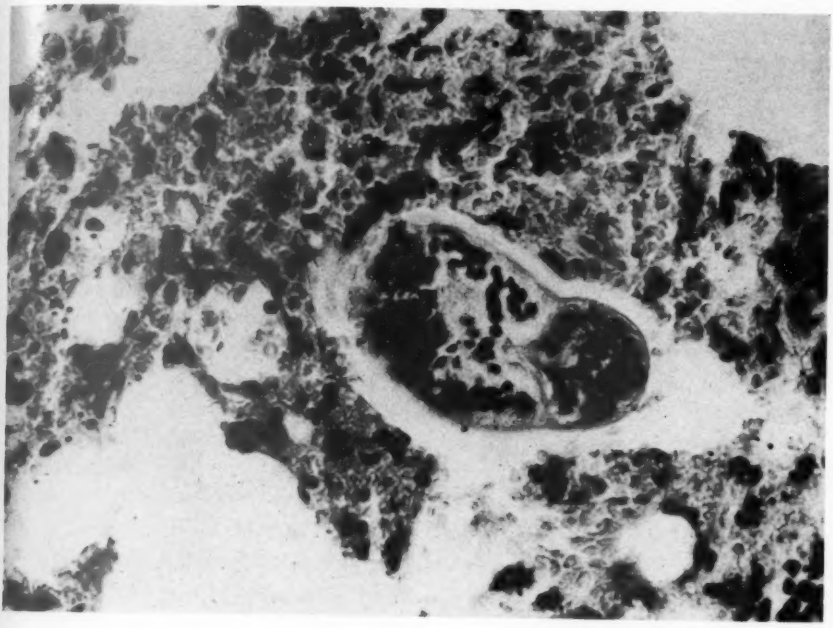

1

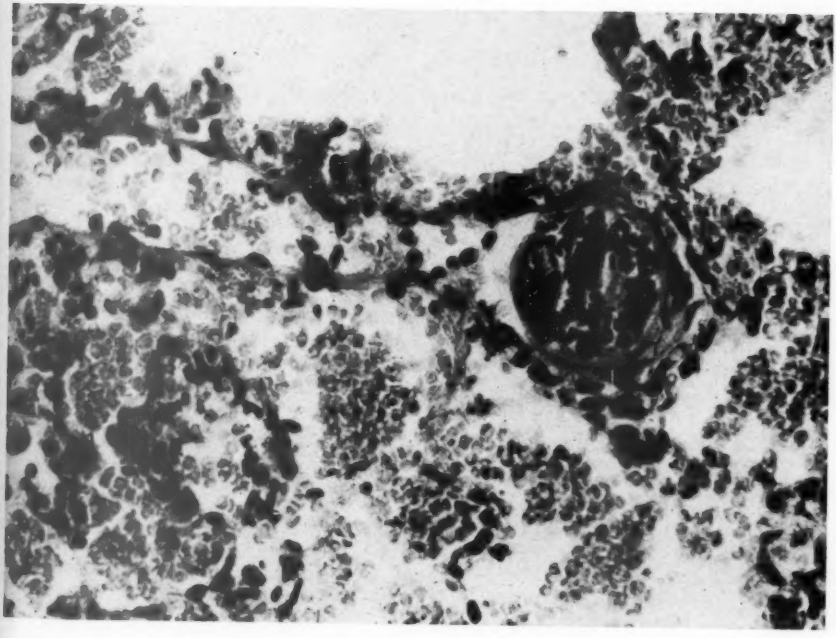

2

CYTOCHEMICAL STUDIES DURING THE DIFFERENTIATION OF NORMAL HUMAN MONOCYTES IN VITRO*

MILTON N. GOLDSTEIN, Ph.D., and TERENCE MCCORMICK, B.S.
From the Department of Biology, Roswell Park Memorial Institute, Buffalo 3, N.Y.

Cytochemical observations indicate that during the formation of macrophages and giant cells *in vitro* and *in vivo*, an active synthesis or accumulation of proteins, nucleic acids, polysaccharides, and enzymes occurs. Some investigators have attempted to correlate the increase in these components with the functional potentialities of the monocytes and the cells derived from them—the macrophages and giant cells.[1-4] Cytochemical studies of chicken monocytes, macrophages, and giant cells in tissue culture have been reported,[2] but no similar studies have been done on human monocytes, except for desoxyribose nucleic acid.[5] Although there are cytochemical studies of inflammatory lesions in humans,[6-10] they are not detailed because of the obvious difficulties involved in obtaining adequate specimens for study during the early stages of inflammation.

Since a simple method was available for the induction of changes in the monocytes which morphologically look like those seen *in vivo*,[11] it was of interest to learn more about the chemical changes occurring in the cells during culture and to determine whether there was any correlation between these changes and those that occur *in vivo* in inflammatory lesions in man.

MATERIAL AND METHODS

Fragments of buffy coat from normal human peripheral blood were explanted on the surface of perforated cellophane in D-35 Carrel flasks in the manner previously described.[11] In addition, some explants were embedded in a thin clot of human plasma formed over the surface of the cellophane. One ml. of a feeding solution consisting of two parts Gey's solution and one part pooled human serum was added to the flasks, which were then stoppered and incubated at 36° C. After varying periods of incubation, from 4 to 160 hours, the disks of cellophane with the adherent cells were washed with Gey's solution, removed from the flasks, fixed and stained.

Necropsy material which had been fixed in buffered 10 per cent formalin was used for cytochemical studies of inflammatory lesions. Paraffin sections, 10 μ in thickness, of liver and lymph nodes con-

* This study was supported in part by the Dorothy and Louis Rosensteil Foundation.
Received for publication, August 4, 1956.

taining granulomas in various stages of organization were used. Although the method of fixation limited the number of cytochemical procedures performed, it was possible to add to the data already recorded in the literature.

Staining Procedures

The method of Manheimer and Seligman[12] was used for the demonstration of alkaline phosphatase. Acid phosphatase was demonstrated by the method of Seligman and Manheimer.[13] Cells which were cultivated for 24 hours or less were incubated as long as 24 hours in the substrate mixture. After 24 hours of cultivation, the cells were incubated for 3 to 5 hours in the substrate. Material for the demonstration of both alkaline and acid phosphatases was fixed in either acetone or 10 per cent neutral formalin at 10° C. for 12 to 24 hours.

Lipids were stained with a saturated solution of Sudan black B in 70 per cent alcohol or with Herxheimer's mixture consisting of acetone, 70 per cent alcohol, and Sudan IV for 2 minutes[14] after fixation in 10 per cent neutral formalin for 24 hours. Baker's acid hematein method[15] was used to demonstrate phospholipids in cultures fixed in 10 per cent formalin-calcium, with controls fixed in dilute Bouin's solution.

Polysaccharides were demonstrated by the periodic acid-Schiff (PAS) reaction[16] after fixation in Carnoy's solution (3 parts alcohol and 1 part acetic acid) or in 10 per cent neutral formalin for 20 minutes. Sections of necropsy material also were stained by the PAS procedure. Some cultures, after varying periods of cultivation *in vitro*, as well as sections of necropsy material, were exposed to (a) chloroform/methanol (1:1) at 60° C. for 24 hours, (b) hyaluronidase* (bovine testis), 1 mg. per ml. in 0.9 per cent saline solution for 3 hours at 37° C. with controls, (c) saliva (three changes) during 1 hour of incubation at 37° C., and (d) malt diastase 1/1000 in phosphate buffer at pH 6.0 for 1 hour at 37° C.[14] Acetylation for 2 hours according to the method described by Lillie[14] with the technique for deacetylation was performed on cultured cells and tissues stained by the PAS technique.

A 0.01 per cent aqueous solution of toluidine blue was applied to cultures and sections for 5 minutes. The tissues were observed immediately after staining, but more permanent mounts were prepared by placing the stained material in 5 per cent ammonium molybdate and

* Obtained from the Worthington Biochemical Corp., Freehold, N.J.

1 per cent potassium ferrocyanide for 2 minutes before dehydrating and mounting in Permount.[17]

The methyl green pyronine technique modified from Trevan and Sharrock[10] was used as an indicator of ribose nucleic acid. Crystalline ribonuclease, 1.0 mg. per ml. in glass distilled water at 37° C. for 1 hour, was used to extract the ribose nucleic acid.

Observations

As previously noted,[11] most of the polymorphonuclear leukocytes and lymphocytes degenerated within the first 48 hours of cultivation. The observations, therefore, will be concerned with the monocytes and the cells which differentiated from them in tissue culture.

Alkaline and Acid Phosphatases

Alkaline phosphatase could not be demonstrated in monocytes, macrophages, giant cells, or in fibroblast-like cells at any period of cultivation.

Acid phosphatase was not demonstrable in the monocytes or macrophages before 24 hours of cultivation *in vitro*. In cultures 24 hours old, a faint reaction was noted in the cytoplasm of the mononuclear cells. This was evident only after 24 hours of incubation in the substrate. After 24 hours of cultivation, the reaction for acid phosphatase became much more intense, so that in cultures 30 to 40 hours old, only 5 hours of incubation was needed to demonstrate an intense deposition of the dye in the cytoplasm. In older cultures the reaction was even more intense, especially in the large multinucleated giant cells. In giant cells with the nuclei arranged in a circular fashion, the deposition of the dye occurred in the central area (Fig. 3), while in those cells containing nuclei with an irregular distribution, the dye was more diffusely deposited. The fibroblast-like cells which developed from monocytes in plasma clot cultures on cellophane also were stained by the reaction for acid phosphatase. These cells developed from monocytes after 3 to 5 days *in vitro*.

The staining reaction for acid phosphatase was negative in the nuclei of the monocytes during the first 24 hours of culture; in older cultures the nuclei were lightly stained. The nucleoli in the older cultures showed a well defined deposition of dye in the region of the "nucleolus associated chromatin," a reaction noted in blood cells by Rabinovitch.[18,19] In addition to the staining of the cytoplasm and nuclei, staining occurred in the lipidic droplets which accumulated in

the cytoplasm of the large mononuclear and giant cells. As noted by others,[20,21] cultures fixed in cold formalin showed better preservation of the enzyme than those fixed in cold acetone.

Lipids

Cultures which were 2 to 6 hours old did not stain with either Sudan IV or Sudan black B. After 24 hours of cultivation, a few lipidic droplets were found in the cytoplasm of the mononuclear cells adjacent to the nuclei. Lipidic droplets accumulated as the cells were cultivated for longer periods. The droplets, which stained a brilliant orange to orange-red with Sudan IV, varied in size, larger ones being present in older cultures (70 to 160 hours). In preparations cultivated for at least 70 hours, many lipidic droplets were found in the peripheral cytoplasmic area and in the cytoplasmic bridges connecting one giant cell with another. Organic solvents such as ethyl alcohol, chloroform, and pyridine removed all stainable lipid. It was not possible to demonstrate a Schultz reaction for the determination of cholesterol because the cellophane interfered with the test. The monocytes and macrophages showed a faint blue coloring of the cytoplasm with Baker's method for phospholipids.[15] After 24 hours, the reaction was more intense, and in older cultures the color varied from deep blue to blue-black. The reaction was localized mainly in the central areas of the giant cells; the cell membrane also was deeply stained in the cultures. In addition to the staining of the cytoplasm, the rims of the lipidic droplets also were stained. The cytoplasm of the controls, fixed in dilute Bouin's solution and extracted with pyridine, gave negative results.

Polysaccharides

No staining reaction was observed in the cytoplasm of the monocytes or macrophages before 24 hours of cultivation. After that period, a faint, diffuse pink was noted around the nuclei of the mononuclear cells (30 to 40 hours). A more intense reaction was observed in the large mononuclear and giant cells of older cultures. The localization of the material stained with Schiff's reagent corresponded to the localization of acid phosphatase (Fig. 4). The PAS reaction was as intense in the large mononuclear cells in the older cultures as it was in the giant cells, although the latter probably contained more PAS-positive material. To make certain that this staining of the cytoplasm was not due to lipid, cells fixed in formalin as well as Carnoy's solution were treated with hot chloroform and methanol. Although all stainable lipid was removed, the PAS reaction was still positive. The material was not

glycogen because the reaction was present after treatment with saliva or malt diastase. Hyaluronidase also was ineffective in abolishing the PAS staining of the cells. The fact that the reaction could be blocked by acetylation with acetic anhydride after oxidation with periodic acid and its reappearance after treatment with dilute potassium hydroxide indicated that 1,2-glycol groups of a polysaccharide were probably involved.

A faint gamma metachromasia* occurred only in older cultures (40 to 150 hours). The metachomasia was most pronounced in the central area of those giant cells with nuclei arranged in a circle. Since it was not possible to remove the PAS-positive material, it was not certain that the metachromasia and the accumulation of the PAS-positive material were closely associated.

Ribose Nucleic Acid

The staining of the cytoplasm of the monocytes with pyronine was faint in recently incubated cultures. As the cultural period was increased (30 to 150 hours), there was a noticeable increase in pyronine staining in the macrophages. The giant cells which developed in the cultures showed a marked increase in pyronine-positive material. The cells of cultures treated with crystalline ribonuclease showed no staining. It was pointed out by Ehrich[22] that macrophages contain little ribose nucleic acid; the observations reported here confirm this, but as the monocyte differentiates into the multinucleated giant cell, ribose nucleic acid accumulates as evidenced by the increase in pyronine staining.

Necropsy Material

The staining reaction for polysaccharide in the cytoplasm of the macrophages and giant cells in tissues from the granulomas was like that seen in the macrophages and giant cells in cultures of buffy coat. Hot chloroform/methanol, hyaluronidase, saliva, or malt diastase did not alter the staining. Acetylation blocked the Schiff reaction after periodic acid oxidation, which could then be reversed by treatment with dilute potassium hydroxide.

When sections of tissue were stained with toluidine blue, a gamma metachromasia was observed in the multinucleated giant cells but not in macrophages. Treating the sections with hyaluronidase did not alter the staining reaction.

Sections stained with the methyl green-pyronine technique of Trevan

* The pink to red color found in tissues which stain metachromatically with toluidine blue (Pearse,[10] page 148).

and Sharrock[10] showed variable staining results. Some of the epithelioid and small multinucleated giant cells showed a pronounced pyronine staining, while in others the reaction was very faint. Treatment with ribonuclease resulted in no staining with pyronine.

Gomori[6] noted the presence of acid phosphatase in macrophages and giant cells in tissues containing inflammatory lesions. The lipids which accumulated in the macrophages and giant cells of man, as well as of other animals, were found to be composed of neutral fats, phospholipids, and sometimes small amounts of cholesterol.[9,10]

Discussion

The rapid accumulation or *de novo* synthesis of acid phosphatase in the macrophages and giant cells in tissue culture was one of the striking cytochemical changes observed. No enzyme could be demonstrated in the monocytes before 24 hours in tissue culture. The induced increase of enzymes has been demonstrated in bacteria and in mammalian tissues.[23] *In vivo* in areas of inflammation, and *in vitro* in the presence of a stimulus such as cellophane, it also appears that induced enzyme formation can occur. Although Grogg and Pearse[1] suggested that a specific substance, a phospholipid fraction of the tubercle bacillus, was necessary for the appearance of acid phosphatase in the macrophages and giant cells, any irritant which can cause a chronic inflammatory reaction will induce the formation of the enzyme. It has been suggested also that the degeneration and phagocytosis of polymorphonuclear leukocytes might be a source of acid phosphatase. In studies of blood from patients with acute leukemias,[24] in which no granular leukocytes were present in the cultures, the differentiating cells showed a large increase in acid phosphatase in the leukemic cells, so that the presence of polymorphonuclear leukocytes cannot be the only explanation for the large increase in this enzyme.

The localization of most of the enzyme in the cytoplasm corresponded to the biochemical data reported on isolated cell fractions of other tissue.[25-27] Palade[25] reported enzyme activity in nuclear fractions of liver cells of about 5 per cent, which he thought may have been due to contamination. The histochemical data reported here on monocytes and their derivatives suggest that the small amount of enzyme found in the nuclei by biochemical techniques may not be due to contamination, but to the presence of small amounts of acid phosphatase.

The function of acid phosphatase in the blood cells is not known. Both Weiss and Fawcett[2] and Grogg and Pearse[1] assumed, on the basis of the increased phagocytic activity of the macrophage, that acid

phosphatase plays an important rôle in this process. Unless there are different specific acid phosphatases, it is difficult, for example, to explain the rôle of acid phosphatase in the prostate or in other cells of the body which are not active phagocytes. The PAS-positive material which accumulated in the cells was probably a mucopolysaccharide or glycoprotein. This material resembled the PAS-positive material found in the erythroblasts of patients with thalassemia major[28] and the Schiff-positive material which was observed in the macrophages and giant cells of chickens.

In addition to the appearance of large amounts of acid phosphatase and polysaccharide, an increase in ribose nucleic acid and protein (as evidenced by a more intense staining with fast green) was observed. These cytochemical reactions indicate that the transformation of monocytes of the blood during inflammation *in vitro* as well as *in vivo* is not a degenerative process. The similarity in structure and cytochemical features of human monocytes, macrophages, and giant cells in tissue culture to those cells seen in human granulomatous tissue suggests that the process studied *in vitro* can be closely correlated with the phenomenon observed *in vivo*.

Summary

Fragments of buffy coat from normal human peripheral blood were explanted on the surface of cellophane in D-35 Carrel flasks. After varying periods of incubation *in vitro*, the cellophane was removed from the flasks and fixed and stained. The staining results indicated that during the formation of giant cells *in vitro* there was an increase in acid phosphatase, in polysaccharide which was probably a glycoprotein or mucopolysaccharide, in ribose nucleic acid, lipid, and in the appearance of a gamma metachromasia. The cytochemical observations in the macrophages and giant cells which formed *in vitro* corresponded to those seen in human granulomatous tissue. It appears from these and previous studies that the two processes are identical.

We should like to thank Dr. Hugh McCorkle, former Resident in Chief in the Department of Pathology, Western Reserve University, Cleveland, Ohio, for supplying the necropsy material.

REFERENCES

1. Grogg, E., and Pearse, A. G. E. The enzymic and lipid histochemistry of experimental tuberculosis. *Brit. J. Exper. Path.*, 1952, 33, 567–576.

2. Weiss, L. P., and Fawcett, D. W. Cytochemical observations on chicken monocytes, macrophages and giant cells in tissue culture. *J. Histochem. & Cytochem.*, 1953, 1, 47–65.

3. Menkin, V. Factors concerned in the mobilization of leukocytes in inflammation. *Ann. New York Acad. Sc.*, 1955, **59**, 956–985.

4. Seabra, P. Oxidase and lipase of the leucocyte. Research work that resulted in a chemical blood test to detect infections by acid-fast bacilli. *Ann. New York Acad. Sc.*, 1955, **59**, 1022–1051.

5. Goldstein, M. N. The desoxyribose nucleic acid (DNA) content of human monocytes and their derivatives during giant cell formation in vitro. *J. Histochem. & Cytochem.*, 1954, **2**, 274–281.

6. Gomori, G. Distribution of acid phosphatase in the tissues under normal and pathologic conditions. *Arch. Path.*, 1941, **32**, 189–199.

7. Gomori, G. Distribution of lipase in the tissues under normal and under pathologic conditions. *Arch. Path.*, 1946, **41**, 121–129.

8. Altshuler, C. H., and Angevine, D. M. Histochemical studies on the pathogenesis of fibrinoid. *Am. J. Path.*, 1949, **25**, 1061–1077.

9. Engle, R. L., Jr. Giant cell foreign body reaction to non-cholesterol lipid plate crystals. A case report with chemical studies. *Am. J. Path.*, 1951, **27**, 317–325.

10. Pearse, A. G. E. Histochemistry, Theoretical and Applied. Little, Brown & Co., Boston, 1953, 530 pp.

11. Goldstein, M. N. Formation of giant cells from human monocytes cultivated on cellophane. *Anat. Rec.*, 1954, **118**, 577–591.

12. Manheimer, L. H., and Seligman, A. M. Improvement in the method for the histochemical demonstration of alkaline phosphatase and its use in a study of normal and neoplastic tissues. *J. Nat. Cancer Inst.*, 1948–49, **9**, 181–199.

13. Seligman, A. M., and Manheimer, L. H. A new method for the histochemical demonstration of acid phosphatase. *J. Nat. Cancer Inst.*, 1948–49, **9**, 427–434.

14. Lillie, R. D. Histopathologic Technic and Practical Histochemistry. The Blakiston Co., Inc., New York, 1954, 501 pp.

15. Baker, J. R. The histochemical recognition of lipine. *Quart. J. Micr. Sc.*, 1946, **87**, 441–471.

16. McManus, J. F. A. Histological demonstration of mucin after periodic acid. *Nature, London*, 1946, **158**, 202.

17. McClung, C. E. Handbook of Microscopical Technique, Jones, R. M. (ed.). Paul Hoeber & Co., New York, 1950, ed. 3, 790 pp.

18. Rabinovitch, M. Nucleolus and "nucleolus associated chromatin" acid phosphatase reaction. *Nature, London*, 1949, **164**, 878.

19. Rabinovitch, M., and Andreucci, D. A histochemical study of "acid" and "alkaline" phosphatase distribution in normal human bone marrow smears. *Blood*, 1949, **4**, 580–594.

20. Stafford, R. O., and Atkinson, W. B. Effect of acetone and alcohol fixation and paraffin embedding on activity of acid and alkaline phosphatases in rat tissues. *Science*, 1948, **107**, 279–281.

21. Seligman, A. M.; Chauncey, H. H., and Nachlas, M. M. Effect of formalin fixation on the activity of five enzymes of rat liver. *Stain Technol.*, 1951, **26**, 19–23.

22. Ehrich, W. E. Cellular Sources of Antibody. In: Blood Cells and Plasma Proteins, Tullis, J. L. (ed.). Academic Press, New York, 1953, p. 188.

23. Lee, N. D. The induced increase in the tryptophan peroxidase-oxidase activity of rat liver: time studies. *J. Biol. Chem.*, 1956, **219**, 211–220.
24. Goldstein, M. N., and McCormick, T. In preparation.
25. Palade, G. E. Intracellular localization of acid phosphatase. A comparative study of biochemical and histochemical methods. *J. Exper. Med.*, 1951, **94**, 535–548.
26. Berthet, J., and DeDuve, C. Tissue fractionation studies. I. The existence of a mitochondria-linked, enzymically inactive form of acid phosphatase in rat-liver tissue. *Biochem. J.*, 1951, **50**, 174–181.
27. Berthet, J.; Berthet, L.; Applemans, F., and DeDuve, C. Tissue fractionation studies. II. The nature of the linkage between acid phosphatase and mitochondria in rat-liver tissue. *Biochem. J.*, 1951, **50**, 182–189.
28. Astaldi, G.; Rondanelli, E. G.; Bernardelli, E., and Strosselli, E. An abnormal substance present in the erythroblasts of Thalassaemia major; cytochemical investigations. *Acta haemat.*, 1954, **12**, 145–153.

[*Illustrations follow*]

LEGENDS FOR FIGURES

FIG. 1. Human giant cell on cellophane derived from monocytes of buffy coat. There is an accumulation of nuclei in the central area of the cell. A nucleus of another giant cell is moving across the bridge of cytoplasm and will eventually be incorporated into the giant cell. Maintained in culture for 72 hours. Leitz positive phase contrast. × 200.

FIG. 2. Giant cell and macrophages on cellophane. The nuclei of the giant cell are arranged around the periphery. Nucleoli are prominent. In fixed cells the staining reactions are concentrated in the central areas of the cells. Maintained in culture for 48 hours. Leitz positive phase contrast. × 500.

FIG. 3. Staining reaction for acid phosphatase. The central areas of the giant cells were intensely stained after 3 hours in the substrate. Fixation in cold 10 per cent formalin. Seligman-Manheimer technique. Cultured for 134 hours. Leitz positive phase contrast. × 200.

FIG. 4. Giant cells on cellophane stained by the Schiff reagent after periodic acid oxidation. The Schiff-positive material showed the same localization as acid phosphatase. Nuclei counterstained with methyl green. Carnoy fixation. Cultured for 72 hours. Leitz bright field. × 100.

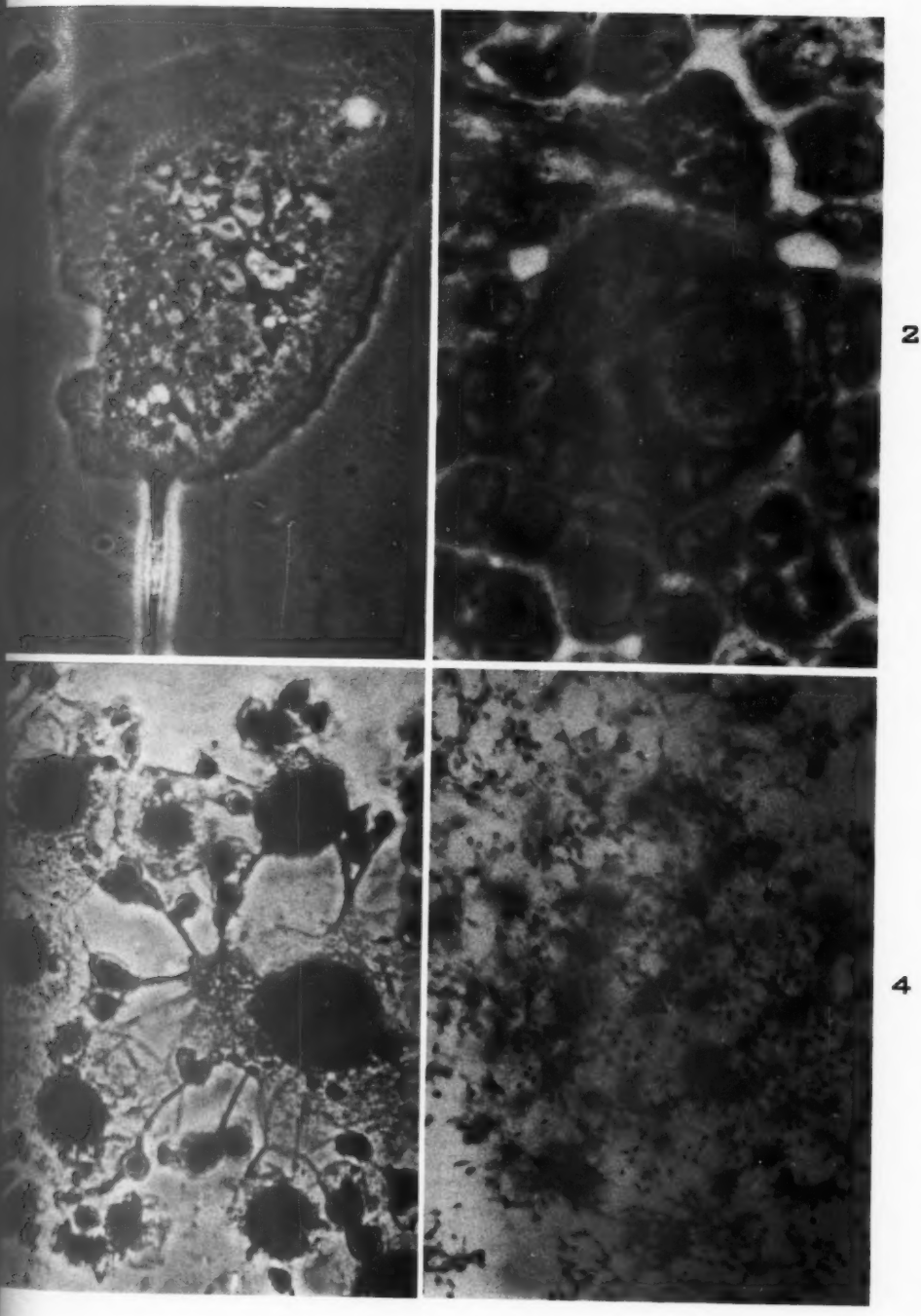

2

4

HOMOLOGOUS BONE MARROW IN THE TREATMENT OF RADIATION INJURY IN MICE*

C. C. Congdon, M.D., and Irene S. Urso, M.S.
From the Biology Division, Oak Ridge National Laboratory, Oak Ridge, Tenn.

In the experimental treatment of lethal total-body irradiation injury in mice by intravenous injection of bone marrow suspensions, most of the work has been carried out with isologous† bone marrow donor animals of the same strain as the irradiated recipient. In these experiments with x-radiation, about 95 per cent 30-day survival was observed. There was no appreciable additional mortality during the next few months. Under similar irradiation conditions the exposed mice receiving homologous bone marrow from donor animals of a different strain showed about 50 per cent 30-day survival with many delayed deaths during the second and third months after irradiation.[1] The nature of the delayed deaths and the clinical features of the disease exhibited by the animals prior to death form the basis of the present report.

Materials and Methods

Animals. Male and female LAF_1 mice were used as irradiated recipients; IOI $\times$ C_3HF_1 or LAF_1 mice were the donor animals. All irradiated mice were about 3 months old at the time of exposure. The mice were kept 10 to a cage; food and water were always available.

X-Ray Conditions. The irradiation conditions were: 250 kvp, 30 ma, and 3 mm. of Al filter; target-object distance, 80 cm.; dose rate, ~100 r./min.; hvl 0.4 mm. of Cu.

Bone Marrow Preparations. The femur of the donor mouse was severed at both ends and the bone marrow flushed into a small cup by means of a needle and syringe containing Tyrode's solution. The tissue was drawn several times through the needle and syringe to make the suspension. All bone marrow suspensions were administered intravenously.

Necropsy. Gross examinations were carried out on nearly all animals dying in certain experiments and on selected animals in other experi-

* Work performed under Contract No. W-7405-eng-26 for the U.S. Atomic Energy Commission.

Received for publication, October 30, 1956.

† Isologous bone marrow refers to transplantation within an inbred strain or between genetically homogeneous F_1 hybrids. Homologous transplantation of bone marrow refers to transplantation between inbred strains or between different F_1 hybrids. Heterologous transplantation is used to denote interspecies experiments; e.g., rat to mouse.

ments, as indicated. Tissues for microscopic study were fixed in Zenker's-formol solution or in 10 per cent formalin. The sections were stained with hematoxylin and eosin.

Results

Survival

The pattern of death in one experiment during the first 30 days after irradiation is shown in Table I for x-ray control animals and those treated with isologous and homologous bone marrow. At a dose level of 900 r., x-ray controls rarely survived beyond the 15th day after irradiation. Mortality in mice treated with isologous bone marrow varied from 0 to 10 per cent during the first 30 days after irradiation. The results were generally uniform from experiment to experiment, and the few animals that did die might have died at any time during the 30-day

Table I

Effect of Isologous and Homologous Bone Marrow on 30-Day Mortality of Total-Body X-Irradiated (900 r.) LAF_1 Male Mice

No. of mice	Donor animal*	Number of animals dying each day after x-ray: Day 6	7	8	9	10	11	12	13–19	20	21	22	23	24	25	26–30	Mortality
																	%
8	None				1	2	4	1									100
15	LAF_1		1														6.6
15	$101 \times C_3HF_1$	1								1		1	1	1	2		46.6

* The bone marrow from one femur given intravenously to each recipient.

Table II

Effect of Isologous and Homologous Bone Marrow on Survival of LAF_1 Mice for 100 Days After 900 r. of Total-Body X-Radiation

No. of mice and sex	Donor*	Number surviving at end of each 10-day period: Day 0	10	20	30	40	50	60	70	80	90	100	Survival
													%
47 M	$101 \times C_3HF_1$	47	44	28	15	11	9	6	4	3	2	1	2.1
32 F	$101 \times C_3HF_1$	32	27	24	15	10	9	8	5	4	4	3	9.4
35 M	LAF_1	35	33	33	33	33	33	33	33	33	33	33	94.3
28 F	LAF_1	28	28	28	28	28	28	28	28	28	28	28	100.0

* Bone marrow from one femur given intravenously to each recipient.

period. During the first 15 days after irradiation, there were often no more deaths among the mice injected with homologous bone marrow (Table I) than in those treated with isologous marrow. The results, however, varied from experiment to experiment. A large percentage of

mice injected with homologous marrow died during the second 15-day period after irradiation (Table I). These deaths were due to a secondary disease process, as described later, and were not caused by lack of bone marrow regeneration.

During the second and third months after irradiation, mice treated with homologous bone marrow continued to die. Table II shows the results obtained in a series of experiments. In both male and female

TABLE III

Long-term Survival of Irradiated Mice Treated with Homologous Bone Marrow

Experiment no.	No. of mice and sex	Post-irradiation (900 r.) treatment and time*	Post-irradiation survival†	
			No. of mice	No. of days
1	4 M	Marrow‡	2	316
2	17 F	Marrow	2	217
3	15 M	Marrow	1	204
4	17 F	Marrow; streptomycin on days 44–53	6	190
5	9 F	Marrow	4	167
6	10 M	Marrow; streptomycin on days 3–24	1	163
7	10 F	Marrow; streptomycin on days 4–30	3	142
8	10 F	Marrow on day 1	7	107
9	10 F	Marrow on day 2	8	107
10	10 F	Marrow on day 3	4	107
11	10 F	Marrow on day 4	1	107

* Bone marrow on day 0 unless otherwise stated.
† As of August 8, 1956.
‡ Marrow from 4 femurs in experiment 1; in all others, 1 femur.

mice, 100-day survival was rare after injection of homologous bone marrow, in sharp contrast to the high percentage of survival in mice treated with isologous bone marrow (Table II). Selected homologous bone marrow experiments in which the animals lived longer than 100 days are shown in Table III.

Appearance and Body Weight

Mice treated with homologous bone marrow closely resembled the isologously treated animals for the first 2 weeks after exposure. During this period the untreated, irradiated mice died of the irradiation syndrome. The body-weight response after bone marrow treatment is shown in Text-figure 1. Mice injected with isologous and homologous bone marrow showed a nearly parallel decline in average body weight

and recovery during the first 2 weeks after irradiation. In the second 2 weeks, the isologous animals continued their recovery; and the average body weight of the homologous mice showed a secondary decline during which many of the mice died.

In the second 2 weeks after irradiation, or later, most of the mice treated with homologous bone marrow had marked ruffling of hair, the skin became atrophic, and a yellow, scaly dermatitis developed. Partial

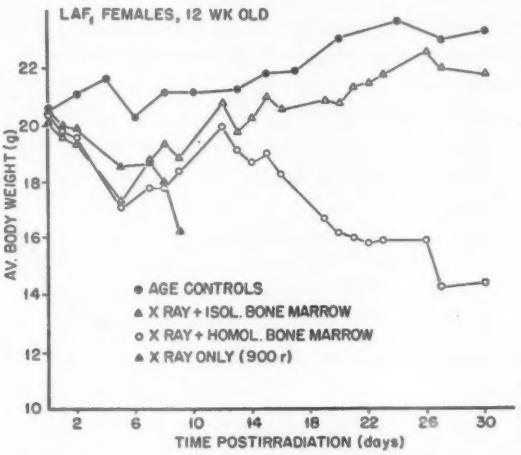

Text-figure 1. Response of body weight in irradiated mice treated with isologous and homologous bone marrow.

epilation often appeared, and the hair was easily pulled out. Radiation-induced graying of hair was well developed in isologous animals by 30 days after irradiation but was absent or markedly reduced in homologous mice unless they lived for prolonged periods.

A few of the sick animals described consumed a normal amount of food, but lost much weight. Normally formed feces were eliminated. During this same period the isologous mice resembled age controls except for the growth of gray hair (Fig. 1).

Gross Necropsy Findings

Gross necropsy examinations were performed on 33 males that died between the 13th and 92nd days after 900 r. and homologous bone marrow treatment. Necropsies were performed also on 24 similarly treated female mice that died on the 6th to 95th days after irradiation. Since there was no marked difference in the findings in males and

females, the observations apply to both sexes. The most striking feature at necropsy was emaciation; many animals weighed only 11 to 15 gm. This was true for nearly all animals examined, whether death occurred early or late. Dermatitis was noted in most of the mice examined but not necessarily in those that died very early. Graying of hair did not appear except in patches even in mice that died 90 days after irradiation. Emaciation was associated with loss of adipose tissue in subcutaneous areas and other sites. Marked atrophy of thymus, lymph nodes, and Peyer's patches characterized the necropsy findings in nearly every mouse. The spleen was normal in many mice and was occasionally hyperplastic. In many mice, localized hemorrhagic lesions were found in the wall of the gastro-intestinal tract at specific anatomical areas. Seven of the 24 females examined showed this lesion, and 16 of the 33 males showed 18 discrete hemorrhagic lesions in the wall of the gastro-intestinal tract. In the females, three of the hemorrhagic lesions were located in the wall of the pylorus; and four were in the wall of the cecum and colon. Two of the pyloric lesions produced acute gastric obstruction and dilatation. The hemorrhage at the pylorus sometimes extended into the adjacent omentum and pancreas. The mucosal surface of the pylorus was often ulcerated, but perforation was not found. In the cecum, the hemorrhage sometimes involved the ileocecal valve and produced obstruction of the small bowel. The 18 hemorrhagic lesions in the males were associated with the pylorus in 12 instances, 5 of which produced acute obstruction, and with the cecum and colon in 6 instances. The ascending, transverse, and descending colon were less frequent sites of mural hemorrhage. Generalized purpuric manifestations of the type associated with the radiation syndrome were not observed. The hemorrhagic lesion occurred in mice that died 20 to 60 days after irradiation.

Another lesion was discovered in the liver in four of the females and in three of the males (Fig. 2). In these, the organ showed a diffuse, often uniformly granular or mottled appearance from the capsular surface. On cut surfaces, the fine or coarse alteration in the parenchyma extended through all lobes. The larger focal lesions (about 2 to 3 mm.) had red centers and white margins, and the intervening tissue had a translucent or gelatinous appearance. More common in the liver than this change were single and multiple yellow abscesses or white areas of necrosis of varying size. These were seen in 6 of the females and 15 of the males; in some, the livers showed no gross abnormalities. In a few mice, abscesses were observed in other organs, primarily the

kidneys and lungs. Some mice showed no gross changes at death other than the emaciation, dermatitis, and atrophy of lymphatic tissues. The bone marrow could not be accurately characterized by gross observation but appeared to be normal.

Microscopic Findings

Tissues from 25 male animals that died 18 to 92 days after 900 r. and homologous bone marrow treatment and from 31 female mice that died 6 to 95 days after similar treatment were examined microscopically. The changes were not significantly influenced by the sex of the animals.

Bone Marrow. The degree of cellularity was estimated on sections through the femur or sternum. Four plus was considered normal. Table IV shows the results.

TABLE IV

Bone Marrow Cellularity at Necropsy of Mice that Died 6 to 95 Days after 900 r. and Treatment with Homologous Bone Marrow

No. of mice and sex	Cellularity of bone marrow				
	++++	+++	++	+	±
25 M	11	10	4	0	0
31 F	22	4	2	2	1

Mild or moderate congestion was the most common cause of reduction in cellularity. Occasional focal areas with loss of blood-forming cells were seen, some of which showed fibrin deposits. In rare instances, foci of necrosis of blood-forming cells were noted. Plasma-cell collections and eosinophilic granulocytes were present in some sections. Granulocyte formation was often increased at the expense of erythropoiesis, presumably in response to the purulent and suppurative inflammations that were often present in other organs. The changes in the bone marrow showed no special relation to time of death. In approximately one half the animals, the bone marrow was considered normal except for the increased granulopoiesis. No abnormality in the formation of megakaryocytes was observed.

Spleen. In two animals, the white pulp was partially intact; in all others, the lymphocytic elements were not present, and only the framework of the white pulp remained. It usually contained some plasma cells. In many animals, an occasional individual splenic nodule was replaced by a dense pink-staining material (Fig. 3). Sometimes the arteriole in the white pulp was obliterated.

The red pulp contained all phases of blood cell formation. However,

formation of blood cells was often markedly reduced. Infiltration of plasma cells was usually present, sometimes to a very marked degree. Some spleens showed erythrophagocytosis. Focal areas of necrosis of blood-forming cells were seen in a few sections. Often, patchy areas in the red pulp were replaced by fibrinous deposits or had undergone fibrosis. None of the spleens could be considered normal.

Lymph Nodes. The brachial and inguinal lymph nodes were always atrophic. In the more extreme cases, the normal architecture was obliterated (Fig. 4). The capsule was thickened. The cortex and medulla were replaced by dense fibrous connective tissue, usually infiltrated by plasma cells and containing pigment-laden macrophages. In some instances, the medullary sinuses were discernible. Blood-forming cells were present in a few lymph nodes.

Thymus. Extreme simple atrophy was present in all cases.

Liver. The unique lesion affecting the entire parenchyma seen in the gross examination consisted of foci of simple necrosis of the hepatic cord cells resembling tiny infarcts (Fig. 5). In some of the cases, there was no inflammatory cell reaction; but when it was present, it usually contained plasma cells in addition to other cells associated with the repair of necrotic foci. Small foci of extramedullary hematopoiesis were present in the portal areas in several animals. Metastatic hepatic abscesses from thrombo-pylephlebitis were observed in several mice. The inflammatory processes, when present, did not differ from those expected in otherwise normal mice.

Stomach and Intestine. On microscopic examination, the hemorrhagic lesions at the pylorus or in the large intestine consisted of necrotic, ulcerating mucosal lesions with extensive bacterial growth and suppurative inflammation. Extensive recent hemorrhage into adjacent tissues was almost invariably present. Septic thrombosis of vessels in the wall of the pylorus or large intestine accompanied the lesion.

Adrenal Gland and Kidney. Usually, microscopic examination showed these organs to be normal. A few kidneys showed embolic abscesses or septic thrombi in blood vessels in the hilum. In one female mouse that died 64 days after irradiation and homologous bone marrow treatment, necrosis of erythropoietic cells was observed in most of the glomeruli of both kidneys.

Lungs. About one third of the mice showed inflammatory lesions in the lungs. These varied from purulent bronchitis and lobular pneumonia to septic emboli that rarely formed abscesses. Large collections of plasma cells around blood vessels and bronchi were observed in a few of the lungs with inflammatory lesions.

Data Obtained on Mice Sacrificed at Intervals after 900 r. and Treatment with Homologous Bone Marrow

A group of 30 LAF_1 female mice that received 900 r. and homologous bone marrow were sacrificed at intervals of 1 to 3 days on days 0 to 30. Equal numbers of un-irradiated normal mice and irradiated mice receiving isologous bone marrow were also sacrificed. Fourteen mice given 900 r. of total-body radiation without additional treatment were sacrificed on days 0 to 13. Organ weights were obtained on thymus and spleen, and histologic sections were taken at selected intervals on thymus, spleen, and lymph nodes. Text-figures 2 and 3 show the data

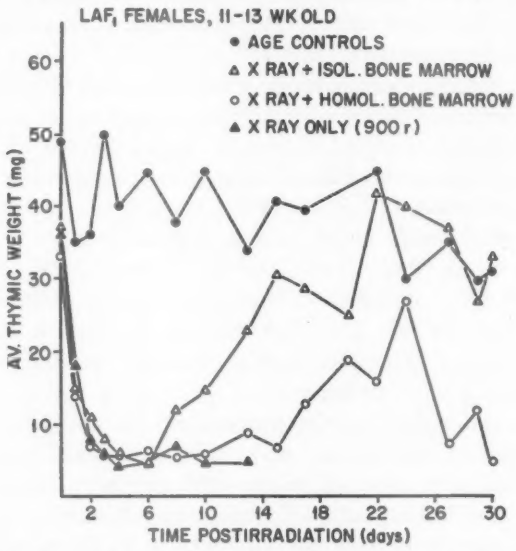

Text-figure 2. Response of thymic weight in irradiated mice treated with isologous and homologous bone marrow.

for weight of thymus and spleen. Microscopically, the thymus showed massive necrosis within 24 hours in all irradiated groups. In the control irradiated group, the animal examined on day 10 showed slight regeneration of thymocytes in cortex and medulla. On day 10, the mouse treated with isologous marrow showed nearly normal architecture with a wide cortex filled with thymocytes. The mouse treated with homologous bone marrow on day 10 showed only slight regeneration of thymocytes. At successive intervals, the thymuses of isologous marrow-treated mice continued to enlarge, having by 10 days reconstituted the normal architecture of the organ. At 15 days, the thymus of the mouse

injected with homologous bone marrow had a normal architecture in one lobe, but part of the other lobe was without a normal cortex. On days 22, 27, and 29, the cortex was irregular with reduction in thymocytes; the sharp corticomedullary junction was no longer discernible.

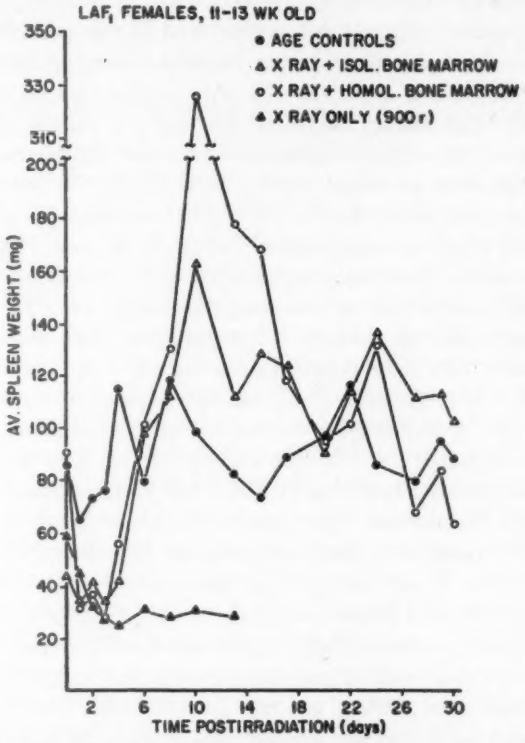

Text-figure 3. Response of splenic weight in irradiated mice injected with isologous and homologous bone marrow.

These findings along with the organ-weight data on the thymus show that partial regeneration after treatment with homologous bone marrow occurs but is followed by secondary degeneration during the fourth week after irradiation.

Marked destruction of the red and white pulp of the spleen occurred in all irradiated groups in the first 24 hours after irradiation. Slight regeneration of lymphocytes in the white pulp of the irradiation controls appeared and remained in this state throughout the observation period. No regeneration took place in the red pulp.

The white pulp in the mice treated with isologous marrow showed

slight regeneration very early. Enlargement and germinal-center formation were present on day 10, and a normal state was reached by day 22. As would be expected, marked regeneration of blood-forming cells in the red pulp had begun by day 4 in the isologous animals and continued to increase thereafter.

Normal white pulp was not regenerated in the mice injected with homologous bone marrow. During the first 2 weeks after irradiation, blood cell formation from the red pulp encroached on the atrophic white pulp. The animal sacrificed on day 15 showed fibrinoid degeneration of two adjacent splenic nodules and infiltration by plasma cells. The number of blood-forming cells in the red pulp near these nodules was markedly reduced. The animal sacrificed on day 8 showed a focal area of reticulo-endothelial cell proliferation. Hyaline degeneration or fibrinoid necrosis in the white pulp was seen also on days 17, 24, and 29. On day 29, however, the remainder of the white pulp had a nearly normal content of lymphocytes. The red pulp in the mice treated with homologous marrow showed massive hyperplasia of blood-forming elements of all phases, paralleling that seen in the mice injected with isologous bone marrow. These changes were reflected in the weight of the spleen (Text-fig. 3). The drop in splenic weight to normal levels during the third and fourth weeks after irradiation reflects the normal reduction in blood-forming cells in the red pulp in mice treated with both isologous and homologous bone marrow.

In the three irradiated groups, microscopic examination of the lymph nodes showed massive necrosis of lymphocytes during the first 24 hours after exposure. Slight regeneration of lymphocytes occurred in relation to the original germinal centers in the irradiated control group. These were present on day 1 after irradiation and persisted as the lymph nodes became smaller and smaller on subsequent days.

The lymph nodes of the mice treated with isologous bone marrow did not differ appreciably from those of the x-ray control mice until day 10. Lymph nodes of the animal sacrificed on this day showed extensive formation of granulocytes in the medullary cords. On day 15, marked accumulation of lymphocytes around the cortical nodules was present. Formation of granulocytes persisted in a reduced amount. Gradual resumption of the normal architecture of the lymph node began between the 15th and 29th days after irradiation.

The lymph nodes in the mice treated with homologous bone marrow did not return to a normal state microscopically. They showed the same findings as the other two groups for about 8 days after irradiation. Formation of granulocytes was minimal compared to that seen

in the lymph nodes of mice treated with isologous bone marrow. Proliferated reticulo-endothelial cells, plasma cells, and scattered multinucleated giant cells were the most striking histologic features in the lymph nodes on day 10. These changes persisted for about 1 week. On day 24, progressive fibrosis of the lymph nodes was taking place with a marked reduction of all other cell types. At subsequent intervals, fibrous atrophy had occurred in nearly all lymph nodes examined.

Attempts to Influence the Delayed Homologous Bone Marrow Reaction

The reaction occurred at all doses of homologous bone marrow administered from 1/32 of the marrow from one femur to a 16-femur bone marrow dose. It developed at all levels of exposure from 600 through 1200 r. but did not develop at exposures from 200 to 500 r. It was not definitely prevented by use of older (6-months-old) irradiated recipients or by administration of homologous fetal blood-forming tissues. The fetal homologous blood-forming tissues, however, may cause less delayed reaction than adult homologous tissues. It was not prevented by chemical protection (S,2-aminoethylisothiuronium·Br·HBr), gonadotrophin, hydrocortisone, diphenhydramine hydrochloride, estrogen, or streptomycin administration under the experimental conditions used. Mixtures of isologous and homologous bone marrow did not prevent the delayed homologous reaction unless excess isologous bone marrow (3:1) was in the mixture. The most promising results in our efforts to circumvent the delayed reaction were seen in mice given homologous bone marrow on day 1 or 2 after irradiation instead of day 0, the usual time for injection. Fifteen of 20 female mice treated in this manner survived 107 days after irradiation (Table III). They resembled mice treated with isologous bone marrow and were gaining weight.

Discussion

The delayed reaction was not observed in the first report on the use of homologous* bone marrow in the treatment of total-body irradiation injury in mice.[2] Loutit[3] noted that spleen homogenate transplantation between strains of mice enhanced 30-day survival but that delayed deaths beyond the 30-day period occurred in the treated mice. He suggested that host iso-antibodies developed that killed the graft and the host animal. Delayed deaths after the 30-day observation period

* In some of the early literature on the use of bone marrow and spleen in the treatment of irradiation injury, the term homologous was used to indicate intrastrain transplantation; now referred to as isologous. Heterologous transplantation was used to indicate interstrain as well as interspecies transplantation.

have now been observed with homologous bone marrow treatment by several investigators.[1,4,5]

The occurrence of delayed deaths of this type in heterologous bone marrow treatment; i.e., rat bone marrow to the lethally irradiated mouse, was reported also.[6,7]

It is clear that the delayed homologous reaction is caused by the homologous bone marrow since, at sublethal radiation exposure (650 r.), only the homologous bone marrow-treated mice develop the reaction. It was not seen in the mice treated with isologous bone marrow or in the untreated-irradiated controls that survived the 650-r. exposure.[1] The amount of radiation administered was also important. Below 600 r., homologous bone marrow injection did not cause the delayed reaction.

An important feature in the pathogenesis of the delayed homologous bone marrow reaction or in the delayed heterologous bone marrow reaction is the proliferation of the foreign bone marrow cells in the irradiated host. Evidence to support the idea that proliferation occurs has been accumulated by several investigators.[8–14]

The delayed foreign bone marrow reactions can be interpreted as evidence of a hypersensitive state resulting from a chronic *in vivo* tissue antigen-antibody reaction.[11,15] In this reaction, however, the host animal is not able to destroy significant numbers of the proliferating foreign bone marrow cells, as evidenced by the nearly intact bone marrow in most of the mice at necropsy. Presumably, the main antibody-producing tissues, the spleen and lymph nodes, are exhausted in the presence of such extreme stimulation. Lesions in these tissues are compatible with this interpretation. An alternative suggestion is that the donor bone marrow cells also transplant the donor type immune mechanism and that this reacts against host tissue antigens and brings about the delayed reaction. The mechanism is not yet settled.

The thymus in mice treated with homologous bone marrow showed a partial, temporary recovery followed by a secondary, simple atrophy. This organ did not show the reactive changes seen in lymph nodes and spleen. Failure of homologous and heterologous bone marrow treatment to allow thymic regeneration after multiple total-body irradiation exposures was reported by Hirsch *et al.*[16] Under the same conditions, treatment with isologous bone marrow caused complete regeneration of the thymus. The effect of treatment with foreign bone marrow on the prevention of radiation-induced thymic lymphosarcoma has not been determined. The secondary atrophy of the thymus in

the present work may be related to the emaciated condition of the animals at necropsy rather than to a failure of the foreign bone marrow to allow its complete regeneration.

The dermatitis seen grossly and the specific lesions of the liver and gastro-intestinal tract cannot be satisfactorily explained at the present time. Nutritional disturbances and severe stress reactions as well as possible allergic phenomena were considered. The failure to develop normal amounts of gray hair after recovery from irradiation injury indicates failure of hair growth and is believed to result from the total metabolic disturbance. The later disturbance in the presence of a nearly normal food intake was not investigated. The structure of the thyroid gland was normal.

Delayed mortality in lethally irradiated mice that received homologous spleen treatment was investigated by Barnes and Loutit.[17] They reported a chronic diarrhea and weight loss as the prominent clinical features of the disease preceding death. No specific lesions were noted at necropsy. Trentin[18] also found no specific lesions at necropsy to explain the delayed deaths in homologous and heterologous bone marrow-treated irradiated mice. Some of the lesions reported by Denko[5] at necropsy of irradiated mice treated with homologous bone marrow resemble those described in the present paper. The extent to which these apparently specific changes depend on the strains of mice used has not been determined.

Some aspects of the delayed homologous bone marrow reaction resembled certain features of parabiosis intoxication in rats[19] and also the syndrome seen in germ-free guinea pigs.[20] The near-total absence of normal lymphocytic tissue in these mice probably favored the development of some of the secondary purulent and suppurative inflammatory conditions. The possibility that prolonged absence of lymphocytic tissue by itself might give rise to a metabolic disorder was considered but not investigated.

The few animals that survived for prolonged periods (Table III) demonstrated the feasibility of preventing or circumventing the delayed foreign bone marrow reaction. It is obvious that such an achievement with persistence of the foreign bone marrow cells would have important implications for the homotransplant problem.

Summary

The 30-day survival of lethally irradiated LAF_1 mice receiving homologous bone marrow intravenously was often comparable to the survival of those receiving isologous bone marrow; however, most of

the mice treated with homologous bone marrow subsequently died of a secondary disease. The histologic changes in the lymph nodes and spleen were compatible with an immunologic tissue reaction. The lesions in the liver, gastro-intestinal tract, skin, and the general state of the mice at the time of death suggested a severe metabolic disturbance, presumably initiated by the immune reaction if not actually a part of the reaction. A few animals survived 107 to 316 days and, in general, resembled isologous bone marrow-treated mice at these intervals.

The ability of a few mice to escape the delayed homologous bone marrow reaction suggests the feasibility of attempts to circumvent the reaction if proper experimental conditions could be found.

REFERENCES

1. Congdon, C. C., and Urso, I. Isologous versus homologous bone marrow in the treatment of irradiated mice. (Abstract.) *Radiation Res.*, 1956, **5**, 474.
2. Lorenz, E.; Congdon, C., and Uphoff, D. Modification of acute irradiation injury in mice and guinea-pigs by bone marrow injections. *Radiology*, 1952, **58**, 863–877.
3. Loutit, J. F. Protection against ionizing radiation. The "recovery factor" in spleen and bone-marrow. *J. Nuclear Energy*, 1954, **1**, 87–91.
4. Trentin, J. J. Relative effectiveness of isologous, homologous, and heterologous bone marrow transfusion against lethal doses of X-radiation, and its effect on tissue transplantation. (Abstract.) *Proc. Am. Assoc. Cancer Res.*, 1956, **2**, 153–154.
5. Denko, J. O. The histopathology of the irradiation syndrome following homologous injections in mice. (Abstract.) *Radiation Res.*, 1956, **5**, 607.
6. Congdon, C. C., and Lorenz, E. Humoral factor in irradiation protection: modification of lethal irradiation injury in mice by injection of rat bone marrow. *Am. J. Physiol.*, 1954, **176**, 297–300.
7. Cole, L. J.; Habermeyer, J. G., and Bond, V. P. Recovery from acute radiation injury in mice following administration of rat bone marrow. *J. Nat. Cancer Inst.*, 1955, **16**, 1–9.
8. Main, J. M., and Prehn, R. T. Successful skin homographs after the administration of high dosage X-radiation and homologous bone marrow. *J. Nat. Cancer Inst.*, 1954–55, **15**, 1023–1029.
9. Lindsley, D. L.; Odell, T. T., Jr., and Tausche, F. G. Implantation of functional erythropoietic elements following total-body irradiation. *Proc. Soc. Exper. Biol. & Med.*, 1955, **90**, 512–515.
10. Merwin, R. M., and Congdon, C. C. Presence of homologous cells in the marrow of mice protected from the effects of irradiation by homologous marrow. (Abstract.) *Federation Proc.*, 1956, **15**, 129.
11. Makinodan, T. Circulating rat cells in lethally irradiated mice protected with rat bone marrow. *Proc. Soc. Exper. Biol. & Med.*, 1956, **92**, 174–179.
12. Nowell, P. C.; Cole, L. J.; Habermeyer, J. G., and Roan, P. L. Growth and continued function of rat marrow cells in X-radiated mice. *Cancer Res.*, 1956, **16**, 258–261.

13. Vos, O.; Davids, J. A. G.; Weyzen, W. W. H., and van Bekkum, D. W. Evidence for the cellular hypothesis in radiation protection by bone marrow cells. *Acta physiol. et pharmacol. neerl.*, 1955–56, **4**, 482–486.

14. Ford, C. E.; Hamerton, J. L.; Barnes, D. W. H., and Loutit, J. F. Cytological identification of radiation-chimaeras. *Nature, London*, 1956, **177**, 452–454.

15. Gengozian, N., and Makinodan, T. Antibody response of lethally X-irradiated mice treated with rat bone marrow. *J. Immunol.*, 1956, **77**, 430–436.

16. Hirsch, B. B.; Brown, M. B.; Nagareda, C. S., and Kaplan, H. S. Comparative activity of isologous vs. homologous or heterologous mouse bone marrow in promoting regeneration of the irradiated mouse thymus. *Radiation Res.*, 1956, **5**, 52–57.

17. Barnes, D. W. H., and Loutit, J. F. Immunological and Histological Response Following Spleen Treatment in Irradiated Mice. In: Progress in Radiobiology, Mitchell, J. S.; Holmes, B. E., and Smith, C. L. (eds.). Oliver & Boyd, Edinburgh, 1956, pp. 291–296.

18. Trentin, J. J. Mortality and skin transplantability in X-irradiated mice receiving isologous, homologous or heterologous bone marrow. *Proc. Soc. Exper. Biol. & Med.*, 1956, **92**, 688–693.

19. Finerty, J. C. Parabiosis in physiological studies. *Physiol. Rev.*, 1952, **32**, 277–302.

20. Lobund Reports, Reyniers, J. A. (ed.). Laboratories of Bacteriology, University of Notre Dame, South Bend, Ind., November, 1946, no. 1, pp. 109–111.

[*Illustrations follow*]

LEGENDS FOR FIGURES

FIG. 1. The animal at the top of the picture was a normal LAF_1 mouse at 4 months of age. The middle animal was an LAF_1 mouse of the same age that received 900 r. and isologous bone marrow 30 days before the picture was taken. Graying hair over most of the body can be seen. The animal at the bottom of the picture was an LAF_1 mouse that received 900 r. and homologous bone marrow 30 days before the picture was taken; it was small, had ruffled hair, and showed very little graying.

FIG. 2. Formalin fixed specimen of liver in a mouse that died 66 days after 900 r. and injection of homologous bone marrow.

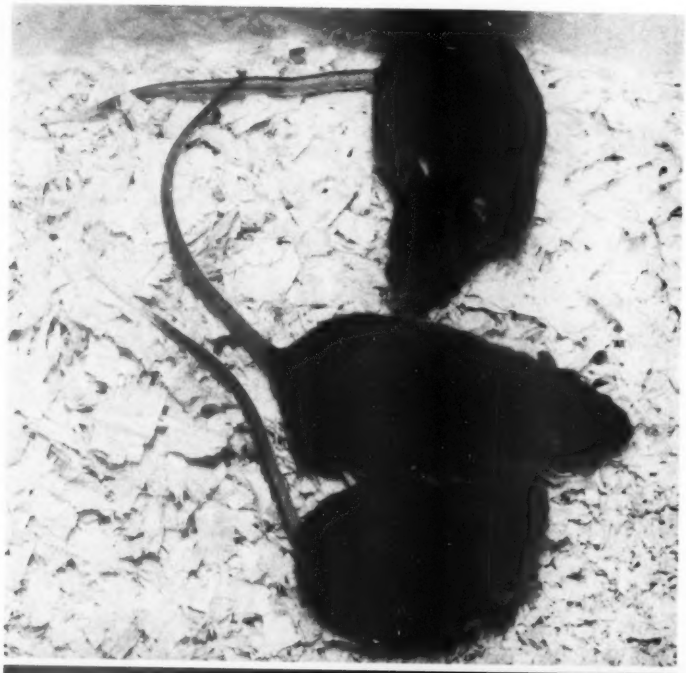

1

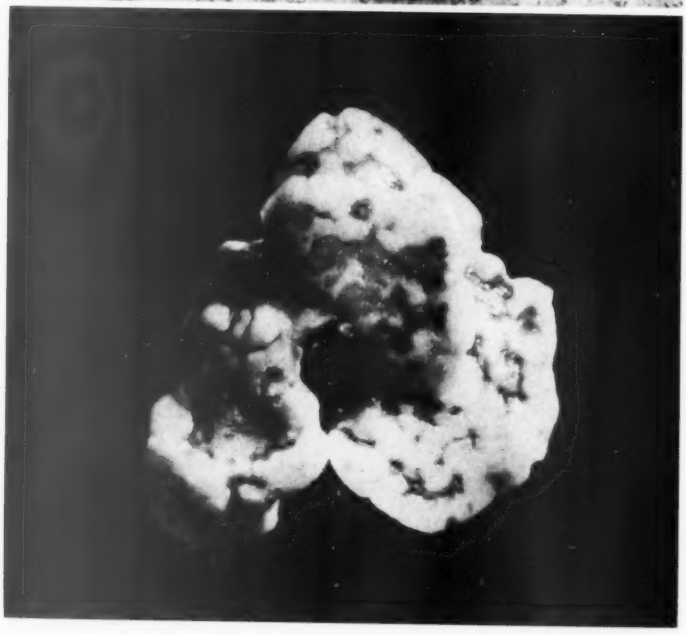

2

FIG. 3. Fibrinoid degeneration of a splenic nodule in an LAF_1 mouse sacrificed 15 days after 900 r. and homologous bone marrow. Hematoxylin and eosin stain. × 145.

FIG. 4. Fibrosis and multinucleated giant cell reaction in the inguinal lymph node of an LAF_1 mouse that died 64 days after 900 r. and homologous bone marrow. Hematoxylin and eosin stain. × 145.

FIG. 5. Simple necrosis in the liver of an LAF_1 mouse that died 33 days after 900 r. and homologous bone marrow. Hematoxylin and eosin stain. × 145.

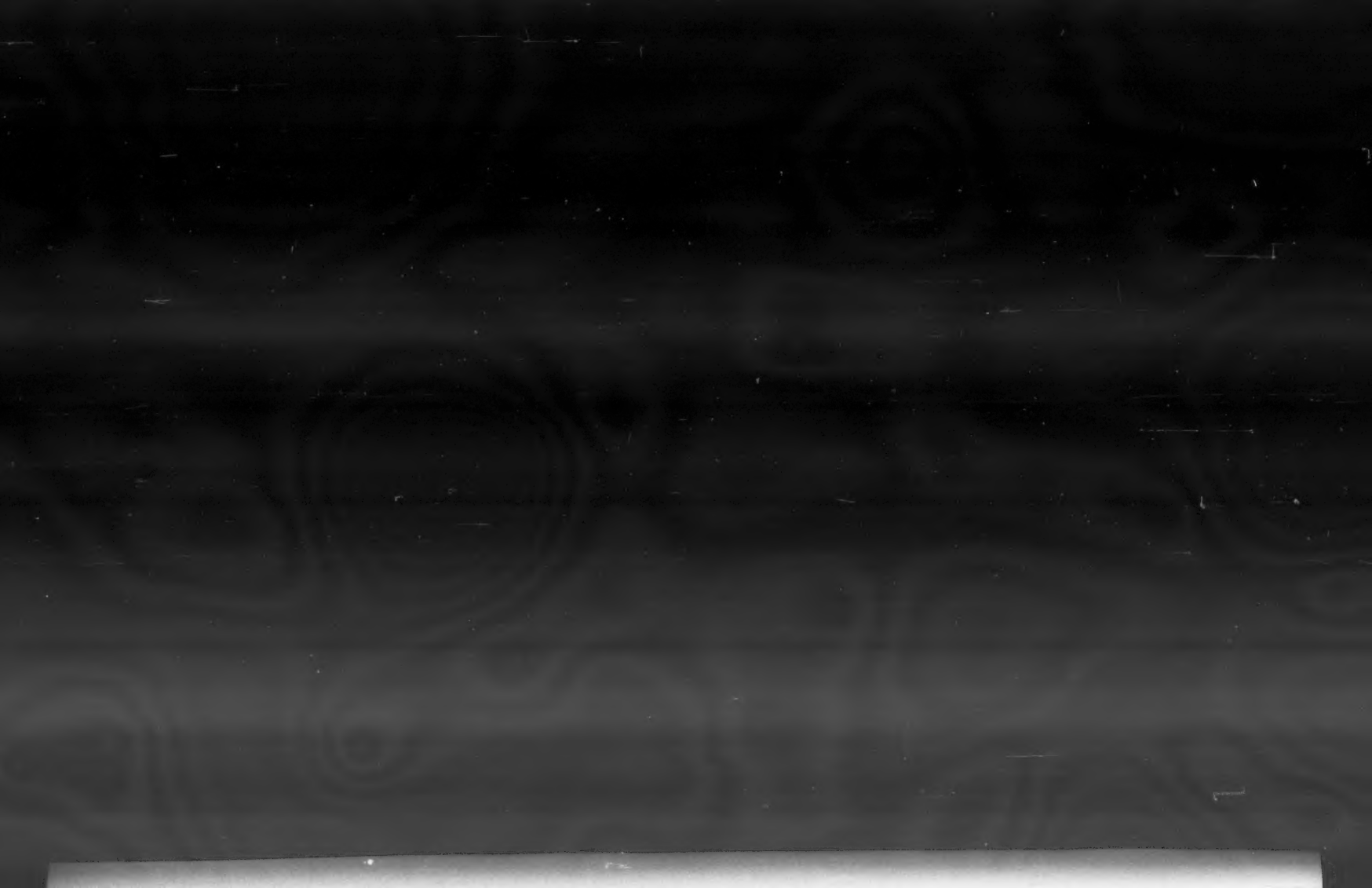

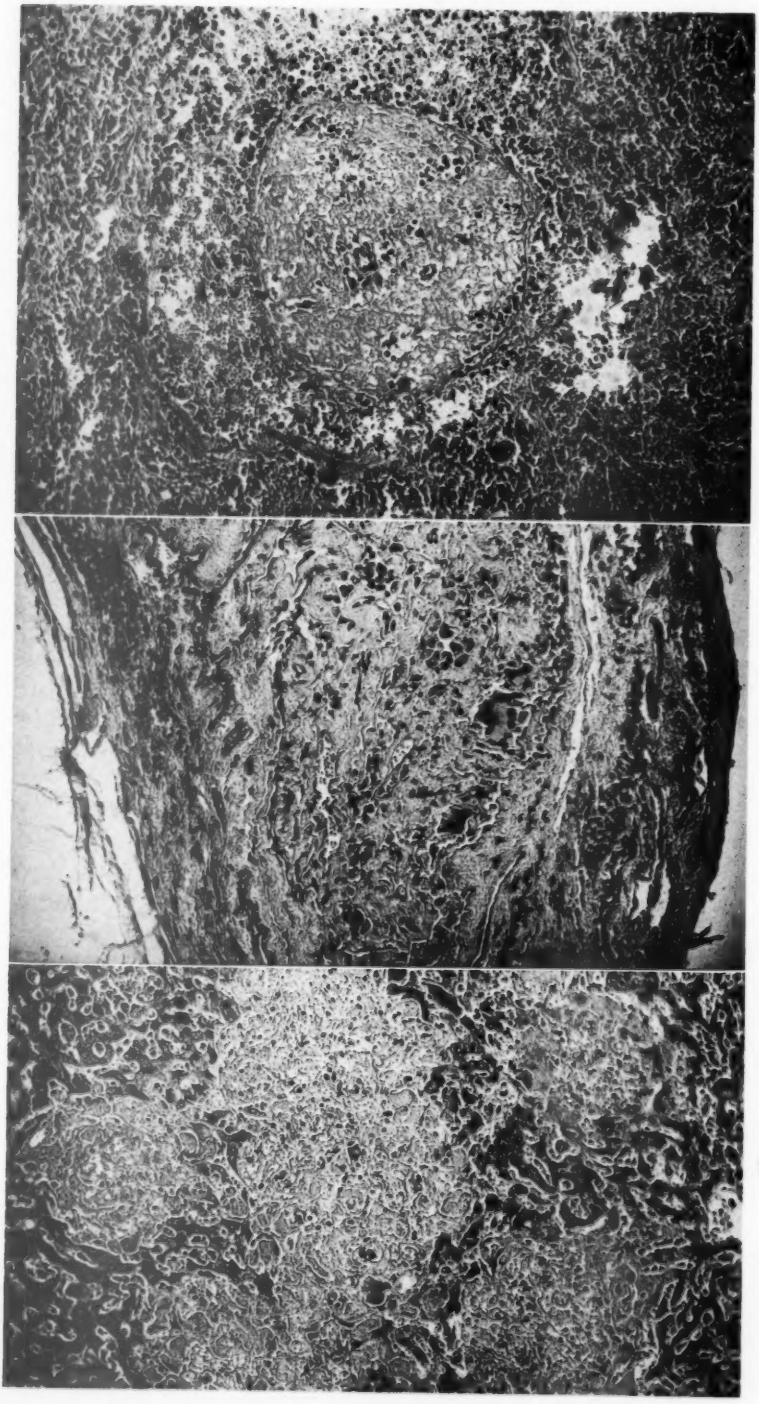

3

4

5

PULMONARY HYALINE MEMBRANES STUDIED WITH THE ELECTRON MICROSCOPE*

V. L. VAN BREEMEN, Ph.D.; H. B. NEUSTEIN, M.D.,† and PAUL D. BRUNS, M.D.
From the Departments of Anatomy, Pathology, and Obstetrics and Gynecology, University of Colorado Medical Center, Denver, Colo.

The "pulmonary hyaline membrane syndrome" has been well established as a clinical entity,[1-3] though its etiology is still debated. The pathologic changes in this disease are characterized by an eosinophilic membrane lining alveolar ducts and filling some alveoli as well as by atelectasis and hyperemia of the lungs.[1,4] The literature concerning this subject has been thoroughly reviewed by De and Anderson.[2]

The precise localization of the hyaline membrane has been in question. Gilmer and Hand[3] have stated that the hyaline membrane lies between an endothelial basement membrane and an epithelial basement membrane. However, most investigators believe that the hyaline membrane lies over the surface epithelium of the alveolar ducts and alveoli.

Histochemical methods have failed to specifically identify components of the hyaline membrane, until the recent work of Gitlin and Craig[5] who used a fluorescein-labeled antibody to demonstrate the presence of fibrin in the hyaline membrane.

The light and electron microscopic studies reported here were undertaken with the hope that the pulmonary hyaline membrane of human infants and experimental animals could be more definitely localized, that their fine structure could be demonstrated, that their content could be identified, and that some light might be shed on their etiology.

MATERIAL AND METHODS

Examinations were made of lung tissue from three sources, as follows: (1) from 37 premature human infants who died in the neonatal period, (2) from ten young adult guinea pigs in which pulmonary hyaline membranes had been experimentally produced, and (3) from five normal guinea pigs as controls for the second group. In about 50 per cent of the 37 human cases, lung specimens were essentially normal and served as controls for the pathologic material.

Immediately after death of infants in the neonatal period, specimens

* Supported in part by research grant (B-605(c)) from the United States Public Health Service.

Presented at the Fifty-third Annual Meeting of the American Association of Pathologists and Bacteriologists, Cincinnati, Ohio, April 26, 1956.

Received for publication, October 5, 1956.

† Maytag Fellow of the American Cancer Society, 1955–56.

of lung were obtained by a technique devised by one of us (H.B.N.). A No. 4 Novak curette was passed into the trachea (under direct vision) and then into a major bronchus; as resistance was encountered, the curette was forced into the lung parenchyma and a piece of lung was removed which measured 2 to 3 mm. The tissue was immediately immersed in fixative. This method fulfilled requirements as follows: The specimens were obtained immediately after death without external mutilation of the body; adequate material was obtained; the procedure was simple and quick, insuring adequate preservation of the tissue for electron microscopy.

Young adult guinea pigs of both sexes were exposed to an atmosphere of about 98 per cent oxygen and about 98 per cent humidity at a pressure of 760 mm. of Hg. After exposure to these conditions for about 72 hours, the guinea pigs were sacrificed by a blow on the head, and pieces of lung were immediately cut and immersed in fixative.

Pulmonic tissue from each infant and from each guinea pig was cut into several pieces for fixation in 10 per cent formalin or in osmium tetroxide. The tissue fixed in formalin was processed routinely for light microscopy, sectioned at 5 μ, and stained with hematoxylin and eosin or with Gomori's trichrome stain. This was done for orientation and comparison, as well as for initial evaluation of the specimen to determine the presence or absence of hyaline membranes. For phase contrast microscopy and electron microscopy, tissue was fixed for 12 to 15 minutes in 1 per cent osmium tetroxide made up in 25 per cent Tyrode solution and adjusted to pH 7.4 to 7.6. After fixation, the tissue was washed in 70 per cent methanol, dehydrated in methanol over a period of about 1 hour, and embedded in n-butyl methacrylate, using dichlorobenzoyl peroxide as polymerizing catalyst.

In order to compare the structure of plasma clot and hyaline membrane, plasma clots were fixed and prepared in the same manner as the pulmonic tissues.

For direct light microscopy, the tissues embedded in plastic were sectioned at 2 μ with a Spencer rotary microtome modified with a wedge for thin sectioning. The sections were treated with toluene for 20 minutes and with xylene for 30 minutes to remove the plastic and were subsequently stained with hematoxylin and eosin; bleaching with hydrogen peroxide before staining produced brighter staining. For phase contrast microscopy, the tissues embedded in plastic were sectioned at 2 μ, treated with xylene for 10 to 15 minutes to remove part of the plastic, and then covered with a coverglass without staining. For electron microscopy, tissues embedded in plastic were sec-

tioned at 0.025 to 0.05 μ with a Sorvall cantilever microtome. As a substrate for mounting the sections, specimen holders for the electron microscope were covered with a very thin film of parlodion which was then covered with a film of carbon in a high vacuum evaporator; the parlodion film was not removed. A Philips electron microscope (EM-100A) was used. The Philips specimen holders have a viewing field 1 mm. long and 0.2 mm. wide, making it possible to study large areas of the sections. The carbon film stabilized the section in spite of this large area.

These four successive phases of study of pulmonic tissue, i.e., stained paraffin sections, stained plastic sections by bright field light microscopy, unstained plastic sections by phase contrast microscopy, and thin plastic sections by electron microscopy, yielded adequate data for orientation, comparison, and interpretation.

Observations

As illustrated by photomicrographs in Figures 1, 2, and 3, typical pulmonary hyaline membrane was found in about one fourth of the pulmonic specimens of the human infant and in about one half of those of the treated guinea pigs studied with the light microscope. Since the hyaline membrane seen in infant and guinea pig was almost identical in structure and in composition,[6] subsequent statements about hyaline membrane will refer to both groups.

When the specimens which contained hyaline membrane were studied with the electron microscope, the membrane was identified and detailed structure and relationships were observed (Figs. 4, 5, and 6). The hyaline membrane is apparently made up of cell débris, plasma proteins, and fibrin in various stages of polymerization. Tentative identification of these components of the hyaline membrane was made on a morphologic basis, as follows: The cell débris was compared to structures occurring in intact cells (structures such as nuclei, mitochondria, vacuoles, and endoplasmic reticulum) Figure 6; the finely granular material in the alveoli was compared to the finely granular plasma proteins in the capillaries (Fig. 5); and the matrix of the hyaline membrane, in which the constituent fibrils sometimes show a periodicity, was compared to the fibrillar structure and periodicity seen in a plasma clot (Figs. 7 and 8). A section of hyaline membrane may be compared directly to a section of a plasma clot, since both show the same component structures, as follows: cell débris, plasma remnants, incompletely polymerized fibrin, fibrin fibrils without periodicity, and fibrin fibrils with periodicity.

In sections studied with the electron microscope the hyaline membrane was found within the air spaces and overlying the epithelium lining the alveoli, alveolar ducts, and bronchioles. The epithelial lining was intact, as in Figure 4, except for scattered small breaks. At some sites, the epithelial cells were vacuolated and appeared to be partly degenerated (Fig. 9) and, more rarely, the basement membrane under the disrupted epithelium seemed to be partly disintegrated also. This was possibly the site of leakage of the plasma.

A complete break-through of the capillary-alveolar wall was rarely seen. At such sites, hemorrhage into the air space was evident. In general, the hyaline membrane contained few erythocytes, the cell débris being mostly from other cell types, probably from macrophages, white blood cells, and epithelial cells.

The presence of the hyaline membrane apparently stimulated phagocytic activity of macrophages, segmented neutrophils, and even epithelial cells. The number of macrophages and segmented neutrophils was increased, so that they often appeared in or near the hyaline membrane (Figs. 1, 2, 3, 9, and 10). Macrophages contained varying amounts of ingested hyaline membrane (Figs. 9 and 10), some cells apparently being full of ingested material. Figures 10 and 11 illustrate a common observation, a macrophage fixed in the process of phagocytosis and pinocytosis.

Discussion

Early during our electron microscopic studies of the structure of the hyaline membrane in lungs of premature human infants and treated guinea pigs, we became convinced that the matrix of the hyaline membrane was fibrin-like material. This led us to examine sections of a plasma clot, in which we found cell débris embedded in a matrix of fine fibrils of fibrin. In some parts of the sections of the clot a characteristic periodicity could be demonstrated in the fibrils (Fig. 7). In some specimens of lung, as in Figure 5, the relationship of un-polymerized plasma-like material and partially polymerized fibrillar matrix of the hyaline membrane was demonstrated. In hyaline membrane that was more completely polymerized or clotted, periodicity characteristic of fibrin fibrils was seen (Fig. 8). Fibrin clots studied with the electron microscope have shown variations with clotting duration, thrombin concentration, and pH.[7-9] When one compares results of such studies with our observations, the varied appearance of the matrix of the hyaline membrane from finely granular to fibrillar can be explained as successive stages of clotting. Because of the appearance of the fibrillar matrix and because we found sites of partial breakdown of the capillary-alveolar wall (Fig. 9), we are convinced, on a morpho-

logic basis, that the source of the matrix of hyaline membrane is the blood plasma which leaks from capillaries into air spaces and that the hyaline matrix is fibrin in various stages of clotting. [6]

While our morphologic studies were in progress, Gitlin and Craig[5] published results of their work with fluorescein-labeled fibrin antibody, demonstrating the abundance of fibrin in pulmonary hyaline membrane. Gitlin and Craig also concluded that hyaline membrane was formed from an effusion from the pulmonary circulation. They further stated that "conversion of fibrinogen to fibrin in pulmonary effusions can and does take place ***in vivo*** without addition of any exogenous materials. Hence, amniotic fluid need not be an essential ingredient for the production of hyaline membranes alone as is apparent in the occurrence of these membranes in various disease states such as uremia (where thromboplastin may be supplied by tissue damage) or even in rats exposed to 100 per cent oxygen for prolonged periods; the membranes in these instances have also been demonstrated to be composed of fibrin." Our conclusions based on morphology are substantiated by the immunologic studies of Gitlin and Craig.

Gilmer and Hand[3] stated that the hyaline membrane may be found between an endothelial basement membrane and an epithelial basement membrane. They believed that this indicated the endogenous origin of the material, which they considered may be derived from the blood stream, may represent a change within the respiratory basement membrane, or may represent a change in the connective tissue substances between the two membranes. In disagreement with the statements of Gilmer and Hand, our studies show that the hyaline membrane lies in the air space over the surface of the epithelium lining the alveolar ducts and alveoli (Figs. 4 and 5). Furthermore, we have noted repeatedly that pulmonary capillary endothelium and alveolar epithelium may *share* a single basement membrane (Fig. 4). It is also true that endothelium and epithelium may be separated by fibrous connective tissue (Fig. 4); in this situation each cell layer has its own basement membrane. However, it is clear that neither the basement membrane nor the connective tissue space is the site of the hyaline membrane.

Various structures were found embedded in the matrix of the hyaline membrane (Fig. 6). In Figure 6 and in other material studied, the following components of the hyaline membrane were identified: a fibrin matrix; scattered remnants of erythrocytes or very few intact erythrocytes; cell débris such as endoplasmic reticulum, mitochondria, cytoplasmic vacuoles as found in macrophages and degenerating epithelial cells, and granules as found in neutrophilic leukocytes.

Our observations of an epithelial lining of the alveoli corroborate

those of Low.[10,11] An attenuated cytoplasmic layer extends from the perinuclear region of the "septal" cell and covers the neighboring capillaries, collagenous connective tissue, and fibroblasts (Fig. 4), forming a normally complete or nearly complete epithelial lining of the alveoli and alveolar ducts. Macrophages and white blood cells of various kinds may occasionally be found enclosed in the connective tissue of the septum. Alveolar cells—that is, free cells in the air space—are mostly macrophages and some are polymorphonuclear leukocytes. Both macrophages and polymorphonuclear leukocytes occur in greater number after irritation of the lung. We often have seen evidence of pinocytosis in the epithelial cells and what appeared to be evidence of phagocytosis in this cell.

As noted previously, broken capillary-alveolar walls were rarely found. The cause of such break-through and hemorrhage into the air spaces was uncertain. This could have been artifact produced by the stress of removal of tissue with the curette. However, such hemorrhage is a common pathologic finding in association with pulmonary hyaline membranes and is to be expected when capillaries are engorged as they are in this syndrome. The broken capillary walls that were observed in sections studied with the electron microscope could have been part of the pathologic picture and had all the appearance of being so. As for the sites of damage to, and partial "erosion" of, the epithelial lining of alveoli and alveolar ducts, these were more prevalent and were more obviously pathologic. The epithelial cells in these regions were vacuolated, loosened from the basement membrane, and disintegrated at some points. At the latter sites, the basement membrane and endothelium may have been sufficiently affected to increase their permeability and allow the passage of plasma proteins. After leakage of the plasma and formation of hyaline membrane, respiratory distress may be aggravated by shock, sludging of the blood, and engorgement of the pulmonary capillaries. Stickiness of the red blood cells, characteristic of sludging, was noted in the electron microscopic studies of much of the pathologic material.

In human infants, the pathogenesis of pulmonary hyaline membranes may depend upon a series of factors, such as "extrinsic," "predisposing," "precipitating," and "aggravating" factors suggested by Bruns and Shields.[12,13] Perhaps the last two factors would constitute the pathogenesis of hyaline membranes in guinea pigs. This report is primarily concerned with the results produced by the precipitating factor, that is, injury to the epithelium of the alveoli and alveolar ducts with resultant formation of hyaline membranes.

Summary and Conclusions

Light and electron microscopic studies were made of pulmonic tissue from premature human infants, young adult guinea pigs which were exposed to an atmosphere of high oxygen and high humidity, and normal guinea pigs. Light microscopy was used to locate specimens of lung which contained typical hyaline membrane. Then the electron microscope was used to study the detailed structure of the hyaline membrane, to identify its components, and to determine its location and relationships to septal structures.

The hyaline membrane was found in the air spaces, overlying the epithelial lining of the alveoli and alveolar ducts. It was made up largely of a finely fibrillar matrix, apparently fibrin, probably derived from plasma which leaked from the pulmonary capillaries. In the fibrin matrix was enmeshed cell débris, such as nuclei, mitochondria, endoplasmic reticulum, and vacuoles.

The presence of the hyaline membrane apparently stimulated phagocytic activity of the macrophages and occasionally of the alveolar epithelial cells. The number of macrophages and neutrophilic leukocytes was increased, so that they often appeared in or near the hyaline membrane.

REFERENCES

1. Potter, E. L. Pathology of the Fetus and the Newborn. Year Book Publishers, Inc., Chicago, 1952, pp. 249–252.
2. De, T. D., and Anderson, G. W. Hyaline-like membranes associated with diseases of the newborn lungs: a review of the literature. *Obst. & Gynec. Surv.*, 1953, **8**, 1–44.
3. Gilmer, W. S., and Hand, A. M. Morphological studies of hyaline membranes in the newborn infant. *A. M. A. Arch. Path.*, 1955, **59**, 207–213.
4. Johnson, W. C., and Meyer, J. R. A study of pneumonia in the stillborn and newborn. *Am. J. Obst. & Gynec.*, 1925, **9**, 151–167.
5. Gitlin, D., and Craig, J. M. The nature of the hyaline membrane in asphyxia of the newborn. *Pediatrics*, 1956, **17**, 64–71.
6. Neustein, H. B., and van Breemen, V. L. Pulmonary hyaline membrane disease: a morphologic study utilizing the electron microscope. (Abstract.) *Am. J. Path.*, 1956, **32**, 613.
7. Morrison, P. R., and Scudder, C. L. Fibrin clot structure during clotting as observed in unsupported films under electron microscope. *Am. J. Physiol.*, 1952, **170**, 147–154.
8. Hawn, C. v. Z., and Porter, K. R. The fine structure of clots formed from purified bovine fibrinogen and thrombin: a study with the electron microscope. *J. Exper. Med.*, 1947, **86**, 285–292.
9. Porter, K. R., and Hawn, C. v. Z. Sequences in the formation of clots from purified bovine fibrinogen and thrombin: a study with the electron microscope. *J. Exper. Med.*, 1949, **90**, 225–232.

10. Low, F. N. Electron microscopy of the rat lung. *Anat. Rec.*, 1952, 113, 437–449.

11. Low, F. N. The pulmonary alveolar epithelium of laboratory mammals and man. *Anat. Rec.*, 1953, 117, 241–263.

12. Bruns, P. D., and Shields, L. V. High oxygen and hyaline-like membranes. *Am. J. Obst. & Gynec.*, 1954, 67, 1224–1236.

13. Shields, L. V. A study of hyaline-like membranes in newborn infants; review of oxygen poisoning; experimental production of hyaline-like membranes in laboratory animals. Thesis for Master of Science Degree, University of Colorado, 1954.

LEGENDS FOR FIGURES

FIG. 1. Premature human infant lung (case 29). The tissue was fixed in formalin, embedded in paraffin, cut at 5 μ, and stained with hematoxylin and eosin. Two alveolar ducts are lined with hyaline membrane and surrounded by atelectatic lung. Photomicrograph, × 155.

FIG. 2. Premature human infant lung (case 29). The tissue was fixed in osmium tetroxide, embedded in plastic, sectioned at 2 μ, and stained with hematoxylin and eosin. Better preservation of cells and tissue is very apparent. Alveolar ducts are lined with hyaline membrane and surrounded by partly atelectatic lung. An alveolus adjacent to the lower duct is filled by hyaline membrane. The lower duct and at least one alveolus contain plasma. Photomicrograph, × 155.

FIG. 3. Lung, guinea pig, exposed to about 98 per cent oxygen and about 98 per cent humidity. The tissue was fixed in osmium tetroxide, embedded in plastic, sectioned at 2 μ, and mounted unstained. In the upper half of the photomicrograph is a large macrophage and hyaline membrane in an alveolar duct. In the lower part of the picture (arrow) is an alveolus containing hyaline membrane and plasma; the alveolus is surrounded by collapsed lung. Phase contrast photomicrograph, × 630.

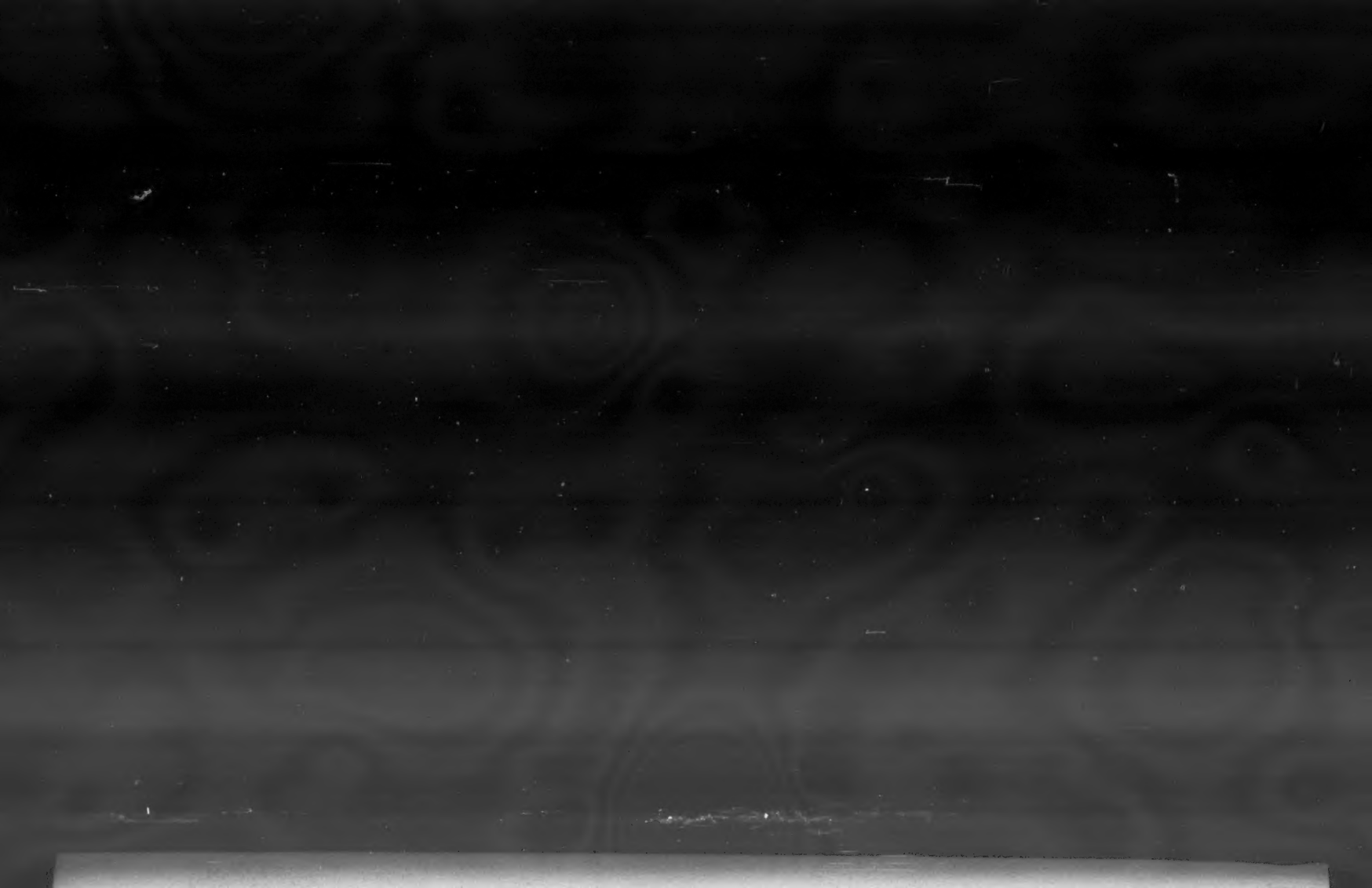

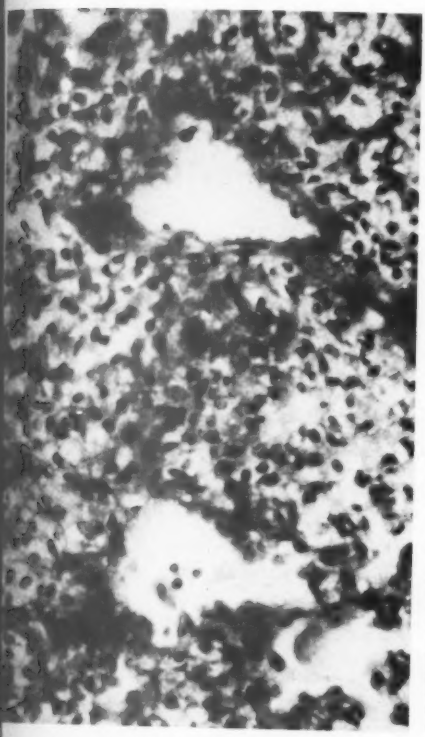

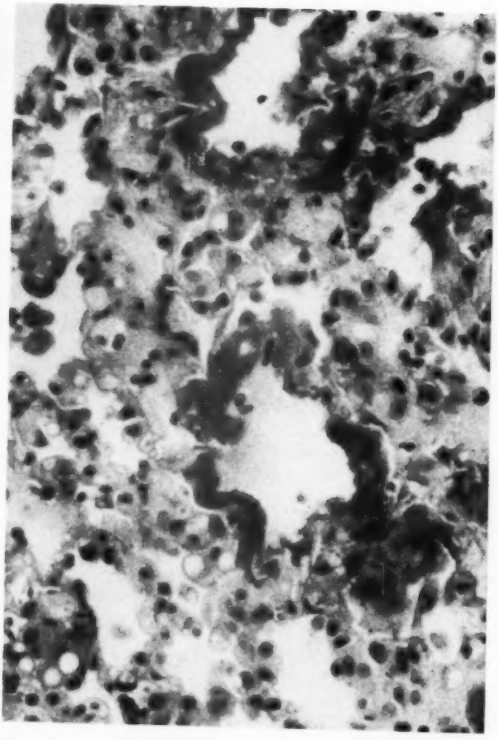

2

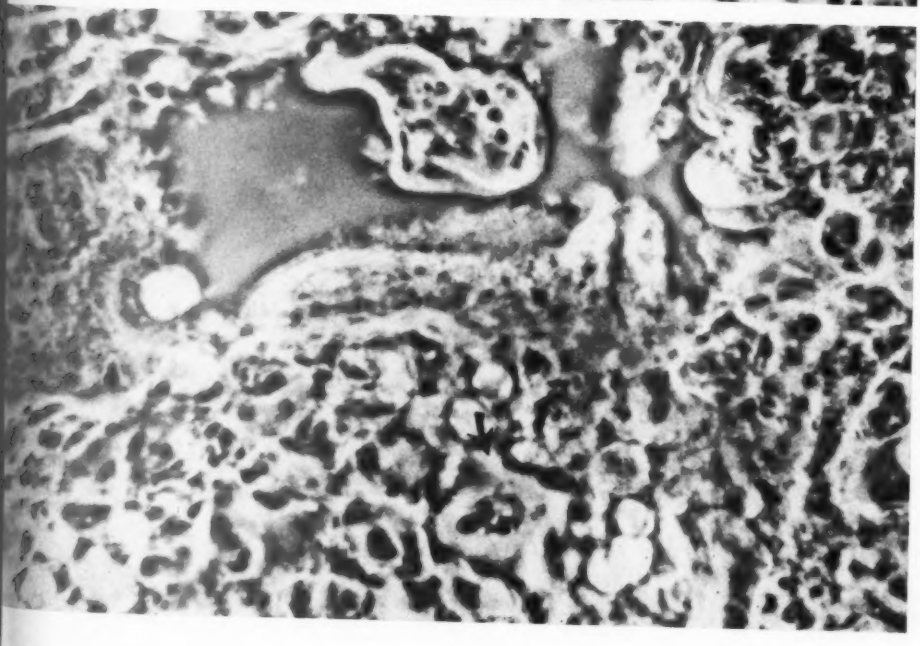

3

FIG. 4. Premature human infant lung (case 29). Hyaline membrane is seen in the air space at the top of the figure. The large cells with round nuclei are epithelial cells, from one of which an attenuated cytoplasmic layer extends over the adjacent capillary (lower left). The epithelium is separated from the endothelium by a single basement membrane (a). At (b) is a subepithelial space containing some collagenous fibrils. In the lumen of the capillary are two red blood cells. Electron micrograph, × 4,620.

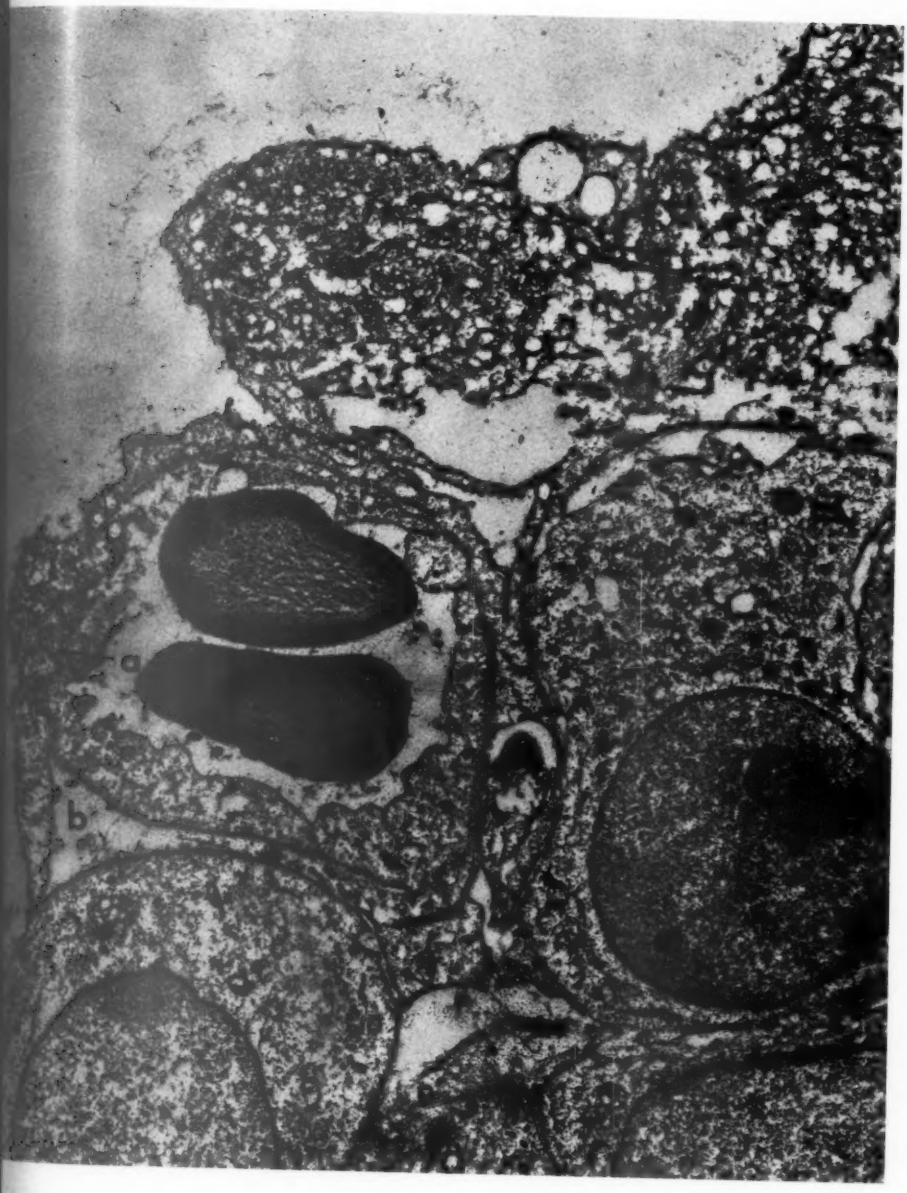

4

FIG. 5. Premature human infant lung (case 29). On the left side of the figure is a portion of a septal capillary. An erythrocyte (E) and plasma appear in the capillary. Endothelium and epithelium are separated by a basement membrane (arrow). In the air space overlying the epithelium is a layer of plasma (P), which, on the right side of the figure, extends into clotted hyaline membrane (H). The magnification is high enough to demonstrate the fibrous nature of the matrix of the hyaline membrane. Electron micrograph, × 6,875.

FIG. 6. Premature human infant lung (case 29). Higher magnification of hyaline membrane shows partially clotted fibrin matrix and cell débris. Electron micrograph, × 13,750.

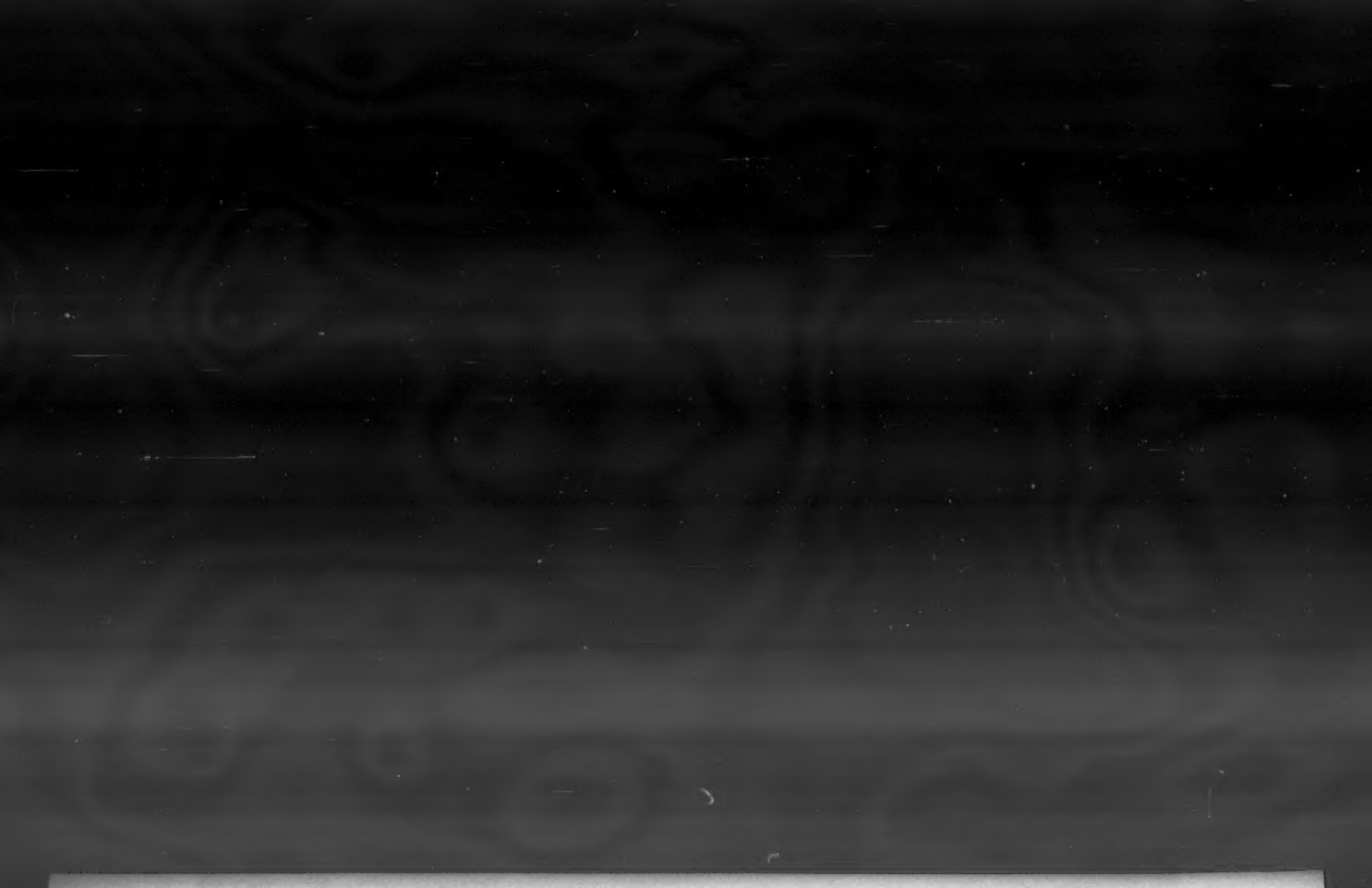

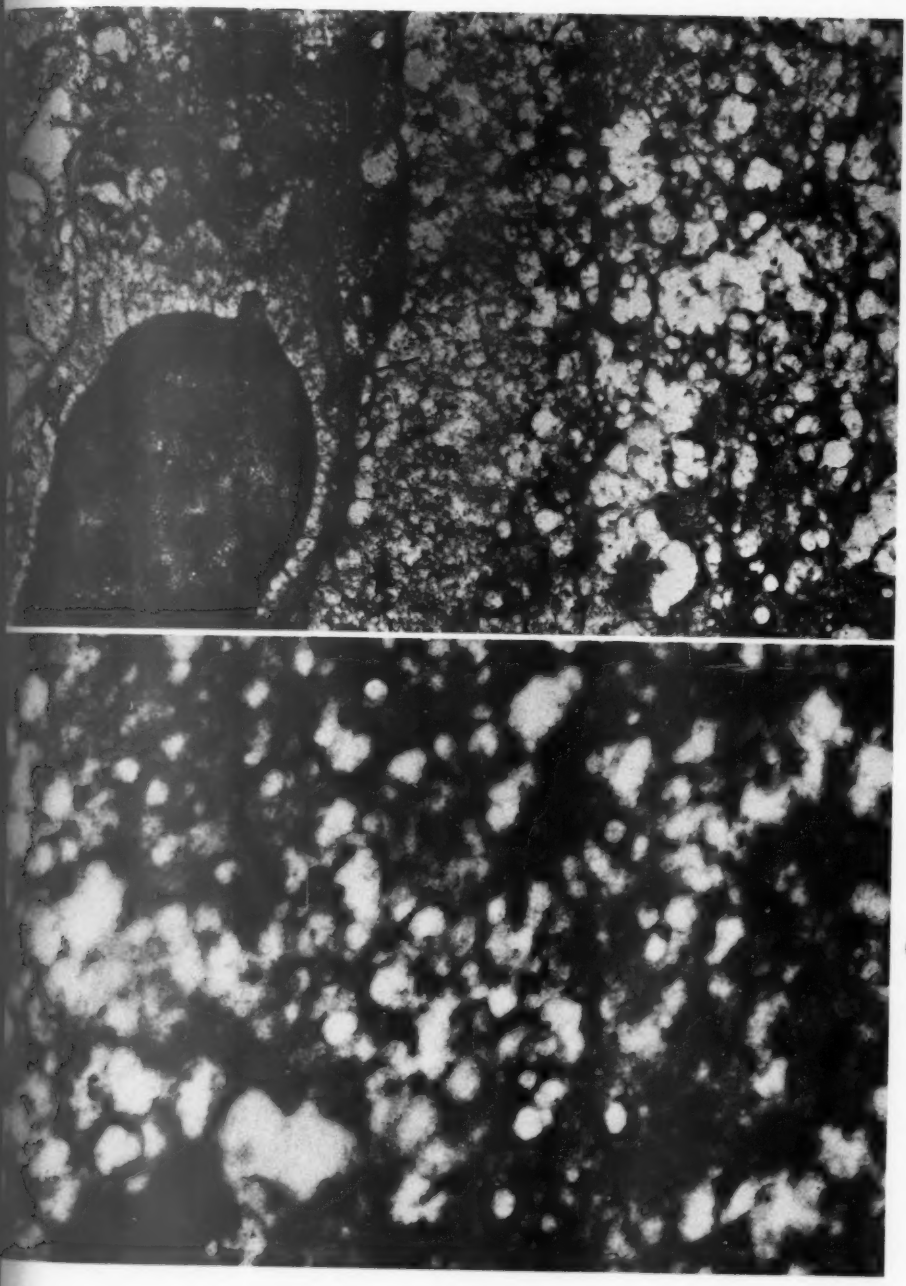

5

6

FIG. 7. Plasma clot. In this part of the section fibrin fibrils are the major constituent of the clot. Periodicity, or beading, is seen in many of the fibrils. Electron micrograph, × 15,170.

FIG. 8. Guinea pig lung. This figure shows the fibrillar matrix of the hyaline membrane at higher magnification, and demonstrates the periodicity, or beading, of the fibrils (example at arrow). Electron micrograph, × 22,760.

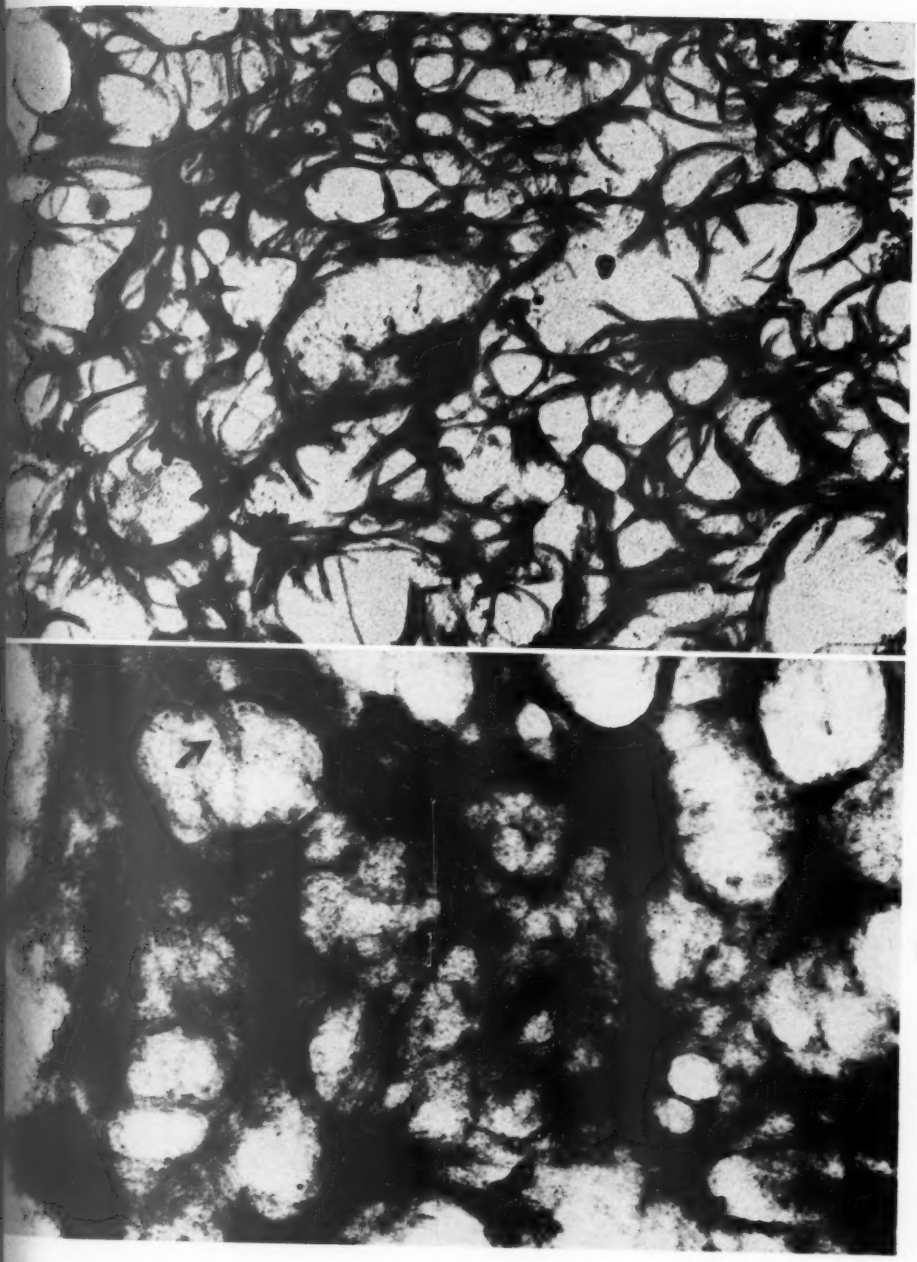

7

8

FIG. 9. Human infant lung (case 29). Parts of three capillaries appear in this figure, one at the top and two at the bottom of the figure. The alveolar duct between the capillaries is filled with a macrophage and hyaline membrane; ingested hyaline membrane may be seen in the macrophage, in which no nucleus appears at the level of section. There are small processes on the surface of the macrophage. At the right of the alveolar duct is an opening into an alveolus, which is full of hyaline membrane. Electron micrograph. × 2.165.

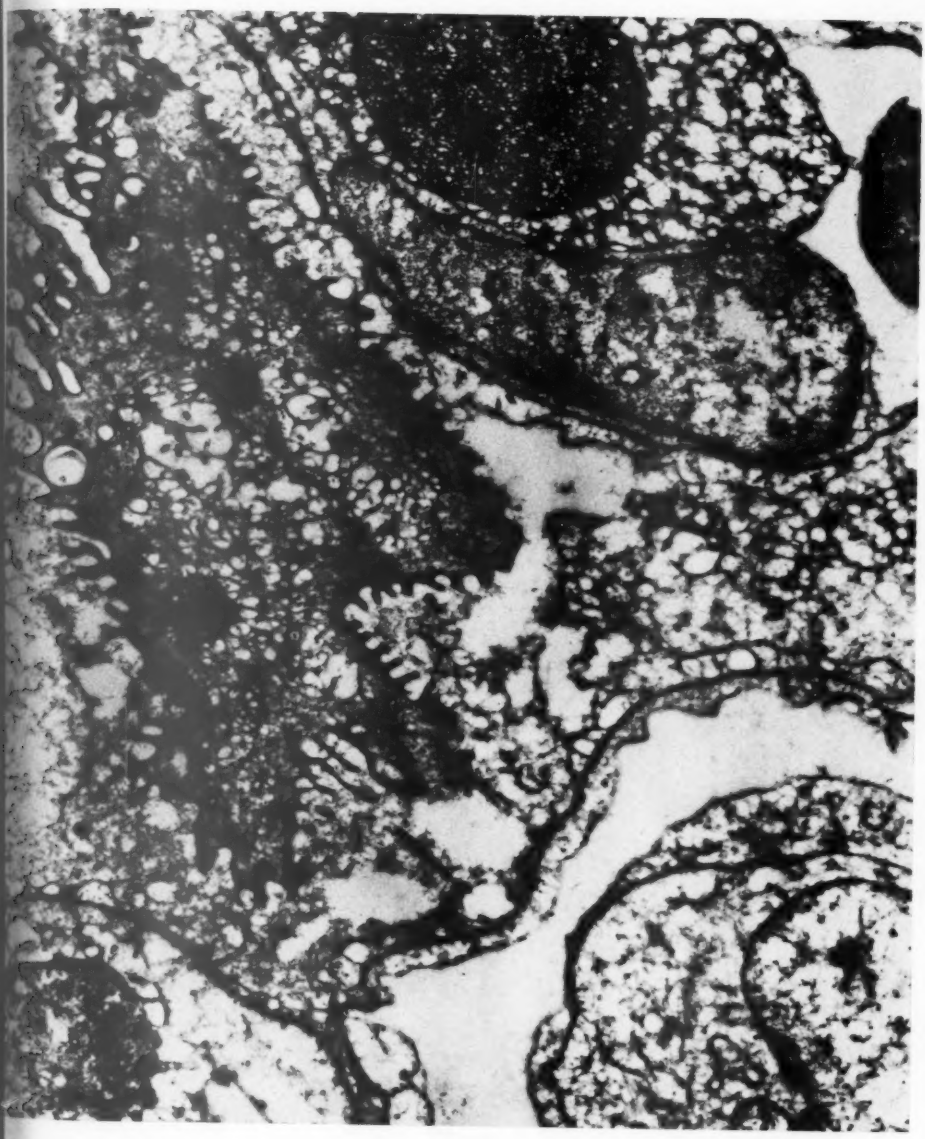

9

FIG. 10. Human infant lung (case 29). A large macrophage seen in a bronchiole (ciliated epithelium may be noted). Ingested hyaline membrane may be seen in the macrophage. Electron micrograph, × 2,600.

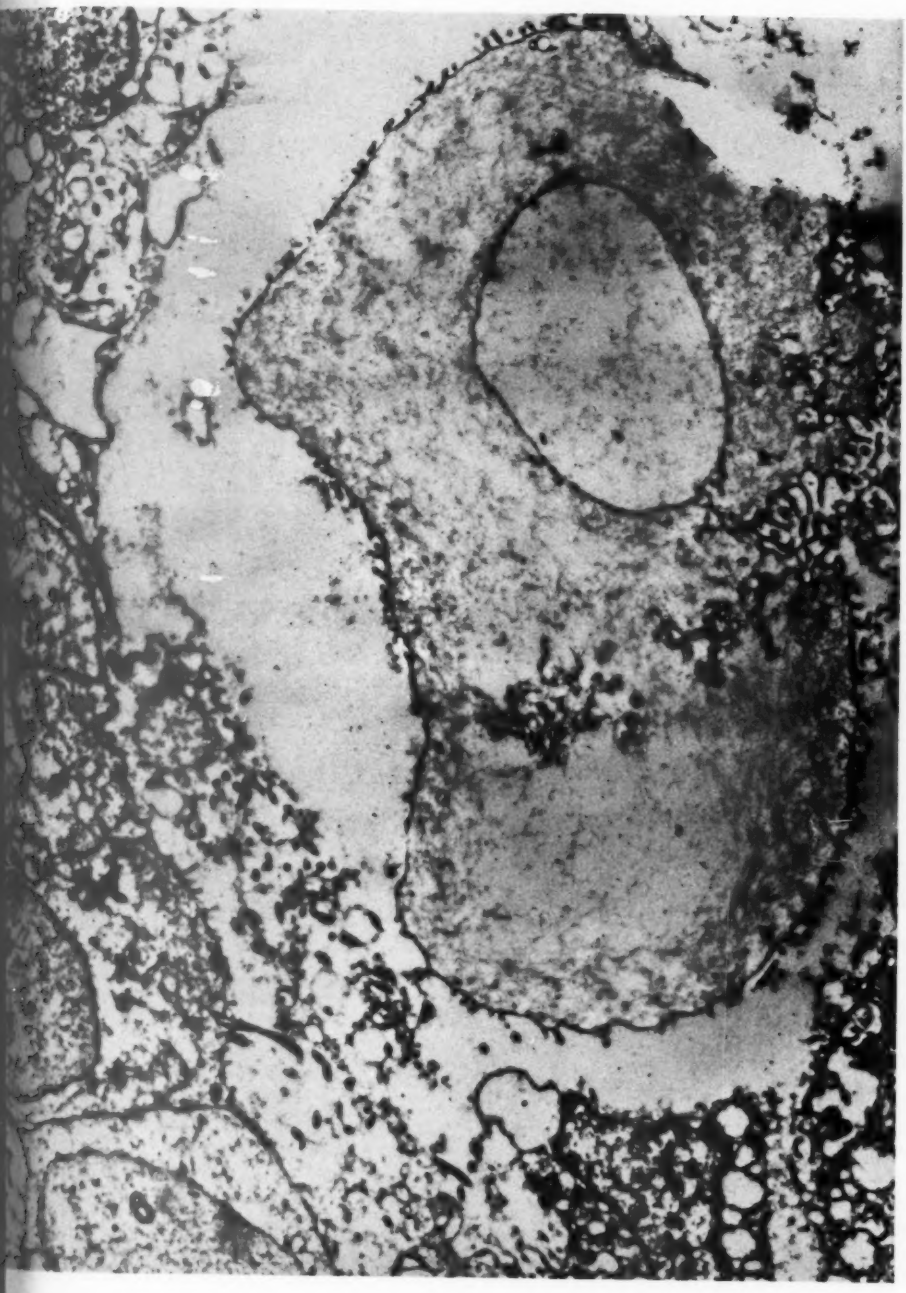

10

FIG. 11. Enlargement from Figure 10, showing the area of the microprojections at the cell surface, with evidence of ingestion of hyaline membrane and of pinocytosis. The very fine filaments seen in the cytoplasm of this macrophage are not from the hyaline membrane but are cytoplasmic components commonly found in cells, especially in macrophages and other ameboid cells. These submicroscopic filaments are believed to be part of the sol-gel mechanism of ameboid movement. Electron micrograph, × 8,500.

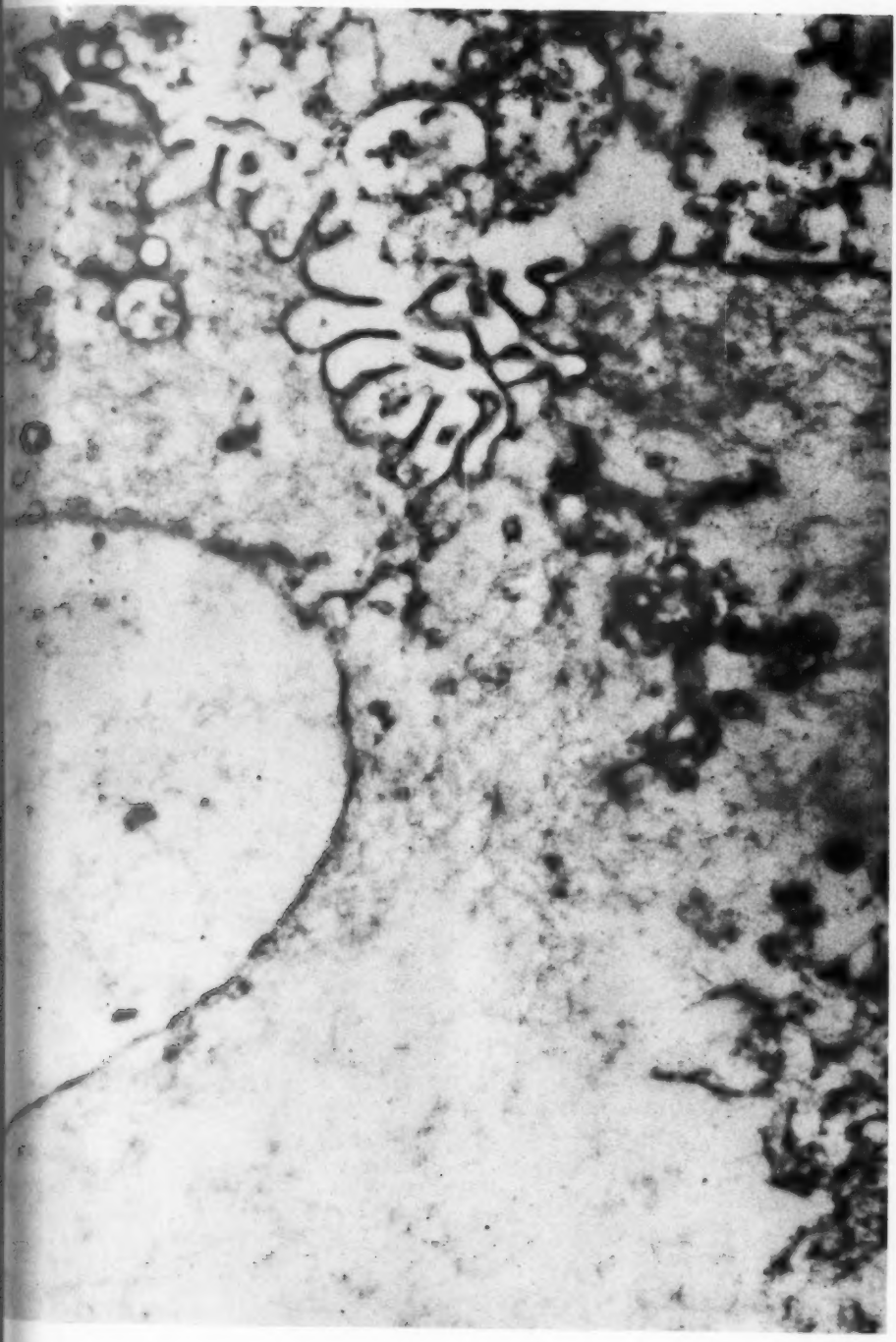

11

STUDIES ON FAMILIAL NEPHROSIS

II. Glomerular Changes Observed with the Electron Microscope*

Marilyn G. Farquhar, Ph.D.; Robert L. Vernier, M.D., and Robert A. Good, M.D.
From the Department of Pathology, University of California School of Medicine, San Francisco, Calif., and the Pediatric Research Laboratories of the Variety Club Heart Hospital, University of Minnesota, Minneapolis, Minn.

The clinical, laboratory, and pathologic data on four children from a single family who showed various manifestations of the nephrotic syndrome were reported in a previous article of this series.[1] The data clearly indicated that cases of the nephrotic syndrome appearing in a single family are indistinguishable from non-familial cases. Furthermore, the variability in the form of the disease is just as pronounced as in non-familial cases. This variation is illustrated by the following clinical designations of the syndrome in four children: case 1, nephrosis with chronic glomerulonephritis; case 2, transient "pure" nephrosis with apparent recovery; case 3, mixed nephrosis-nephritis; case 4, chronically active "pure" nephrosis.

The purpose of this report is to describe and illustrate the changes observed with the electron microscope in the glomeruli of the four children from this family and to discuss the physiologic and pathologic significance of our observations.

The normal renal glomerulus has been the subject of numerous electron microscopic studies.[2-16] Inasmuch as adequate techniques for tissue preparation were not generally available until relatively recently, early studies[2-5] were of limited value. However, following the introduction of improved technical methods, the structure of the normal glomerulus has been adequately described.[6-16] Only certain details of the fine structural features of glomeruli and the interpretations of their physiologic significance remain controversial.

Inasmuch as the fine structure of the normal glomerular capillary has been delineated, investigations of glomerular pathology and ex-

* This investigation was aided in part by research grants from the American Cancer Society (Institutional Grant 43G) and the National Heart Institute of the National Institutes of Health, Public Health Service (H-1542) to the Department of Pathology, University of California School of Medicine, San Francisco, and by grants to the Pediatric Research Laboratories of the Variety Club Heart Hospital, University of Minnesota, from the National Heart Institute, United States Public Health Service (E-798 and H-2085), Helen Hay Whitney Foundation, American Heart Association, Minnesota Heart Association, and the Graduate Research Fund of the University of Minnesota.

* Received for publication, August 29, 1956.

perimental lesions can now be undertaken with the electron microscope. To date we know of only four such investigations,[17–20] three of which were carried out in small animals.[17,18,20] The availability of fresh kidney tissue by direct surgical biopsy or needle biopsy has made the present electron-microscopic study of human renal lesions feasible.

Materials and Methods

Renal tissues from each of the four children with "familial nephrosis" were studied with the electron microscope. At least ten glomeruli from each patient were examined, with the exception of case 2; only three glomeruli from this case were available. The segment of tissue obtained from each child by biopsy was cut into two pieces immediately upon removal. One piece was fixed in formalin and was subsequently utilized for light microscopy.[1] The other piece was immersed in osmic acid and prepared for electron microscopy in the following manner: Blocks of 1 cmm. were cut from the tissue and fixed in 1 per cent buffered osmium tetroxide,[21] dehydrated in graded alcohols, infiltrated and embedded in n-butyl methacrylate,[22] and sectioned in a Porter-Blum microtome[23] equipped with a glass knife.[24] The sections obtained were examined in an RCA EMU-2 electron microscope, equipped with a biased gun, intermediate lens, and 10-mil condenser aperture. The objective lens had been compensated for astigmatism and contained an aperture measuring 25 to 30 μ. Pictures were taken at initial magnifications of 300 to 10,000 and were enlarged photographically as desired.

In addition to the ultrathin sections for electron microscopy, sections 1 μ thick were cut from tissue fixed in osmium tetroxide and embedded in methacrylate.[25] These were stained with Ehrlich's hematoxylin and studied by light microscopy. It was thus possible to study sections from the same glomerulus by both methods.

Observations

The Normal Glomerulus

Before describing the pathologic changes observed in the glomeruli of children with lipoid nephrosis, the anatomy of the normal glomerulus, as seen with the electron microscope, will be reviewed briefly. The structures to be described are identical in all mammalian species investigated up to the present; i.e., the rat,[7,10,11-13] mouse,[8,14,16,18] rabbit,[7] dog,[7,9] and man.[7,9,15]

It is generally agreed that the glomerular capillary has three distinct components: the endothelium, the basement membrane proper, and

the epithelium (Figs. 5 and 6). The endothelial cells lie closest to the lumen of the capillary. They are three to four times as numerous as epithelial cells, and their nuclei are somewhat smaller and denser than those of the latter. Cytoplasmic extensions of endothelial cells appear to line completely the inner aspect of the glomerular loop. Endothelial cytoplasm is abundant in the region near the nucleus and contains the usual components, i.e., mitochondria,[26] a few canaliculi of the endoplasmic reticulum[27] or ergastoplasm, and closely associated small basophilic particles.[28] At a greater distance from the cell body the cytoplasm becomes extremely attenuated and shows apparent interruptions. Some researchers[7,11,16] have described these discontinuities as regularly spaced pores, whereas others have suggested that they may represent intracytoplasmic vesicles[10] or a postmortem degenerative change.[8]

Directly adjoining the endothelium is the basement membrane proper. It consists of a nearly homogeneous layer, approximately 0.08 μ in thickness, possessing a moderate electron density. The basement membrane is considered to be an endothelial derivative,[5,6] for in places endothelial cytoplasm merges almost imperceptibly with the basement membrane. In other areas, particularly away from the endothelial cell body, a zone of lighter density separates the basement membrane from the endothelial cytoplasm. A similar zone of light density can usually be seen between the basement membrane and the epithelial foot processes. Pease[11] suggested that these areas of low density may be cement substance, attaching the endothelium on one side and partially embedding the epithelial foot processes on the other. Hall[6] believed he could distinguish a fine porosity in the basement membrane. Reid[8] suggested that the basement membrane possibly possesses a delicate fibrillary character, and Rhodin[14] also believed that there is an indication of a lamellated structure. A number of workers[9-12] were unable to find any regular fine structure. This is in contrast to the basement membrane of Bowman's capsule which shows a distinct lamellated structure.[9]

The outer layer of the glomerular capillary wall is the epithelium. The pale epithelial nuclei are surrounded by abundant cytoplasm which has a rather light background density and contains scattered formed elements—vesicles, mitochondria, Golgi material,[29] and a few canaliculi of the endoplasmic reticulum. In the normal glomerulus, epithelial cells possess a very remarkable and elaborate organization. Their cytoplasm is divided into a number of branches; each branch in turn is divided into a number of secondary branches or "foot processes" which are applied to the outer aspect of the basement membrane. The portion

of the foot process directly adjacent to the basement membrane possesses greater density than the remainder of the epithelial cyptoplasm. Ordinarily, a small space separates adjoining foot processes, and a similar space separates the foot process and the basement membrane.

Several workers[12,16] believe that, in addition to the endothelium, epithelium, and basement membrane, a fourth component of the glomerular tuft can be distinguished in electron micrographs. This component is the intercapillary layer or "mesangium" of Zimmermann.[30] Hall[6,7] and Mueller *et al.*[9] pointed out that what has been interpreted as mesangium by some actually represents sections through the base of endothelial cells at places where they form intimate attachments to the basement membrane. Furthermore, Irvine *et al.*[19] failed to find "intercapillary spaces" or mesangial cells in renal tissues taken for biopsy from patients with diabetic glomerulosclerosis. We can find no evidence for the existence of a mesangial layer in either normal or pathologic glomeruli. We believe that the endothelium, epithelium, and basement membrane are the only glomerular components. Furthermore, our observations,[5,15] in accordance with those of others,[6,9,12] indicate that there is no collagen in the normal glomerulus.

Glomerular Structure in Lipoid Nephrosis

Striking alterations from normal glomerular architecture were observed in all the glomeruli from the children with nephrosis which we examined. The most constant and definitive changes were observed in the epithelium, although in some instances changes were seen in the endothelium and basement membrane.

Marked alterations were evident in the organization of the epithelium. Foot processes were greatly decreased in number and in some areas were virtually absent. Instead, broad masses of epithelial cytoplasm covered the surface of the loops, and only occasional and irregularly spaced interruptions were present (Figs. 7, 8, 9, 11, and 12). It is interesting that the portion of the epithelial cytoplasm which directly adjoins the basement membrane retained the greater density normally seen at the base of each foot process. Sometimes there even appeared to be a greater accumulation of dense material than normal (Fig 11).

One could speculate that this area of greater density in the portion of the epithelium directly adjoining the basement membrane may possibly be due to a concentration of an enzyme which is active at the site of filtration. A heavy metal activator could cause greater electron absorption and, therefore, render the area more dense in appearance.

In addition to the lack of foot processes, the epithelial cytoplasm commonly showed other changes. Although vacuoles and vesicles were encountered in both epithelial and endothelial cytoplasm of the normal glomerulus, vacuolar bodies were much more frequently seen in the cytoplasm of the epithelial cells of the nephrotic glomerulus (Figs. 7, 8, and 11). These vacuoles were of varying size and in some instances were quite large—up to 3 to 4 μ. They were separated from the remainder of the cytoplasm by a membrane. Sometimes microvilli or filiform processes, formed by infolding of the limiting membrane, projected into the lumen of the vacuole. A scattering of flocculent material sometimes was seen within the vacuoles, but otherwise they contained material of little or no electron density.

We have gained the impression that the formed cytoplasmic elements —the mitochondria, Golgi material, endoplasmic reticulum, and basophilic particles—were present in greater amounts in the epithelium of the nephrotic glomerulus than in that of the normal glomerulus (Fig. 7). Golgi material, particularly, appeared to be abundant.

It should be emphasized that, although the severity of the changes varied from one case to another, these alterations in epithelial structure were present in the glomeruli of all the children studied regardless of the clinical phase of the disease or the state of the pathologic process as observed by light microscopy. Furthermore, this lesion is not merely a characteristic of the particular group described here, but has been observed in all of the other cases, regarded clinically as "pure" nephrosis, which we have studied.

Sometimes changes were seen also in the endothelium and basement membrane proper. In contrast to the changes in the epithelium described above, those in the endothelium and basement membrane varied a great deal, not only from one case to another, but also among glomeruli from the same child. The basement membrane was either of normal thickness, slightly thickened, or obviously thicker than normal. Often, the typical homogeneous character of the basement membrane was lacking. Instead, it presented a rather moth-eaten appearance, consisting of the usual more or less homogeneous material interrupted by lighter areas of little or no density (Figs. 8 and 9). Furthermore, in some instances the basement membrane showed a delicate fibrillar appearance suggesting that it possesses a lamellated structure similar to that of the basement membrane of Bowman's capsule.

When the basement membrane appeared thicker than normal its outer or epithelial edge remained smooth, and the clear separation between epithelium and basement membrane was still present. However,

the endothelial border of the basement membrane was very irregular, and in many areas there was no distinct separation from endothelial cytoplasm. The endothelial edge of the basement membrane showed nodular areas of various sizes and configurations which resembled knots on a tree (Fig. 9). This frequent finding of an intimate association between the basement membrane and endothelium under conditions wherein the basement membrane is presumably undergoing a thickening further supports the belief[5,6,15] that the basement membrane is an endothelial product.

Like the changes in the basement membrane, the changes in the endothelium were quite variable both from one child to another and among glomeruli from the same child. An increase in the number of endothelial cells (endothelial proliferation, Fig. 12) was sometimes observed, particularly in case 1 and to a lesser extent in case 3. In addition, great irregularity was observed in the luminal cytoplasmic border of the endothelium due to the presence of numerous tiny cytoplasmic processes. When the processes were cut tangentially, they took on a very interesting and sometimes puzzling appearance, suggesting a meshwork (Fig. 10). In addition, the endothelial cytoplasm contained many small fluid droplets or vesicles and often appeared quite swollen or distended. It has been suggested[21] that fluid may be transported across the endothelium via minute vesicles. The presence of an apparent increase in activity at the cell border of the endothelium in nephrosis, together with the presence of abundant cytoplasmic vesicles, suggest that the endothelium is more active than normal in taking up fluid from the blood stream. The possible significance of this finding will be discussed in a later section.

As contrasted to alterations in epithelial structure, the presence and severity of changes of the endothelium and basement membrane observed with the electron microscope seem to be related to the duration of the disease and its severity as interpreted by light microscopy. For instance, in case 4, in which the duration of the disease was only 2 to 3 months, the glomeruli appeared virtually normal under the light microscope (Fig. 4). By electron microscopy only epithelial changes were apparent (Fig. 8). No increase in the number of endothelial cells was noted. The basement membrane appeared quite thin, but this was probably because of the very young age (3 months) of the child. The glomeruli of case 3, which was of longer duration (2 years), showed changes characteristic of subacute glomerulonephritis when examined with the light microscope (Fig. 3). When viewed with the electron microscope, not only were epithelial changes present, but

moderate thickening of the basement membrane and a moderate increase in the number of endothelial cells were observed in most of the glomeruli (Figs 7 and 11). Case 1, which was of longest duration (6 years), showed the greatest pathologic changes under the light microscope (Fig. 1). By electron microscopy the changes varied considerably from glomerulus to glomerulus. Epithelial lesions were observed in all of the glomeruli, but additional alterations ranged from a slight thickening of the basement membrane and a moderate increase in the number of endothelial cells, such as seen in case 3, to almost complete obliteration of some glomeruli. The most severely altered glomeruli were shrunken and were composed of a few endothelial cells and small epithelial cells embedded in a mass of homogeneous basement membrane-like material (Fig. 12). Few, if any, open blood channels could be found.

Case 2 showed symptoms of nephrosis over a period of 7 to 8 months with subsequent recovery. This time interval is intermediate between that of case 3 and that of case 4 (case 2 was biopsied 1 year after apparent recovery). However, this patient showed only mild manifestations of the nephrotic syndrome at virtually a subclinical level, and the renal tissue appeared normal with the light microscope (Fig. 2). The three glomeruli available for electron microscopic examination showed only mild distortion of the epithelial foot processes, and no changes of endothelium or basement membrane were observed. These glomeruli were more nearly normal than those from any of the other children of the family.

Proximal Convoluted Tubules

Although this report is concerned chiefly with glomerular changes seen in nephrosis, because of the prominent tubular changes seen in this condition a few brief remarks on the cells of the proximal convoluted tubules seem appropriate. The structure of cells from the normal proximal convoluted tubules has been the subject of detailed reports by Sjöstrand and Rhodin,[32] Rhodin,[33] and Pease.[34] The important aspects of tubular structure delineated by electron microscopy include (1) the description of an elaborate system of membranes dividing the basal cytoplasm of tubular cells into compartments which contain mitochondria and (2) clarification of the nature of the "brush border" which has been shown to consist of simple extensions of the apical cytoplasm of the cell.

It is well known that the cytoplasm of these cells as well as tubular lumina of nephrotic patients frequently contain lipidic droplets.[35]

When the lipidic accumulations were small, they usually appeared quite dense under the electron microscope. However, when the accumulations were large, they typically were dense on the surface and empty in the center. The latter appearance is presumably due to poor penetration by osmic acid into lipidic droplets.[36]

We observed several other interesting changes in these cells of the kidneys from each of the children with nephrosis with the exception of case 2. First of all, we noted that frequently the cells showed a complete absence of the brush border (Fig. 13). In other instances the number of cytoplasmic projections forming the brush border was greatly diminished. Secondly, we noted a variable number of large granules in the cytoplasm of some of the cells (Figs. 13 and 14). These granules most certainly are the structures called hyaline droplets and appear to be derived from mitochondria as originally suggested by Oliver.[37] Rhodin[33] studied these cells in mice subjected to egg white injections and found that the ultrastructure of the mitochondria was destroyed. Parallel with this destruction the mitochondria fused to form large granules. In the proximal convoluted tubular cells of nephrotic patients we noted all gradations in size from granules to mitochondria, and frequently some of the granules showed remnants of mitochondrial structure. These findings appear to confirm the studies of Oliver and Rhodin, indicating the derivation of hyaline droplets or granules from altered mitochondria.

Rhodin[33] and Pease[34] failed to find evidence of internal structure in the basement membranes of the normal proximal convoluted tubule. However, we have frequently observed a definite laminated structure in the basement membranes of tubules of patients with nephrosis. It may be that the disease process causes the removal of some component from both tubular and glomerular basement membranes which normally binds the layers together and results in the homogeneous appearance seen with the electron microscope.

Discussion

The previous paper of this series[1] indicated the variability of the clinical and pathologic manifestations of nephrosis in four children of a family in which a single pathogenic mechanism was presumed to underlie the disease. The results of the present study indicate that a common pathologic alteration can be observed with the electron microscope in the kidney of each of the four children studied. This lesion is present regardless of the clinical state of the patient, the duration of the disease process, or the pathologic changes as observed with the

light microscope. The common pathologic change revealed by the electron microscope consists of alterations in the epithelial component of the glomerular capillary wall. The same lesion has been seen in all other cases regarded clinically as "pure nephrosis" which we have studied. Furthermore, these early changes seen in nephrosis differ markedly from those we have observed in the glomeruli of patients with classical acute and subacute glomerulonephritis and with disseminated lupus erythematosus. Likewise, the changes differ from those observed in patients with diabetic glomerulosclerosis.[10]

Since the light microscopic appearance of the kidneys of children who have succumbed to nephrosis is variable,[35] the finding of a common submicroscopic lesion of the glomerulus in nephrosis, irrespective of the stage of the process, should contribute to an understanding of the pathogenesis of the disease.

It is not surprising that many capable investigators fail to find evidences of glomerular abnormality on light microscopic examination of the kidneys of children succumbing to lipoid nephrosis.[35,38-42] Likewise, it is easy to understand how others, such as Allen,[43] can recognize only an abnormal thickening of the glomerular capillary wall in this condition, for most of the details of glomerular structure, such as the attenuated endothelial cytoplasm, basement membrane proper, spaces between foot processes, and the endothelial interruptions or "pores," are of a size well below that resolvable with the ordinary light microscope. Only with the electron microscope can the components of the glomerular capillary wall be adequately delineated. Hall[6,7] pointed out that what light microscopists generally refer to as the basement membrane probably includes: (1) the attenuated endothelial cytoplasm, (2) the basement membrane proper, and (3) the epithelial foot processes, seen by electron microscopy. A thickening of any one of these components would probably appear to the light microscopist as a thickening of the basement membrane. Conversely, when a thickening of the glomerular wall can be discerned with the light microscope, the exact site of the alteration in terms of fine structural features cannot be determined. Furthermore, the present study indicates that a disease process must be well advanced before changes become clearly demonstrable at the level of the light microscope. However, by combining the techniques of renal biopsy and electron microscopy, the exact site of very early changes in the glomerulus may be detected. In nephrosis, changes in the epithelium are seen before changes in either the endothelium or basement membrane proper become evident. Therefore, we consider the epithelium to be the probable

site of early glomerular injury in lipoid nephrosis. By defining the site of early injury, further insight may be gained into the nature and mechanism of this disease.

Concepts of Glomerular Filtration Based on Fine Structure

Most investigators who have studied glomerular structure with the electron microscope have developed similar ideas about the possible pathway of the glomerular filtrate. These ideas stem chiefly from the studies of Hall[6,7] who postulated that filtration may occur through the interruptions or "large pores" in the endothelium and between the slits separating the epithelial foot processes. Therefore, according to Hall's concept, the basement membrane proper (or "lamina densa" of his terminology) acts as the chief barrier, restricting the passage of proteins while allowing the passage of fluid and salts.

Rinehart,[10] on the other hand, was of the opinion that the nature and structure of the endothelium and epithelium were such as to indicate that both are quite active in the filtration process. He regarded the endothelial pores of Hall, Pease, and others as intracytoplasmic vesicles and suggested that the transfer of fluid across endothelial cytoplasm to reach the basement membrane occurs via small vesicles. The latter would then serve as an effective filter for protein. He suggested that the filtrate then passes through the basement membrane, is taken up by the epithelial foot processes, and is subsequently transferred to the urinary spaces and to the proximal convoluted tubules. He believed that the delicate, spongy cytoplasm of adjacent foot processes are actually in contact in life so that the filtrate must pass through epithelial cytoplasm.

Our observations on the glomeruli from patients with lipoid nephrosis appear to lend support to certain aspects of Rinehart's[10] concept of glomerular filtration. We have noted that the organization of epithelial cytoplasm into foot processes is diminished or virtually absent in patients with nephrosis. Instead, broad masses of epithelial cytoplasm are applied to the basement membrane and only occasional interruptions are seen. If filtration were presumed to occur between adjacent foot processes, the surface area for filtration should be greatly reduced in nephrosis, and one would expect the filtration rate to be correspondingly reduced. However, such was not the case, for early in the course of the disease all of the children were shown to have normal or supernormal glomerular filtration rates as measured by inulin clearance.[1]

In addition, the epithelial cells contain large fluid vacuoles and

increased amounts of Golgi material, endoplasmic reticulum, and basophilic particles. These cytologic changes are suggestive of increased functional activity. The finding of diminished numbers of foot processes and evidences of increased cytoplasmic activity in the presence of normal or supernormal glomerular filtration rates suggest that the filtrate may pass through the cytoplasm of epithelial cells.

We have noted also an increase in the number of vesicles at the luminal cytoplasmic border of the endothelial cells of the nephrotic glomerulus and a swelling and increase in the number of vesicles in the endothelial cytoplasm in general. These findings suggest that the endothelium is actively taking up fluid droplets from the plasma. Such changes may simply reflect the generalized edema which occurs in these patients presumably due to hypo-albuminemia.

There is another possible explanation for the occurrence of decreased numbers of epithelial foot processes in the presence of proteinuria and supernormal or normal glomerular filtration rates. It is possible that the epithelial alteration is not a primary change but may be secondary to changes in the basement membrane proper. We have noted that later in the disease the basement membrane shows areas of light density which give it a moth-eaten appearance. The initiation of this process of disruption and distortion of the basement membrane may occur on such a fine level early in the course of the disease that it cannot be readily distinguished with the electron microscope. Such "holes" in the basement membrane might allow a considerable amount of leakage of protein and salts from the glomerular capillary and might also be responsible for an increase in the glomerular filtration rate. The epithelial changes could then be interpreted as resulting from an attempt by the capillary to repair the large holes in its filtration apparatus.

At any rate, it appears that it is too early to engage in anything except speculation about the mechanisms involved in glomerular filtration under either normal or pathologic conditions. Explanations of the physiologic implications of many of the observations made must await further correlated studies.

Comment

The results of this study together with preliminary studies of renal tissue taken for biopsy from other non-familial nephrotic patients and from patients with classical acute and subacute glomerulonephritis [44,45] indicate that the clinical expressions of these diseases correlate remarkably well with glomerular lesions demonstrable at the

electron microscope level. Those patients who are designated clinically as manifesting "pure nephrosis" early in the disease show primarily changes in the epithelial component of the glomerular tuft, while those patients with classical acute or subacute glomerulonephritis characteristically show a striking proliferation of endothelial cells and basement membrane-like material. It appears that if the clinical picture is mixed, the histopathologic changes visible with the electron microscope in the glomeruli are likewise mixed and therefore show various combinations of alterations in structure of epithelium, endothelium, and basement membrane.

Thus the fine structure of the glomeruli from patients with nephrosis or nephritis may to a certain extent be predicted from knowledge of the clinical history. In contrast, the pathologic diagnoses based on light microscopic studies are of limited value in predicting submicroscopic lesions unless the disease process is well advanced.

Summary

Renal tissues taken for biopsy from four children of a single family with various manifestations of the nephrotic syndrome were studied with the electron microscope. The clinical designations of the four children, reported in a previous paper of this series,[1] included: pure nephrosis, mixed nephrosis and nephritis, and chronic glomerulonephritis. The pathologic diagnoses based on light microscopy, also reported in the previous paper, ranged from normal kidney to chronic glomerulonephritis.

When ultrathin sections of the tissues were studied with the electron microscope, a striking change in the organization of the epithelium of the glomerular capillary was seen to be common to all of the children. These changes were present regardless of the clinical phase of the disease or state of the pathologic process observed by light microscopy. The alteration consisted of a loss of the characteristic differentiation of epithelial cytoplasm into numerous foot processes which normally insert on the outer aspect of the basement membrane. Instead, it was noted that broad masses of epithelial cytoplasm covered large areas of the capillary loops, and only occasional, irregularly spaced interruptions were present. The epithelial cells also showed increased numbers of large vacuoles, canaliculi of the endoplasmic reticulum, basophilic particles, and Golgi material in cytoplasm.

Changes sometimes were seen also in the endothelium and basement membrane proper. The presence and severity of these changes appeared to be related to the duration of the disease as well as its

severity, as interpreted by light microscopy. The range in changes of the endothelium and basement membrane was considerable, being quite severe in the child with the disease of longest duration (6 years) and indiscernible in the child with the disease of shortest duration (2 to 3 months). The alterations in the basement membrane consisted of an irregular thickening and loss of homogeneity which was interrupted by clear, empty-appearing areas. The chief endothelial alterations noted were a swelling and proliferation of cells along with great irregularity in the luminal cytoplasmic border.

The possible significance of the glomerular changes in relationship to the pathogenesis of nephrosis as well as to the concepts of glomerular filtration is discussed. Also included is a discussion of the correlation between the clinical picture and the electron microscopic findings.

In addition, a few observations on changes observed with the electron microscope in the cells of the proximal convoluted tubules are presented.

Finally, it is suggested that studies with the electron microscope may help a great deal to clarify the basic pathologic changes which occur in nephrosis and other types of renal disease, for only with the electron microscope can the fine structural components of the glomerulus be adequately visualized.

REFERENCES

1. Vernier, R. L.; Brunson, J., and Good, R. A. Studies on familial nephrosis. I. Clinical and pathologic study of four cases in a single family. *Am. J. Dis. Child.*, 1957, 93, 469–485.
2. Pease, D. C., and Baker, R. F. Electron microscopy of the kidney. *Am. J. Anat.*, 1950, 87, 349–389.
3. Oberling, C.; Gautier, A., and Bernhard, W. La structure des capillaires glomérulaires vue au microscope électronique. *Presse méd.*, 1951, 59, 938–940.
4. Dalton, A. J. Structural details of some of the epithelial cell types in the kidney of the mouse as revealed by the electron microscope. *J. Nat. Cancer Inst.*, 1950–51, 11, 1163–1185.
5. Rinehart, J. F.; Farquhar, M. G.; Jung, H. C., and Abul-Haj, S. K. The normal glomerulus and its basic reactions in disease. *Am. J. Path.*, 1953, 29, 21–31.
6. Hall, B. V. Studies of normal glomerular structure by electron microscopy. Proceedings of the Fifth Annual Conference on the Nephrotic Syndrome, Philadelphia, November 5–7, 1953. National Nephrosis Foundation, Inc., New York, 1953, 39 pp.
7. Hall, B. V. Further studies of the normal structure of the renal glomerulus. Proceedings of the Sixth Annual Conference on the Nephrotic Syndrome, Cleveland, November 5–6, 1954. National Nephrosis Foundation, Inc., New York, 1954, 40 pp.

8. Reid, R. T. W. Observations on the structure of the renal glomerulus of the mouse revealed by the electron microscope. *Australian J. Exper. Biol. & M. Sc.*, 1954, **32**, 235–239.

9. Mueller, C. B.; Mason, A. D., Jr., and Stout, D. G. Anatomy of the glomerulus. *Am. J. Med.*, 1955, **18**, 267–276.

10. Rinehart, J. F. Fine structure of renal glomerulus as revealed by electron microscopy. *A. M. A. Arch. Path.*, 1955, **59**, 439–448.

11. Pease, D. C. Electron microscopy of the vascular bed of the kidney cortex. *Anat. Rec.*, 1955, **121**, 701–721.

12. Policard, A.; Collet, A., and Giltaire-Ralyte, L. Recherches au microscope électronique sur la structure du glomérule rénal des mammifères. *Arch. d'anat. micr.*, 1955, **44**, 1–19.

13. Bargmann, W.; Knoop, A., and Schiebler, T. H. Histologische, cytochemische und elektronen-mikroskopische Untersuchungen am Nephron, mit Berücksichtigung der Mitochondrien. *Ztschr. f. Zellforsch. u. mikr. Anat.*, 1955, **42**, 386–422.

14. Rhodin, J. Electron microscopy of the glomerular capillary wall. *Exper. Cell Res.*, 1955, **8**, 572–574.

15. Rinehart, J. F.; Farquhar, M. G., and Gould, E. Fine structure of the renal glomerulus. Histochemical and electron microscopic observations. (Abstract.) *Am. J. Path.*, 1955, **31**, 587–588.

16. Yamada, E. The fine structure of the renal glomerulus of the mouse. *J. Biophys. & Biochem. Cytol.*, 1955, **1**, 551–566.

17. Simer, P. H. Electron microscopic study of the glomerulus, especially its basement membrane in normal and nephritic mice. (Abstract.) *Anat. Rec.*, 1955, **121**, 416.

18. Piel, C. F.; Dong, L.; Modern, F. W. S.; Goodman, J. R., and Moore, R. The glomerulus in experimental renal disease in rats as observed by light and electron microscopy. *J. Exper. Med.*, 1955, **102**, 573–580.

19. Irvine, E.; Rinehart, J. F.; Mortimore, G. E., and Hopper, J., Jr. The ultrastructure of the renal glomerulus in intercapillary glomerulosclerosis. (Abstract.) *Am. J. Path.*, 1956, **32**, 647–648.

20. Reid, R. T. W. Electron microscopy of glomeruli in nephrotoxic serum nephritis. *Australian J. Exper. Biol. & M. Sc.*, 1956, **34**, 143–150.

21. Palade, G. E. A study of fixation for electron microscopy. *J. Exper. Med.*, 1952, **95**, 285–298.

22. Newman, S. B.; Borysko, E., and Swerdlow, M. Ultra-microtomy by a new method. *J. Res. Nat. Bureau Standards*, 1949, **43**, 183–199.

23. Porter, K. R., and Blum, J. A study in microtomy for electron microscopy. *Anat. Rec.*, 1953, **117**, 685–710.

24. Latta, H., and Hartmann, J. F. Use of a glass edge in thin sectioning for electron microscopy. *Proc. Soc. Exper. Biol. & Med.*, 1950, **74**, 436–439.

25. Farquhar, M. G. Preparation of ultrathin tissue sections for electron microscopy. Review and compilation of procedures. *Lab. Investigation*, 1956, **5**, 317–337.

26. Palade, G. E. The fine structure of mitochondria. *Anat. Rec.*, 1952, **114**, 427–451.

27. Porter, K. R. Electron microscopy of basophilic components of cytoplasm. *J. Histochem.*, 1954, **2**, 346–375.

28. Palade, G. E. A small particulate component of the cytoplasm. *J. Biophys. & Biochem. Cytol.*, 1955, 1, 59–68.

29. Dalton, A. J., and Felix, M. D. Cytologic and cytochemical characteristics of the Golgi substance of epithelial cells of the epididymis—in situ, in homogenates and after isolation. *Am. J. Anat.*, 1954, 94, 171–207.

30. Zimmermann, K. W. Über den Bau des Glomerulus der Säugerniere, Weitere Mitteilungen. *Ztschr. f. mikr.-anat. Forsch.*, 1933, 32, 176–278.

31. Palade, G. E. Fine structure of blood capillaries. *J. Applied Physics*, 1953, 24, 1424.

32. Sjöstrand, F. S., and Rhodin, J. The ultrastructure of the proximal convoluted tubules of the mouse kidney as revealed by high resolution electron microscopy. *Exper. Cell Res.*, 1953, 4, 426–456.

33. Rhodin, J. Correlation of Ultrastructural Organization and Function in Normal and Experimentally Changed Proximal Convoluted Tubule Cells of the Mouse Kidney. Privately printed for the Department of Anatomy, Karolinska Institutet by Artiebolaget Godvil, Stockholm, 1954, 76 pp.

34. Pease, D. C. Electron microscopy of the tubular cells of the kidney cortex. *Anat. Rec.*, 1955, 121, 723–743.

35. Bell, E. T. Renal Diseases. Lea & Febiger, Philadelphia, 1950, ed. 2, 448 pp.

36. Bahr, G. F. Continued studies about the fixation with osmium tetroxide. Electron stains IV. *Exper. Cell Res.*, 1955, 9, 277–285.

37. Oliver, J. The structure of the metabolic process in the nephron. *J. Mt. Sinai Hosp.*, 1948–49, 15, 175–222.

38. Dunn, J. S. Nephrosis or nephritis? *J. Path. & Bact.*, 1934, 39, 1–25.

39. Murphy, F. D.; Warfield, L. M.; Grill, J., and Annis, E. R. Lipoid nephrosis. A study of nine patients, with special reference to those observed over a long period. *Arch. Int. Med.*, 1938, 62, 355–376.

40. Pantin, C. G. A study of the relation between nephritis and nephrosis. *Guy's Hosp. Rep.*, 1938, 88, 456–481.

41. Heymann, W., and Startzman, V. Lipemic nephrosis. *J. Pediat.*, 1946, 28, 117–133.

42. Schwarz, H.; Kohn, J. L., and Weiner, S. B. Lipid nephrosis: observations over a period of 20 years. *Am. J. Dis. Child.*, 1943, 65, 355–363.

43. Allen, A. C. The clinicopathologic meaning of the nephrotic syndrome. *Am. J. Med.*, 1955, 18, 277–314.

ADDENDUM TO REFERENCES

44. Farquhar, M. G.; Vernier, R. L., and Good, R. A. The application of electron microscopy in pathology: study of renal biopsy tissues. *Schweiz. med. Wchnschr.*, 1957, 87, 501–510.

45. Farquhar, M. G.; Vernier, R. L., and Good, R. A. An electron microscope study of the glomerulus in nephrosis, glomerulonephritis, and lupus erythematosus. (In preparation.)

[*Illustrations follow*]

LEGENDS FOR FIGURES

Figures 1 to 4 are light photomicrographs of sections stained with hematoxylin and eosin prepared from specimens from cases 1 to 4, respectively. Detailed descriptions of the light microscopic appearance of these tissues are included in the previous paper of this series.[1]

FIG. 1. A portion of the surgical biopsy specimen from case 1, which clinically showed chronic glomerulonephritis. Many of the glomeruli in this kidney were shrunken and hyalinized with complete obliteration of the capillary loops. The remaining glomeruli were large, bloodless, and distinctly lobulated with a varying degree of coalescence and obliteration of capillary loops. Epithelial crescents (not seen in this field) also were observed scattered throughout the section. Many of the tubules appeared atrophic whereas others were markedly dilated. There was considerable proliferation of interstitial fibrous tissue with localized accumulations of lymphocytes. The changes present in this kidney were considered to be compatible with active chronic glomerulonephritis.

FIG. 2. A portion of the needle biopsy specimen from case 2, which clinically showed transient "pure" nephrosis with apparent recovery. The glomeruli appeared to be of normal size, and there was no readily apparent thickening of the basement membrane. This kidney was considered to be histologically normal.

FIG. 3. A field from the surgical biopsy specimen from case 3 which clinically showed a mixed picture of nephrosis and nephritis. The glomeruli were distinctly enlarged and relatively bloodless. There was a definite increase in the number of endothelial nuclei, but the capillary basement membranes did not appear to be thickened. In some fields occasional hyalinized glomeruli were observed as well as scattered glomeruli showing epithelial proliferation and early crescent formation. These changes were considered to be consistent with the late stage of acute glomerulonephritis or the early stage of subacute glomerulonephritis.

FIG. 4. Part of a section from the surgical biopsy specimen from case 4. These glomeruli appeared to be of normal size, and no increase in the number of endothelial or epithelial cells was evident. The capillaries contained numerous erythrocytes, and the capillary basement membranes did not appear thickened either in sections stained with hematoxylin and eosin or following special staining.

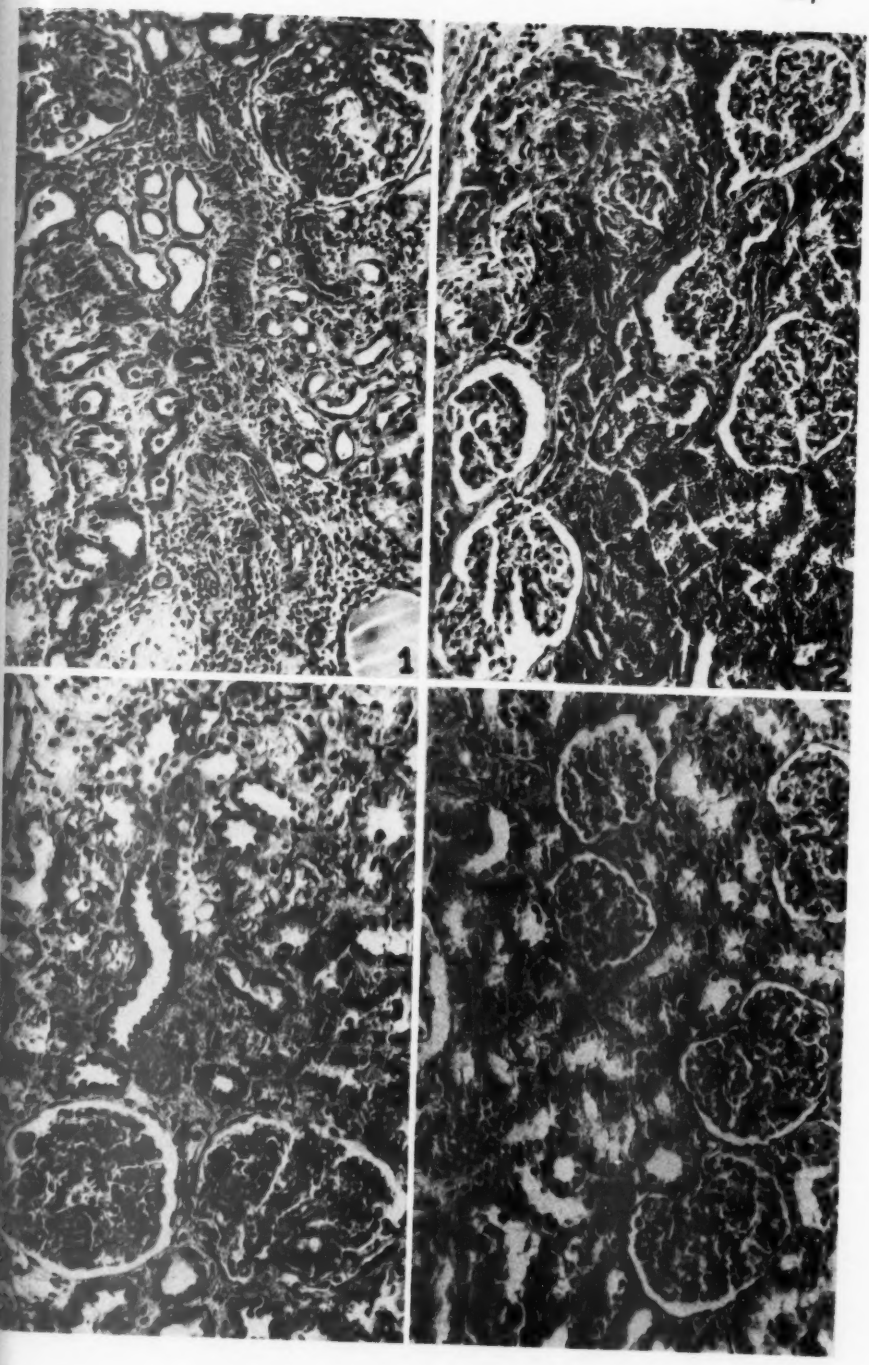

Figures 5 to 14 are electron micrographs taken of ultrathin tissue sections prepared from the renal biopsy specimens. Abbreviations for Figures 5 to 14 follow:

BB = brush border
BM = basement membrane
CAP = capillary
CM = cell membrane
END = endothelial cell
EP = epithelial cell
ER = endoplasmic reticulum
FP = foot process
G = Golgi material
GR = granules or "hyaline droplets"
M = mitochondria
RBC = red blood cell
VAC = vacuole

Figures 5 and 6 show portions of glomeruli from a human renal biopsy specimen that was presumed to be normal. The three elements which enter into the composition of the glomerular loops of man and other species, i.e., endothelium, basement membrane proper, and epithelium, can be readily distinguished.

FIG. 5. A red blood cell marks the lumen of a glomerular capillary. An endothelial nucleus can be seen on the upper left. The perinuclear endothelial cytoplasm is relatively abundant and contains scattered formed elements. Opposite the endothelial nucleus is a thin layer of more peripheral endothelial cytoplasm (arrows) which is seen to be quite attenuated. It forms a complete lining for the capillary with the exception of minute and characteristic interruptions. The latter have been interpreted as regularly spaced pores by some[7,11,16] and as intracytoplasmic vesicles by others.[8] Directly adjoining the endothelium is the basement membrane proper. It has a fairly uniform, intermediate density. In some places a thin, relatively clear area can be seen between the endothelium and basement membrane; however, in other places, particularly closer to the cell body, no clear separation can be distinguished. Portions of several epithelial cells are indicated. These cells show abundant cytoplasm containing scattered formed elements, i.e., mitochondria, Golgi material, vesicles, vacuoles, and a few canaliculi of the endoplasmic reticulum and small basophilic particles. The epithelial cytoplasm is elaborately organized into a number of foot processes which are applied to the outer aspect of the basement membrane. A small space generally can be seen between adjacent foot processes. That portion of the foot process which directly adjoins the basement membrane shows a greater density than the remainder of the epithelial cytoplasm. × 10,300.

FIG. 6. A large epithelial cell occupies most of this field. Its cytoplasm contains scattered formed elements. Numerous cytoplasmic extensions of the epithelial cells (foot processes) are seen to insert on the outer aspect of the basement membrane. The lumina of two capillaries are indicated. Attenuated endothelial cytoplasm can be seen to line the inner surfaces of the capillaries completely. × 11,300.

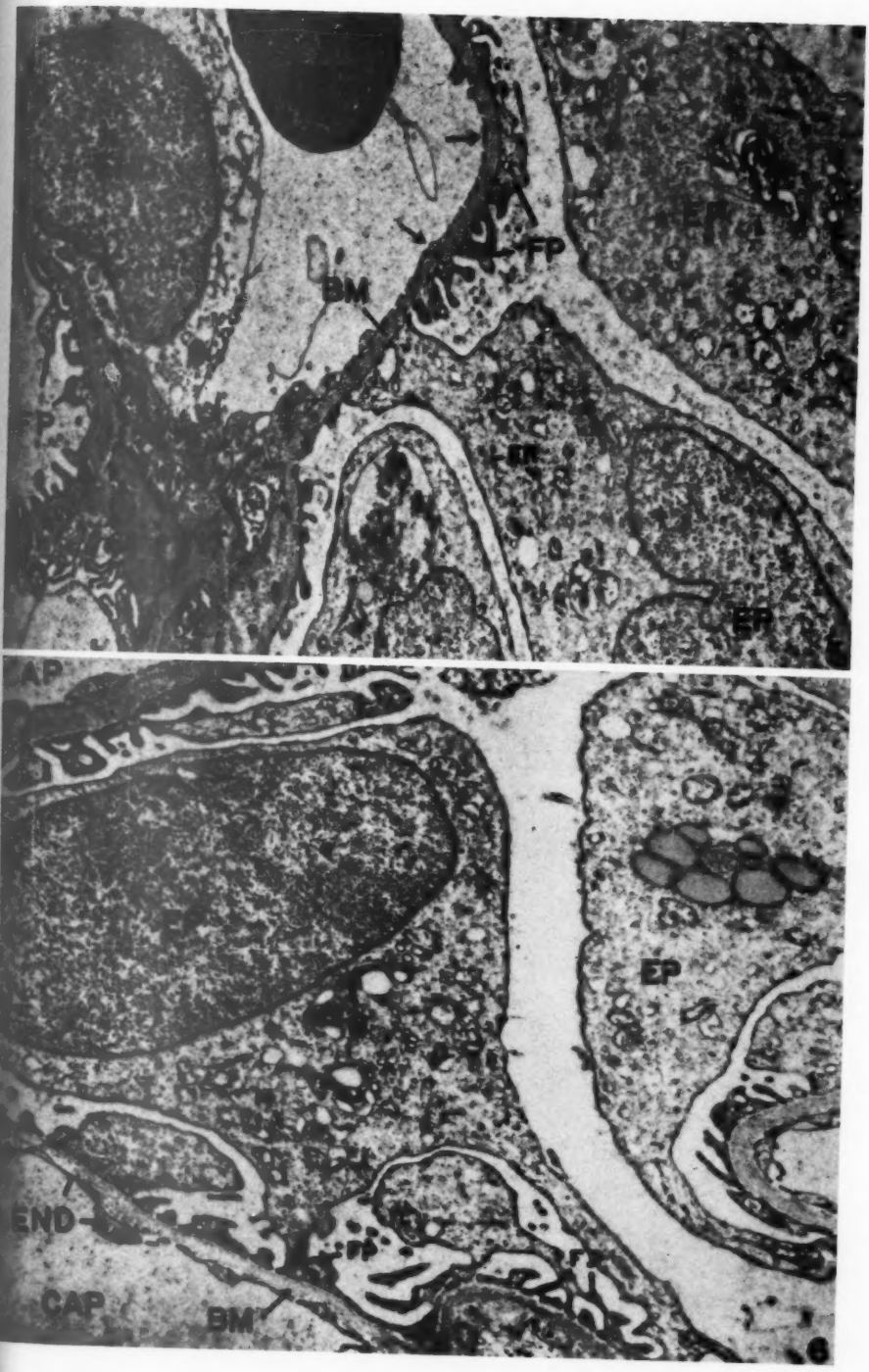
FP
BM
EP
EP
CAP
EP
END
CAP
BM

FIG. 7. Field from a typical glomerulus of case 3 which, clinically, showed mixed nephrosis and nephritis. When the tissue was examined with the light microscope, it showed changes considered diagnostic of subacute glomerulonephritis. Two epithelial cells can be seen in this field. A striking alteration of the epithelium is apparent here, for the organization of epithelial cytoplasm into foot processes is lacking. Instead, broad masses of epithelial cytoplasm cover large areas of the two loops which are partly included in the field. That portion of the epithelial cytoplasm which directly adjoins the basement membrane has retained the greater density normally seen at the base of each foot process. These epithelial changes are common to the glomeruli of each of the children of this study. The cytoplasm of the large epithelial cell to the left contains a number of large vacuoles. In addition there is abundant Golgi material, a few canaliculi and "cisternae" of the endoplasmic reticulum, and many small, dense particles. The formed cytoplasmic elements are concentrated in the area of the cytoplasm which lies between the nucleus of the cell and the basement membrane of the capillary. The endothelium and basement membrane do not show any obvious deviation from the normal. × 13,100.

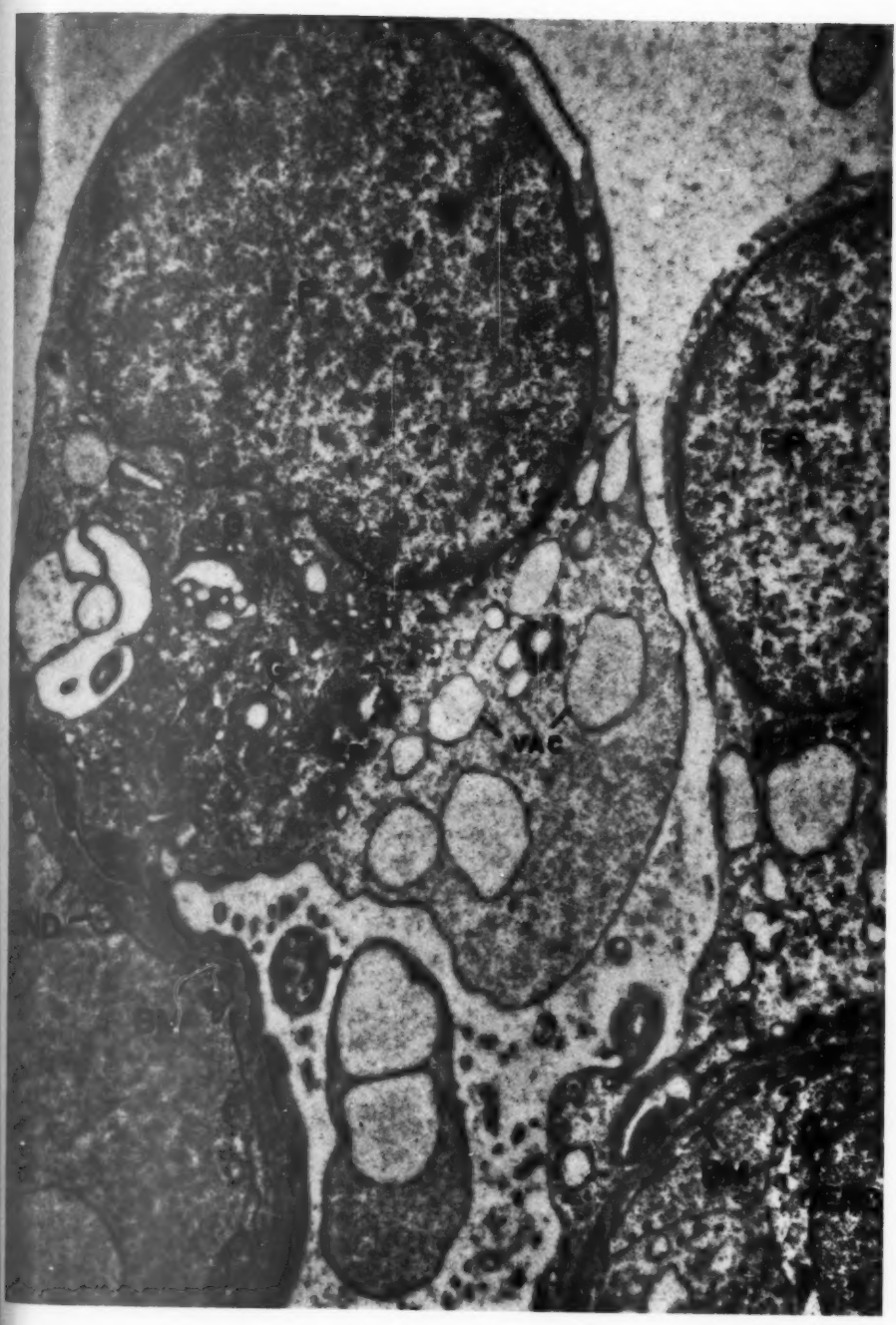
VAC

FIG. 8. A portion of a typical glomerulus from case 4 is illustrated. Clinically, this child showed chronically active "pure" nephrosis. The tissue from the renal biopsy appeared normal with the light microscope, but with the electron microscope changes in the epithelium are evident. An epithelial cell is present in the center of the field. Two capillaries are indicated. Again, epithelial cytoplasm is seen to cover the basement membrane everywhere, and no regular organization into foot processes is seen. The basement membrane appears quite thin, but this is probably because of the very young age (3 months) of the child. × 10,600.

FIG. 9. This figure (from case 3) illustrates alterations in the basement membrane which are frequently seen in nephrosis. The segment of basement membrane seen above has lost its normal homogeneity, for irregular, clear areas are evident below. The endothelial edge of the basement membrane shows nodular areas of various sizes and configurations resembling knots on a tree. In contrast, the epithelial border of the basement membrane appears relatively smooth. Both segments of basement membrane are thicker than normal. × 24,200.

FIG. 10. In this figure (from case 3) a portion of an endothelial cell and basement membrane are seen at high magnification. The lumen of the capillary is indicated to the left. The luminal cell border of the endothelium shows numerous fine processes resembling a meshwork (arrows). Although this irregularity in the luminal cytoplasmic border of the endothelium is encountered in normal glomeruli, it is much more frequently seen and much more elaborately organized in glomeruli from patients with nephrosis. × 20,600.

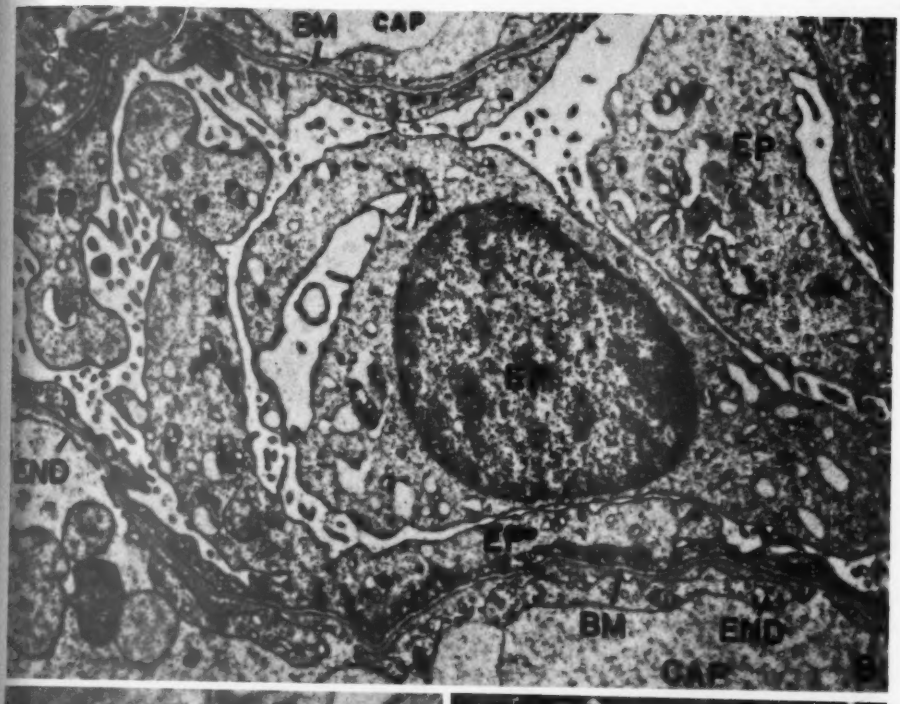
BM
CAP
EP
END
BM
END
CAP

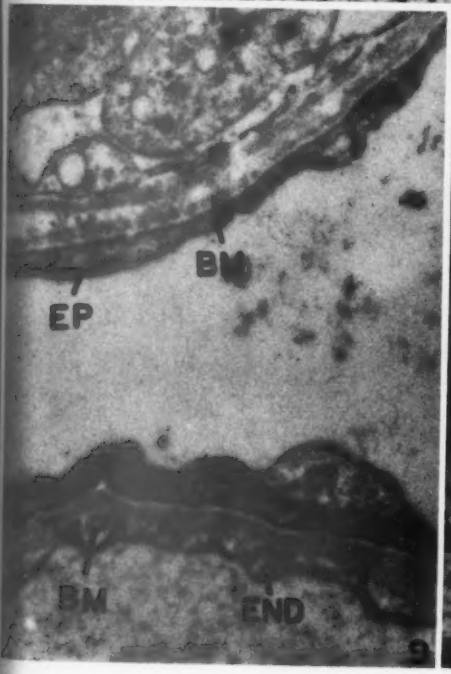
BM
EP
BM
END

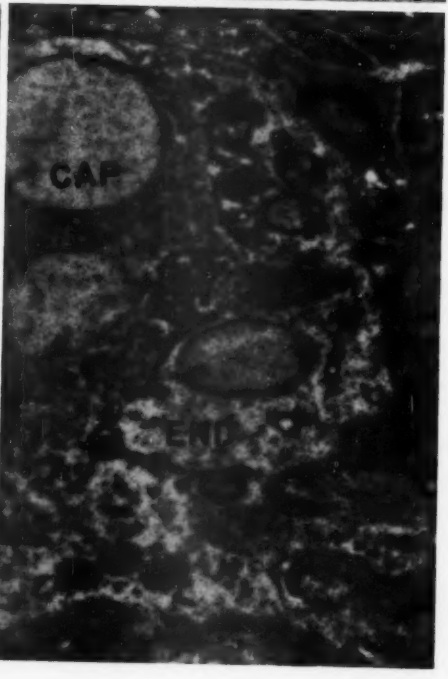
CAP
END

FIG. 11. This figure (case 3) illustrates again the striking lack of foot processes characteristically seen in nephrosis. Here a typical epithelial cell completely covers and appears to clasp the surface of the glomerular loop. Particulate dense material is concentrated in the band of epithelial cytoplasm which directly adjoins the basement membrane. It is somewhat more plentiful than is ordinarily seen at the base of foot processes in normal glomeruli (Figs. 5 and 6). Part of another capillary which is also entirely covered by epithelial cytoplasm can be seen on the lower left. × 10,300.

FIG. 12. A portion of a severely altered glomerulus from case 1 is illustrated here. Clinically, this case showed nephrosis with chronic glomerulonephritis. By light microscopy the tissue showed changes characteristic of chronic glomerulonephritis. With the electron microscope, many of the glomeruli appeared shrunken and showed groups of endothelial and epithelial cells embedded in masses of basement membrane-like material. Often no open blood channels could be found. In this field, greatly thickened and distorted basement membranes and basement membrane-like material surround numerous proliferating endothelial cells. Several of the endothelial nuclei are visible and are indicated. In other places the plane of section passes through endothelial cytoplasm alone. Portions of epithelial cytoplasm which lack organization into foot processes can be identified. × 7,100.

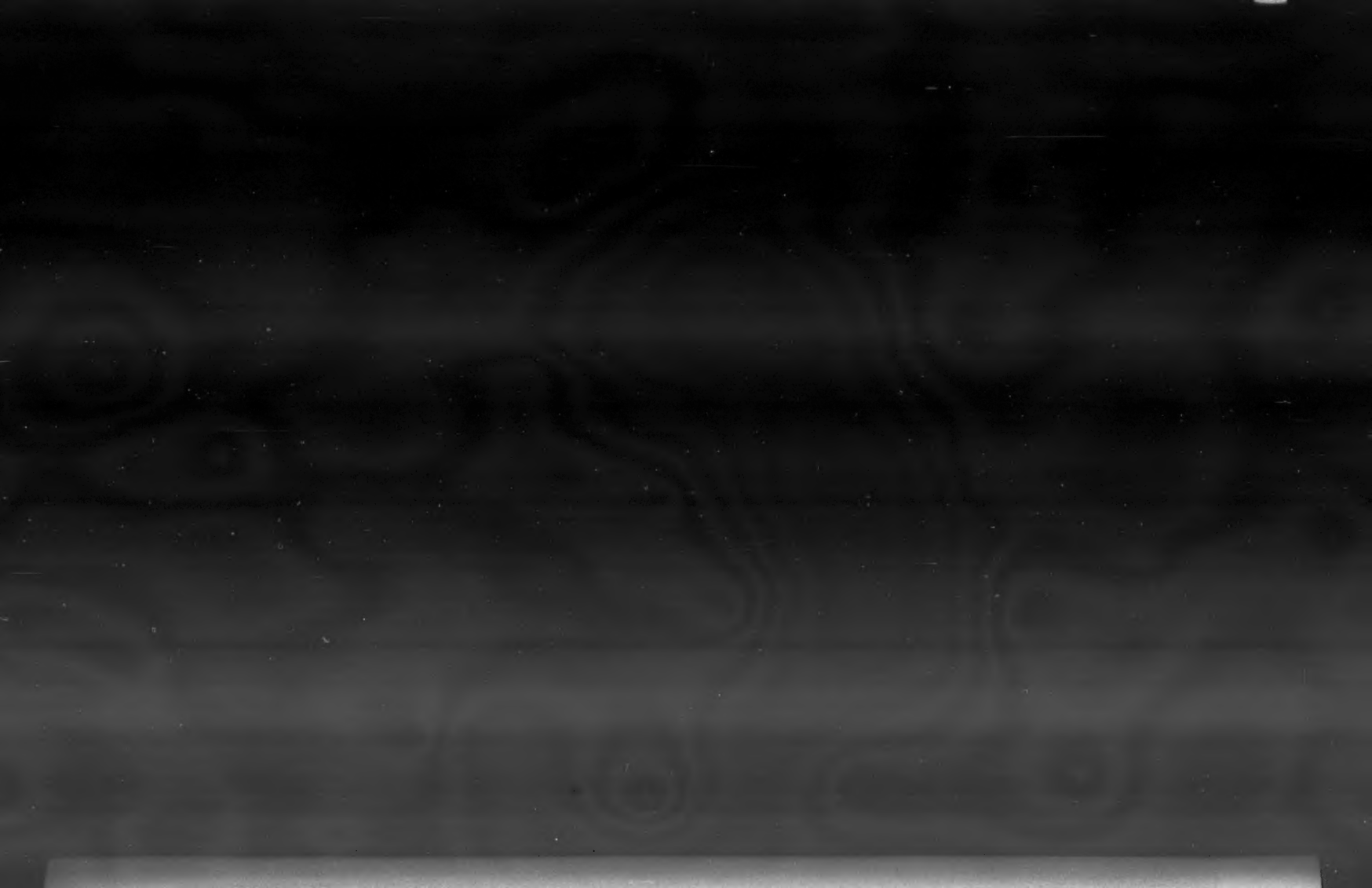

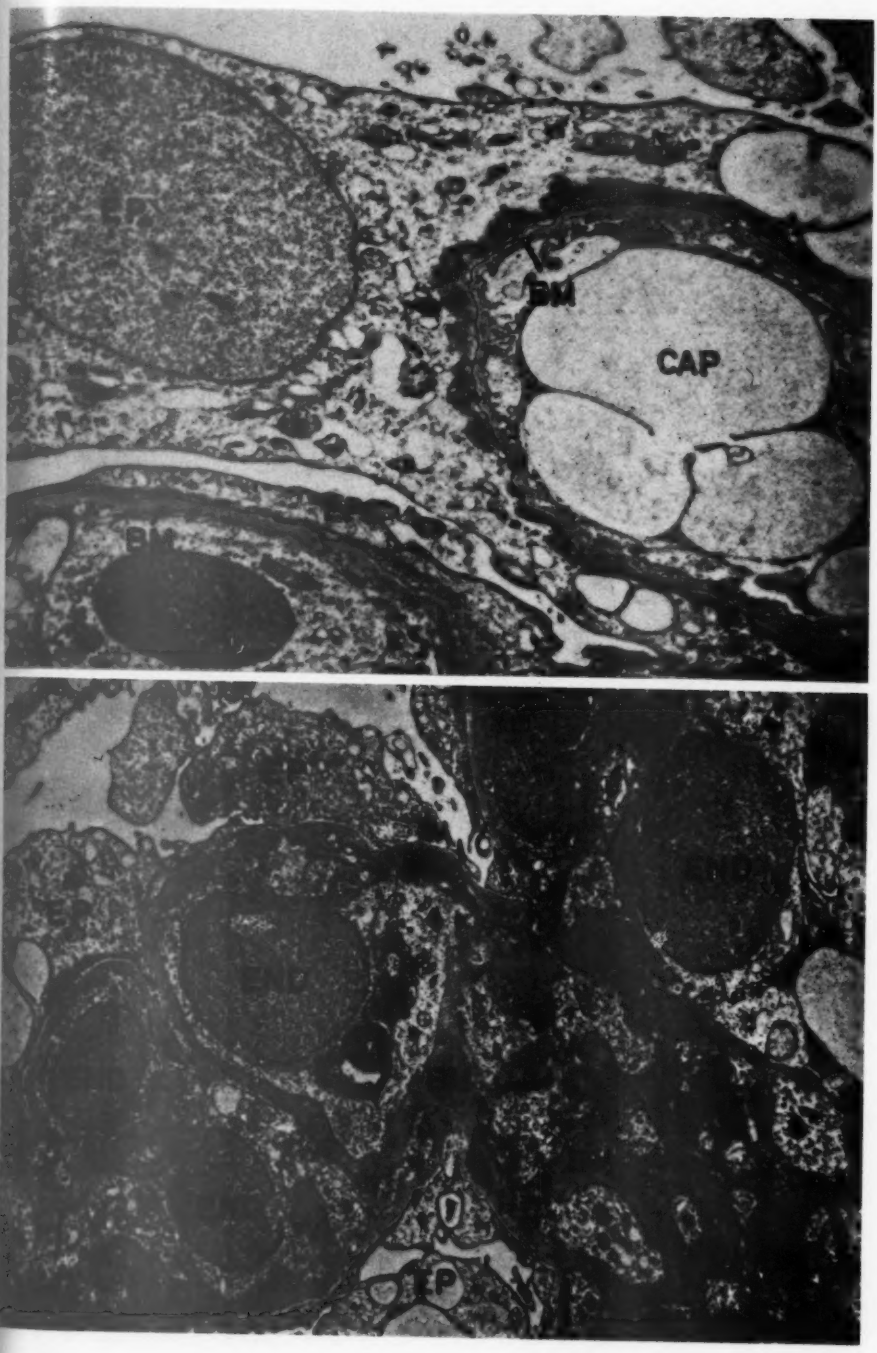
BM
CAP
P

FIG. 13. Part of a proximal convoluted tubule from case 1. Portions of two tubule cells are included in the field. The cell above shows a typical brush border which can be seen to be formed by simple extensions of the apical cytoplasm. The cell below has lost its organization into a brush border. The cytoplasm of the cell above is filled with formed elements. Some of these can be clearly identified as mitochondria on the basis of presence of internal crests. Other typical, denser, rounded granules undoubtedly represent the "hyaline droplets" of light microscopy. A number of transitional forms, with both mitochondrial crests and the denser background of the granules, are present also. The cytoplasm of the cell below contains fewer formed elements. Only a few mitochondria and large granules are present. The basement membrane of the tubule, seen to the right of the field, is somewhat thickened. It appears to be lamellated and is composed of alternating layers of greater and lesser density. × 9,400.

FIG. 14. Portion of a proximal convoluted tubule cell from case 4. Mitochondria can be identified by the presence of internal membranes or crests and occasional dark dots. Several large granules, i.e., "hyaline droplets," are visible also. These appear to be derived from mitochondria, for they show occasional remnants of internal membranes and the finely granular background density seen in mitochondria. The elaborate system of membranes which divides the basal cytoplasm of tubule cells into compartments can be seen above the basement membrane of the tubule. These membranes are formed by infolding of the basal cell membrane. Part of the cell membrane between two adjacent tubule cells also is visible on the left. × 19,500.

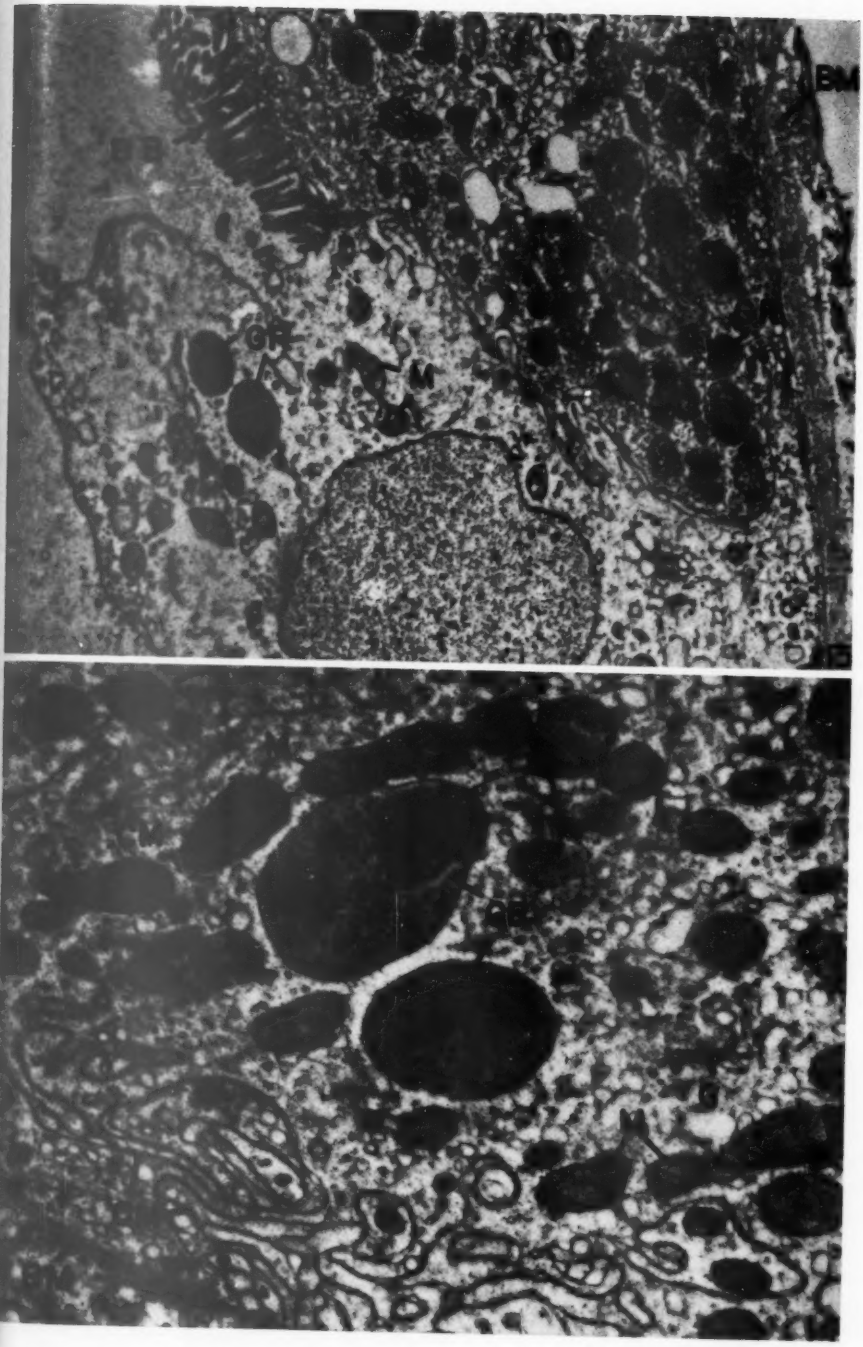
BM
GF

ANEURYSMS OF THE CORONARY ARTERIES

Report of Three Cases in Infants and Review of the Literature*

Diane W. Crocker, M.D.†; Sidney Sobin, M.D., and Wilbur C. Thomas, M.D.‡
From the Departments of Cardiology and Pathology of the Los Angeles Childrens Hospital and the University of Southern California School of Medicine, Los Angeles, Calif.

This paper reports three cases of aneurysms of the coronary artery in infants. Heretofore, such rare lesions have been reported only in association with polyarteritis nodosa. The literature is reviewed and the cases which have been reported since the last comprehensive review[1] in 1948 are tabulated and discussed. A brief discussion of possible etiologic factors is presented.

Since the first case of aneurysm of the coronary artery was reported in 1812 by Bougon,[2] there have been 67 case reports to date, of which 47 were described prior to 1947. The first extensive review of the literature is that of Packard and Wechsler[3] (1929). They collected 29 cases of localized aneurysm of the coronary artery not associated with polyarteritis nodosa, and added one case. The etiology in most instances was attributed either to arteriosclerosis or to a mycotic-embolic origin, although the existence of other possible etiologic factors was recognized. The average age at necropsy was 27 years in the mycotic-embolic group and 57 years in the arteriosclerotic group. The age range of the entire group was 5 to 77 years. A threefold greater incidence of aneurysms of the coronary artery in men than in women was noted. The left coronary artery was more frequently involved than the right. Rupture of an aneurysm of a coronary artery occurred in 12 of 30 cases and was outstanding as a cause of sudden death. Occlusion of the coronary artery was found in two instances, in one of which it was attributed to a septic embolus. Endocarditis involving the aortic valve was noted in seven cases.

In the following year (1930), Forbus[4] introduced the concept of the congenital etiology of cerebral aneurysms and suggested that aneurysms of the coronary artery might also be ascribed to a con-

* Conducted under a Research Fellowship grant by the Los Angeles County Heart Association.
Received for publication, August 14, 1956.
† Research Fellow of the Los Angeles County Heart Association. Now at Department of Pathology, the Babies Hospital, New York 32, N.Y.
‡ Now at the Meadville City Hospital, Meadville, Pa.

genital origin on the same basis, i.e., a developmental deficiency involving the elastica and media at the bifurcation of vessels. This etiologic possibility was referred to frequently in subsequent reports, including several review articles.[5,6] Scott[1] (1948) revised Packard and Wechsler's[3] etiologic classification and concluded that many aneurysms previously considered arteriosclerotic were in fact congenital. He also reviewed 17 additional cases of localized coronary aneurysm and several features became apparent. The left coronary artery was confirmed as the site of predilection, and the preponderance of males in the group was again noted. The primary mechanism of death was different. Occlusion of the coronary artery by thrombus in 9 cases predominated as a cause of death. The thrombosis occurred within the aneurysm in two instances and was distal to the aneurysm in five. Rupture of the aneurysm occurred in only three cases as contrasted with the much larger proportion in Packard and Wechsler's series. Subacute bacterial endocarditis was a concomitant feature in two cases exhibiting occlusion of the coronary artery and in two cases of aneurysm with rupture.

Reports of localized aneurysms of the coronary artery are comparatively more common in the recent literature, from which 20 cases are collected (Table I). The similarities between these cases and the earlier literature include the wide age range and the 3:1 ratio of males to females. Several differences are noted. The marked preponderance of involvement of the left coronary artery was not a feature of the recent cases; in fact, aneurysmal formation involving the right coronary artery was slightly more frequent, with eight instances on the right and seven on the left. Both coronary arteries were involved in five cases. Rupture of an aneurysm of the coronary artery was not encountered in the recent cases whereas this was a common occurrence in the early literature. Rupture of an abdominal aortic aneurysm was noted in three cases. The common causes of death were occlusion of the coronary artery and myocardial infarction. Myocardial fibrosis was generally present. Subacute bacterial endocarditis was diagnosed in only one case. Hypertensive heart disease was present in two cases.

The etiology listed in Table I for each lesion is that suggested by the original authors. An arteriosclerotic origin predominates, the ages in this group ranging from 42 to 82 years. In the congenital category the ages range from 9½ to 85 years. Two of the three children had mycotic aneurysm, the other myocardial infarction. Syphilis was the etiologic factor in only one instance.

TABLE I

Reports of Cases of Localized Aneurysms of the Coronary Artery, 1947 to 1956

Auth

TABLE I

Reports of Cases of Localised Aneurysms of the Coronary Artery, 1947 to 1956

Author	Year	Age	Sex	Location of aneurysm	Etiology	Cause of death
1. Mitchell[7]	1947	42	M	Left circumflex branch; right coronary artery	Arteriosclerotic	Occlusion of aneurysm of right coronary artery; acute myocardial infarction
2. Ott[8]	1947	76	M	Left anterior descending branch	Arteriosclerotic	
3. Benesova & Houstek[9]	1947	7½	M	Left anterior descending branch	Mycotic	Rupture
4. Ashton & Monro[10]	1948	23	M	Left coronary artery; right coronary artery	Congenital	Sudden occlusion of aneurysm of left coronary artery by calcified mass
5. Bowden[11]	1949	74	F	Left coronary artery; 2 aneurysms of right coronary artery	Arteriosclerotic	Occlusion of aneurysms of both right main coronary arteries; myocardial infarction, acute
6. Bowden[11]	1949	62	M	Left interventricular branch	Arteriosclerotic	Occlusion of aneurysm
7. O'Neill & Laipply[12]	1949	53	M	Right coronary artery	Arteriosclerotic	Rupture of abdominal aortic aneurysm
8. O'Neill & Laipply[12]	1949	46	M	Right coronary artery	Arteriosclerotic	Occlusion of aneurysm
9. Dordi[13]	1950	60	F	Left coronary artery	Arteriosclerotic and congenital	Acute cardiac insufficiency
10. Sarkisian[14]	1950	78	M	Right coronary artery	Arteriosclerotic	Cerebral hemorrhage
11. Denham[15]	1951	81	M	Left descending branch	Syphilitic	Occlusion of aneurysm; acute myocardial infarction
12. Kempton[16]	1951	9½	F	Left coronary artery; right coronary artery	Congenital	Occlusion of right coronary artery
13. Prentice & Penfold[17]	1952	66	M	Right coronary artery	Arteriosclerotic	Aneurysm partly filled by old thrombus; myocardial infarction, acute
14. Prentice & Penfold[17]	1952	82	F	Branch of right coronary artery	Arteriosclerotic	Rupture of abdominal aortic aneurysm
15. Velázquez[18]	1952	16	F	Left anterior descending branch	Mycotic	Myocardial infarction, acute
16. Rukstinat[19]	1952	67	M	6 aneurysms of right coronary artery	Arteriosclerotic	Rupture of abdominal aortic aneurysm
17. Minder[20]	1953	63	M	Right coronary artery	Congenital	Hypertensive heart disease with congestive heart failure
18. Trinidad *et al.*[21]	1953	59	M	Left circumflex branch	Arteriosclerotic	Coronary thrombosis; myocardial infarction, acute
19. Colbeck & Shaw[22]	1954	85	M	Right coronary artery	Congenital	Arteriosclerotic heart disease
20. Loring[23]	1955	58	M	3 aneurysms of right coronary artery; left anterior descending branch; left circumflex branch	Arteriosclerotic	Hypertensive heart disease

The diagnosis of this lesion is rarely entertained clinically; however, in case 2 it was suggested by the fluoroscopic finding of a mass pulsating asynchronously with the left ventricle in the left atrioventricular groove.

Report of Cases

Case 1

M. L. P. (C.H. no. 43–1542), a 2 month old white female infant, had been cyanotic since birth and had had an upper respiratory infection for 1 week. Upon admission to Childrens Hospital she was intensely cyanotic and dehydrated, respirations were gasping, the heart sounds were almost imperceptible, and the extremities were cold. She expired several hours later.

Necropsy Description

At necropsy (A-57-43) the body was that of a well developed and well nourished white female infant with marked generalized cyanosis. The main findings were in the heart, which weighed 35 gm. (normal weight,[24] 23 gm.) and occupied two thirds of the transverse diameter of the chest. The anterior descending branch of the right coronary artery was prominently dilated, its wall had a distinctly yellow tint, and was firm. This vessel terminated abruptly in a thick-walled, saccular knob-like dilatation about four fifths of the distance from the base to the apex. No other vessels communicated with the aneurysm. The remainder of the coronary circulation was normal.

The superior and inferior venae cavae were dilated as was the right atrium into which they emptied. There was a defect, 0.8 cm. in diameter, of the septum secundum over the foramen ovale. The tricuspid valve was stenotic, measuring 2 cm. in circumference; the valve ring exhibited poor differentiation of its leaflets. The right ventricle was hypoplastic and the myocardium was thickened. The pulmonic valve was atretic. The hypoplastic pulmonary artery arose blindly at the base of the heart in its usual location. The left side of the heart was normal. The mitral valve measured 4.5 cm. in circumference. The ductus arteriosus measured 0.3 cm. in diameter.

Microscopic examination of the heart revealed hypertrophy of groups of muscle fibers, particularly in the subepicardial region. No infarction was noted. The endocardium was not thickened. Unfortunately, no sections of the aneurysm were available. There was generalized visceral congestion.

Anatomical Diagnoses. Saccular aneurysm of the right anterior descending coronary artery. Tricuspid stenosis. Pulmonic atresia. Hypoplasia of the pulmonary artery. Hypoplastic right ventricle.

Dilatation and hypertrophy of the heart. Defect of the septum secundum. Patent ductus arteriosus. Congestion and edema of the lungs. Generalized visceral congestion.

Case 2

R. G. (C.H. no. 68477), a 3½ month old white male infant, had a sudden onset of cough, abdominal maculopapular eruption, and rhinorrhea associated with fever of 103° F. 3 days prior to admission. On the following day, the rash had spread. He refused feedings and the rectal temperature rose to 104° F. Aspirin and intramuscular penicillin were given. On the day prior to admission, the eruption had spread further, temperature was 105° F., and the patient was lethargic.

Physical examination on admission revealed an acutely ill male infant exhibiting a generalized maculopapular skin eruption with confluent erythematous areas, bilateral palpebral conjunctivitis, cheilitis, and slightly injected posterior pharynx with edema and white exudate. Suboccipital, cervical, and axillary lymph nodes were enlarged. The point of maximum cardiac impulse was in the fifth interspace, 2 cm. to the left of the sternum. The heart tones were of good quality without murmurs or palpable thrill. The lungs were clear to auscultation. The liver and spleen were not enlarged to palpation. A right hydrocele was noted.

During the first week of hospitalization, stomatitis, generalized lymphadenopathy, and hepatosplenomegaly developed. During the second week the patient developed cyanosis, a gallop rhythm, coarse breath sounds in both upper lobes, and pitting edema of the ankles. Roentgenograms of the chest revealed an enlarged heart and pneumonitis of the right and left upper lobes. The electrocardiographic pattern was that of a posterior myocardial infarction. Hematologic studies revealed leukocytosis, eosinophilia, and anemia. The white blood cell count was 32,100 per cmm. with 20 per cent eosinophils; hemoglobin, 8 gm. per 100 ml.; erythrocyte count, 3.2 million per cmm.

Gram-positive micrococci were cultured from both conjunctivae. Alpha streptococci were isolated from the nasopharynx. Cultures of catheterized urine, blood, and spinal fluid were sterile. No agglutination was noted against antigens for typhoid, paratyphoid A and B, and *Brucella abortus*. Urinalysis revealed a trace of albumin, no sugar or acetone, 15 to 20 white blood cells, and occasional red blood cells per high power field.

During the third week of hospitalization, a grade II blowing apical systolic murmur became audible. Its intensity increased to grade IV, and a diastolic component was heard as the heart tones became more distinct. The heart rate was rapid, with multiple ectopic beats. Respiratory distress and cyanosis became pronounced. Roentgenologic examination exhibited a marked increase in the size of the cardiac shadow during this period. Pericardiocentesis yielded a small amount of serosanguineous fluid. Respirations ceased following this procedure. The clinical impression was collagen disease with myocarditis and pericardial effusion.

Necropsy Description

At necropsy (A-156-52) the body was that of a well developed, well nourished white male weighing 7,105 gm. and measuring 63 cm. in crown-heel length. No skin lesions or cyanosis were evident. The conjunctivae were minimally injected. Four needle puncture wounds were visible at the lower left sternal border. There was minimal pitting

edema of the extremities. Needle puncture wounds were noted on the anterior surface of the pericardium; otherwise the pericardial surfaces were smooth and glistening. The pericardial sac was distended by serosanguineous fluid. The coronary arteries arose in their usual position; the ostia were patent and of normal diameter. The left coronary artery branched at a distance of 0.5 cm. from its origin to form the anterior descending and circumflex branches. Immediately distal to the point of origin of the left anterior descending branch, a prominent, smooth, red-blue saccular enlargement, 1 cm. in diameter, was filled by organized thrombus (Fig. 1). The wall of the aneurysm appeared thickened. Distal to the aneurysm, the left anterior descending branch was tortuous. The left circumflex coronary artery exhibited slight tortuosity and thickening of its wall. The right coronary artery was moderately dilated, patent, and tortuous throughout its course with thickening of its wall.

The heart weighed 75 gm. (normal weight,[24] 27 gm.) and showed dilatation of all chambers. The right and left ventricular walls were hypertrophied. The myocardium of the left ventricle was soft and the posterior wall was pale and yellow-tan. The endocardium was thin and transparent. No cardiac anomalies were noted.

The left lung weighed 45 gm. (normal weight,[24] 33 gm.); the right, 50 gm. (normal weight,[24] 37 gm.). Numerous dark red-brown hemorrhagic areas, 0.1 to 0.3 cm. in diameter, were present in the substance of both lobes. Six superficial erosions of the gastrointestinal tract were noted along the lesser curvature of the stomach. The spleen, liver, and kidneys were congested. The right scrotal sac was distended with watery, pale yellow fluid. The right testis was soft and mottled red-brown and yellow.

Microscopic Findings. The aneurysm was completely occluded by thrombus composed predominantly of polymorphonuclear leukocytes and nuclear débris. A moderate number of polymorphonuclear leukocytes extended through all layers of the vessel wall. The intima was not thickened. The entire wall was composed of fibrous tissue and a few fragments of elastica. No fibrinoid degeneration was seen. Adjacent to the aneurysm was a coronary artery (Fig. 2) with no inflammation of its wall. There was marked subintimal fibrosis in addition to a hyalinized thrombus in the wall which further narrowed the lumen. Verhoeff's stain demonstrated fragmentation of the internal elastica. The media was replaced by fibrous tissue in one portion. The left circumflex coronary artery was dilated and occluded by a thrombus composed chiefly of polymorphonuclear leukocytes. Lymphocytes and plasma cells were present in all layers of the vessel

wall. Another section of coronary artery demonstrated striking subintimal fibrous proliferation and a small early thrombus lying free in the lumen. No fibrinoid degeneration was noted; however, the media and internal elastica had a disorderly pattern in several segments of the vessel circumference. The entire vessel wall and periadventitial fibrous tissue were sparsely infiltrated by polymorphonuclear leukocytes, lymphocytes, plasma cells, and histiocytes. The coronary arteries within the myocardium did not demonstrate any of the changes seen in the larger coronary vessels. Large areas of the left ventricular myocardium demonstrated acute necrosis of muscle fibers with granularity of the cytoplasm, loss of striations, poor nuclear staining, and extensive red cell extravasation.

Pulmonary congestion was diffuse, with dilatation and tortuosity of alveolar capillaries, hemorrhage into the alveoli, and hemosiderin pigment within macrophages. Polymorphonuclear leukocytes were more abundant in some areas than could be attributed to the hemorrhage. In addition, many alveoli contained fibrin and protein precipitate. The liver contained small areas of necrosis with polymorphonuclear leukocytic infiltration. In addition, polymorphonuclear leukocytes were noted in the capsule of the liver and the spleen, and were present in large numbers in the splenic substance.

The tunica vaginalis was thickened, partially hyalinized, and densely infiltrated by cells showing acute and chronic inflammation. Several arteries adjacent to the vas deferens and to the epididymis were occluded by organized thrombi with recanalization (Fig. 4). The elastica was intact. The media contained an increased amount of fibrous tissue. The vessels were surrounded by dense fibrous tissue containing cells with chronic inflammation. The right testis and epididymis were not infarcted. The only other vascular lesion noted consisted of slight subintimal fibrous thickening of the abdominal aorta.

Main Anatomical Diagnoses. Diffuse dilatation and tortuosity of the coronary arteries. Saccular aneurysm of the left anterior descending coronary artery with thrombosis and acute myocardial infarction of the left ventricle. Hemorrhagic pneumonitis. Focal necrosis of the liver. Acute splenitis. Superficial gastric ulcerations of the lesser curvature. Infected hydrocele, right.

Case 3

M. L. (C.H. no. 59360), a 6 month old white male infant, became irritable 1 month prior to admission and was considered to have an upper respiratory infection which was treated with intramuscular penicillin. The following day, conjunctivitis, cough, and pharyngitis were noted. An erythematous eruption appeared behind

the ears and on the scalp, became generalized, and then faded within 1 week. Intramuscular penicillin therapy was continued. Later, a macular eruption appeared on the thighs, rapidly became generalized, and then faded. The infant appeared to be improving until 1 week prior to admission when a blood-tinged nasal discharge and grunting on urination were noted.

When first seen at Childrens Hospital, this infant was lethargic, pale, and appeared chronically ill. Heart tones were of fair quality with a regular sinus rhythm and no murmurs. Roentgenogram of the chest revealed a large globular heart shadow. Hematologic examination revealed a white blood cell count of 28,000 per cmm., with 4 per cent eosinophils, 46 per cent segmented neutrophils, 4 per cent band neutrophils, 11 per cent monocytes, and 35 per cent normal lymphocytes. The white blood cell count decreased to 8,500 per cmm. with the following differential: 3 per cent eosinophils, 19 per cent segmented neutrophils, 8 per cent band forms, 8 per cent monocytes, and 62 per cent normal lymphocytes. *Salmonella typhimurium* was isolated from the stools. *Pseudomonas aeruginosa* and hemolytic *Staphylococcus aureus,* coagulase positive, were cultured from a catheterized urine specimen. Cystogram and intravenous pyelogram were normal. The infection of the urinary tract was treated. The patient was discharged 2 weeks after admission, to be followed as an out-patient.

When seen in Emergency Clinic at 8 months of age, he appeared acutely ill, and dyspneic. There had been a fleeting maculopapular eruption on the face and trunk, and vomiting 2 days previously. The heart was enlarged but there was no increase in size by roentgenologic examination as compared to roentgenograms taken during the first admission. The apical rate was 150 beats per minute with a gallop rhythm. The liver was markedly enlarged. Despite rapid digitalization, the gallop rhythm persisted, with poor heart tones. The leukocyte count was 25,900 white blood cells per cmm. with a differential count of 31 per cent segmented neutrophils, 3 per cent band forms, 63 per cent lymphocytes and 3 per cent monocytes. Kahn test was negative. He expired on the fourth hospital day, 2 months after the onset of first symptoms. Clinical impression: acyanotic congenital heart disease, possible endocardial sclerosis or glycogen storage disease.

Necropsy Description

Necropsy (A-31-52) was limited to examination of the heart and liver. Body was that of an 8 month old white male infant, measuring 69 cm. in length and weighing 18½ lbs. External examination was normal.

The heart weighed 70 gm. (normal weight,[24] 37 gm.). The epicardial surface was marked by the exaggerated size and tortuosity of the coronary arteries, particularly the left coronary artery (Figs. 3 and 5). The sinuses of Valsalva and the ascending aorta were negative. The coronary arteries arose normally from the aorta. The coronary ostia were patent and of slightly increased circumference. The left coronary artery was markedly dilated just beyond the ostium, to form a raised, firm, thick-walled, fusiform enlargement, 1.5 cm. in internal diameter, filled with adherent, firm, red-brown thrombus. The anterior descending branch, 2 cm. in diameter, was dilated and tortuous for a distance of 3 cm. from its origin.

The external diameter was considerably decreased in the distal portion of this vessel, although marked tortuosity persisted. Due to the extreme thickness of the vessel wall, 0.2 to 0.3 cm., the lumen was almost completely obliterated. Aneurysmal dilatation of the left circumflex branch extended from its origin at the bifurcation of the left coronary artery for a distance of 1.5 cm. The wall was markedly thickened in the dilated portion. Beyond this area, the lumen was almost completely obliterated by the thickened vessel wall. All dilated portions of the left coronary artery were filled with adherent brown-red thrombi. Just beyond the right coronary ostium, the main right coronary artery presented a saccular aneurysmal dilatation measuring 1.5 cm. in diameter which was filled with firmly adherent thrombus. Distally, the vessel was thick-walled and tortuous with marked narrowing of its lumen.

The myocardium of the interventricular septum and anterior wall of the left ventricle was extremely soft, pale tan, and had red hemorrhagic areas. The remainder of the myocardium was brown-red and of normal consistency. The right ventricular wall measured 0.3 cm. in thickness; the left, 0.9 cm. The endocardium of all chambers was thin, transparent, smooth and glistening. No cardial anomalies were noted.

The liver extended 3 cm. below the right costal margin and had a characteristic nutmeg pattern.

Microscopic Examination. The intima of the main coronary arteries and their major branches had undergone striking fibrous proliferation. This was the major factor responsible for marked thickening of the vessel walls. The subendothelial proliferation was seen in both the dilated and undilated portions of coronary arteries and was characterized by abundant fibroblasts and fibrocytes in a homogeneous ground substance, taking a pink to pale blue stain in hematoxylin and eosin preparations. Infrequent foci of calcification of the outer one third of the intima were found in the dilated portions of coronary arteries. Small thrombi with ingrowth of fibroblasts were present in the dilated portions and formed niduses for layering of fibrin and platelets to make up the major portion of clots which filled these dilated portions. The intima of the non-dilated portions was thickened sufficiently in some areas to produce almost complete occlusion of the lumen. Several smaller branches, including those within the myocardium, exhibited subendothelial fibrous proliferation of varying degrees. The media was thickened by increase of fibromuscular elements. No medial necrosis was seen. Adventitial fibrosis extended to

periadventitial tissue with inclusion of nerves, small vessels, and lymphatics in dense fibrous tissue. There was conspicuous absence of acute inflammatory reaction. Few lymphocytes could be found in the endothelium of the aneurysms; no inflammatory cells were found in the media. The adventitia and periadventitial fibrous tissue contained clusters of lymphocytes, plasma cells, and occasional polymorphonuclear leukocytes. Verhoeff stains of the dilated segments revealed splitting of the thinned internal elastic lamina, with areas of fragmentation and scattering of elastic fibers (Fig. 6). The non-dilated portions with intimal fibrous proliferation showed reduplication and thickening of the internal elastica (Fig. 7). The veins were normal.

The myocardium of the left ventricle and interventricular septum revealed extensive recent infarction with the oldest portions at the periphery showing proliferation of fibroblasts, macrophages with engulfed amber pigment, and lymphocytic infiltration. Central areas exhibited pyknosis of muscle nuclei, fragmentation of nuclei and cytoplasm, extensive red blood cell extravasation, and polymorphonuclear leukocytic infiltration. Fibrotic areas were scattered throughout the right ventricle and the atria. The endocardium of the atria and atrial appendages was prominently thickened. Subendocardial sclerosis of the left ventricle corresponded in location with the underlying infarction. The valves were normal.

The liver showed marked central congestion with foci of central hemorrhage and necrosis.

Anatomical Diagnoses. Diffuse aneurysmal dilatation involving the main left coronary artery, the left circumflex coronary artery, and the left anterior descending coronary artery with occlusion and recent infarction of the interventricular septum and anterior wall of the left ventricle. Localized aneurysm of the right main coronary artery. Endocardial sclerosis of the atria. Central hemorrhagic necrosis of liver.

Aneurysms in Infants and Children

A group of reported cases, including our three cases of aneurysms of the coronary arteries in infants and children and omitting cases of periarteritis nodosa, are summarized in Table II. Only those cases are included which are cited by Packard and Wechsler[8] and Scott,[1] and those referred to in Table I, in addition to our three cases. The ages range from 2 months to 16 years. Our three cases are the only ones which were necropsied in infancy. The right coronary artery alone was involved in two cases, the left alone in five cases, and both coronary arteries presented aneurysms in five cases. Occlusion of

TABLE II

Aneurysms of the Coronary Artery in Infants and Children Listed Serially by Age

TABLE II

Aneurysms of the Coronary Artery in Infants and Children Listed Serially by Age

Author	Year	Sex	Clinical features	Location of aneurysms		Other pathologic findings	Etiology
				Right coronary	Left coronary		
1. Crocker *et al.*	1957	F	Cyanosis since birth; 1-week history of upper respiratory infection	+		Congenital heart disease	Congenital
2. Crocker *et al.*	1957	M	4-week course, died in congestive heart failure; onset with cough, rash, and fever; developed stomatitis, conjunctivitis, pharyngitis, and eosinophilia		+	Thrombosis, aneurysm of left coronary artery	Unknown
3. Crocker *et al.*	1957	M	2-month course: conjunctivitis, pharyngitis, rash; died in congestive heart failure	+	+	Occlusion, left coronary artery; myocardial infarction	Unknown
4. Rae[25]	1937	M	10-month history of cyanotic episodes; 1-month history of pallor and listlessness, fever, lymphadenopathy, and joint tenderness; sudden death	+	+	Thrombosis, aneurysm of right coronary artery; exudative necrotizing vasculitis; rheumatic carditis	Rheumatic heart disease
5. Malet & Evans[26]	1887	M	3-week history of thirst and polyuria, sudden death		+	Rupture, aneurysm of left coronary artery	Congenital
6. Gee[27]	1871	M	"Scarlatinal dropsy," meningitis, and pneumonia	+	+	Few atheromas of ascending aorta and aortic leaflet of mitral valve	Congenital
7. Benesova & Houstek[9]	1947	M	17-day illness with sudden onset of pain in left shoulder and arm, followed by fever, meningeal irritation, and progressive cardiac decompensation		+	Rupture of aneurysm, purulent pericarditis	Mycotic
8. Kempton[16]	1951	F	Well child; died suddenly while playing hockey	+	+	Thrombosis, right coronary artery	Congenital
9. Clarke[28]	1896	F	1-month history of mass of right buttock; 1-week history of mass in left axilla	+	+	Thickening of mitral valve	Probable periarteritis
10. Trevor[29]	1912	F	22-day course with chills and fever; harsh tricuspid to and fro murmur 5 days before death; *Strep. viridans* isolated from blood culture	+		Rupture of aneurysm into right ventricle	Mycotic-embolic
11. Ruge[30]	1905	M	Osteomyelitis, head of femur, followed by pyemia and signs of cardiac disease		+	Acute purulent pericarditis	Mycotic
12. Velázquez[18]	1952	F	Rheumatic heart disease with subacute bacterial endocarditis		+	Myocardial infarction	Mycotic-embolic

coronary arteries was noted in five cases. Rupture of the aneurysm occurred in three of 12 cases. The etiology did not appear to be related to the location or to the occurrence of thrombosis or rupture. A congenital etiology was postulated in four cases and a mycotic origin established in four cases. In case 4, rheumatic heart disease with carditis was considered to be related to the acute exudative and necrotizing vasculitis with formation of aneurysms of the coronary artery. The extracardiac nodules and the multiple aneurysms in case 9 suggested the possibility of periarteritis nodosa. The nature of the extracardial nodules had not been ascertained. Because the etiology was not conclusively periarteritis nodosa, this case was included in Table II. In none of the cases was arteriosclerosis implicated.

Etiologic Considerations

There are a multiplicity of possible etiologic factors in the formation of localized aneurysms of the coronary arteries. The major categories of those which might be indicted are discussed.

Congenital Defect. The etiology of aneurysms of the coronary artery has been ascribed with increasing frequency to a congenital basis since Forbus' concept was introduced. Forbus demonstrated incomplete development of some vessels at their bifurcation and concluded that this constitutes a potential site for formation of aneurysms because of weakening of the elastica and muscularis. This concept is strengthened by the fact that aneurysms are frequently situated at or near a point of bifurcation.[5,13]

The assumption of congenital etiology is warranted in most cases in which there are other congenital cardiovascular anomalies, particularly when these involve the coronary circulation as well, as illustrated by our case 1. Aneurysmal dilatation associated with arteriovenous fistulae will be considered elsewhere.

Arteriosclerosis. Atherosclerosis is one manifestation of the arteriosclerotic process.[21] Only the broader term is used here although it should be understood that arteriosclerotic changes in the coronary arteries may include atherosclerosis.

Arteriosclerosis of the coronary arteries has been implicated as the most common cause of formation of aneurysms, chiefly in the older age group. The absence of advanced arteriosclerosis of the coronary arteries in some of the cases makes this interpretation doubtful. In those cases presenting adequate evidence of arteriosclerosis of the coronary arteries there is justification for ascribing the etiology to

arteriosclerosis. The arteriosclerotic process may also involve other vessels, particularly the abdominal aorta, with resultant formation of aneurysms. In three cases listed in Table I, death was due to rupture of an abdominal aortic aneurysm.

Several microscopic studies have indicated a difference between the coronary arteries of male and female infants, the former sometimes exhibiting a much thicker intima than the latter. Dock[32] observed that the newborn male has an intima three times the thickness of that in the female newborn. Whether this constitutes an inherent anatomical peculiarity[32] or the earliest stage of arteriosclerosis[33] is a matter of conjecture. Nonetheless, it is a significant finding worthy of further investigation and raises the possibility of an arteriosclerotic origin for aneurysms occurring even in infancy. This observation may have its corollary in the higher incidence of arteriosclerosis of the coronary arteries in non-diabetic adult males as compared to females of the same age.[34]

Hypertension. Hypertension may be a contributory factor by hastening the arteriosclerotic process but is noted infrequently in reports of aneurysms of the coronary artery. Only two of the cases in Table I had hypertensive heart disease and the aneurysms in both instances were attributed to arteriosclerosis.

Infectious Arteritis. Bacterial infection of the coronary arteries can result from direct extension of pericardial or myocardial infection, and from mycotic embolic spread from a primary source within or without the heart. Subacute bacterial endocarditis with involvement of the aortic valve due to *Streptococcus viridans* was the predominant type of infection leading to formation of aneurysms in the coronary vessels,[1,3] but this complication is now reported less frequently than in the past.

Syphilitic arteritis also is less frequently encountered today. This tertiary manifestation of syphilitic infection can involve the coronary arteries, and instances of formation of aneurysms have been reported.[1,3,15] Syphilitic arteritis is not seen in early childhood, and almost never occurs in late congenital syphilis.[35]

Necrotizing Arteritis. In the category of necrotizing arteritis, the disease which most commonly affects the coronary arteries is polyarteritis nodosa, a systemic and often diffuse disease characterized by necrosis, degeneration, and inflammation of a variable number of small and medium-sized arteries. The clinical manifestations depend on the site of major vascular involvement. Cases of polyarteritis

apparently localized to one organ have been encountered; this applies to the coronary circulation.[36,37] The main complications of coronary arterial involvement have been described in children as well as adults and consist of thrombosis[38] and formation of aneurysms.[37] The aneurysms may become occluded or may rupture.[39]

Necrotizing angiitis of the coronary arteries may also occur during the course of rheumatic carditis and can result in formation of aneurysms.[25]

Other Causes of Arteritis. Chronic inflammation of the coronary arteries can result from inflammation or obstruction of the perivascular lymphatics. Metastatic tumor in the pericardial lymphatics may have been a factor in formation of aneurysms in one case.[8]

Trauma. There are no recorded cases of aneurysms of the coronary artery in which trauma is considered to be an etiologic factor.

Arteriovenous Fistula. Diffuse aneurysmal dilatation of a coronary vessel usually is associated with an anomalous arteriovenous communication. Rarely, localized aneurysms may result from such communications.[1,22] The basic defect is the anomalous communication between vessels of high and low intraluminal pressure without an intervening capillary bed. Secondary dilatation of the vessel having the higher pressure results from the increased flow and the local hemodynamic alterations. The right coronary artery or one of its larger branches is the most frequent site of diffuse dilatation and may communicate directly with a coronary vein,[40-42] with the coronary sinus,[43] or with the right auricle.[6] Arteriovenous fistulas involving the left coronary artery are seldom encountered.[1]

That the congenital fistula may be well tolerated is evidenced by the absence of clinical symptoms and the long survival of several patients who demonstrated an arteriovenous shunt of the coronary circulation as an incidental finding at necropsy.[6,43] The youngest patient,[41] a 9 year old boy, had a continuous murmur in the right parasternal region. A preoperative diagnosis of arteriovenous fistula was made, several sites being considered. Exploration confirmed the presence of a shunt: the right coronary artery which was extremely dilated and tortuous communicated with the coronary vein at its junction with the coronary sinus. Removal was not attempted and the patient did well postoperatively.

In most instances the arteriovenous communication constitutes a congenital malformation. However, an arteriovenous fistula can result from rupture of an aneurysm of a coronary artery into one of the cardiac chambers. This appears to be what occurred in the case of

an 11 year old girl[29] who demonstrated an aneurysm of the descending branch of the right coronary artery which communicated with the right ventricular cavity by a ragged opening. This was correlated with the sudden appearance of a to-and-fro precordial murmur 5 days before death.

Discussion

Case 1, a 2 month old female infant with cyanosis since birth, had multiple congenital cardiac anomalies involving the right side of the heart, and consisting primarily of pulmonic atresia. In the absence of septal defects, it was imperative for the foramen ovale to remain patent as the only egress for venous blood returning to the right auricle. Blood reached the pulmonary arteries by way of the ductus arteriosus. In view of the small caliber of this vessel, it evidently was closing, thereby precipitating the rapid sequence of events leading to this infant's demise. Closure of the ductus in such a case would be incompatible with life unless sufficient blood supply could reach the lungs through the bronchial arteries. Taussig[44] stated that in cases of this type death usually occurs between 3 and 5 months of age.

The right anterior descending coronary artery terminated abruptly in a saccular aneurysm. Since no vessel could be found leaving the aneurysm, this arterial branch was considered to be an end-artery. Coronary arteries are not normally end-arteries and, therefore, the right anterior descending branch was malformed. This anomaly of a coronary vessel, although unusual, is in keeping with the incomplete development of the right side of the heart. The anatomical findings constitute adequate evidence for the congenital origin of the aneurysm in this case.

In cases 2 and 3, the etiology of the aneurysms of the coronary artery is not apparent. Both patients were male infants, 4 and 8 months of age. The duration of illness was 26 days and 3 months, respectively. The clinical manifestations included stomatitis, conjunctivitis, dermatitis, and pharyngitis in case 2; dermatitis, conjunctivitis, pharyngitis, bronchitis, and cystitis in case 3. Necropsy demonstrated occlusion of an aneurysm in each case with resultant acute myocardial infarction. The coronary arteries were tortuous and diffusely diseased; the intima was strikingly thickened, producing narrowing of the lumen, and the media was hypertrophied. This pathologic picture in an adult would be compatible with arteriosclerosis of the coronary arteries. In infants it may represent extension of the process previously described, and considered to be either an overproduction of tissue[32] or premature arteriosclerosis.[23]

The symptomatology is not dissimilar from that observed in cases of polyarteritis nodosa. The ages of our patients would not preclude this diagnosis for polyarteritis has been described even in the neonatal period.[45] Cases of polyarteritis occurring in infancy and early childhood have been reported with clinical findings similar to those described in cases 2 and 3. Particularly in case 2, polyarteritis nodosa should be considered seriously in view of the clinical history, the marked eosinophilia, and the vascular changes. Yet there is conspicuous absence of fibrinoid degeneration, of intramyocardial disease of the coronary arteries, and of vascular disease in other viscera. Furthermore, the microscopic appearance of the thrombus in the coronary aneurysm suggests a mycotic-embolic origin. The source may have been the infected hydrocele; no other possible source was located. The pathologic process in the visceral organs is suggestive of a septic process also. Case 3 demonstrated none of the histologic features of an *acute* panarteritis of the coronary vessels.

The clinical manifestations also are suggestive of a mild Stevens-Johnson syndrome. The etiology of this febrile illness was assumed by the original authors to be infectious.[46] That angiitis can occur in the course of an acute infection has been well documented.[47] Not only bacteria and spirochetes have been implicated; one of the most striking examples of infectious arteritis is seen in Rocky Mountain Spotted Fever, which is caused by a rickettsia.

A viral etiology of angiitis is as yet unexplored and probably merits consideration. The recent literature contains reports of lesions of the coronary vessels[48] and of muscular arteries of small and medium size throughout the body,[49] the etiology of which is open to speculation.

Until more is known concerning the etiologic factors producing lesions of the type exemplified by cases 2 and 3, we prefer not to categorize the cases but to consider the causative factor to be as yet undetermined. This may stimulate further studies.

Summary

Aneurysms of the coronary arteries are not common. To date, 67 cases have appeared in the literature. Most of these aneurysms occurred in adults, with the exception of the mycotic-embolic variety, and those associated with rheumatic carditis, or with polyarteritis nodosa, which occurred both in adults and in children. Aneurysms of the coronary artery in infancy are rare and have been attributed to polyarteritis. The most frequently considered etiologies of such aneurysms are discussed briefly.

Three cases from the files of the Los Angeles Childrens Hospital are presented, each occurring in the first year of life. In one case the aneurysm was associated with congenital malformations of the right coronary artery and of the right side of the heart and therefore is considered to be of congenital etiology. In the other two cases, the etiology was not determined. Several possibilities are suggested.

REFERENCES

1. Scott, D. H. Aneurysm of the coronary arteries. *Am. Heart J.*, 1948, **36**, 403–421.
2. Bougon. *Biblioth. méd.*, 1812, **37**, 183. (Cited by Packard and Wechsler.[3])
3. Packard, M., and Wechsler, H. F. Aneurysm of the coronary arteries. *Arch. Int. Med.*, 1929, **43**, 1–14.
4. Forbus, W. D. On the origin of miliary aneurysms of the superficial cerebral arteries. *Bull. Johns Hopkins Hosp.*, 1930, **47**, 239–284.
5. Rigdon, R. H., and Vandergriff, H. Aneurysms of the coronary arteries. Review of the literature and report of a case. *Am. J. Surg.*, 1943, **61**, 407–413.
6. Harris, P. N. Aneurysmal dilatation of the cardiac coronary arteries. Review of the literature and report of a case. *Am. J. Path.*, 1937, **13**, 89–98.
7. Mitchell, N. Arteriosclerotic aneurysm of the cardiac coronary arteries. Report of a case. *Am. Heart J.*, 1947, **33**, 112–120.
8. Ott, A. Ein Fall von Aneurysma der Kranzarterie. *Wien. klin. Wchnschr.*, 1947, **59**, 718–720.
9. Benesova, D., and Houstek, J. Aneurysma koronarni arterie. *Časop. lék. česk.*, 1947, **86**, 663–668.
10. Ashton, N., and Munro, M. Coronary artery aneurysm with occlusion due to a calcified thrombus. *Brit. Heart J.*, 1948, **10**, 165–166.
11. Bowden, K. M. Coronary aneurysms: report of a case. *M. J. Australia*, 1949, **1**, 209–211.
12. O'Neill, J. B., and Laipply, T. C. Aneurysms of coronary arteries. Report of two cases. *Quart. Bull. Northwestern Univ. M. School*, 1949, **23**, 77–82.
13. Dordi, F. Descrizione di un raro caso di aneurisma dell'arteria coronarica sinistra. *Pathologica*, 1950–51, **42**, 239–244.
14. Sarkisian, S. S. Aneurysm of the coronary artery: report of a case. *U.S. Armed Forces M. J.*, 1950, **1**, 1281–1283.
15. Denham, S. W. Syphilitic aneurysm of the left coronary artery. *A. M. A. Arch. Path.*, 1951, **51**, 661–665.
16. Kempton, J. J. Calcified aneurysms of the coronary arteries. *Proc. Roy. Soc. Med.*, 1951, **44**, 733–734.
17. Prentice, A. I. D., and Penfold, J. B. Aneurysm of the coronary arteries. *Brit. Heart J.*, 1952, **14**, 87–90.
18. Velázquez, T. Aneurisma micótico de la arteria coronaria; presentación de un caso y revision de la literatura. *Arch. Inst. cardiol. México*, 1952, **22**, 49–64.
19. Rukstinat, G. J. Multiple aneurysm of the right coronary artery; death from a ruptured aneurysm of the abdominal aorta. *J. A. M. A.*, 1952, **149**, 1129–1131.

20. Minder, W. H. Aneurysma congenitum arteriae coronariae. *Cardiologia,* 1953, **22,** 35–44.

21. Trinidad, S.; Grayzel, D. M.; Rapoport, P., and Lee, N. Aneurysm of the coronary artery. *Ann. Int. Med.,* 1953, **39,** 1117–1124.

22. Colbeck, J. C., and Shaw, J. M. Coronary aneurysm with arteriovenous fistula. *Am. Heart J.,* 1954, **48,** 270–274.

23. Loring, W. E. Multiple arteriosclerotic aneurysms of coronary arteries. *A. M. A. Arch. Path.,* 1955, **59,** 449–452.

24. Coppoletta, J. M., and Wolbach, S. B. Body length and organ weights of infants and children. A study of the body length and normal weights of the more important vital organs of the body between birth and twelve years of age. *Am. J. Path.,* 1933, **9,** 55–70.

25. Rae, M. V. Coronary aneurysms with thrombosis in rheumatic carditis. Unusual occurrence accompanied by hyperleukocytosis in a child. *Arch. Path.,* 1937, **24,** 369–376. (Cited by Scott.[1])

26. Malet and Evans, A. Aneurysm of coronary artery; rupture; necropsy; remarks. *Lancet,* 1887, **2,** 67. (Cited by Packard and Wechsler.[3])

27. Gee, S. J. Aneurysms of coronary arteries in a boy. *St. Barth. Hosp. Rep.,* 1871, **7,** 148. (Cited by Packard and Wechsler.[3])

28. Clarke, J. J. Embolic aneurysms of the heart, buttock, and axilla. *Tr. Path. Soc. London,* 1896, **47,** 24–25. (Cited by Packard and Wechsler.[3])

29. Trevor, R. S. Aneurysm of the descending branch of the right coronary artery, situated in the wall of the right ventricle, and opening into the cavity of the ventricle, associated with great dilatation of the right coronary artery and non-valvular infective endocarditis. *Proc. Roy. Soc. Med.,* 1911–12, **5,** 20–26. (Cited by Scott.[1])

30. Ruge, E. Infektiöses Aneurysma der linken Coronararterie als Teilerscheinung einer Septicopyämie nach Osteomyelitis acuta infectiosa femoris. *Deutschr. Ztschr. f. Chir.,* 1905, 80, 150–164. (Cited by Packard and Wechsler.[3])

31. Anderson, W. A. D. Pathology. C. V. Mosby Co., St. Louis, 1948, pp. 565–566.

32. Dock, W. The predilection of atherosclerosis for the coronary arteries. *J. A. M. A.,* 1946, **131,** 875–878.

33. Fangman, R. J., and Hellwig, C. A. Histology of coronary arteries in newborn infants. (Abstract.) *Am. J. Path.,* 1947, **23,** 901–902.

34. Marble, A. Coronary artery disease in the diabetic. *Diabetes,* 1955, **4,** 290–297.

35. Nelson, W. E. (ed.). Textbook of Pediatrics. W. B. Saunders Co., Philadelphia, 1954, ed. 6, p. 461.

36. Sinclair, W., Jr., and Nitsch, E. Polyarteritis nodosa of the coronary arteries. Report of a case in an infant with rupture of an aneurysm and intrapericardial hemorrhage. *Am. Heart J.,* 1949, **38,** 898–904.

37. Spector, S. Scarlet fever, periarteritis nodosa, aneurysm of coronary artery with spontaneous rupture, hemopericardium. *Arch. Pediat.,* 1939, **56,** 319–324.

38. Pickard, C. M.; Owen, J. G., and Dammin, G. J. Aneurysms of the coronary arteries due to polyarteritis nodosa occurring in an infant. Report of a case with coronary artery thrombosis and myocardial infarction. *J. Lab. & Clin. Med.,* 1947, **32,** 1513–1514.

39. Scott, E. P., and Rotondo, C. C. Periarteritis nodosa; report of two cases, one complicated by intrapericardial hemorrhage. *J. Pediat.*, 1944, **25**, 306–310.

40. Emminger, E. Arterio-venöses Aneurysma der rechten Herzkranzschlagader. *Klin. med.*, 1947, **2**, 652–656.

41. Paul, O.; Sweet, R. H., and White, P. D. Coronary arteriovenous fistula; case report. *Am. Heart J.*, 1949, **37**, 441–445.

42. Löwenheim, I. Eine seltene Missbildung der Coronargefässe. *Frankfurt. Ztschr. f. Path.*, 1932, **43**, 63–68.

43. Halpert, B. Arteriovenous communication between the right coronary artery and the coronary sinus. *Heart*, 1929–31, **15**, 129–133.

44. Taussig, H. B. Congenital Malformations of the Heart. The Commonwealth Fund, New York, 1947, 618 pp.

45. Wilmer, H. A. Two cases of periarteritis nodosa occurring in the first month of life. *Bull. Johns Hopkins Hosp.*, 1945, **77**, 275–286.

46. Stevens, A. M., and Johnson, F. C. A new eruptive fever associated with stomatitis and ophthalmia. Report of two cases in children. *Am. J. Dis. Child.*, 1922, **24**, 526–533.

47. Middleton, W. S. Infectious arteritis. *Ann. Int. Med.*, 1948, **29**, 1093–1103.

48. Blankenhorn, M. A., and Gall, E. A. Clinicopathologic conference. *Am. J. Clin. Path.*, 1955, **25**, 543–553.

49. McLetchie, N. G. B., and Gillis, D. A. Disseminate endarteritis. Report of a case. *Am. J. Clin. Path.*, 1955, **25**, 502–509.

[*Illustrations follow*]

LEGENDS FOR FIGURES

FIG. 1. Case 2, a 4 month old male infant. Gross appearance of the heart. Saccular aneurysm of the left anterior descending coronary artery.

FIG. 2. Case 2. Photomicrograph of the coronary artery. Striking subintimal thickening. Breaks may be noted in the continuity of the internal elastica. Verhoeff and van Gieson's stains. × 45.

1

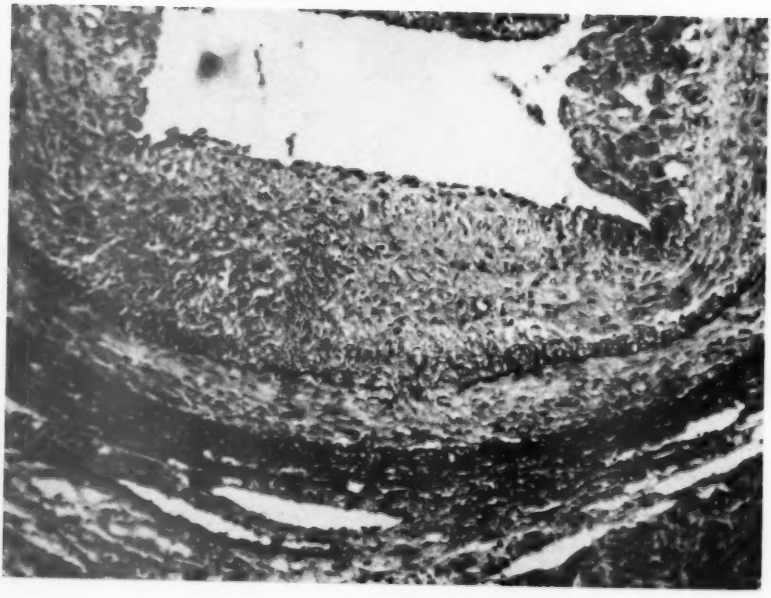

2

FIG. 3. Case 3, an 8 month old male infant. Gross appearance of the heart. Anterior view. Striking diffuse dilatation and tortuosity of the left anterior descending and circumflex coronary arteries. Saccular aneurysm of the main right coronary artery.

FIG. 4. Case 2. Photomicrograph of small vessels adjacent to the right epididymis. Arterial occlusion with recanalization. Perivascular fibrosis. Verhoeff and van Gieson's stains. × 75.

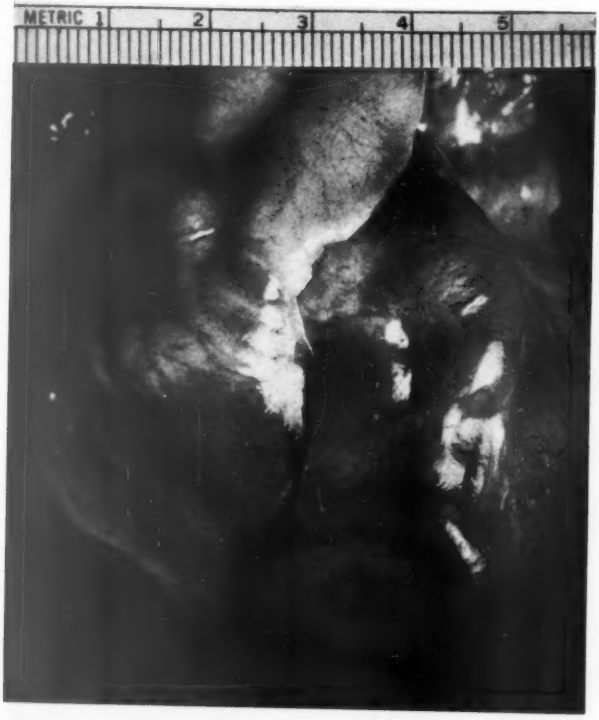

3

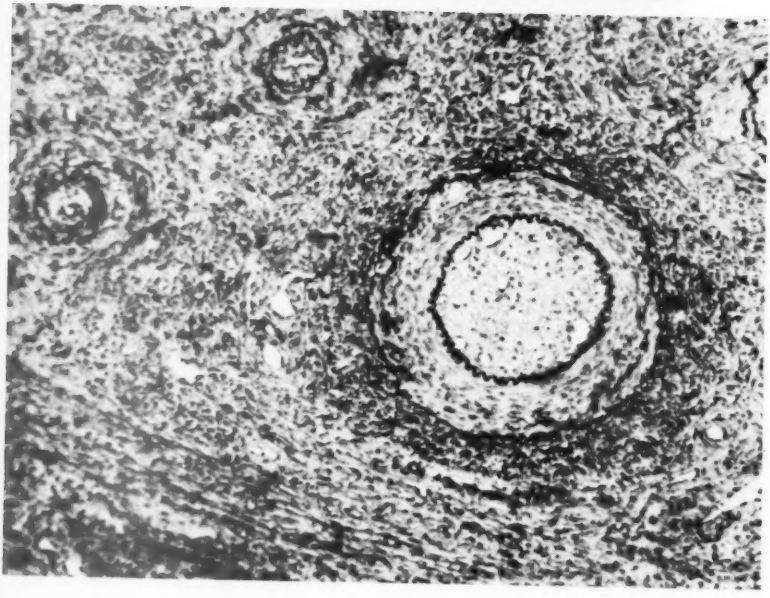

4

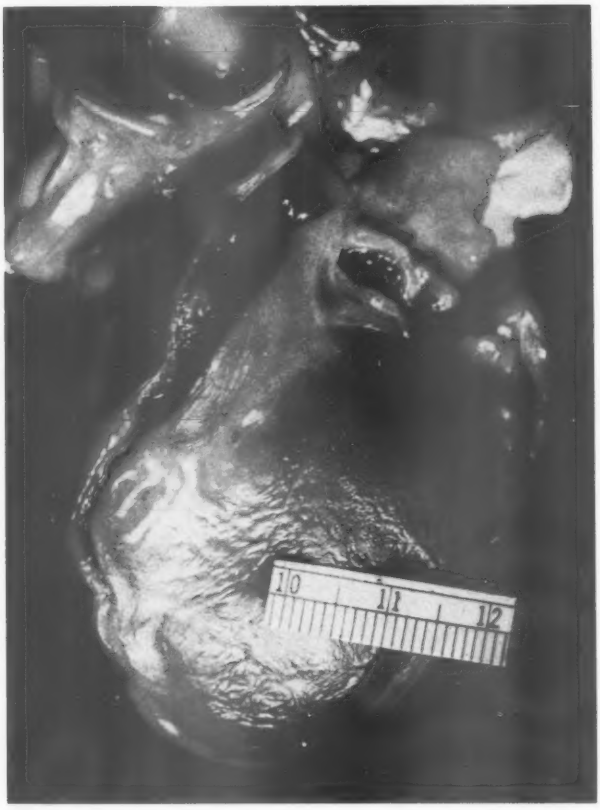

FIG. 5. Case 3. Gross appearance of the heart. Lateral view. The left main coronary artery, left anterior descending and left circumflex branches have been opened.

FIG. 6. Case 3. Aneurysm of the right main coronary artery. Extreme subintimal fibrosis. Fragmentation and disruption of elastica. Verhoeff and van Gieson's stains. × 45.

FIG. 7. Case 3. Small coronary artery demonstrating endothelial proliferation, subendothelial fibrosis, splitting with reduplication of the elastica, and periadventitial fibrosis. Verhoeff and van Gieson's stains. × 75.

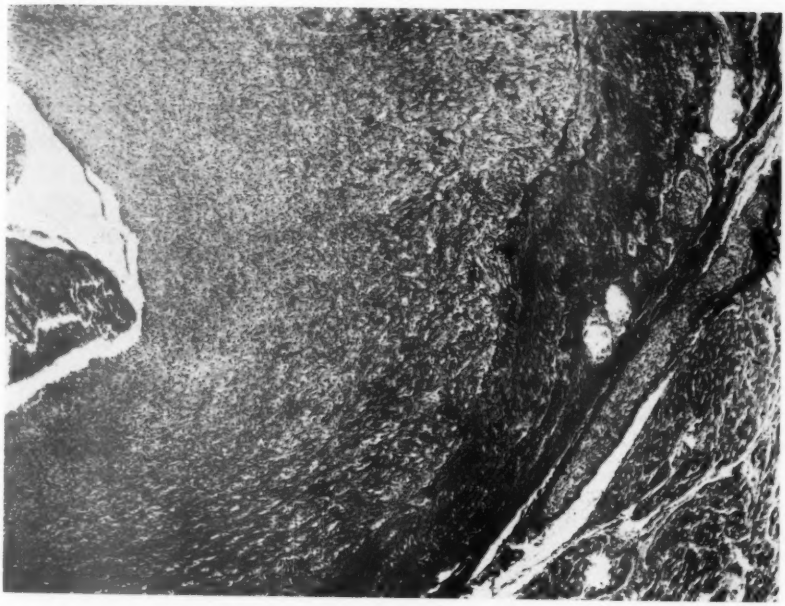

6

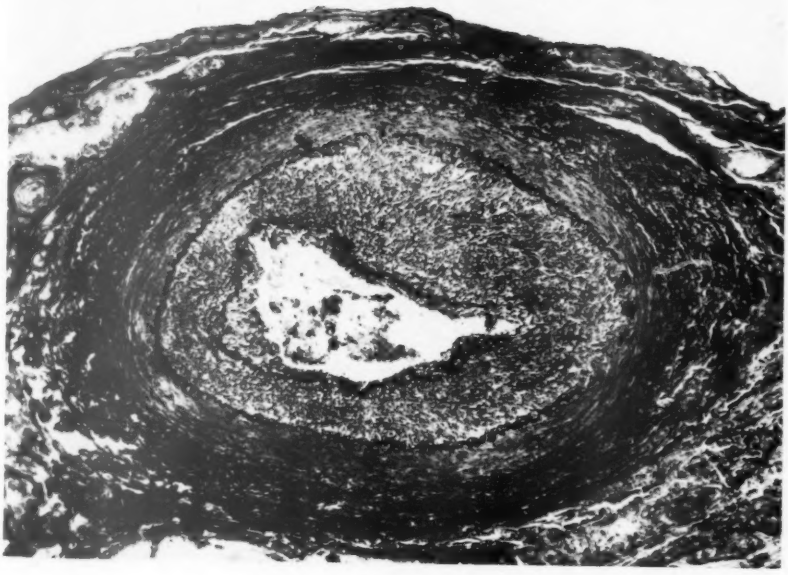

7